Universidad Nacional Autónoma de México

Instituto de Investigaciones Biomédicas

Facultad de Medicina

Caracterización de células germinativas de *Taenia crassiceps*

TESIS

Que para obtener el grado de Licenciado en

Investigación Biomédica Básica presenta el alumno

Arturo Alejandro Calderón Gallegos

Director de tesis: Dr. Juan Pedro Laclette

Ciudad Universitaria, CD. MX. 2022

Dedicatoria

A mi mamá Elvia quien ha sido una madre modelo y a mi papá Arturo quien fue un gran ejemplo a seguir. Por ser y haber sido excelentes padres quienes bajo cualquier adversidad estuvieron presentes brindando todo su apoyo para la conclusión de mis estudios y para mi formación personal.

A mis queridos abuelos, María Luisa y Jorge, quienes me procuraron y brindaron todo su amor durante la infancia.

A mis tíos Herón, Irma y Rosaura, quienes me han cuidado y querido incondicionalmente.

A mis primos, Karen, Maggy, Alan y Jorge por haberme acompañado mientras crecía y por su gran cariño.

A mi amada Ximena por estar incondicionalmente todos los días entregándome lo mejor de su persona y demostrándome su hermoso cariño.

A Miss Gile por haberme recibido y apoyado en una etapa difícil y de muchos cambios.

A mi profesor de preparatoria Arturo Quero Mota, quien me preparó para enfrentarme a los obstáculos que se me presentarían en la carrera.

A todos mis compañeros de laboratorio de mis distintas rotaciones con quienes he pasado muy buenos momentos.

A mi mentor el Dr. Juan Pedro Laclette por enseñarme el camino de la investigación, por integrarme en su grupo de investigación y por toda la sabiduría que ha compartido conmigo hasta el momento.

Agradecimientos

Al Dr. Julio Carrero, Dr. Raúl Bobes, Dra. Edda Sciutto, Dra. Gladis Fragoso, Investigadores titulares del Instituto de Investigaciones Biomédicas, por sus invitaciones para colaborar en distintos proyectos y por su excelente apoyo intelectual, asimismo agradezco la revisión de esta tesis al Dr. Abraham Landa, Dra. Ana Flisser y al Dr. Luis Vaca. Finalmente extiendo mi gratitud a la Dra. Diana Ríos, Dr. Miguel Tapia, Dra. Adriana Ayón, Dra. Marisela Hernández, Dra. Georgina Díaz, y a la M. en C. Patricia de la Torre, por todo su apoyo técnico brindado para la elaboración de los experimentos del presente trabajo de tesis.

Índice

I. Resumen

Los parásitos son organismos de gran interés científico, no sólo por su capacidad para infectar a los humanos, sino porque se trata del modo de vida más común en la naturaleza. Además, participan en numerosas interacciones ecológicas con otros organismos y presentan diversas estrategias que han desarrollado a lo largo de su historia evolutiva para su coexistencia con el hospedero. Una característica de los céstodos, todos ellos parásitos, los cuales son una clase importante de los platelmintos, es la aparición del tegumento que marca la frontera entre el gusano y el hospedero. Los céstodos, así como en el resto de los platelmintos, poseen una extraordinaria capacidad regenerativa relacionada con la existencia de células totipotenciales (neoblastos). En esta tesis de investigación, se definió como objetivo principal la identificación, el aislamiento, la caracterización y el cultivo de las células replicativas de *Taenia crassiceps* que pueden estar relacionadas con los neoblastos. La *T. crassiceps* es una especie que afecta a roedores y lagomorfos en su fase larvaria y cánidos en su fase adulta. Este ténido está cercanamente emparentado con *Taenia solium,* que en su fase larvaria puede afectar gravemente la salud humana causando la neurocisticercosis y afecta la porcicultura rústica causando la cisticercosis porcina. La cisticercosis por *T. crassiceps* ha sido ampliamente utilizada como modelo experimental para el estudio de la cisticercosis humana y porcina. Para la realización de esta tesis se emplearon metodologías adaptadas de estudios similares en otros platelmintos de vida libre, tales como la incorporación del análogo de timidina (EdU), el marcaje con un anticuerpo contra DDX4/VASA el cual ha sido identificado en células germinales de la planaria, la utilización de la citometría de flujo para la separación de las poblaciones celulares del tejido larvario, asimismo se probaron distintas condiciones de cultivo. También se determinó el número cromosómico de los citones replicativos. Nuestros resultados muestran que las células replicativas están presentes principalmente en regiones proliferativas de la pared vesicular y del escólex del cisticerco. Se observó que los anticuerpos contra DDX4/VASA reconocen a una proteína muscular del cisticerco y no a la helicasa que se ha utilizado para identificar las células de línea germinal. Se estudiaron las poblaciones de citones obtenidas por disgregación del tejido parasitario por medio de citometría de flujo y se logró caracterizar los estadios del ciclo celular de algunas poblaciones. Se establecieron las condiciones para el cultivo *in vitro* de los citones aislados durante al menos 14 días. Finalmente se obtuvieron los cariotipos de las cepas WFU y ORF de *T. crassiceps,* encontrándose que la ausencia de escólex en la cepa ORF no se debe a una aneuploidía (pérdida de un par cromosómico) como se ha propuesto anteriormente. Esta tesis contribuye información básica al respecto de características de las células proliferativas de *T. crassiceps*, que será complementada en estudios posteriores para el establecimiento de líneas celulares estables de este parásito.

I. Summary

Parasites are organisms of great scientific interest, not only due to their capacity to infect humans, but also because parasitism is the most common lifestyle in nature. Also, the variety of ecological interactions with other organisms and their strategies acquired or developed during their evolution to coexist with their hosts. One characteristic of cestodes, which are an important class of Platyhelminthes, is the apparition of the tegument, which is a structure that establishes the frontier between the worm and the host. Cestodes, as in other flatworms, have a remarkable regenerative capacity related to the existence of totipotential cells (neoblasts). In this research thesis, the main objective was the identification, isolation, characterization, and cultivation of replicative cells of *Taenia crassiceps* that may be related to the regenerative capacity in these organisms. The *Taenia crassiceps* is a species which infects lagomorphs and rodents in its juvenile stage and canids in the adult stage. This taeniid is closely related to *Taenia solium* which in its larval stage can have a harmful impact on human health, causing neurocysticercosis and affecting rustic pig farming by causing porcine cysticercosis. *Taenia crassiceps* cysticercosis has been widely used as an experimental approach for the study of human and porcine cysticercosis. The methodologies used were adapted from similar studies in other free-living worms such as the incorporation of an analog of thymidine (EdU), the identification of the target of the antibody anti-DDX4/VASA which has been involved with germinative cells of planarians, the utilization of flow cytometry to separate cell populations of the tegument and the standardization of *in vitro* culture conditions. Finally, the chromosomic number of replicative cells in the larvae was determined. Our results show that replicative cells are mainly present in the proliferative regions of the vesicle and in the scolex of the cysticerci. It was observed that the antibodies directed against DDX4/VASA recognize a muscular protein of the cysticerci and not the helicase which has been used to identify germinal cells. The cyton populations obtained by tissue disaggregation were studied and the cell cycle of some populations could be observed. The *in vitro* culture conditions were determined and the isolated cytons could be maintained for at least 14 days. Finally, the karyotypes of the WFU and ORF strains were obtained, finding that the absence of scolex in the ORF strain is not due to an aneuploidy (loss of a chromosome pair), which has been proposed previously. This thesis contributes basic knowledge about the characteristics of proliferative cells of *T. crassiceps*, which may be complemented in future studies to obtain stable cell lines of this parasite.

II. Introducción

II.1 Los organismos invertebrados

En la naturaleza los organismos invertebrados son, con mucho, los más abundantes. Existe una gran variedad de especies que son el resultado de centenas de millones de años de evolución. La fecha de aparición de algunos grupos de invertebrados ha sido difícil de elucidar debido a que sus tejidos blandos han dejado muy pocos registros fósiles. Sin embargo, se dispone de una amplia variedad de fósiles de algunos grupos como los artrópodos, braquiópodos o moluscos. De los 32 *phyla* de metazoarios actuales, 14 son exclusivamente marinos, lo que apoya la idea de que la invasión de los ambientes terrestres significaba un reto para muchos organismos y solamente algunos pudieron desarrollar sistemas de intercambio de gases o de regulación osmótica para poder sobrevivir en el ambiente terrestre [8, 39].

La vida en la Tierra indudablemente comenzó en el mar, la oportunidad que representa este nicho para albergar vida es única debido a las propiedades fisicoquímicas del agua. Existe evidencia de la presencia de invertebrados en estratos correspondientes al periodo Proterozoico (hace 2,500 Ma), se puede afirmar que durante el periodo Ediacarano (~635 Ma) aparecieron algunos organismos invertebrados marinos, ya que los fósiles de la fauna durante este periodo representan las primeras evidencias de *phyla* modernos [8, 13]. Un claro ejemplo es el hallazgo de animales con simetría bilateral en la formación geológica de Ediacara. Una especie (*Ikaria wariootia*) es consistente con las predicciones basadas en los estudios filogenéticos de invertebrados modernos, respaldando la idea de que ya existían algunos *phyla* que precedían a los que se han encontrado en los registros fósiles correspondientes al periodo Proterozoico (Fig. 1) [16]. Para el estudio de cualquier organismo, fósil o actual, ha sido necesario establecer diferentes criterios de clasificación que agrupen la gran cantidad de organismos descritos. Por ello se han tomado en consideración la simetría corporal y el patrón de desarrollo.

Figura 1. Reconstrucción de *Ikaria wariootia* según el fósil de rastro encontrado en el sur de Australia (tomada de Evans et. al., 2020).

II.1.1 Simetría corporal

La clasificación con base en la simetría corporal se divide en dos; aquellos que son bilateralmente simétricos (Fig. 2a), usualmente acompañado de cefalización, que consiste en la congregación de órganos y tejidos en uno de los extremos del organismo, lo que define un eje anteroposterior del animal. Los organismos bilaterales entonces pueden dividirse en dos secciones simétricas cuando se realiza un corte paralelo al eje anteroposterior, el cual resulta en una imagen en espejo del cuerpo. Sin embargo, un corte perpendicular con respecto a su eje crea dos imágenes disimilares incluso pasando por el centro. La segunda forma de simetría corporal que se observa en la naturaleza es la radial (Fig. 2b), la cual ocurre en organismos en los que es posible realizar un corte desde cualquier lado, siempre y cuando pase por su centro y se divide igualitariamente el cuerpo. Los cnidarios y los equinodermos en sus fases adultas, son ejemplos de esta clase de simetría [8, 23 38, 39].

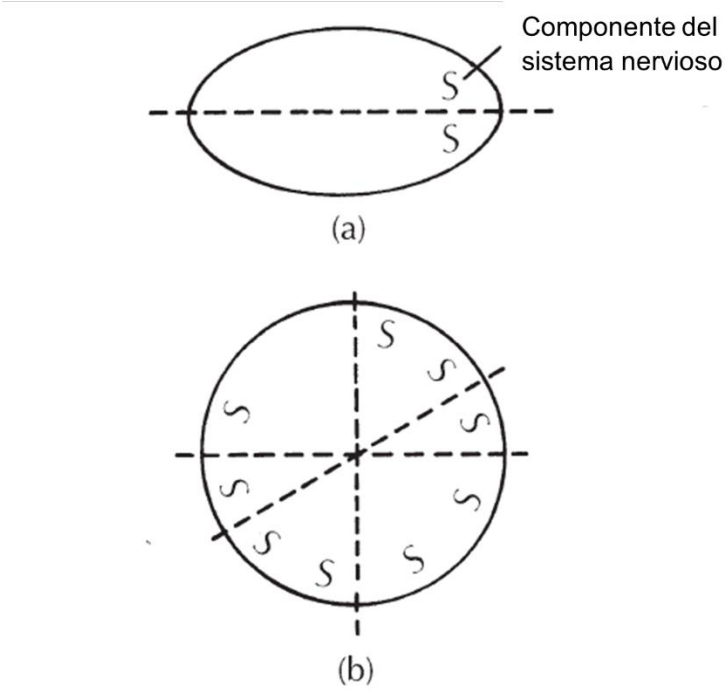

Figura 2. Diferentes tipos de simetría corporal. a) Simetría bilateral y b) radial (tomada y traducida de Pechenik, 2014)

II.1.2 Patrones de desarrollo

Para la clasificación con base en los patrones de desarrollo de los metazoarios se utilizan los términos diploblásticos o triploblásticos, que están basados en el número de capas germinales durante su embriogénesis, las cuales dan lugar a distintos tejidos y sistemas. Los organismos diploblásticos muestran dos capas dentro del embrión; el ectodermo, que es la capa más superficial y el endodermo, la capa más interna. La mayoría de los metazoarios son triploblásticos, en los que ocurre una tercera capa además del endodermo y del ectodermo. Esta tercera capa se denomina mesodermo, la cual yace entre las otras dos. Dentro de la clasificación de los organismos triploblásticos existen tres tipos de *bauplan* (plan organizacional del cuerpo), basándose en la presencia de una cavidad interna llena de fluido independiente del tracto digestivo, que por su origen durante la embriogénesis permite clasificarlos como acelomados, pseudocelomados o celomados. Los acelomados carecen de esa cavidad; en los pseudocelomados la aparición del espacio interior se desarrolla del blastocelo, dando lugar a una cavidad que no está cubierta por tejido derivado del mesodermo. En el último grupo de animales triploblásticos se encuentran los celomados, la aparición de este tipo de arquitectura, denominada celoma, permitió el desarrollo de nuevas estructuras en el cuerpo, incluyendo una cavidad para el resguardo de distintos órganos

corporales, así como un medio de circulación de fluidos para el funcionamiento del esqueleto hidrostático. La formación del celoma puede ocurrir por dos procesos distintos, lo que permite distinguir los grupos de los protostomados, en los cuales se origina el celoma por la aparición y elongamiento de una hendidura en el mesodermo denominada esquizocelo y los deuterostomados, en los cuales el celoma se forma por la evaginación del arquenterón hacia el blastocelo embriónico. Debido al origen del celoma en estos organismos, a partir del arquenterón, el cual es una parte del tejido que también da origen al intestino, en ocasiones se le denomina también como enterocelo. Existen otras características que pueden ayudar a distinguir entre los protostomados y deuterostomados. Otro ejemplo es el origen embriónico de la boca, la cual surge en los protostomados a partir del blastoporo y además es la primera abertura que aparece durante su desarrollo embrionario; en cambio, en los deuterostomados la boca se desarrolla después de la aparición del ano a partir del blastoporo y se considera una segunda abertura en otra parte del embrión [8, 23, 38, 39].

II.1.3 Formas de locomoción y soporte del cuerpo

Entre las notables adaptaciones evolutivas de los invertebrados también podemos destacar las diferentes formas de locomoción que han aparecido, que están relacionadas con diferentes estructuras de soporte desarrolladas a lo largo de la evolución. Existen tres tipos básicos de sistemas de soporte, los esqueletos hidrostáticos, los exoesqueletos y los endoesqueletos. El esqueleto hidrostático se basa en las propiedades de los líquidos, la incompresibilidad del agua y su capacidad de asumir la forma del recipiente. Haciendo uso de los músculos longitudinales y circulares, de la cavidad hueca del cuerpo, de una membrana deformable y del fluido interno se puede obtener locomoción basada en el antagonismo de las contracciones musculares, que producen cambios en la presión interna del fluido para la elongación de los músculos previamente contraídos y del cuerpo, permitiendo recuperar su forma inicial y avanzar sobre el sustrato en el que se encuentra (Fig. 3). Uno de los *Phylum* que utiliza el esqueleto hidrostático y que ha sido de los más estudiados por sus características únicas es el de los platelmintos, los cuales son organismos frecuentemente utilizados como modelos experimentales para diferentes disciplinas científicas. En contraste, los organismos con esqueleto “duro” (endoesqueleto o exoesqueleto) en los invertebrados previenen la deformación del cuerpo, confiriendo ventajas como un aumento de tamaño y de coordinación del movimiento. Un ejemplo de organismos que utilizan el exoesqueleto son los artrópodos. Asimismo, un ejemplo del uso de un endoesqueleto ocurre en los cordados, organismos que presentan una notocorda durante alguna etapa de su desarrollo. La notocorda es un conducto protector que se extiende a lo largo del cuerpo del animal para conducir y proteger el sistema nervioso; también provee soporte durante la locomoción del organismo [8, 27, 39].

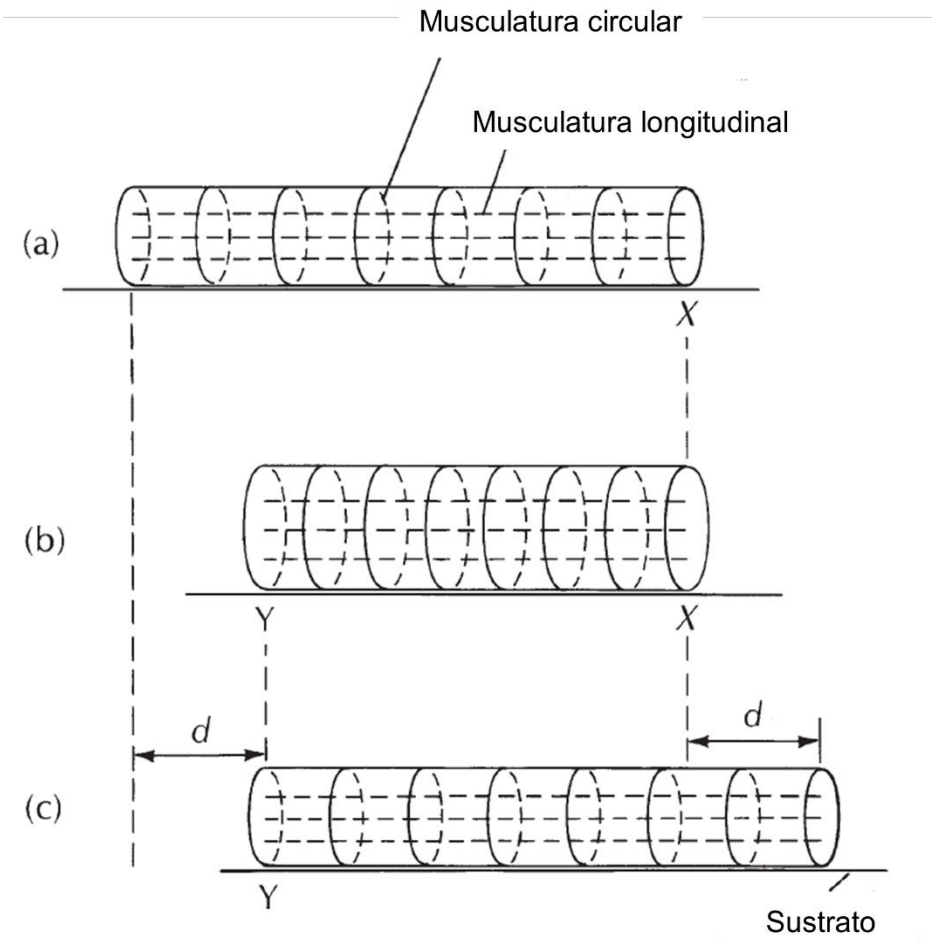

Figura 3. Representación esquemática del movimiento de un gusano con músculos longitudinales y circulares que le permiten la contracción y relajamiento de la cavidad corporal llena de fluido. (a) Representación de las musculaturas circular y longitudinal; (b) Ocurre la contracción de los músculos longitudinales con un anclaje en la posición X y se contrae la parte posterior formando un punto de anclaje en Y; (c) se relajan los músculos longitudinales soltando el anclaje en X. Los anclajes se deben a la contracción de los músculos circulares para poder avanzar la distancia d en la parte anterior del organismo (tomada y traducida de Pechenik, 2014).

II.2 Modos de vida, simbiosis y parasitismo

En los animales existe una gran diversidad en los patrones de asociación que se pueden clasificar como homogénicas o heterogénicas; estos términos se refieren a las interacciones entre organismos de la misma o de diferente especie, respectivamente. Para referirse a todas las relaciones entre especies se utiliza el término simbiosis, sin embargo, distintos términos tratan de abarcar el espectro de interacciones, basándose en criterios tales como el beneficio o daño de un miembro

al otro. Los términos que permiten la identificación del tipo de relación simbiótica son: foresis, mutualismo, comensalismo y parasitismo. Foresis se refiere a la relación en la cual un organismo transporta a otro; comensalismo se refiere a las relaciones en donde ambos organismos comparten su alimento; mutualismo se refiere a las relaciones en donde ambos organismos resultan beneficiados de su interacción; finalmente en el parasitismo uno de los organismos, denominado parásito, recibe un beneficio a costa del bienestar del otro, llamado huésped u hospedero. Para que una relación parasítica tenga éxito, se requiere que el daño conferido tenga un impacto moderado sobre la capacidad reproductiva del hospedero (parásito eficiente) [32, 45, 54]. El parasitismo es la relación simbiótica antagonista más exitosa que podemos encontrar en la Tierra, ya que se estima que entre el 50-70% de las especies se relacionan a través del parasitismo [35]. Existen registros fósiles del parasitismo que se remontan al periodo Cámbrico temprano, los cuales se encontraron en el sur de China. Esta asociación consistía de un braquiópodo en el cual estaban incrustados varios “tubos parasíticos”, con una orientación en dirección de las corrientes de flujo laminar que el hospedero generaba para alimentarse, resultando en la disminución de la biomasa del braquiópodo [66]. Algunos ejemplos de los efectos que pueden provocar los parásitos son lesiones mecánicas, manipulación del sistema inmunológico o robo de nutrientes del hospedero. Además, dependiendo de la localización del parásito se les denomina de distinta manera, “ectoparásitos” son aquellos que habitan en la parte externa del hospedero y “endoparásitos” son los que viven dentro del organismo. Las características que han aparecido en los diferentes organismos parásitos durante la evolución son dependientes del sitio de invasión del hospedero y además pueden ser afectados por la convivencia con otros organismos y sus hábitos.

Otra adaptación al hospedero es la especificidad, esta característica varía entre parásitos y puede exhibir diferentes grados de exclusividad con un organismo, un ejemplo es *Taenia solium* que solamente alcanza su forma adulta como parásito en el tubo digestivo del ser humano [31, 32]. En contraste, una especie cercanamente relacionada: *Taenia crassiceps*, puede parasitar distintas especies de cánidos y dar lugar a huevos fértiles. Existen ocasiones donde un parásito puede encontrar un hospedero paraténico (o de transporte) en el cual no sufre ningún cambio con respecto a su ciclo de vida, pero puede funcionar como un puente ecológico entre un hospedero intermediario y uno definitivo [45]. También existen los hospederos reservorios que se caracterizan por ser organismos alternativos en donde los parásitos pueden continuar con su ciclo de vida a pesar de no estar en un hospedero ideal para su desarrollo, sin embargo, debido a la carencia de hospederos principales puede continuar su transmisión.

II.3 Los platelmintos

Los platelmintos son organismos acuáticos, mayoritariamente de vida libre (Turbellaria) aunque existen tres grupos que mantienen un modo de vida parasitario. Algunos afectan al ser humano y son de importancia médica (Monogenea, Digenea y Cestoda). Se conocen aproximadamente 30,000 especies de platelmintos [9]. Su característica principal es que son gusanos aplanados; la diversidad morfológica de estos organismos es amplia y pueden carecer de caracteres en común. En el caso de los platelmintos parásitos, la adquisición de un cuerpo aplanado les permitió invadir sitios tubulares dentro del hospedero, como los tubos digestivos, en donde se alojan para su desarrollo, nutrición y reproducción. Son organismos acelomados, triploblásticos y bilateralmente simétricos [38]. El *bauplan* de los platelmintos es único, poseen estructuras que permiten la circulación de fluidos basados en el movimiento de cilios pertenecientes a células altamente especializadas denominadas células flama, las cuales están conectadas a tubos colectores y que participan en procesos de excreción y osmorregulación. Otra estructura única en los platelmintos es la aparición del tegumento, la cual está conformada de una superficie externa membranosa y es metabólicamente activa. Por debajo del tegumento, y separados por la llamada membrana basal, existen citones subtegumentales, glandulares y sensoriales que forman un tejido laxo con una característica excepcional: se trata de un sincicio en el que todas las estructuras celulares están interconectadas por lo que sólo existe especialización regional; a ello se debe que en lugar de utilizar el término “célula” se utilice el de “citón”. El tegumento también funciona como un medio de comunicación con el exterior, ya que a través de él se mueven productos de excreción/secreción, inmunomodulares (en el caso de aquellos parásitos), etc [54]. El sistema nervioso de los platelmintos es variable entre las diferentes clases, puede estar muy simplificado y en algunos casos carecen de ojos o también pueden poseer un sistema nervioso centralizado, formado por un ganglio cerebral conectado longitudinal y transversalmente a lo largo del cuerpo del organismo [39]. Con respecto a la forma de reproducción de los platelmintos, pueden ser sexuales o asexuales, inclusive algunas especies pueden utilizar uno u otro método sexual o asexual durante su ciclo de vida, un ejemplo es *Taenia crassiceps*, que pueden reproducirse asexualmente en el hospedero intermediario (roedores) por medio de gemación, mientras que dentro de su hospedero definitivo (cánidos) puede reproducirse solamente por reproducción sexual. Los sistemas digestivos de los platelmintos pueden estar conformados por un intestino ciego el cual puede ser recto o ramificado y pueden poseer bocas con diferente morfología como una faringe protráctil o incluso una probóscide que les permite la adquisición de alimento que se almacena para su digestión en un intestino o enterón. También existen algunos platelmintos parásitos que carecen completamente de tubo digestivo, debido a que llevan a cabo la adquisición de

nutrientes a través del tegumento. Otra capacidad relevante de los platelmintos es su regeneración de tejidos, que no sólo implica la reparación de una parte del cuerpo, sino la formación de órganos, estructuras o incluso de otro organismo completo. Esta habilidad se le atribuye a la presencia de una población denominada neoblastos, que son equivalentes a las células troncales de otros organismos. Los neoblastos son células versátiles capaces de retomar programas de diferenciación propios de tejidos especializados [3, 4, 38, 42, 43]. Entre la gran diversidad de platelmintos, destacan, por su biología, aquellos que han adoptado el parasitismo como su modo de vida, no solamente por estar involucrados en el ámbito médico, sino por ser organismos especiales dentro del reino animal habiendo adquirido complejas estrategias para su supervivencia dentro de los hospederos, ya que han coevolucionado durante largos periodos y bajo presiones selectivas que han resultado en mecanismos altamente especializados para la invasión y permanencia en distintos órganos y tejidos de los hospederos, influyendo importantemente en la ecología de los hábitats en donde se encuentran, debido a su influencia sobre distintas cadenas tróficas [8, 35, 45].

II.4 Céstodos

Los gusanos pertenecientes a la clase Cestoda, pueden dividirse en dos subclases, Cestodaria y Eucestoda, los primeros no se dividen en segmentos, tienen un solo juego de órganos reproductivos, carecen de escólex (órgano de fijación) y tienen una larva decacanto (10 ganchos), mientras que los miembros del segundo grupo poseen un cuerpo elongado y acintado, además carecen de tubo digestivo. Residen principalmente en el tracto digestivo de los hospederos donde hay disponibilidad de nutrientes para afrontar la demanda energética por su alta tasa de crecimiento. Los órdenes de mayor interés médico pertenecen a la subclase Eucestoda [54]. El origen de los céstodos sigue siendo incierto hasta el día de hoy, aunque se ha demostrado que el origen del modo de vida parasitario entre los platelmintos de vida libre, incluyendo los tres grupos principales: Digenea, Monogenea y Cestoda, es monofilético [11]. Es decir, que el parasitismo surgió entre los platelmintos de vida libre en una sola ocasión. En esos análisis filogenéticos el grupo hermano a los tres taxa parásitos son los Seriata. Los céstodos poseen diversos órganos de sujeción que se pueden clasificar en tres grupos, bothria, bothridia y acetábula, que se han adaptado dependiendo de las presiones selectivas a las cuales se han enfrentado durante su evolución, principalmente por la forma del órgano (*v. gr.* intestino) de la especie que parasitan. Pueden además poseer ganchos, pliegues, glándulas, tentáculos o diferentes variantes que les facilitan la fijación dentro del hospedero [10, 45 y 54]. Existen excepciones en algunos organismos como *Fimbriaria fasciolaris* en el cual su escólex pierde la función de sujeción debido al desarrollo

de un pseudoescólex a partir de la porción anterior del estróbilo. Además de las modificaciones del escólex para la fijación al tubo digestivo del hospedero, los céstodos han desarrollado una adaptación única entre los diferentes platelmintos: el tegumento. Esta estructura además de funcionar como una cubierta protectora es una capa metabólicamente activa, formada por un sincicio conectado a los citones subtegumentales, lo que define dos regiones: el citoplasma distal y el citoplasma perinuclear, las cuales han sido extensamente descritas ultraestructuralmente [5, 18, 55]. En el citoplasma distal se pueden encontrar vesículas, que están involucradas en el intercambio de material con la membrana o con el medio externo, en esta región también se pueden observar las microtricas, que se dividen en dos secciones, el eje basal, que posee un núcleo formado por delgados filamentos lo que confiere flexibilidad y la punta distal, que se observa electrón-densa en el microscopio electrónico y puede tener distintas formas según la especie (Fig. 4). Se ha estimado que el factor de amplificación de la membrana externa del tegumento debido a las microtricas, para distintos céstodos, puede variar entre 2.2 a 16.3 [55]. Si se toma en cuenta que la punta distal de la microtrica no está involucrada en la absorción, se puede obtener el factor de amplificación funcional, el cual resulta en un intervalo de 1.73 a 11.75, el cual es comparable con las microvellosidades intestinales.

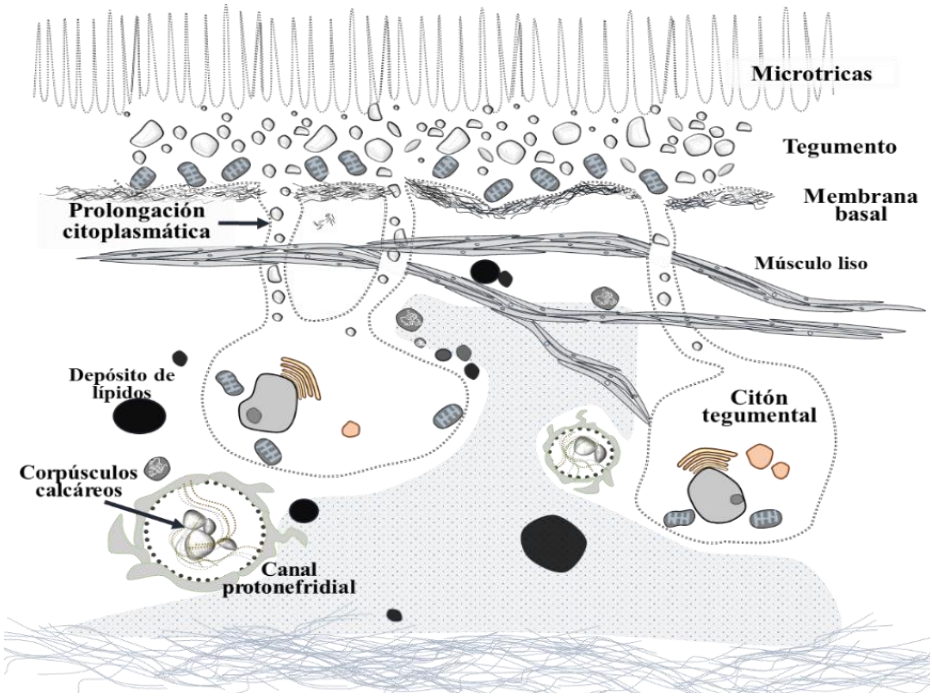

Figura 4. Esquema representativo del tegumento en un céstodo (tomado de la tesis doctoral de Flores-Bautista, 2019) [18].

El desarrollo de la estrobilación en los céstodos es único y consiste en una serie de segmentos que contienen los órganos reproductivos de cada sexo a los cuales se les denomina proglótidos. Conforme se va desarrollando el gusano adulto se producen proglótidos o segmentos que constituyen unidades reproductivas separadas. El proceso de estrobilación consiste en la producción de nuevos proglótidos y en su maduración conforme avanzan hacia el extremo posterior del gusano adulto. Cuando los proglótidos maduros están llenos de huevos se les denomina grávidos. Este proceso de reproducción le permite a los céstodos liberar una gran cantidad de huevos que pueden infectar al siguiente hospedero en su ciclo de vida [45, 54]. En varias especies, los gusanos adultos, son capaces de producir cientos de miles de huevos diarios. Un extraordinario ejemplo de este proceso de reproducción es el organismo *Polygonoporus giganticus*, el cual es un céstodo que habita el intestino de los cachalotes y puede medir hasta 30 metros de largo, con cada proglótido de hasta 5 metros de longitud [67].

II.4.1 Clasificación taxonómica

La taxonomía de los distintos órdenes de céstodos actuales ha tenido cambios a lo largo de la historia. Recientemente se realizó el recuento del número de especies totales estimándose en 4,810 hasta 2017, con un número total de 833 géneros. Sin embargo, constantemente se siguen describiendo nuevas especies de céstodos. Las especies que forman el orden Cyclophyllidea son las más numerosas, incluyendo más del 50% de los céstodos. La descripción de especies se basa principalmente en caracteres morfológicos (tipo de órgano de sujeción, número de ganchos, disposición de los órganos reproductivos, forma de los proglótidos, etc.), pero recientemente se ha integrado la biología molecular para poder realizar estudios filogenéticos de los distintos órdenes que conforman la clase Cestoda [10]. Los marcadores utilizados para la clasificación de estos organismos fueron dos genes nucleares (28S rDNA y 18S rDNA) y dos genes mitocondriales (COI y 16S rDNA) los cuales se han secuenciado para más de 950 especies, logrando separar en 19 órdenes a los céstodos, de los cuales los Eucestoda conforman 17 de estos órdenes [10, 11]. El nombre de los órdenes, los hospederos principales en su ciclo de vida, los genomas secuenciados y el número de géneros y de especies se muestran a continuación, con especial énfasis en el orden Cyclophyllidea, en donde se encuentran la familia Taeniidae (Tabla 1).

Tabla 1. Información de los órdenes actuales de céstodos

Orden	Hospederos principales	Número de géneros	Número de especies	Especies con genomas en WormBase ParaSite
Amphilinidea	Peces óseos, tortugas	6	8	N/A
Bothriocephalidea	Peces óseos	48	132	N/A
Caryophyllidea	Peces óseos	42	122	N/A
Cathetocephalidea	Elasmobranquios	3	6	N/A
Cyclophyllidea	Aves, mamíferos, lagartijas, serpientes, anfibios	437	3,034	*Echinococcus granulosus*, *E. multilocularis*, *E. oligarthrus*, *E. canadensis*, *Hymenolepis microstoma*, *H. diminuta*, *Mesocestoides corti*, *Taenia asiatica*, *T. solium*, *T. multiceps*, *T. saginata*
Diphyllidea	Elasmobranquios	6	59	N/A
Diphyllobothriidea	Mamíferos	18	70	*Spirometra erinaceieuropaei*, *Dibothriocephalus latus*, *Schistocephalus solidus*
Gyrocotylidea	Holocéfalos	1	10	N/A
Haplobothriidea	Peces óseos	1	2	N/A
Lecanicephalidea	Elasmobranquios	29	90	N/A
Litobothriidea	Elasmobranquios	1	9	N/A
Nippotaeniidea	Peces óseos	1	6	N/A
Onchoproteocephalidea	Grupo I: Peces óseos, lagartijas, serpientes, anfibios, tortugas y mamíferos Grupo II: Elasmobranquios	Grupo I: 68 Grupo II:11	Grupo I: 316 Grupo II: 246	N/A
Phyllobothriidea	Elasmobranquios y holocéfalos	24	69	N/A
Rhinebothriidea	Elasmobranquios	22	136	N/A
Spathebothriidea	Peces óseos	5	6	N/A
Tetrabothriidea	Aves y mamíferos	6	70	N/A
“Tetraphyllidea” relics	Elasmobranquios	25	104	N/A
Trypanorhyncha	Elasmobranquios	81	315	N/A

II.5 Ténidos

Dentro de los organismos que pertenecen al orden Cyclophyllidea se encuentran los integrantes de la familia Taeniidae, la cual está conformada por 4 géneros y 50 especies. Son parte de los gusanos parásitos de mayor importancia médica y veterinaria. Los adultos parasitan carnívoros, usualmente en el intestino delgado mientras que los hospederos intermediarios suelen ser las presas de los hospederos definitivos. Existen ocasiones en las que los carnívoros pueden infectarse con el estadio larvario del organismo [32, 45, 54].

Los taénidos pueden tener distintos tipos de larvas: el cisticerco es una vesícula llena de líquido, que rodea un solo escólex invaginado (Fig. 5B); el estrobilocerco es una larva con el escólex usualmente evaginado, conectado por un estróbilo largo, sólido y segmentado a una pequeña vesícula llena de líquido (Fig. 5D); el coenuro/cenuro es una bolsa parecida al cisticerco, pero dentro de ella se desarrollan varios escólices que se mantienen unidos a la pared de la vesícula (Fig. 5A); el quiste hidatídico es una larva similar al cisticerco, sin embargo, una diferencia fundamental es que lleva a cabo el proceso de gemación dentro de la misma vesícula en la cual se depositan escólices que pueden formar a un adulto en el hospedero definitivo (Fig. 5C); finalmente, el quiste alveolar es otro tipo de larva la cual también puede ser denominada “quiste hidatídico multilocular”, la cual produce un quiste sin uniformidad y sin una membrana definida en el tejido que parasita. Produce una estructura poliquística con vesículas proliferativas que se “posan” en un estroma denso y fibroso, de este tejido larvario se producen escólices [54].

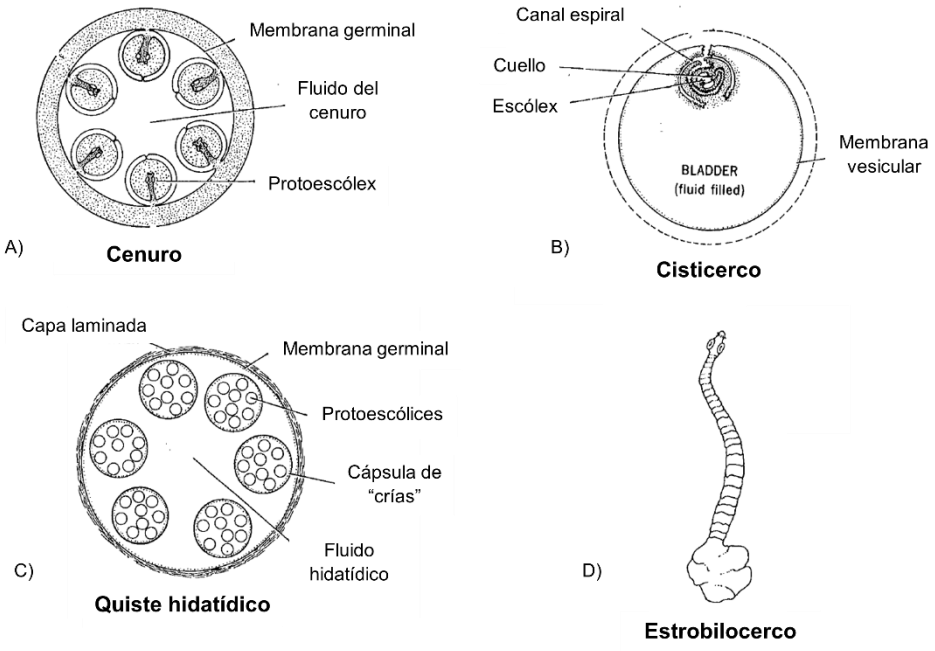

Figura 5. Tipos de larvas que ocurren en los taénidos. A) Cenuro, B) Cisticerco, C) Quiste hidatídico y D) Estrobilocerco (tomada y modificada de Smyth, 1962).

II.6 *Taenia solium*

Uno de los organismos pertenecientes a la familia Taeniidae más conocidos es *Taenia solium*, el cual es un parásito adaptado a las condiciones que presenta el tejido de sus hospederos (humano o porcino). Su ciclo de vida se basa en dos organismos vertebrados que han convivido gracias al establecimiento de la cría de animales, los humanos albergan al gusano adulto mientras que el cerdo es el hospedero intermediario de la larva cisticerco [31]. Existen dos hipótesis acerca de la aparición de la parasitosis por *T. solium* en el humano y en el cerdo; la primera consiste en que la adquisición de la tenia fue debido a la íntima relación de los humanos con los cerdos que fueron domesticados hace unos 15,000 años, ya que eran portadores de la larva y era común el consumo de su carne. Una segunda hipótesis que cuenta con evidencia molecular muy sólida muestra que los homínidos carroñeros primitivos se alimentaban de los restos de las cazas llevadas a cabo por hienas y otros cánidos, de quienes adquirieron estos parásitos. Una especie relacionada, *Taenia saginata,* fue similarmente adquirida de los depredadores felinos (leones) [7].

En el caso de la *T. solium,* el ser humano es el único hospedero definitivo; accidentalmente puede actuar también como hospedero intermediario cuando se ingieren alimentos con contaminación fecal. Esta infección por la larva (cisticerco) se denomina cisticercosis y puede ocurrir en distintos sitios como el cerebro, músculo, ojo, tejido subcutáneo. Cuando el cisticerco se encuentra en el sistema nervioso central, la enfermedad se denomina neurocisticercosis, que es la principal infección parasitaria del sistema nervioso del humano [18, 51]. La investigación llevada a cabo en este organismo ha revelado una gran cantidad de información acerca de su fisiología, relaciones ecológicas, evolución y también sobre la inmunología del humano y del cerdo. En diversos países se han diseñado programas dedicados a la erradicación de la cisticercosis. En México la teniasis/cisticercosis constituía un considerable problema de salud pública y de economía en la producción de carne de cerdo; la modernización de la explotación porcina, el desarrollo de herramientas diagnósticas y preventivas, así como el establecimiento de una normativa para la salud en relación con esta parasitosis han logrado que la teniasis/cisticercosis ya no constituya una amenaza para la salud pública actual [49].

II.7 El modelo animal de cisticercosis murina por *Taenia crassiceps*

Debido a la dificultad para la obtención de muestras de parásitos provenientes de infecciones naturales y de su mantenimiento *in vitro*, se ha adoptado el modelo de infección de *T. crassiceps* para el estudio de la biología de la larva y en algunos casos también del adulto. La similitud de *T. crassiceps* con *T. solium* ha permitido el estudio de la biología básica de la larva, de las interacciones hospedero-parásito, el desarrollo de vacunas y de tratamientos contra la cisticercosis, no solo en el humano sino también en el cerdo.

Taenia crassiceps es un céstodo íntimamente emparentado con *T. solium*, su ciclo de vida requiere dos hospederos; la fase larvaria (cisticerco) se desarrolla en roedores pequeños (*v. gr. Apodemus sylvaticus, Microtus arvalis, Mus musculus, Rattus norvergicus*) y la fase adulta ocurre en cánidos (*v. gr. Canis lupus, Canis lupus familiaris, Vulpes lagopus, Vulpes vulpes*) (Fig. 6) [41]. Los cisticercos de *T. crassiceps* tienen una característica importante para su utilización como modelo animal, ya que es capaz de reproducirse asexualmente en el hospedero intermediario mediante gemación [21]. Esta particularidad ha permitido su mantenimiento en el laboratorio mediante la transferencia de cisticercos de un ratón infectado a otro sano (naïve) lo que ha permitido mantener en el laboratorio varias cepas de esta especie por más de 60 años. Se han establecido distintas cepas que se utilizan experimentalmente. Una de ellas es WFU la cual es considerada silvestre, pero también existe una muy particular, denominada ORF, la cual ha perdido la capacidad de infectar a su hospedero definitivo debido a la carencia de escólex en comparación con las otras cepas KBS o WFU [17]. Puesto que ORF posee una velocidad reproductiva más acelerada [20], ha sido ampliamente utilizada en el estudio de diversos aspectos de la relación hospedero-parásito en la cisticercosis.

El mantenimiento de la *T. crassiceps* en condiciones de laboratorio consiste en la inyección de por lo menos 10 larvas pequeñas (0.5-1.0 mm de diámetro) en el peritoneo de ratones hembra de la cepa BALB/c de tres meses de edad. El tiempo de incubación y el sitio de infección óptimo, se determinó por distintos ensayos de inoculación que demostraron que la inyección peritoneal permitía la obtención de una gran cantidad de larvas después de 45 a 90 días [21, 64].

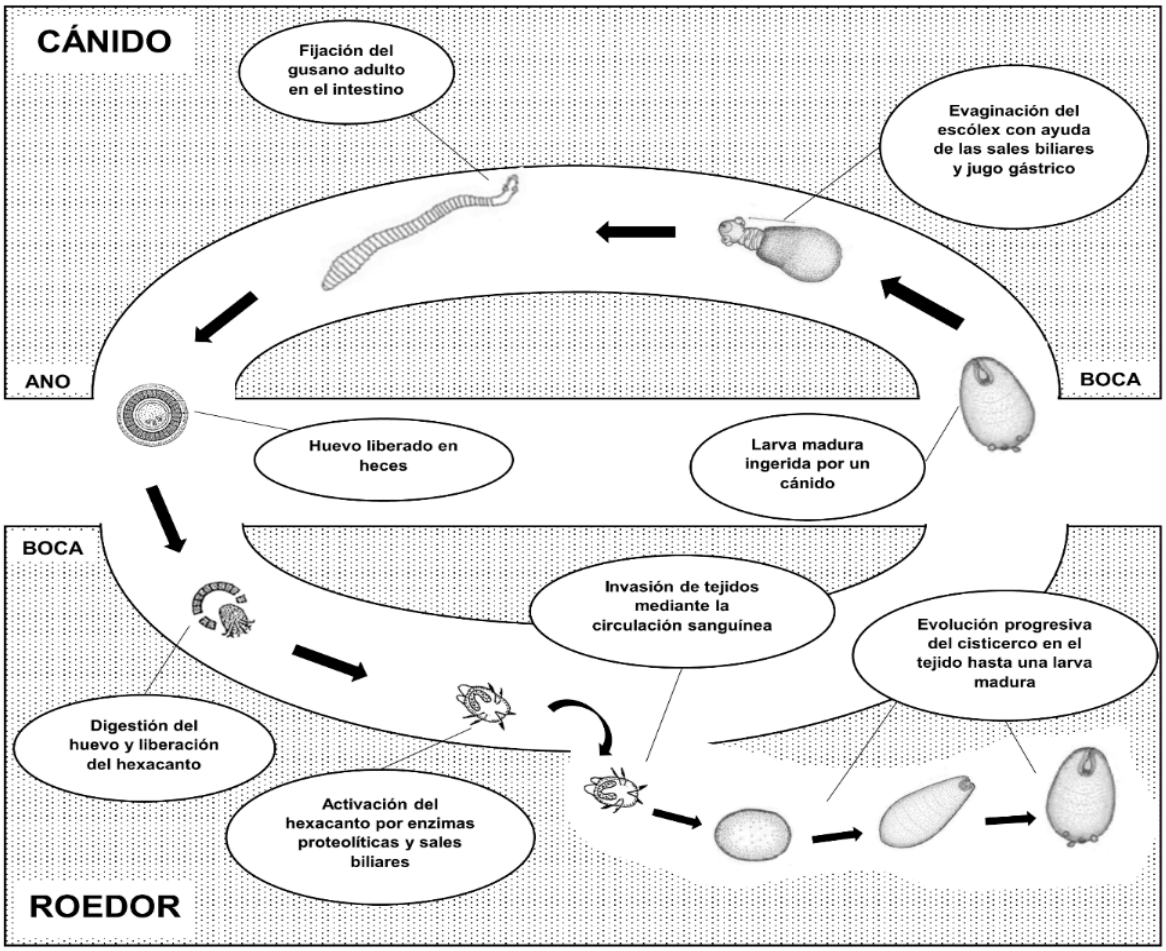

Figura 6. Ciclo de vida de *Taenia crassiceps* en su hospedero definitivo (cánido) y en su hospedero intermediario (roedor) (elaboración propia tomando ilustraciones de Smyth, 1962 y Freeman, 1962).

La cepa ORF ha sido comúnmente empleada en distintos grupos de investigación. Se ha intentado determinar la diferencia entre la cepa silvestre y la cepa mutante carente de escólex. Se ha propuesto que la pérdida del escólex es debida a una anomalía cromosómica, la falta del par cromosómico II debido a una nulisomía, lo cual es considerado un evento catastrófico durante la historia evolutiva del cisticerco de la cepa ORF [52]. También se ha estudiado la replicación celular mediante la incorporación de análogos de nucleótidos o incubación con colchicina y la síntesis de RNA en este organismo [53], con la intención de describir a detalle el sistema de células replicativas que pueden estar involucradas en el mantenimiento de los distintos tejidos que forman a la larva o al adulto. Sin embargo, no hay más estudios actuales al respecto que hayan podido determinar las poblaciones involucradas en la homeostasis del tejido.

II.8 Cariotipos de céstodos

Los cariotipos de algunos céstodos han sido detalladamente reportados por distintos autores. Las técnicas utilizadas comúnmente para la visualización de cromosomas consisten en la utilización de células sexuales del adulto, la incubación con colchicina y la tinción de los cromosomas para su observación bajo el microscopio [58]. Recientemente se han incorporado otras técnicas modernas como la hibridación *in situ* (FISH) o la utilización de sondas fluorescentes (DAPI) para el mapeo y descripción detallada de los cromosomas [36]. Los primeros estudios realizados sobre cariotipos de céstodos se centraban únicamente en su número cromosómico [25, 46, 58]. Conforme se adaptaban técnicas de citogenética originadas en otros organismos, se pudieron realizar descripciones más formales sobre la estructura y composición de los cromosomas de céstodos. Una de las limitantes para el estudio de los cariotipos es la adquisición de células replicativas, ya que su presencia es escasa o inexistente en algunas etapas del desarrollo. El aislamiento celular es una tarea difícil de realizar puesto que se trata de tejidos sinciciales [55]. Los números cromosómicos en céstodos van desde los 6 hasta los 28 pares y la mayoría de las especies presentan una ploidía de 2n=16 o 18. Sin embargo, los organismos del orden Cyclophyllidea tienen una mayor diversidad de cariotipos [58]. En el caso de *T. crassiceps,* se han reportado dos números de cromosomas en su cariotipo [52]. Estos reportes destacan la urgente necesidad de la corroboración de los números cromosómicos para entender la biología básica del parásito y contribuir al conocimiento sobre los céstodos para su utilización como modelos experimentales. Además de que pueden funcionar como herramientas para el establecimiento de las relaciones filogenéticas entre los organismos que conforman este orden. Es por ello que en el presente trabajo de tesis se decidió caracterizar el cariotipo de *T. crassiceps.*

II.9 Secuenciación de genomas

El acceso a las tecnologías de secuenciación masiva ha permitido la caracterización de una gran cantidad de genomas, entre ellos, el de algunos céstodos (Fig. 7). Comenzando con la creación de la base de datos de información genómica de *Schmidtea mediterranea* [44] y con la publicación de los genomas completos de *Schistosoma mansoni y japonicum* [6, 60], el acervo de información genómica de los platelmintos ha crecido notablemente durante la última década. Los parásitos de importancia médica y veterinaria han sido seleccionados para su caracterización genómica. La comparación de los genomas ha permitido comprender el origen filogenético de estos organismos, así como también las adaptaciones a la vida parasitaria que han sucedido durante su historia evolutiva. Los genomas de estos

organismos parásitos son accesibles gracias a un proyecto organizado por el Consorcio Internacional de Genomas de Helmintos, que pueden encontrarse en la base de datos WormBase Parasite, donde se encuentran registrados 197 genomas, de los cuales 19 pertenecen a céstodos [26]. Cabe mencionar que los primeros cuatro genomas de céstodos fueron publicados en el año 2013; entre ellos se describió el genoma de *T. solium* que fue realizado por un consorcio liderado por el Dr. Laclette [62]. En 2019, el registro de genomas creció importantemente, con 17 organismos nuevos registrados en la base de datos. El desarrollo de metodologías que permitan mejorar la calidad de la secuenciación y del armado facilitará el diseño de nuevos fármacos para el tratamiento de enfermedades causadas por estos organismos, así como la producción de vacunas y de métodos diagnósticos.

Se han descrito las células germinativas en planaria y más recientemente en otros organismos parásitos como digeneos y céstodos. Se denominan células "germinativas", "replicativas", "troncales", "de regeneración" o "neoblastos", dependiendo del organismo que se discute, sin embargo, tienen diversas funciones en común, siendo una de ellas la capacidad regenerativa y de crecimiento indefinido, que es una capacidad característica de los platelmintos. Las células germinativas en la clase Cestoda han sido descritas en organismos como Mesocestoides corti, Hymenolepis diminuta, Echinococcus multilocularis, Taenia solium y Taenia crassiceps [28, 29, 33, 37, 47, 53, 65]. A pesar de que se reconoce la existencia de células germinales en estas especies de céstodos, solamente se han logrado caracterizar en E. multilocularis y a H. diminuta, mediante la utilización de métodos de eliminación de células replicativas (radiación o incubación con hidroxiurea), junto con la utilización de marcadores específicos de la línea germinal como mcm2, h2b y ago2 que se han identificado en planaria y en otros organismos parásitos [29, 47]. Otro marcador de la línea germinal que se ha identificado en platelmintos de vida libre es el gen ddx4/vasa, el cual ha sido reemplazado en el genoma de los céstodos por al menos dos genes descritos como pl10, que han tomado las funciones de vasa en el mantenimiento de la población replicativa [62].

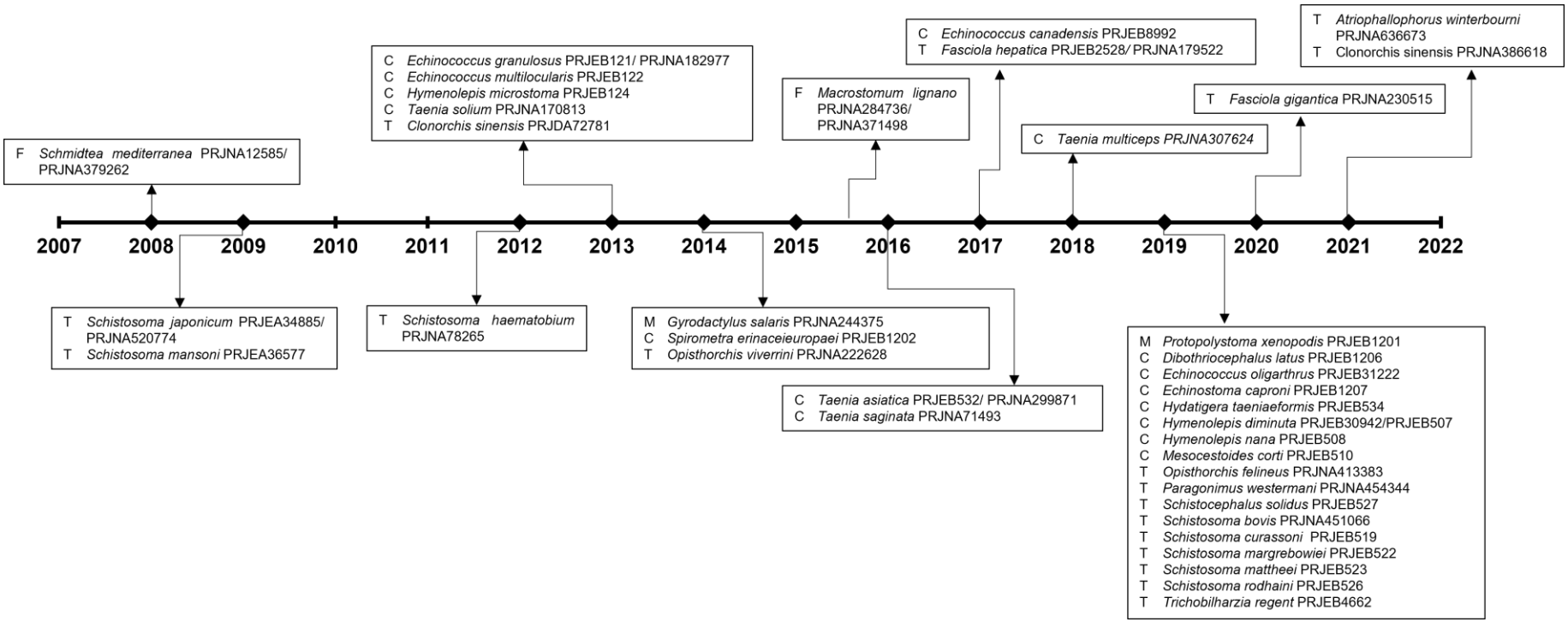

Figura 7. Línea del tiempo con los genomas de platelmintos de interés que se han caracterizado. F, Platelmintos de vida libre; M, Monogenea; C, Cestoda; T, Trematoda

III. Hipótesis

Se pueden identificar poblaciones de citones germinativos del cisticerco de *Taenia crassiceps* mediante el rastreo de la incorporación del análogo de timidina (EdU), la presencia del marcador DDX4/VASA, además de su caracterización mediante citometría de flujo, hasta lograr el aislamiento y cultivo *in vitro* de una línea de citones replicativos.

IV. Objetivos de la tesis

IV.1 Objetivo general

Avanzar en la identificación, aislamiento, caracterización y cultivo de los citones germinativos de cisticerco de *Taenia crassiceps*.

IV. 2 Objetivos específicos

a. Utilizar el marcador EdU para identificar la población celular replicativa (citones) en el cisticerco de *T. crassiceps*.
b. Realizar estudios de localización de la proteína DDX4/VASA en el tejido del cisticerco para determinar su utilidad como marcador de células germinales.
c. Aislar y cultivar la población celular replicativa (citones) en el tejido del cisticerco para establecer un método de cultivo apropiado.
d. Caracterizar mediante citometría de flujo las poblaciones de citones que existen en el tejido del cisticerco.
e. Determinar la ploidía y realizar la descripción del cariotipo de los citones replicativos de WFU y ORF en el tejido del cisticerco.

IV. Materiales y Métodos

V.1 Obtención de cisticercos y aislamiento de citones

Los cisticercos de las cepas WFU y ORF de *Taenia crassiceps*, se mantuvieron por pasaje intraperitoneal de ratones infectados a ratones no infectados. Normalmente se utilizan hembras de la cepa BALB/c de 4-6 semanas de edad. Se inyectaron intraperitonealmente 10 cisticercos por ratón y después de 90 días se sacrificaron para la recuperación de las larvas. Los cisticercos aislados se lavaron tres veces con PBS esterilizado para ser utilizados inmediatamente. Para el fraccionamiento del tejido y el aislamiento de los citones se utilizó un protocolo descrito anteriormente con algunas modificaciones [29, 61]. En breve, se fragmentan los cisticercos por tamizado a través de una organza y una coladera de té. Posteriormente se incuba la suspensión de tejido con una solución de maceración que contenía tripsina-EDTA 0.25% (Gibco) durante 30 minutos a 37 °C y el macerado se centrifugó a 4,000 rpm durante cinco minutos (Eppendorf, 5415C). Se retiró el sobrenadante y se resuspendió la pastilla con 500 µL de medio RPMI 1640 suplementado (Gibco), finalmente se realizó un conteo celular con cámara de Neubauer, antes de realizar citometría de flujo, inmunofluorescencia o cultivo.

V.2 Marcaje con EdU de células proliferativas en el cisticerco completo

Para el marcaje de células proliferativas en cisticercos WFU y ORF, se utilizó 5-etinil-2'-desoxiuridina (EdU) (Thermo Fisher Scientific) siguiendo un protocolo ya establecido anteriormente [48]. Se incubaron los cisticercos recién obtenidos del peritoneo de ratón con medio suplementado con EdU (25µM) por 5 horas a 37 °C, posteriormente se cambió por medio fresco y se dejó incubar por 5 horas más para terminar el marcaje de DNA.

V.3 Montaje completo de los cisticercos

Para mantener la morfología original de los cisticercos y observar la presencia de células proliferativas por microscopía de fluorescencia se utilizó un protocolo reportado anteriormente con algunas modificaciones [28, 29, 47]. Se fijaron los cisticercos incubados con EdU utilizando formaldehído al 4% en solución salina fisiológica pH 7.4 (PBS) durante una hora a temperatura ambiente con agitación moderada. Se colocaron los cisticercos en una placa de 48 pozos y se realizaron cinco lavados con PBS para eliminar el exceso de EdU. Para la permeabilización de los cisticercos se incubaron en acetona (≥99.9%, Sigma) por cinco minutos en agitación y se realizaron cinco lavados con PBS. Para la detección del EdU

se utilizó el kit Click-iT™ EdU Alexa 555 (Life Technologies) siguiendo las instrucciones del fabricante. Para la visualización de núcleos celulares se incubaron los cisticercos con DAPI (1µg/mL) durante 30 minutos y se realizaron cinco lavados con PBS. El montaje de los cisticercos se llevó a cabo en placas de 96 pozos, colocando un cisticerco por pozo con una solución de glicerol al 30% en PBS (Sigma).

V.4 Inmunofluorescencia en cisticercos completos y en cortes histológicos

La obtención de cortes histológicos se realizó mediante la inclusión de los cisticercos previamente fijados con formaldehído y congelados a -70 °C en Tissue-Tek (Sakura). Se obtuvieron cortes histológicos de 10 µm de grosor utilizando un criotomo (Tissue-Tek, modelo Cryo3 Plus). Los cortes obtenidos se montaron en laminillas SuperFrost y se permeabilizaron con TritónX-100 (0.25% Tritón-PBS) durante 30 minutos. En cambio, los cisticercos completos se permeabilizaron con acetona (≥99.9%) por 10 minutos; posteriormente se realizaron tres lavados con PBS y se incubaron con el anticuerpo α-VASA (policlonal de conejo, Abcam ab13840) a una dilución de 1:200, seguido por la incubación con un anticuerpo secundario acoplado a un fluorocromo Alexa 568 (policlonal de cabra, Thermo Fisher Scientific A-11011) a una dilución de 1:1000. Para observar los núcleos de las células se utilizó una tinción con DAPI (1µg/mL). Las muestras se visualizaron y fotografiaron utilizando un microscopio de epifluorescencia (Olympus, modelo IX71) y un microscopio confocal (Nikon, modelo AR1+ STORM).

V.5 Marcaje con CFDA-SE de la suspensión celular

Para la visualización de las poblaciones celulares de los cisticercos, se incubó la suspensión celular con medio RPMI 1640 adicionado con CFDA-SE (Thermo Fisher Scientific) siguiendo las instrucciones del fabricante, a una concentración de 5 y 10 µM durante 15 minutos a 37 °C. Posteriormente se realizaron tres lavados con PBS a 3,000 rpm durante cinco minutos y se prepararon para citometría de flujo.

V.6 Citometría de flujo

Para la visualización de las poblaciones celulares de los cisticercos de *T. crassiceps,* se marcaron con CFDA-SE, DAPI y DDX4/VASA. Se fijaron las células por 30 minutos con formaldehído (4% FA-PBS) y se realizaron tres lavados con PBS a 3,000 rpm por 5 minutos, se permeabilizaron con acetona durante 5 minutos y se lavaron tres veces con PBS por centrifugación a 3,000 rpm por 5 minutos. Las muestras se resuspendieron en 300 µL y se visualizaron utilizando el citómetro de flujo (Cytoflex S, Beckman Coulter).

V.7 Cultivo *in vitro* de las células germinativas

Las células obtenidas por el método de aislamiento con EDTA-Tripsina se mantuvieron en cultivo en placas de 12 pozos, en 2 mL de medio RPMI 1640 suplementado (Gibco) con 10% SFB a 37 °C y en una atmósfera de 5% CO_2. Se realizaron cambios de medio cada dos días. Nuestros intentos de conteo celular resultaron especialmente difíciles debido al pequeño tamaño de los cuerpos celulares.

V.8 Visualización de los cromosomas de WFU y ORF

Con el objeto de visualizar y realizar el conteo de los cromosomas de *T. crassiceps* durante su estado larvario, se adaptaron dos métodos que se habían descrito para planarias y otros céstodos [24, 36]. Se incubaron cisticercos en una solución de colchicina 0.25% (en medio RPMI 1640 suplementado con 1% de suero bovino fetal) durante 6 horas a 37° C. Posteriormente se realizó un lavado de 20 minutos con agua desionizada a temperatura ambiente y finalmente se fijaron con metanol:ácido acético 3:1 durante 30 minutos a 4°C. Una vez obtenidos los parásitos fijados, se colocaron en laminillas SuperFrost (Thermo Fisher Scientific) y se presionaron para disminuir su grosor utilizando un cubreobjetos. Después de montar los cisticercos, se dejaron incubar toda la noche a 4°C y se sumergieron en nitrógeno líquido. Posteriormente, se removió el cubreobjetos intentando no dañar el tejido. Finalmente se permeabilizó durante 5 minutos con PBS-Tritón X-100 (1%) y se tiñó con DAPI 1:500 por 20 minutos para montar los portaobjetos con la muestra en VectaShield (Sigma). Las muestras se visualizaron y fotografiaron en un microscopio de epifluorescencia (Olympus, modelo IX71) y en un microscopio confocal (Nikon, modelo AR1+ STORM).

V. Resultados

VI.1 Identificación de células proliferativas de *Taenia crassiceps*

Una característica de las células germinativas que permite su identificación en el tejido larvario es su alta tasa de replicación, por lo tanto, se decidió utilizar una tinción con EdU, que es un reactivo que permite marcar a todas aquellas células que estén incorporando nucleótidos para la síntesis de DNA necesaria en la duplicación celular. Se realizaron estos ensayos utilizando cisticercos de dos cepas de *T. crassiceps*: ORF y WFU. La primera es una cepa mutante que ha perdido la capacidad de formar el escólex y la segunda es una cepa a la que se podría considerar silvestre, ambas son capaces de reproducirse asexualmente mediante gemación. Sin embargo, la velocidad de proliferación es mayor en ORF que en

WFU; la cantidad de gemas en WFU es menor y más lento el proceso de gemación. Las micrografías obtenidas inicialmente por microscopía de epifluorescencia y confocal de la cepa ORF, demostraron un enriquecimiento de células proliferativas en el polo germinal de los cisticercos completos marcados con EdU, específicamente en los sitios donde se encuentran las gemas nacientes y en su parte más distal (Fig. 8). En contraste, en el tejido de la vesícula madre, la pared vesicular mostraba una tinción mucho menor de EdU.

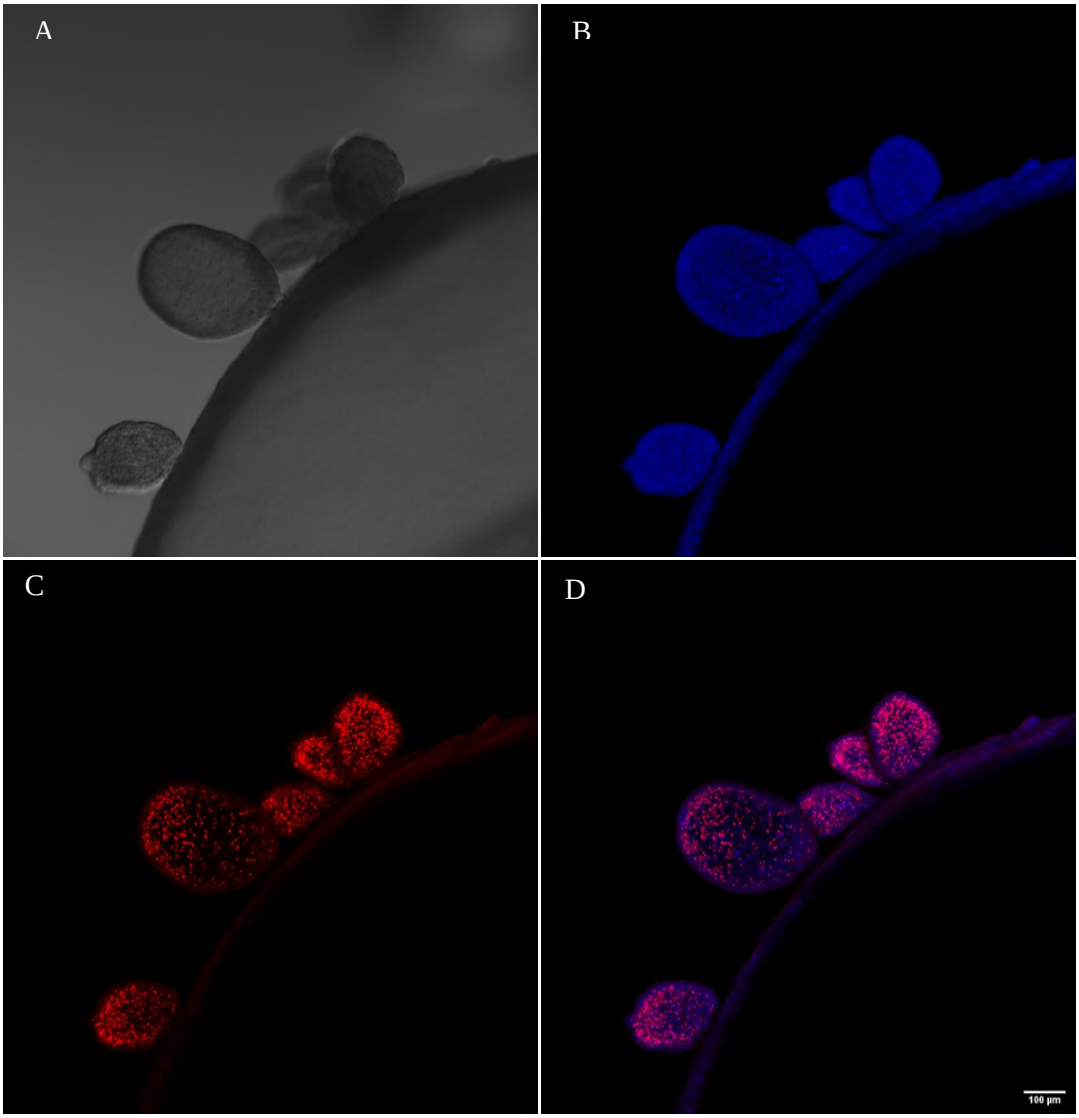

Figura 8. Localización por microscopía confocal de células proliferativas en la pared vesicular de una larva de la cepa ORF de *Taenia crassiceps*. A) Polo germinal mostrando gemas por microscopía confocal DIC; B) imagen equivalente con tinción de DAPI; C) imagen equivalente con tinción de EdU; D) Imagen sobrepuesta de las tinciones con EdU y DAPI. Las micrografías se obtuvieron con un microscopio confocal con los láseres C-FL DAPI (325-375 nm) y C-FL Red (530-560 nm).

En el cisticerco de la cepa WFU la tinción de las gemas con EdU y DAPI fue idéntica a la observada para ORF (teniendo en cuenta que WFU posee una menor cantidad de gemas), sin embargo, se observó también el marcaje con EdU en el escólex (Fig. 9), tanto en las ventosas como en el cono rostelar (Fig. 10). De manera similar a la cepa ORF, la pared vesicular mostró una tinción mucho más pobre del EdU.

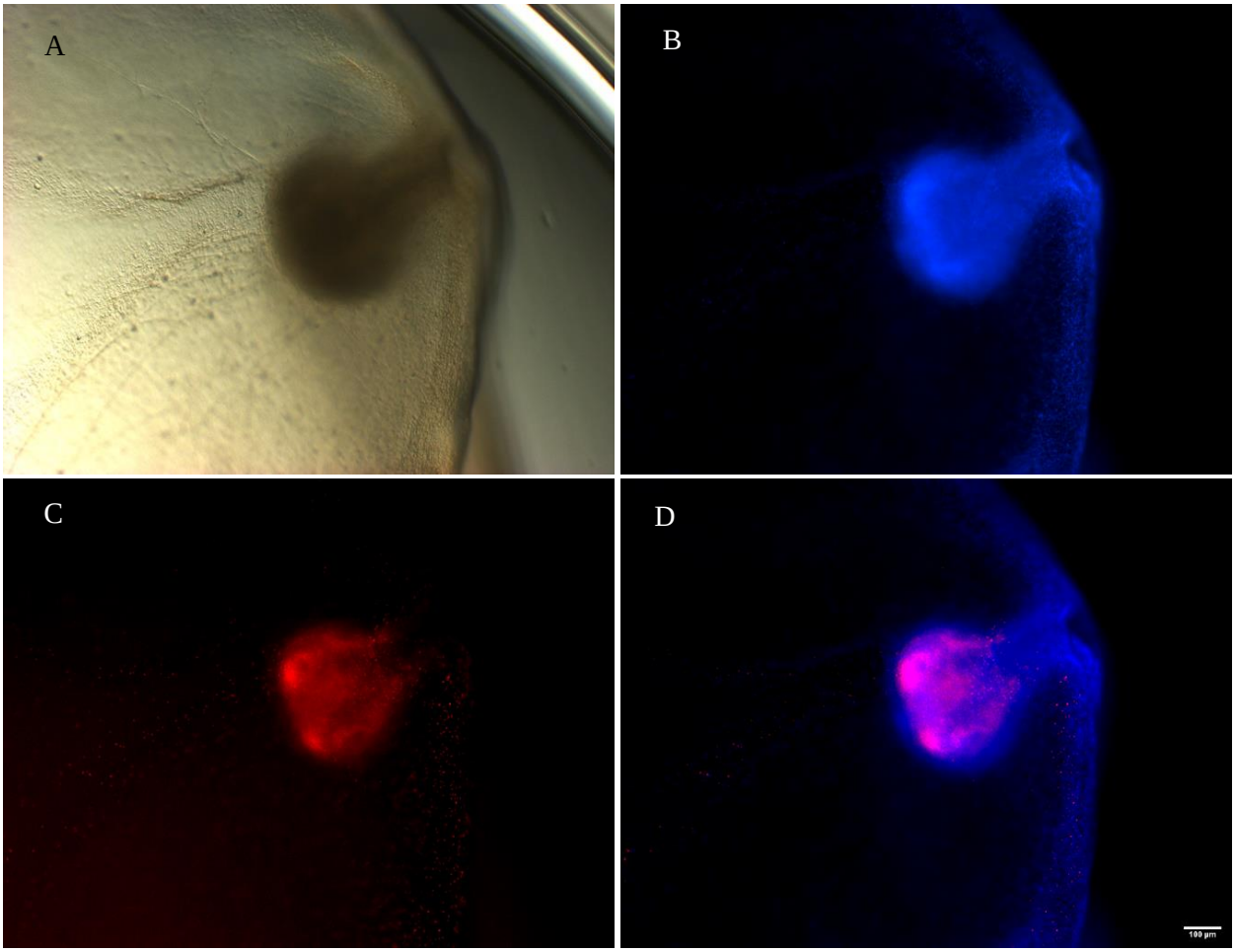

Figura 9. Escólex sin evaginar de cisticerco de la cepa WFU de *Taenia crassiceps*. A) Escólex observado por contraste de fases; B) DAPI; C) EdU; D) Imagen compuesta de EdU y DAPI. Las micrografías se obtuvieron con un microscopio invertido de epifluorescencia con los filtros para observar DAPI (358 nm) y Alexa (568 nm).

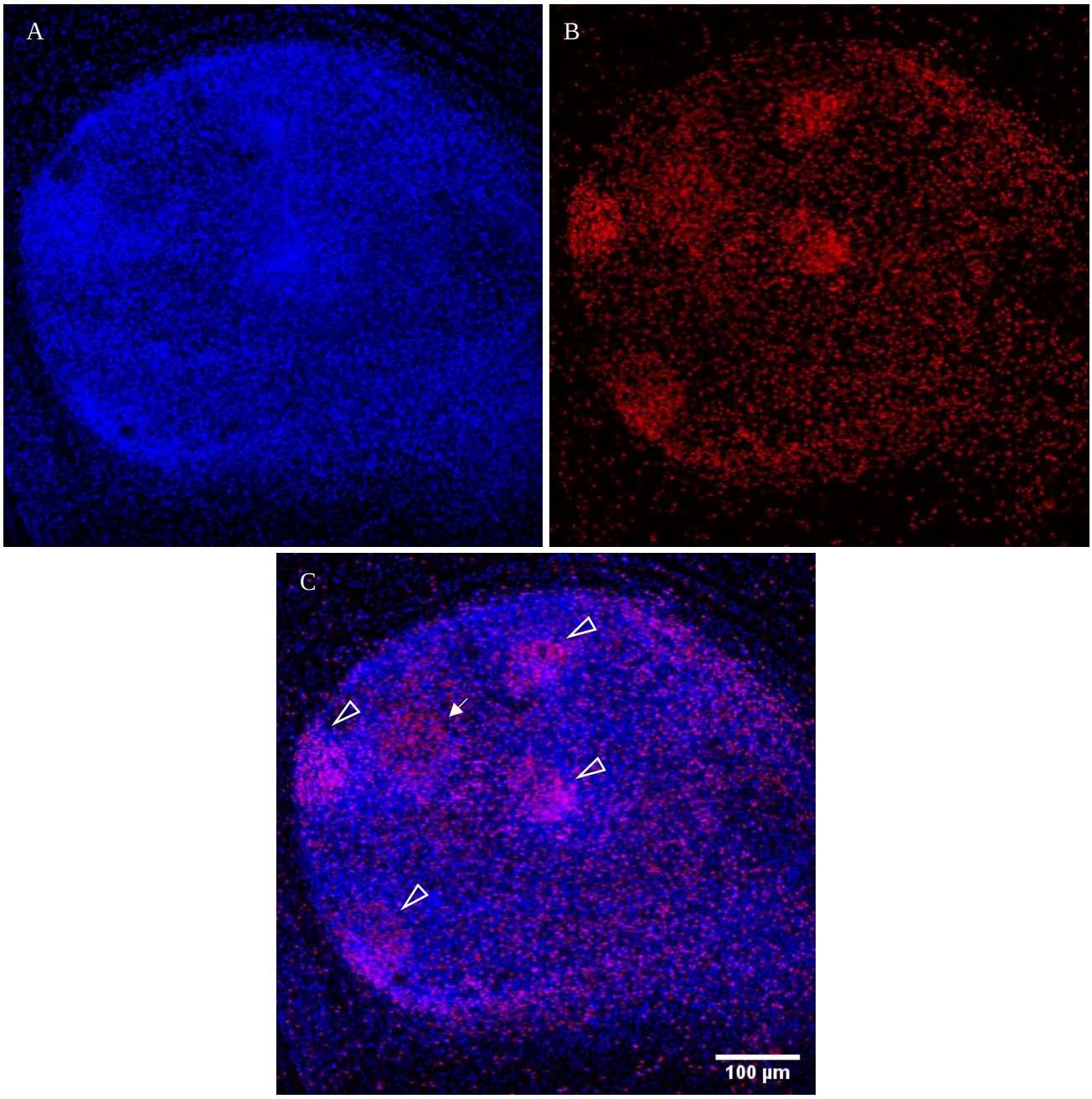

Figura 10. Escólex sin evaginar de cisticerco de la cepa WFU de *Taenia crassiceps*. A) DAPI B) EdU; C) Imagen compuesta de EdU y DAPI. Los triángulos indican la posición de las cuatro ventosas y la flecha muestra el sitio del cono rostelar del escólex del cisticerco. Las micrografías se obtuvieron con un microscopio confocal con los láseres C-FL DAPI (325-375 nm) y C-FL Red (530-560 nm).

VI.2 Localización de DDX4/VASA (PL10) por inmunofluorescencia en cortes histológicos y montaje completo de cisticerco de la cepa ORF de *Taenia crassiceps*

El marcador VASA que corresponde a una helicasa, ha sido ampliamente utilizado como marcador de células germinales en células de mamífero y de planaria [12, 50]. En platelmintos, VASA corresponde con una familia de proteínas denominadas DDX. En el caso de los céstodos esta familia se denomina PL10. Las inmunofluorescencias realizadas en cortes histológicos de cisticercos con el anticuerpo policlonal α-DDX4/VASA, mostraron que la proteína está presente en el músculo liso en la región subtegumental de la pared vesicular. Se pueden diferenciar las regiones de la pared vesicular: en la zona más apical se concentra la señal de DAPI (azul) y por debajo de la membrana basal se observa la red de músculo liso (rojo) (Fig. 11). Para comprobar los resultados de los cortes histológicos, se realizó un montaje completo del cisticerco y la morfología observada coincidió con las micrografías de los cortes histológicos, evidenciando la red de músculos lisos en la región subtegumental de la pared vesicular del cisticerco (Fig. 12).

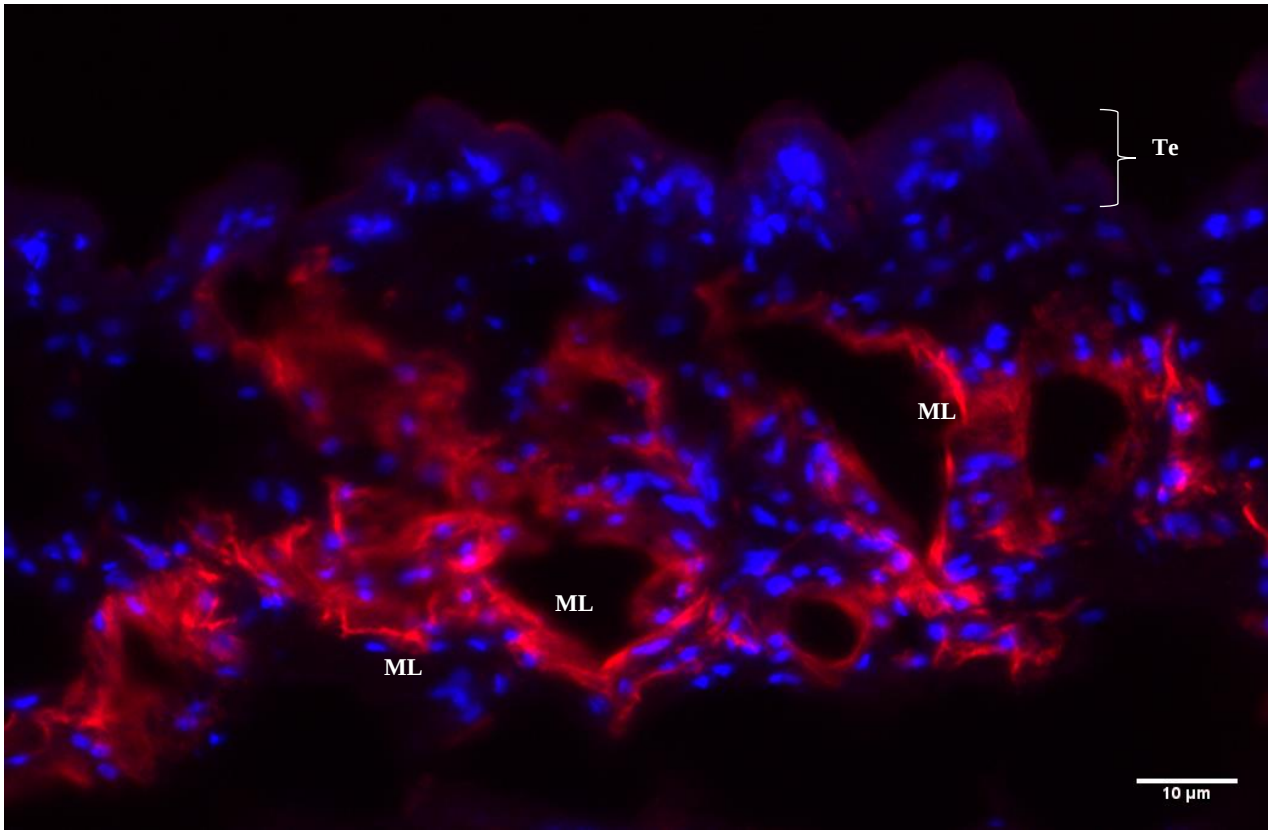

Figura 11. Corte histológico de la pared vesicular de un cisticerco de la cepa WFU de *Taenia crassiceps* marcada con DAPI (azul) y α-DDX4/VASA (rojo). Te, tegumento; ML, músculo liso. Las micrografías se obtuvieron con un microscopio invertido de epifluorescencia con los láseres para observar DAPI (358 nm) y Alexa (568 nm).

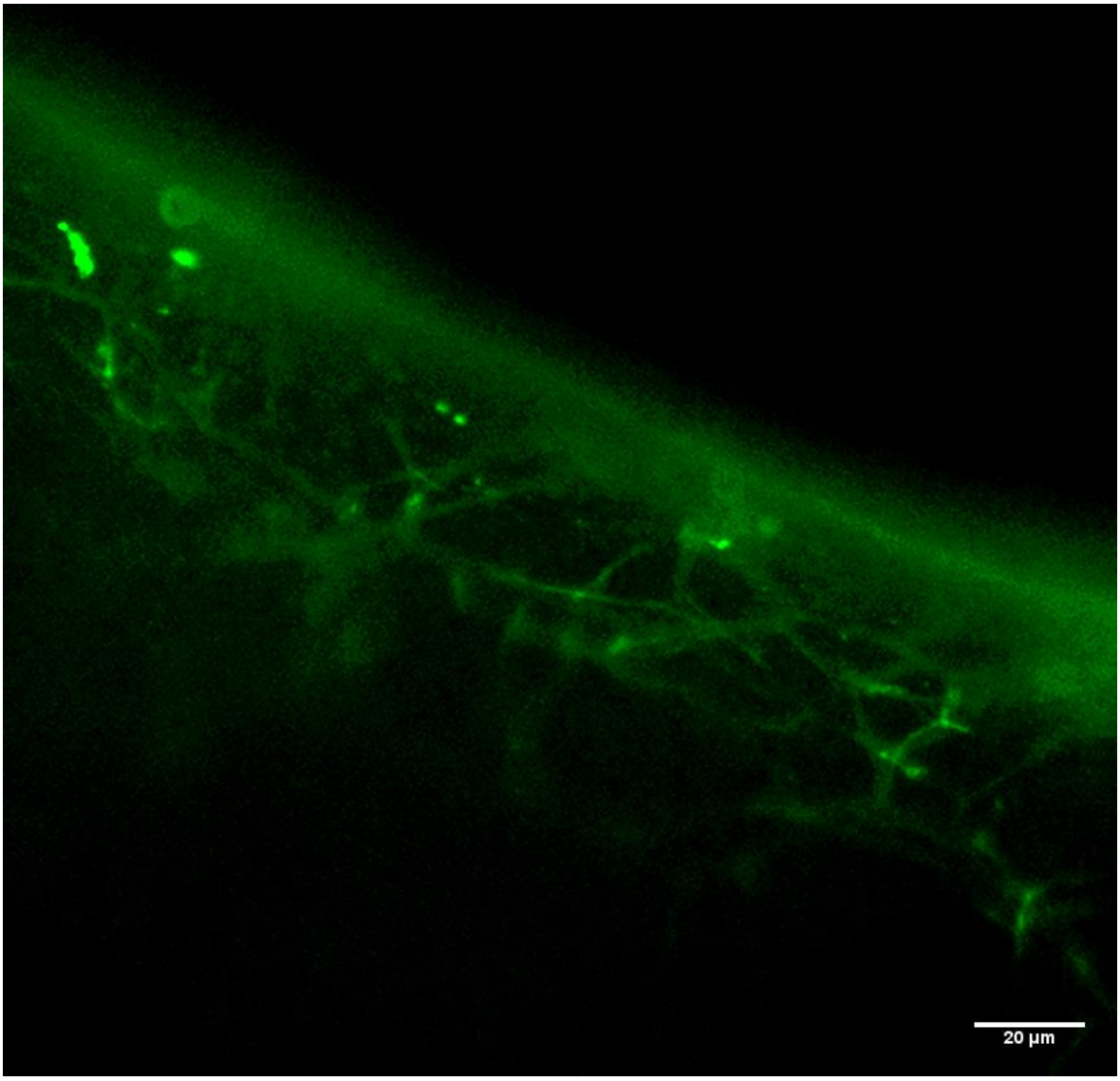

Figura 12. Inmunofluorescencia de la pared vesicular de un cisticerco WFU de *T. crassiceps* utilizando un suero policlonal α-DDX4/VASA. Se observa la red de músculo liso en la región subtegumental de la pared vesicular. Las micrografías se obtuvieron con un microscopio invertido de epifluorescencia con filtro para FITC (488 nm).

VI.3 Caracterización por citometría de la suspensión celular obtenida de los cisticercos de *Taenia crassiceps*

La utilización de marcadores generales también podría permitirnos la identificación de células germinativas presentes en el tejido del cisticerco, por ello se intentó el uso de CFDA-SE y DAPI para identificar células individuales por medio de citometría de flujo. El marcador celular CFDA-SE permite el marcaje de esterasas y de otras proteínas intracelulares. Los ensayos de marcaje con CFDA-SE utilizando dos concentraciones (5 y 10 µM) permitieron discernir la fracción celular de los cisticercos de la cepa ORF de *T. crassiceps* de otros fragmentos tisulares resultantes de la maceración del tejido. La citometría mostró una población de fragmentos que podrían corresponder con citones propiamente dichas, así como otros fragmentos que podrían corresponder con restos celulares (Fig. 13). Desafortunadamente no se logró realizar el ensayo equivalente con los cisticercos de la cepa WFU.

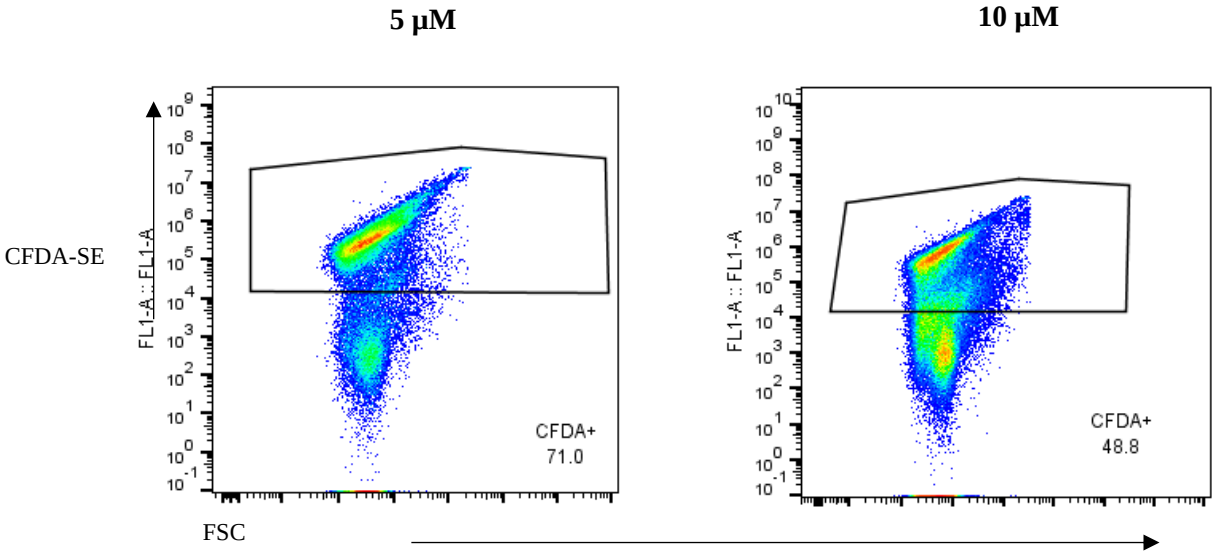

Figura 13. Células de cisticercos de la cepa ORF teñidas con dos concentraciones de CFDA-SE.

Se utilizó también la tinción por DAPI que permitió observar las distintas fases del ciclo celular en ambas cepas. En las figuras 15 y 16 se muestran los resultados correspondientes para ORF y WFU, respectivamente. Resultados preliminares mostraron que el 63 al 76% de la población muestreada se encontraba en fase G1, el 7 al 9% en fase S y el 15 al 19% en fase G2 en la cepa ORF. También se obtuvieron las poblaciones para la fase G1 (75-77.7%), S (5.09-8.24%) y G2 (13-14.5%) de la cepa WFU (Fig. 15). Sin embargo, la validación de estos porcentajes requiere análisis más exhaustivos.

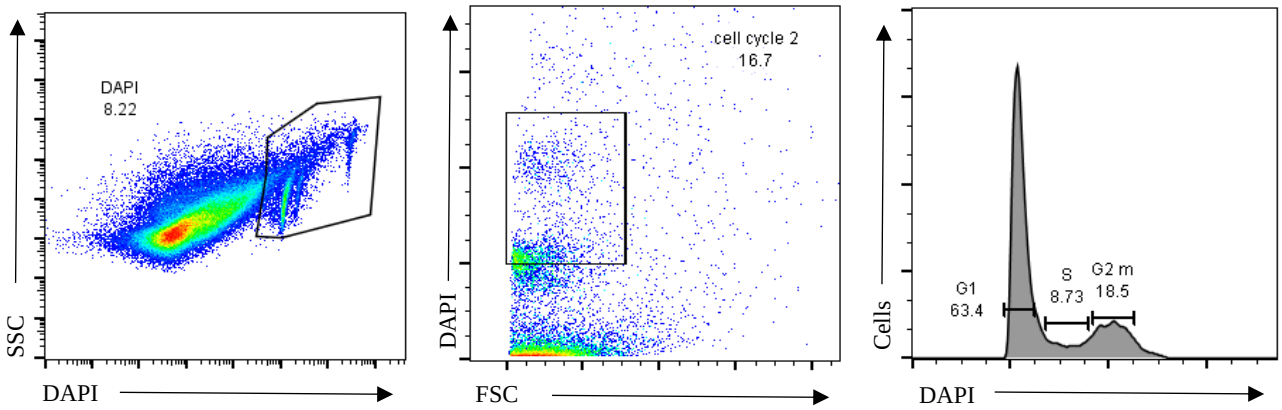

Figura 14. Células de cisticercos de la cepa ORF, DAPI+ en tres fases distintas del ciclo celular.

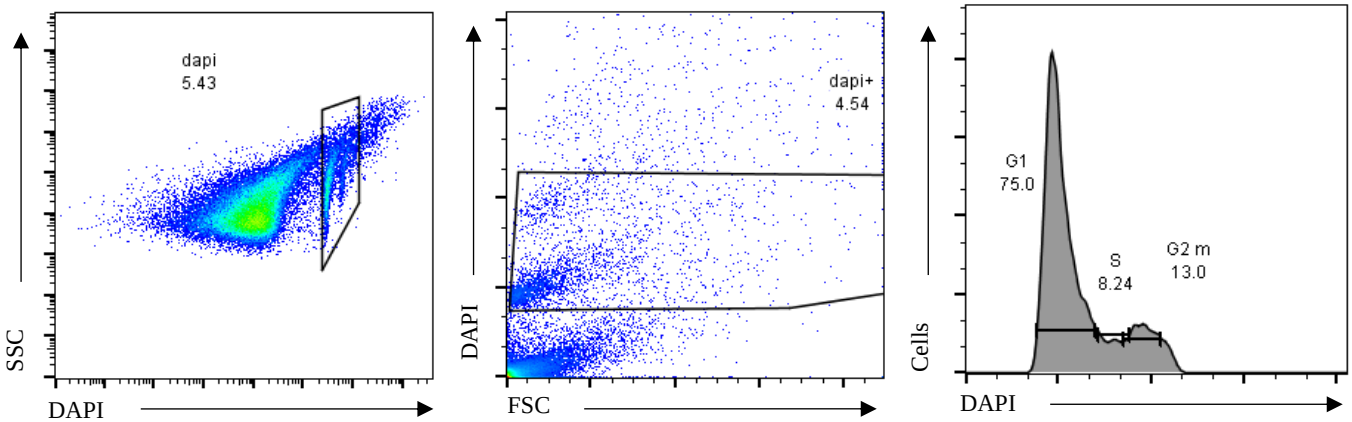

Figura 15. Células de cisticercos de la cepa WFU, DAPI+ en tres fases distintas del ciclo celular.

Finalmente, también se realizaron tinciones con un anticuerpo dirigido a DDX4/VASA de la suspensión celular obtenida a partir de la maceración de los cisticercos. La población celular positiva al anticuerpo se identificó y cuantificó, encontrándose que sólo una proporción pequeña del total de células aisladas (3.84%) en la cepa ORF podría corresponder a la presencia de citones positivos a DDX4/VASA. En la cepa WFU se encontró una población de citones DDX4/VASA+ de 3.66% (Fig. 16). En la figura 16 A y B se debe considerar que los citones positivos a DDX4/VASA sólo incluyen las indicadas dentro del rectángulo y marcadas con color rojo.

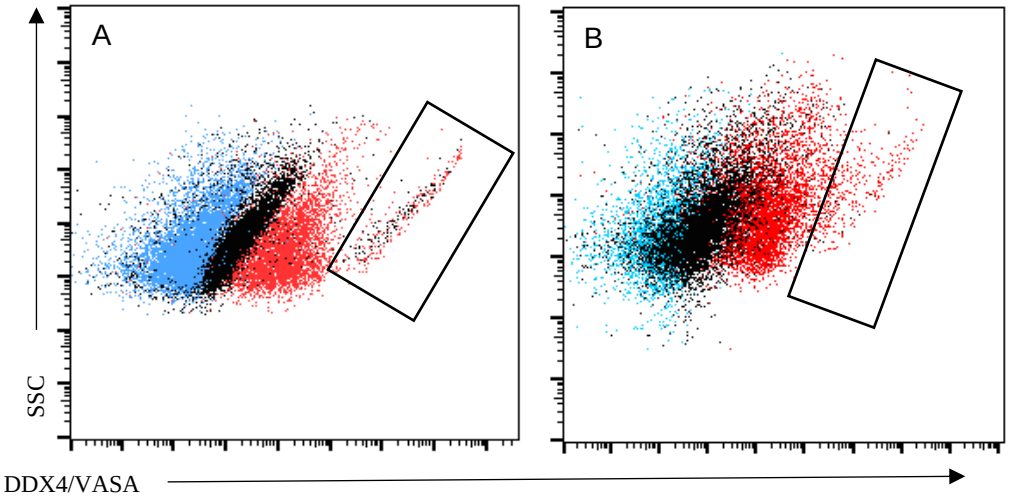

Figura 16. Citometría de flujo de la suspensión celular obtenida por aislamiento celular de los tejidos de los cisticercos WFU y ORF. A: ORF y B: WFU. Se muestran resultados de un experimento representativo. Azul: control sin teñir; Negro: anticuerpo secundario; Rojo: VASA+

En resumen, los resultados de citometría utilizando los marcadores CFDA-SE y DAPI, permitieron identificar citones individuales a partir de los cisticercos macerados. Este es un resultado de gran interés considerando que se trata de un tejido sincicial que resulta después del tratamiento que aplicamos en la producción de fragmentos de los citones. En particular la tinción con DAPI permitió la diferenciación de las diferentes etapas del ciclo celular. Es concebible que la depuración de esta técnica permita realizar la separación de citones individuales por FACS con base en marcadores de la línea germinal que se hayan utilizado en otros platelmintos o también con EdU. Es necesario señalar que para desarrollar una línea celular estable también es necesario el establecimiento de condiciones de cultivo óptimas, así como la obtención de una suspensión celular limpia. Una gran parte de nuestras fracciones celulares obtenidas está conformada por corpúsculos calcáreos, lo que podría limitar la obtención de una línea celular germinal.

VI.4 Cultivo de la suspensión celular obtenida de los cisticercos de *Taenia crassiceps*

El tratamiento de los tejidos de cisticerco con EDTA-Tripsina permitió el aislamiento y cultivo de citones viables por hasta 14 días. La suspensión celular obtenida estuvo compuesta por numerosos fragmentos celulares, corpúsculos calcáreos y una gran cantidad de otras estructuras que no es posible diferenciar por su morfología. La mayoría de los citones obtenidos eran muy pequeños (1-2 µm) y poseían un núcleo grande y muy poco citoplasma. Para la obtención de la fracción celular de los cisticercos de ambas cepas se llevó a cabo un proceso de centrifugación diferencial.

Inicialmente, la fracción se centrifugó a 2,000 rpm durante 5 minutos para sedimentar la mayor parte de los corpúsculos calcáreos (Fig. 17). Posteriormente se llevó a cabo una centrifugación a 4,000 rpm que permitió obtener una población heterogénea de fragmentos, citones y unos pocos corpúsculos calcáreos (Fig. 18 A). Posteriormente, esta fracción heterogénea fue cultivada *in vitro* por 14 días lográndose observar algunos agregados celulares (Fig. 18 B). En resumen, logramos establecer las condiciones para la disgregación y separación de citones de los cisticercos, sin embargo, no se logró mantener los cultivos por más tiempo debido a problemas de contaminación bacteriana. Asimismo, debido a las limitaciones sufridas durante el confinamiento por la pandemia, no fue posible llevar a cabo los experimentos con los cisticercos de la cepa WFU.

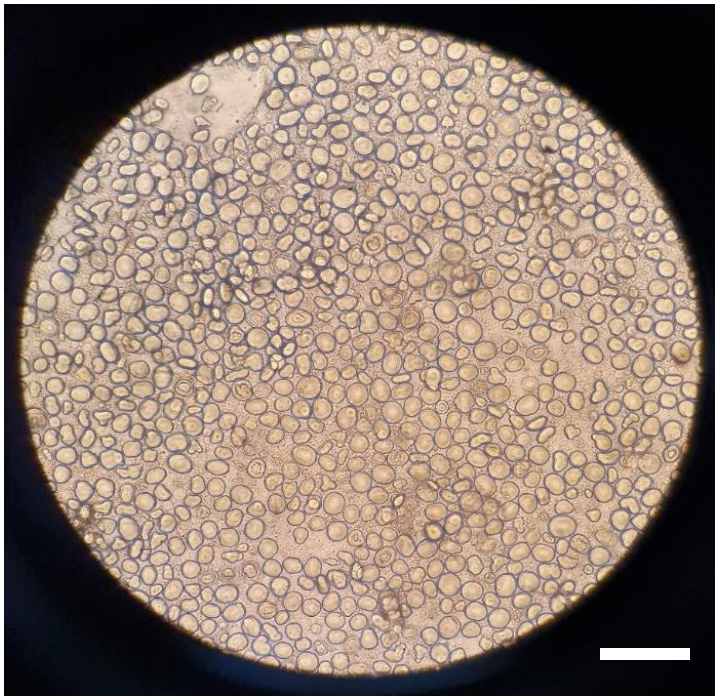

Figura 17. Corpúsculos calcáreos obtenidos por centrifugación del lisado del tejido de cisticerco de la cepa ORF a 2,000 rpm durante 5 minutos. Microscopía de campo claro, 40X. (Escala aproximada 5 um)

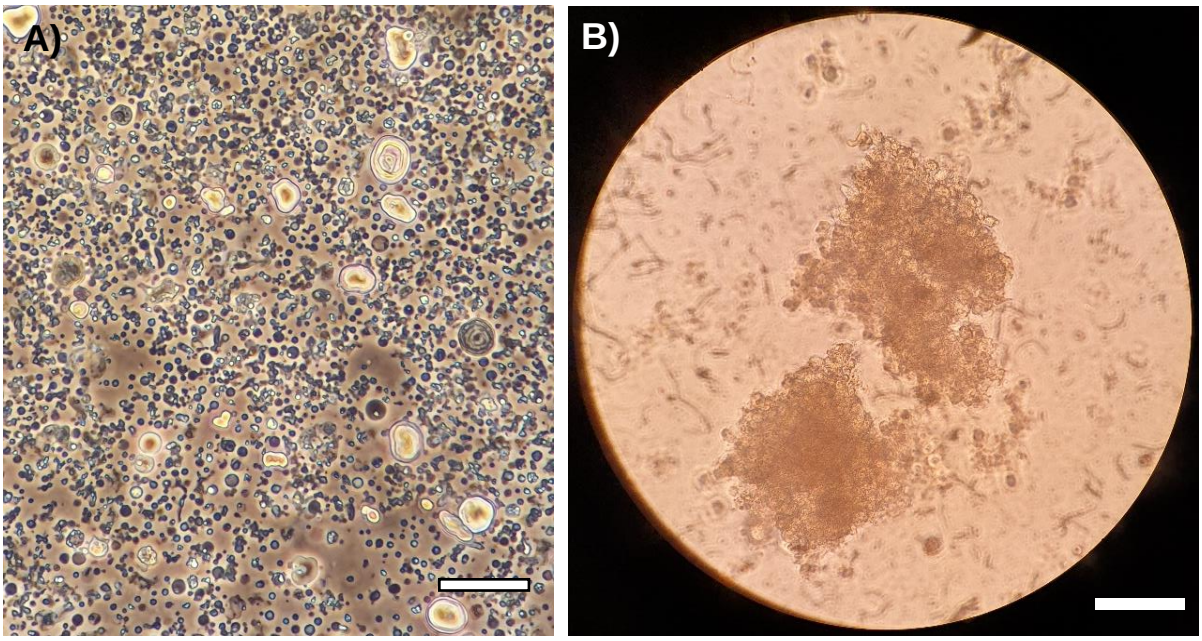

Figura 18. Fracción celular obtenida de los cisticercos de *Taenia crassiceps.* Después de la eliminación de la mayor parte de los corpúsculos calcáreos, se llevó a cabo una centrifugación a 4.000 rpm. A) Fracción heterogénea formada por citones, diversos fragmentos celulares y una pequeña cantidad de corpúsculos calcáreos; B) Agregados celulares después de 14 días en cultivo. Microscopía de campo claro, 40x (Escala aproximada 5 µm)

VI.5 Cariotipo de *Taenia crassiceps*

La información genómica de diferentes platelmintos parásitos ha sido publicada recientemente y ha permitido conocer más a fondo las adaptaciones genéticas para sobrevivir dentro de sus hospederos [14, 62]. Para complementar la información genómica que se ha obtenido de *T. crassiceps*, se realizó un registro fotográfico de los cromosomas de células mitóticas que probablemente formen parte del sistema de citones proliferativos en el cisticerco de las cepas ORF y WFU. El único registro previo discute que la diferencia entre ambas cepas radica en una aneuploidía. Específicamente, se ha propuesto una nulisomía del par cromosómico II en la cepa ORF con respecto a la cepa KBS (la cual también puede ser considerada silvestre). De un total de 602 micrografías se pudo realizar un conteo de los cromosomas. Se hallaron diferentes “juegos cromosómicos” en el tegumento de ambas cepas y se determinó su frecuencia. A pesar de la variabilidad del número cromosómico, la moda siempre fue de 16 cromosomas como se había reportado antes, sin embargo, se pudieron hallar casos de 17 y 18 cromosomas en ambas cepas los cuales están

representados por 2n=16, 2n+1=17 y 2n=18 (Figs. 19 y 20). En ninguna de las fotografías se observaron 14 cromosomas como se había descrito previamente.

Debido al tamaño de los cromosomas de *T. crassiceps* solamente se pudo realizar el conteo y no la descripción morfológica de los cromosomas ya que son de un tamaño menor al que permite obtener una buena resolución mediante microscopía óptica y confocal. Solamente se logró completar el apareamiento en una célula con 17 cromosomas, en la cual únicamente hace falta un integrante de uno de los pares (Fig. 21). No obstante, hacen falta experimentos para determinar si las observaciones realizadas por microscopia de epifluorescencia no son un artefacto debido a la manipulación del tejido y por la falta de resolución en las fotografías.

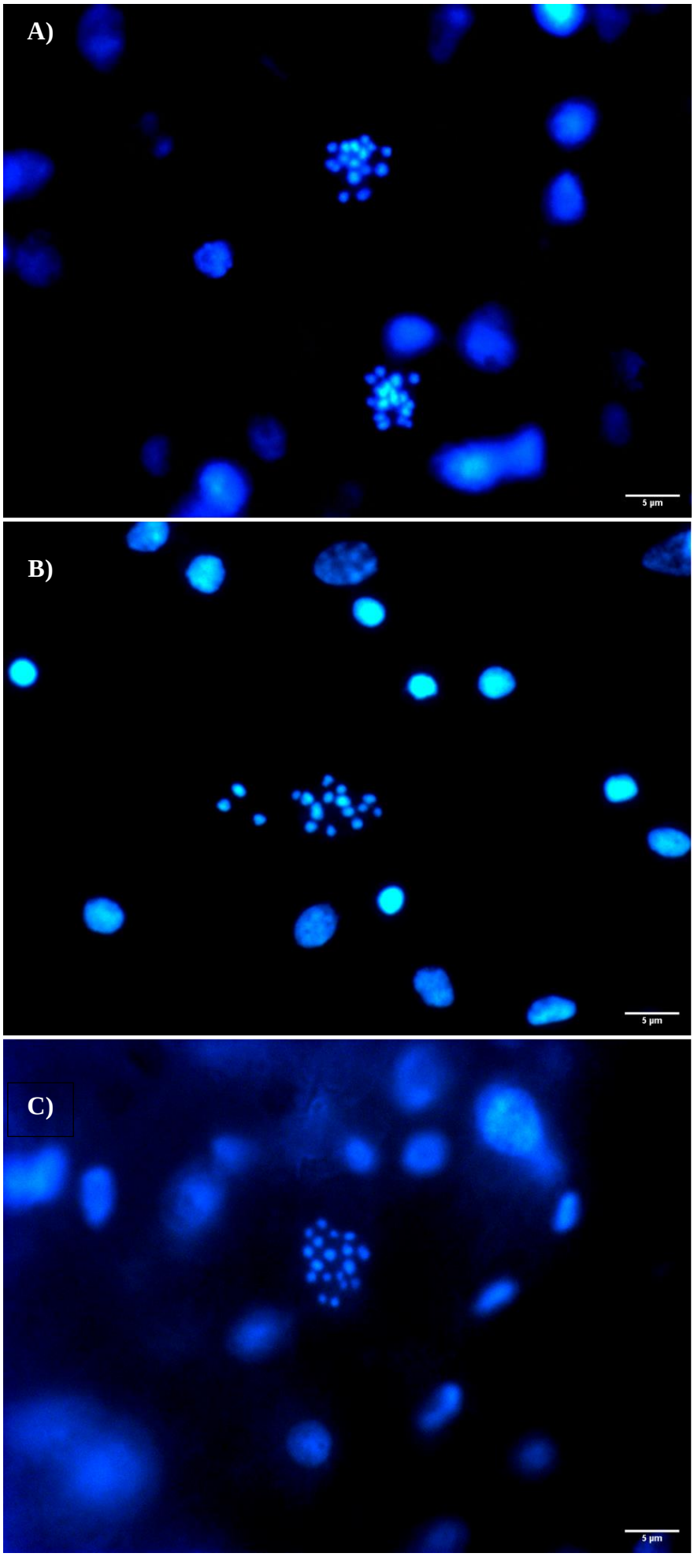

Figura 19. Micrografías representativas de los distintos números cromosómicos hallados en los cisticercos de la cepa ORF. Se pudieron observar tres juegos distintos de cromosomas en células mitóticas ubicadas en el tegumento. A) 2n=16, B) 2n+1=17 y C) 2n=18. Microscopía de epifluorescencia, 100x.

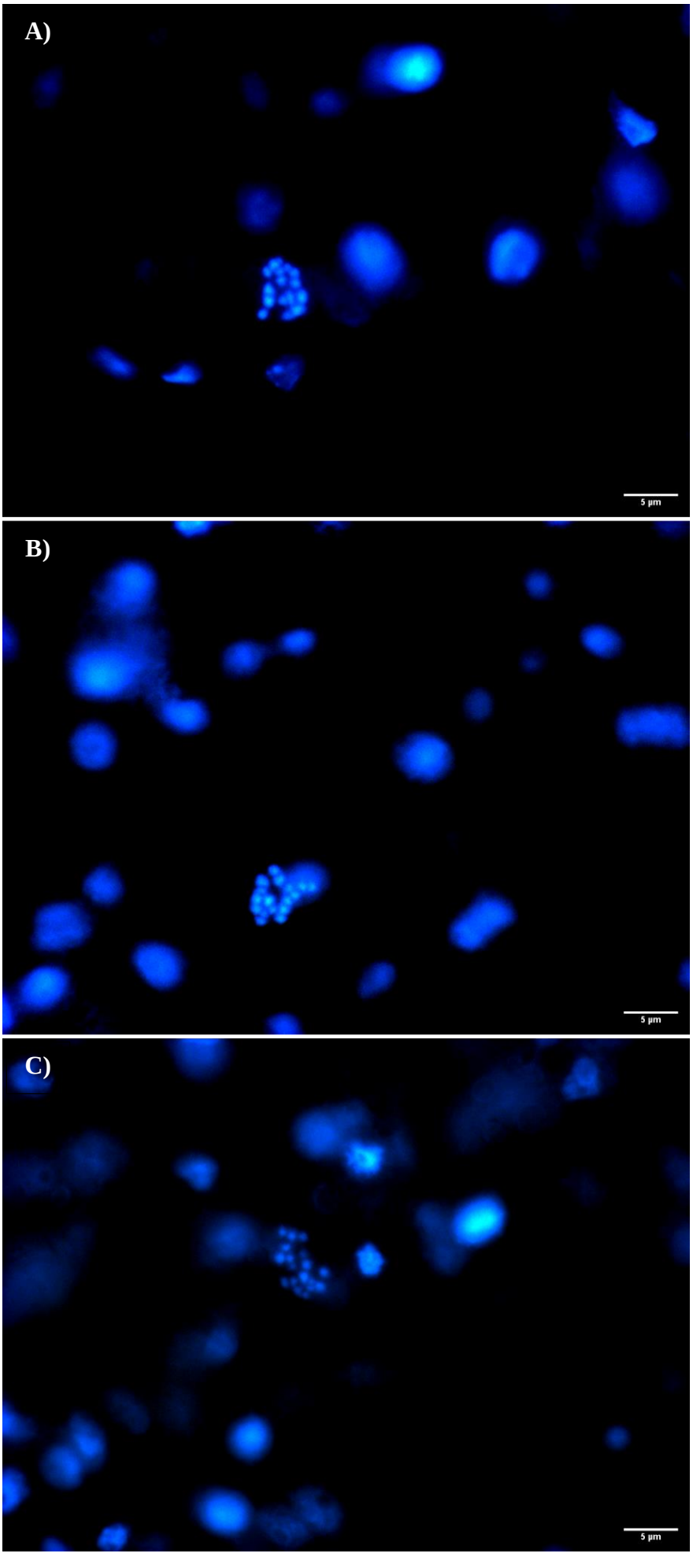

Figura 20. Micrografías representativas de los distintos números cromosómicos hallados en los cisticercos de la cepa WFU. Se pudieron observar tres juegos distintos de cromosomas en células mitóticas ubicadas en el tegumento. A) 2n=16, B) 2n+1=17 y C) 2n=18. Microscopía de epifluorescencia, 100x.

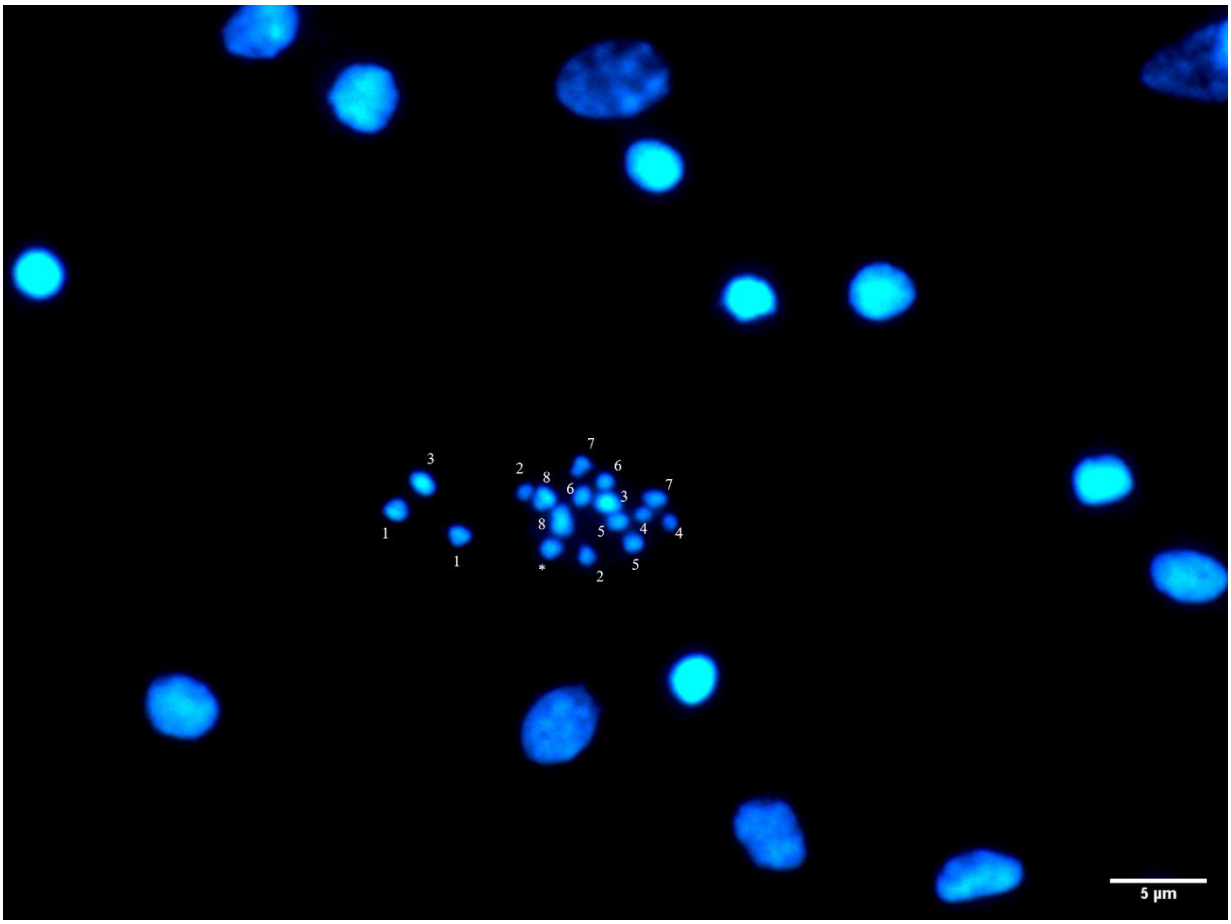

Figura 21. Cromosomas mitóticos apareados de *T. crassiceps*. Se muestran los distintos pares de cromosomas visualizados bajo microscopía de fluorescencia en el tegumento de un cisticerco de la cepa ORF. Se distingue claramente la falta de un par cromosómico resultando en una ploidía de 2n+1=17. Microscopia de epifluorescencia, 100x

VI. Discusión

Los platelmintos tienen una extraordinaria capacidad regenerativa debida a la abundante presencia de células troncales en sus tejidos. Desde hace varios siglos se conoce el ejemplo de las planarias que son capaces de regenerar porciones considerables del cuerpo y tejidos especializados [43]. En estos organismos, a las células troncales se les ha denominado células germinativas, que han sido caracterizadas principalmente en turbelários [3]. El interés por el estudio de la capacidad regenerativa de los platelmintos se ha extendido a la descripción de células multipotenciales en embriones, formas larvarias y en adultos, incluyendo algunos parásitos platelmintos, que han recibido considerable atención como

agentes causales de enfermedad [28, 29, 33, 37, 47, 65]. Se han utilizado como modelos experimentales para el estudio de la respuesta inmunológica, para el desarrollo de vacunas o tratamientos experimentales, entre otros temas. A pesar de que se había perdido el interés por el estudio de su biología básica, recientemente se ha retomado la experimentación en tremátodos, e incluso en céstodos para el aislamiento y descripción de las células germinativas o troncales [28, 29, 37, 47].

Las principales técnicas para el estudio de los sistemas de regeneración se basan en la eliminación de células replicativas por medio de irradiación, cultivo con hidroxiurea o silenciamiento de genes asociados al fenotipo germinal. Además, se han utilizado marcadores de replicación como análogos de nucleótidos (*v. gr.* BrdU, EdU), sondas para hibridación (FISH) o citometría de flujo y más recientemente por scRNA-seq. Esto ha resultado en el establecimiento de líneas celulares capaces de regenerar larvas completas e infecciosas en *Echinococcus granulosus* y en *Echinococcus multilocularis* [1, 2, 15, 22, 59]. En nuestro grupo de investigación se ha decidido obtener una línea celular de *T. crassiceps*, para la experimentación *in vitro*. Es por ello que se ha realizado una revisión exhaustiva de los antecedentes donde se reportan células replicativas en el cisticerco o en el adulto y también en *T. solium*, ya que poseen características fisiológicas similares entre ambas especies.

Los resultados de varios autores demuestran la presencia de células que incorporan los análogos de nucleótidos en la pared vesicular, en el cuello y en el escólex del cisticerco [37, 53, 65]. También se ha intentado realizar previamente la regeneración de un cisticerco completo de *T. crassiceps* mediante la inyección de agregados celulares en el peritoneo del ratón [61]. Estos antecedentes respaldan la idea de que *T. crassiceps* posee citones con capacidades del sistema germinal. Además de la incorporación de timidina tritiada, BrdU o EdU, se han propuesto marcadores de línea germinal como vasa, piwi o tudor los cuales se han empleado en otros platelmintos [40, 50, 56]. En *T. crassiceps* no existen reportes del empleo de marcadores de la línea germinal.

En el presente proyecto de tesis se diseñó un plan de trabajo para abordar tres preguntas principales acerca de la biología básica de *T. crassiceps*:

1.- ¿Dónde se encuentran las células replicativas en el tejido de cisticercos de las cepas WFU y ORF?

2.- ¿Se pueden utilizar EdU, DAPI y DDX4/VASA como marcadores de células proliferativas y de línea germinal?

3.- ¿Es posible desarrollar un procedimiento para el aislamiento y cultivo eficiente de células de la línea germinal?

La primera aproximación para demostrar la presencia y localización de células replicativas en el cisticerco de *T. crassiceps* consistió en la utilización de EdU. La incorporación de este análogo de timidina demostró que en el tejido del cisticerco existe una población de citones altamente replicativa (Figs. 8, 9, 10 y 11). La abundancia de la tinción con EdU en las gemas nacientes del cisticerco destacan la importancia las células replicativas en la reproducción asexual de la larva. Es probable que la localización de una población de células replicativas en esta región esté relacionada con la demanda biosintética del tejido para el desarrollo de una nueva larva. En la pared vesicular también se observó la incorporación de EdU, aunque en menor abundancia que en las gemas. La tinción en esta región puede ser debida a la presencia de una población de células progenitoras a partir de la cual se desarrollan varios tipos celulares, incluyendo los citones subtegumentales, que son abundantes en la pared vesicular. Este progenitor "multipotencial" podría estar involucrado en la reproducción asexual de la larva y también en el recambio constante de citones que conforman el tejido del cisticerco, como se ha descrito en otros platelmintos [4, 28, 29 y 47].

Estas primeras evidencias están respaldadas por los experimentos antes mencionados de incorporación de análogos radiactivos o de BrdU, que coinciden con la distribución del marcaje en el cuello, escólex y pared vesicular. En el caso de *E. multilocularis*, el cual es un céstodo filogenéticamente cercano con *T. crassiceps* y *T. solium,* se ha observado que las células que incorporan EdU están presentes en la capa germinal, a partir de la cual se desarrollan no solo las cápsulas hijas y los protoescólices, sino también los demás tipos celulares del quiste hidatídico [29].

Una vez confirmada la presencia y la localización de las células replicativas en el tejido del cisticerco, se procedió a utilizar vasa que es un marcador de línea germinal en planaria [50]. La proteína VASA es una helicasa de RNA que en el caso de los taénidos como *T. crassiceps* corresponde a una familia de genes conocida como pl10. En nuestro grupo se ha utilizado un anticuerpo dirigido a VASA de mamíferos que resultó en el reconocimiento de una proteína de aproximadamente 100 kDa, la cual se localizó en la musculatura de la zona subtegumental de la larva (Fig. 12 y 13). El análisis reciente de espectrometría de masas llevado a cabo purificando la banda reconocida por los anticuerpos anti-VASA, confirmó que la proteína de alrededor de ~100 kDa no corresponde a la familia pl10 sino a paramiosina, que es una proteína de 110 kDa asociada funcionalmente al complejo actina-miosina en el músculo de los invertebrados; cuya función permite el mantenimiento del tono muscular sin gasto energético [63]. Su reconocimiento por el anticuerpo parece ser un resultado espurio y podría deberse a su capacidad para unir C1q que a su vez se une a la porción Fc de las inmunoglobulinas [30]. Por lo tanto, se debe descartar el uso de anticuerpos anti-DDX4/VASA para la identificación de células de línea germinal en cisticercos de *T. crassiceps*.

También se realizaron intentos para identificar poblaciones celulares en el tejido del cisticerco a través de citometría de flujo, haciendo uso de los marcadores fluorescentes CFDA-SE y DAPI. El primero permite un marcaje intracelular mediante su unión a residuos amino de diversas proteínas, mientras que el segundo permite la visualización de DNA. El marcaje con CFDA-SE resultó en la separación parcial de poblaciones celulares heterogéneas del cisticerco (Fig. 14), sin permitir la separación de poblaciones específicas. Al respecto, se debe considerar que el tejido de la larva es un sincicio y por lo tanto este marcador puede incluir restos de tejido con tamaños similares a los citones. Es por ello que la utilidad de CFDA-SE es limitada y representa una opción poco eficiente para la separación de citones individuales. En contraste, el DAPI permitió la visualización de citones individuales en las tres fases del ciclo celular: G1, S, G2/M (Figs. 15 y 16). A pesar de que el DAPI permitió mejorar la separación de las poblaciones celulares, también se observó una gran cantidad de restos celulares o de fragmentos de tejido. Para futuros experimentos de citometría de flujo se requiere adaptar una metodología adicional que permita "limpiar" la suspensión celular de escombros y de esta manera enriquecer el número de citones totales. Como estrategia adicional para observar las poblaciones germinales del cisticerco, se había utilizado el marcaje con el anticuerpo contra DDX4/VASA, dando como resultado una fracción poco numerosa de eventos positivos a este marcador (Fig. 17). Esto probablemente se deba a que el anticuerpo reconoce la musculatura del cisticerco, como se demostró antes (Figs. 12 y 13).

Después de haber estudiado las poblaciones de células replicativas mediante el marcaje con EdU, DDX4/VASA, CFDA-SE y DAPI, se intentó realizar cultivos celulares a partir de los macerados de cisticercos. Las suspensiones celulares obtenidas permitieron el mantenimiento del cultivo hasta por 14 días. Este resultado es alentador ya que sugiere que las condiciones de cultivo empleadas son razonablemente adecuadas. Los agregados celulares resultantes no se mantuvieron durante más tiempo por problemas de contaminación, sin embargo, fueron muy parecidos a los obtenidos previamente [61]. Estos agregados probablemente son una mezcla de citones y de fragmentos tisulares resultantes de la maceración del tejido. Asimismo, se obtuvo una gran proporción de corpúsculos calcáreos en la suspensión celular, por lo que la pureza de los citones que se obtuvieron no fue óptima. Se necesitará eliminar del macerado obtenido a los corpúsculos calcáreos en experimentos futuros, que van más allá del alcance de esta tesis de licenciatura para implementar un método de selección más eficiente de las células proliferativas del cisticerco. Cabe mencionar que el desarrollo de este proyecto de tesis está planeado como una etapa inicial de mi formación como investigador que será continuado durante mis estudios de posgrado.

Como parte de mi estancia en este grupo para realizar la tesis de licenciatura tuve también la oportunidad de participar en el equipo que elucidó el genoma de las cepas WFU y ORF de *T. crassiceps*. Ambas cepas han sido ampliamente utilizadas como sistemas modelo para el estudio de una diversidad de aspectos de la cisticercosis que se describieron en la introducción. En particular, se ha debatido la idea de que la cepa ORF perdió la capacidad de formar el escólex debido a un evento genómico catastrófico; se ha propuesto que esta cepa perdió el par II cromosómico, resultando en una variante aneuploide. Sin embargo, durante el desarrollo del proyecto de caracterización genómica quedó claro que las diferencias entre ambas cepas son mínimas, lo que indica que la cepa ORF no perdió un par cromosómico. Para confirmar este hallazgo se decidió llevar a cabo la determinación del cariotipo de WFU y ORF. Por consiguiente, en la presente tesis se describe también la metodología y los resultados de la caracterización de los cariotipos.

La incubación de las larvas con colchicina nos permitió observar figuras mitóticas en el tejido. Las micrografías obtenidas representan pruebas de la presencia de células mitóticamente activas que pueden formar parte del sistema germinal en el cisticerco (Figs. 20 y 21). También se contabilizaron los cromosomas encontrados en cada una de las cepas por la técnica de dispersión de cromosomas (chromosome spreading) en el contexto del tejido completo (Tabla 2). Se encontraron en ambas cepas células con 16, 17 y 18 cromosomas, representados por las ploidías 2n o 2n+1, en ambas cepas (ORF y WFU). Una posible explicación de este hallazgo es que el número cromosómico de *T. crassiceps* sea variable, como se ha reportado en distintos platelmintos parásitos [58], específicamente en céstodos. Otra hipótesis es que *T. crassiceps* posea cromosomas B, los cuales son fragmentos que se han separado de las cromátides originales con algunos genes [57]. Los cromosomas B pueden estar presentes con una frecuencia de entre 1 a 10 fragmentos extra y por lo tanto afectan la ploidía observada del organismo cuando se realiza el conteo por microscopía. Cualquiera de las dos hipótesis están sujetas a comprobación. Sin embargo, para los objetivos de los proyectos genómicos, lo que vale la pena resaltar es que no se observaron diferencias en los cariotipos de ambas cepas. Cabe destacar, que a pesar de que se han publicado diferentes reportes sobre el cariotipo de una misma especie de céstodo, no siempre coinciden las ploidías observadas. Hasta el momento no hay más publicaciones que indaguen en este fenómeno acerca de la variabilidad de los cariotipos en platelmintos parásitos, específicamente en céstodos. Las micrografías obtenidas de las células replicativas marcadas con EdU en el tejido del cisticerco de *T. crassiceps* sugieren la existencia de una población o poblaciones de citones involucradas en el constante recambio celular del tejido. Por ello, la búsqueda de marcadores de la línea germinal, como se planteó originalmente, se mantiene como un objetivo válido, que pretendo abordar durante mi proyecto de posgrado.

En resumen, los resultados aquí descritos tienen una gran similitud con otros obtenidos previamente en *T. crassiceps* mediante la incorporación de BrdU, que demostraron una incorporación similar a los ensayos realizados con EdU en el tejido larvario. Esto permitió describir a detalle la localización de esta población replicativa en las gemas nacientes y en las ventosas del escólex, así como en otros organismos, incluyendo la larva de *E. multilocularis* que tiene tipos celulares similares también identificados mediante incorporación de EdU o mediante la depleción de esta población celular por métodos químicos (hidroxiurea). Asimismo, nuestros resultados son similares a los descritos para las formas adultas de *T. solium, H. diminuta* y *M. corti.* Además, como se detalló arriba, se descarta el uso de anticuerpos específicos para el marcador vasa de mamíferos. Finalmente, los resultados de la caracterización cariotípica demostraron que no hay diferencias en el número cromosómico entre las cepas WFU y ORF; similarmente a lo observado en otros organismos céstodos.

VII. Conclusiones

- Se logró identificar citones replicativos mediante la incorporación de EdU en las larvas pertenecientes a las cepas WFU y ORF de *T. crassiceps* y se describieron sus diferencias con respecto al órgano de sujeción y el polo de gemación.

- Se determinó la localización de las células positivas a DDX4/VASA en cortes histológicos y en la larva completa, determinando que el marcaje ocurre en la musculatura del cisticerco. Estos hallazgos descartan la utilidad de esta proteína como marcador de células germinativas.

- Se visualizaron las poblaciones celulares del cisticerco mediante citometría de flujo, utilizando marcadores como CFDA-SE y DAPI, que permitió identificar citones en diferentes fases del ciclo celular (G1, S y G2/M).

- Se aislaron y se mantuvieron *in vitro* los citones aislados del tejido del cisticerco de *T. crassiceps* durante 14 días y se logró la formación de agregados.

- Finalmente se visualizaron los cromosomas de *T. crassiceps*, tanto en la cepa silvestre (WFU) y en la cepa mutante (ORF) y se determinó la frecuencia de los distintos juegos cromosómicos encontrados en las distintas células replicativas que se localizan en el tegumento del cisticerco.

Estos hallazgos son de utilidad para futuros esfuerzos de establecer una línea de células germinativas del cisticerco de *Taenia crassiceps*.

VIII. Bibliografía

1. Albani, C. M., Cumino, A. C., Elissondo, M. C.,y y Denegri, G. M. (2013). *Development of a cell line from Echinococcus granulosus germinal layer*. Acta Tropica, 128(1), 124–129.
2. Albani, C. M., Elissondo, M. C., Cumino, A. C., Chisari, A. y Denegri, G. M. (2010). *Primary cell culture of Echinococcus granulosus developed from the cystic germinal layer: Biological and functional characterization*. International Journal for Parasitology, 40(11), 1269–1275.
3. Baguñà J. (2012). *The planarian neoblast: the rambling history of its origin and some current black boxes*. The International journal of developmental biology, 56(1-3), 19–37.
4. Baguñá, J., Saló, E. y Auladell, C. (2005*). Regeneration and pattern formation in planarians III. Evidence that neoblasts are totipotent stem cells and the source of blastema cells.* Development 107, 77-86
5. Baron P. J. (1968). *On the histology and ultrastructure of Cysticercus longicollis, the cysticercus of Taenia crassiceps Zeder, 1800, (Cestoda, Cyclophyllidea)*. Parasitology, 58(3), 497–513.
6. Berriman, M., Haas, B., LoVerde, P. *et al.* The genome of the blood fluke *Schistosoma mansoni*. *Nature* **460,** 352–358 (2009).
7. Bobes, R. J., Fragoso, G., Fleury, A., García-Varela, M., Sciutto, E., Larralde, C., & Laclette, J. P. (2014). *Evolution, molecular epidemiology and perspectives on the research of taeniid parasites with special emphasis on Taenia solium.* Infection, genetics and evolution: journal of molecular epidemiology and evolutionary genetics in infectious diseases, 23, 150–160.
8. Brusca, R. C., & Brusca, G. J. (1990). *Invertebrates*. Sinauer Associates.
9. Caira, J. N. (2013) *Worms, Platyhelminthes. Encyclopedia of Biodiversity* 437–469.
10. Caira, J. N. and K. Jensen (eds.). 2017. *Planetary Biodiversity Inventory (2008–2017): Tapeworms from Vertebrate Bowels of the Earth.* University of Kansas, Natural History Museum, Special Publication No. 25, Lawrence, KS, USA, 463 pp.
11. Campos, A., Cummings, M. P., Reyes, J. L., & Laclette, J. P. (1998). *Phylogenetic relationships of platyhelminthes based on 18S ribosomal gene sequences.* Molecular phylogenetics and evolution, 10(1), 1–10.
12. Castrillon, D. H., Quade, B. J., Wang, T. Y., Quigley, C., & Crum, C. P. (2000). *The human VASA gene is specifically expressed in the germ cell*

lineage. Proceedings of the National Academy of Sciences of the United States of America, 97(17), 9585–9590.

13. Cohen, K.M., Finney, S.C., Gibbard, P.L. & Fan, J.-X. (2013; updated) The ICS International Chronostratigraphic Chart. Episodes 36: 199-204.

14. Diana G. Ríos-Valencia, José Navarrete-Perea, Arturo Calderón-Gallegos, Jeannette Flores-Bautista and Juan Pedro Laclette (2021). *To Be or Not to Be a Tapeworm Parasite: That Is the Post-Genomic Question* in *Taenia solium Cysticercosis, Current State of the Art in Cysticercosis and Neurocysticercosis*, Jorge Morales-Montor, Abraham Landa and Luis Ignacio Terrazas, IntechOpen,

15. Echeverría, C. I., Isolabella, D. M., Gonzalez, E. A. P., Leonardelli, A., Prada, L., Perrone, A. y Fuchs, A. G. (2010). *Morphological and biological characterization of cell line developed from bovine Echinococcus granulosus.* In Vitro Cellular & Developmental Biology - Animal, 46(9), 781–792.

16. Evans, Scott D.; Hughes, Ian V.; Gehling, James G.; Droser, Mary L. (2020). *Discovery of the oldest bilaterian from the Ediacaran of South Australia.* Proceedings of the National Academy of Sciences, (), 202001045.

17. Fatima Mujib Bilqees and Reino S. Freeman. *Histogenesis of the rostellum of Taenia crassiceps (Zeder, 1800) (Cestoda), with special reference to hook development.* Canadian Journal of Zoology. 47(2): 251-261.

18. Flisser, A., Willms, K., Laclette, J.P., Larralde, C., Ridaura, C. y Beltran, F. (1982). *Cysticercosis: present state of knowledge and perspectives*. Academic Press, Guanajuato, México, 700 p.

19. Flores-Bautista, J. (2019). *Degradación y aprovechamiento de las proteínas del huésped internalizadas por cisticercos de Taenia solium y Taenia crassiceps*. Tesis de doctorado. Universidad Nacional Autónoma de México.

20. Francis J. D. y Gerald W. E. (1969). *Growth rate of two Taenia crassiceps strains.* Experimental Parasitology *25, 0–398.*

21. Freeman, R. S. (1962). *Studies on the Biology of Taenia crassiceps (Zeder, 1800) Rudolphi, 1810 (Cestoda).* Canadian Journal of Zoology, 40(6), 969–990.

22. Furuya, K. (1991*). An established cell line of larval Echinococcus multilocularis*. International Journal for Parasitology, 21(2), 233–240.

23. Gilbert, S. F. (2000). *Developmental biology*. Sunderland, Mass: Sinauer Associates.

24. Guo, L., Accorsi, A., He, S. *et al.* (2018) *An adaptable chromosome preparation methodology for use in invertebrate research organisms*. BMC Biol 16, 25.

25. Jones, A. W., & Wyant, K. D. (1957). *The chromosomes of Taeniarhynchus saginatus (=Taenia saginata)* Goeze, 1782. *The Journal of parasitology*, 43(1), 115–116.

26. Kevin L. Howe, Bruce J. Bolt, Myriam Shafie, Paul Kersey, and Matthew Berriman. *WormBase ParaSite − a comprehensive resource for helminth genomics. Molecular and Biochemical Parasitology* 2017 215 2-10
27. Kier, W. M. (2012). *The diversity of hydrostatic skeletons. Journal of Experimental Biology, 215(8), 1247–1257.*
28. Koziol, U., Domínguez, M. F., Marín, M., Kun, A. y Castillo, E. (2010). *Stem cell proliferation during in vitro development of the model cestode Mesocestoides corti from larva to adult worm*. Frontiers in Zoology, 7(1), 22.
29. Koziol, U., Rauschendorfer, T., Zanon Rodríguez, L., Krohne, G. y Brehm, K. (2014). *The unique stem cell system of the immortal larva of the human parasite Echinococcus multilocularis*. EvoDevo, 5(1), 10.
30. Laclette, J. P., Shoemaker, C. B., Richter, D., Arcos, L., Pante, N., Cohen, C., Bing, D., y Nicholson-Weller, A. (1992). *Paramyosin inhibits complement C1*. *Journal of immunology (Baltimore, Md.: 1950)*, *148*(1), 124–128.
31. Larralde C., De Aluja A.S. *Cisticercosis. Guía para profesionales de la salud.* México, DF: FCE.
32. Lucius, R., Loos-Frank, B., Lane, R. P., Poulin, R., Roberts, C., Grencis, R. K., Shankland, R. FitzRoy, R. (2017). *The Biology of Parasites*. John Wiley & Sons
33. Mead R. W. (1982). *Changes in germinative cell frequencies in the germinative region of Hymenolepis diminuta during development.* The Journal of parasitology, 68(1), 95–99.
34. Moguel, B., Moreno-Mendoza, N., Bobes, R. J., Carrero, J. C., Chimal-Monroy, J., Díaz-Hernández, M. E., Herrera-Estrella, L., y Laclette, J. P. (2015). *Transient transgenesis of the tapeworm Taenia crassiceps.* SpringerPlus, 4, 496.
35. National Research Council (US); Avise JC, Hubbell SP, Ayala FJ, editors. *In the Light of Evolution: Volume II: Biodiversity and Extinction.* Washington (DC): National Academies Press (US); 2008. *4, Homage to Linnaeus: How Many Parasites? How Many Hosts?*
36. Orosova, M., & Spakulová, M. (2018). *Tapeworm chromosomes: their value in systematics with instructions for cytogenetic study*. Folia parasitologica, 65, 2018.001.
37. Orrego-Solano, Miguel Ángel, Cangalaya, Carla, Nash, Theodore E, & Guerra-Giraldez, Cristina. (2014). *Identificación de células proliferativas en quistes de Taenia solium*. Revista Peruana de Medicina Experimental y Salud Publica, 31(4), 702-706.
38. Pandian, T. J. 2020. *Reproduction and development in platyhelminthes*. CRC Press
39. Pechenik, J.A. 2014 *Biology of the Invertebrates*. Fifth Edition. Mc-Graw-Hill. New York, USA. 590 p.

40. Reddien, P. W., Oviedo, N. J., Jennings, J. R., Jenkin, J. C., & Sánchez Alvarado, A. (2005*). SMEDWI-2 is a PIWI-like protein that regulates planarian stem cells. Science* (New York, N.Y.), 310(5752), 1327–1330.

41. Rietschel, G. (1981). *Beitrag zur Kenntnis von Taenia crassiceps (Zeder, 1800) Rudolphi, 1810 (Cestoda, Taeniidae).* Zeitschrift Für Parasitenkunde Parasitology Research, 65(3), 309–315.

42. Rink J. C. (2013). *Stem cell systems and regeneration in planaria.* Development Genes and Evolution, 223(1-2), 67–84.

43. Robb, S. M. C., y Alvarado, A. S. (2014). *Histone Modifications and Regeneration in the Planarian Schmidtea mediterranea.* Current Topics in Developmental Biology, 71–93.

44. Robb, S. M.C.; Ross, E.; Alvarado, A. S. (2007). *SmedGD: the Schmidtea mediterranea genome database. Nucleic Acids Research*, 36(Database), D599–D606.

45. Roberts, L. S., Janovy, J., & Schmidt, G. D. (2009). Gerald D. Schmidt & Larry S. Roberts*. Foundations of parasitology*. Boston: McGraw-Hill.

46. Romanenko, L., Movsessian, S. (1988). *Embryonal development of Taenia pisiformis and T. hydatigena (Cestoda, Cyclophyllidea). Parazitologiya* (Leningrad) 22, 216–223

47. Rozario T., Quinn E. B., Wang J., Davis R. E. y Newmark P. A. (2019). *Region-specific regulation of stem cell-driven regeneration in tapeworms*. Developmental Biology Microbiology and Infectious Disease. eLife, 8, e48958.

48. Salic A. y Mitchison T. J. (2008) *A chemical method for fast and sensitive detection of DNA synthesis in vivo.* Proceedings of the National Academy of Sciences, 105 (7) 2415-2420

49. Sánchez-Torres, N.Y., Bobadilla, J.R., Laclette, J.P. et al. (2019). *How to eliminate taeniasis/cysticercosis: porcine vaccination and human chemotherapy (Part 2)*. *Theor Biol Med Model* 16, 4

50. Shibata, N., Umesono, Y., Orii, H., Sakurai, T., Watanabe, K., & Agata, K. (1999). *Expression of vasa(vas)-related genes in germline cells and totipotent somatic stem cells of planarians. Developmental biology*, 206(1), 73–87.

51. Singh, G., & Prabhakar, S. (2002). *Taenia solium cysticercosis: From basic to clinical science.* Wallingford, Oxon, UK: CABI Pub.

52. Smith, J. K., Esch, G. W. y Kuhn, R. E. (1972*). Growth and development of larval Taenia crassiceps (Cestoda)—I: Aneuploidy in the anomalous ORF strain*. International Journal for Parasitology, 2(2), 261–262.

53. Smith, J. K., Parrish, M., Esch, G. W. y Kuhn, R. E. (1972). *Growth and development of larval taenia Crassiceps (Cestoda)—II: RNA and DNA synthesis in the ORF and KBS strains determined by autoradiography.* International Journal for Parasitology, 2(3), 383–384.

54. Smyth, J. D. (1962). *Introduction to Animal Parasitology.* (3era edición). Cambridge University Press, Londres, Reino Unido, 549 p.

55. Smyth, J., & McManus, D. (1989). *The Physiology and Biochemistry of Cestodes*. Cambridge: Cambridge University Press.
56. Solana, J., Lasko, P., & Romero, R. (2009). *Spoltud-1 is a chromatoid body component required for planarian long-term stem cell self-renewal. Developmental biology,* 328(2), 410–421.
57. Spakulová, M., & Casanova, J. C. (2004). *Current knowledge on B chromosomes in natural populations of helminth parasites: a review*. Cytogenetic and genome research, 106(2-4), 222–229.
58. Spakulová, M., Orosová, M., & Mackiewicz, J. S. (2011). *Cytogenetics and chromosomes of tapeworms (Platyhelminthes, Cestoda)*. Advances in parasitology, 74, 177–230.
59. Spiliotis, M., Lechner, S., Tappe, D., Scheller, C., Krohne, G. y Brehm, K. (2008). *Transient transfection of Echinococcus multilocularis primary cells and complete in vitro regeneration of metacestode vesicles*. International Journal for Parasitology, 38(8-9), 1025–1039.
60. The Schistosoma japonicum Genome Sequencing and Functional Analysis Consortium. The *Schistosoma japonicum* genome reveals features of host–parasite interplay. *Nature* **460,** 345–351 (2009).
61. Toledo, A., Cruz, C., Fragoso, G., Laclette, J. P., Merchant, M. T., Hernández, M., y Sciutto, E. (1997). *In vitro* Culture of *Taenia crassiceps* Larval Cells and Cyst Regeneration after Injection into Mice. The Journal of Parasitology, 83(2), 189.
62. Tsai, I., Zarowiecki, M., Holroyd, N. et al. (2013). The genomes of four tapeworm species reveal adaptations to parasitism. Nature, 496, 57–63.
63. Watabe S. y Hartshorne D.J. (1990). *Paramyosin and the catch mechanism., 96(4), 639–646.*
64. Willms, K. y Zurabian, R. (2009). *Taenia crassiceps: in vivo and in vitro models*. Parasitology, 137(03), 335.
65. Willms, K., Merchant, M. T., Gómez, M., & Robert, L. (2001). *Taenia solium: germinal cell precursors in tapeworms grown in hamster intestine*. Archives of medical research, 32(1), 1–7.
66. Zhang, Zhifei; Strotz, Luke C.; Topper, Timothy P.; Chen, Feiyang; Chen, Yanlong; Liang, Yue; Zhang, Zhiliang; Skovsted, Christian B.; Brock, Glenn A. (2020). *An encrusting kleptoparasite-host interaction from the early Cambrian.* Nature Communications, 11(1), 2625–.
67. А. С. Скрябин (1967) *Гигантская дифиллоботриида* (Difilobótrido gigante) *Polygonoporus giganticus n.g., n.sp. Паразит кашалота* (Parásito del cachalote). Р Паразитология (Parasitología). 1,2 131-136

IX. Anexos

Manuscritos publicados

1.- Ríos-Valencia D. G., Navarrete-Perea J., **Calderón-Gallegos A.**, Flores-Bautista J. y Laclette J. P. (2021). To Be or Not to Be a Tapeworm Parasite: That Is the Post-Genomic Question in "*Taenia solium* Cysticercosis, Current State of the Art in Cysticercosis and Neurocysticercosis*"*, J. Morales-Montor, A. Landa and L.I. Terrazas (editores), IntechOpen (London, UK).

2.- Bobes R. J., Estrada K., Rios-Valencia D. G., **Calderón-Gallegos A.**, De La Torre P., Carrero J. C., Sánchez-Flores A y Laclette J. P. (2022). *The genomes of two strains of Taenia crassiceps the animal model for the study of human cysticercosis. Frontiers in Cellular and Infection Microbiology.*

Manuscritos aceptados para publicación

3.- Giraldo-Velásquez M. F., Pérez-Osorio N. I., Espinosa-Cerón A., Bárcena B. M., **Calderón-Gallegos A.**, Fragoso G., Torres-Ramos M., Páez-Martínez N. y Sciutto E. (2021) Intranasal Methylprednisolone Ameliorates Neuroinflammation Induced by Chronic Toluene Exposure. *Pharmaceutics,* 13, (en prensa)

Manuscritos sometidos para publicación

4.- Cervantes-Torres J., Rosales S., Cabello C., Montero L., Hernandez-Aceves J., Granados G., **Calderón-Gallegos A.**, Zúñiga-Flores F., Ruiz-Rivera M., Abarca-Magaña J. C., Ortega-Francisco S., Olguin-Alor R., Díaz G., Paczka-Garcia F., Zavala-Gaytan R., Vázquez-Ramírez R., Dolores Ayón-Nuñez D. A., Carrero J. C., Rios-Valencia D. G., Jasso-Ramírez M., Vázquez-Hernández R., Venegas D., Garzón D., Cobos L., Segura-Velázquez R., Villalobos N., Meneses G., Zúñiga J., Gamba G., Cárdenas G., Hernández M., Parkhouse M. E., Romano M. C., Herrera L. A., Bobes R. J., Pérez-Tapial M., Huerta L., Fierro N., Gracia I., Soldevilla G., Fragoso G., Suárez-Güemes F., Laclette J. P. y Sciutto E. (2021). *Towards the development of an epitope-focused peptide vaccine for SARS-CoV-2*. Vaccine.

Anexo 1

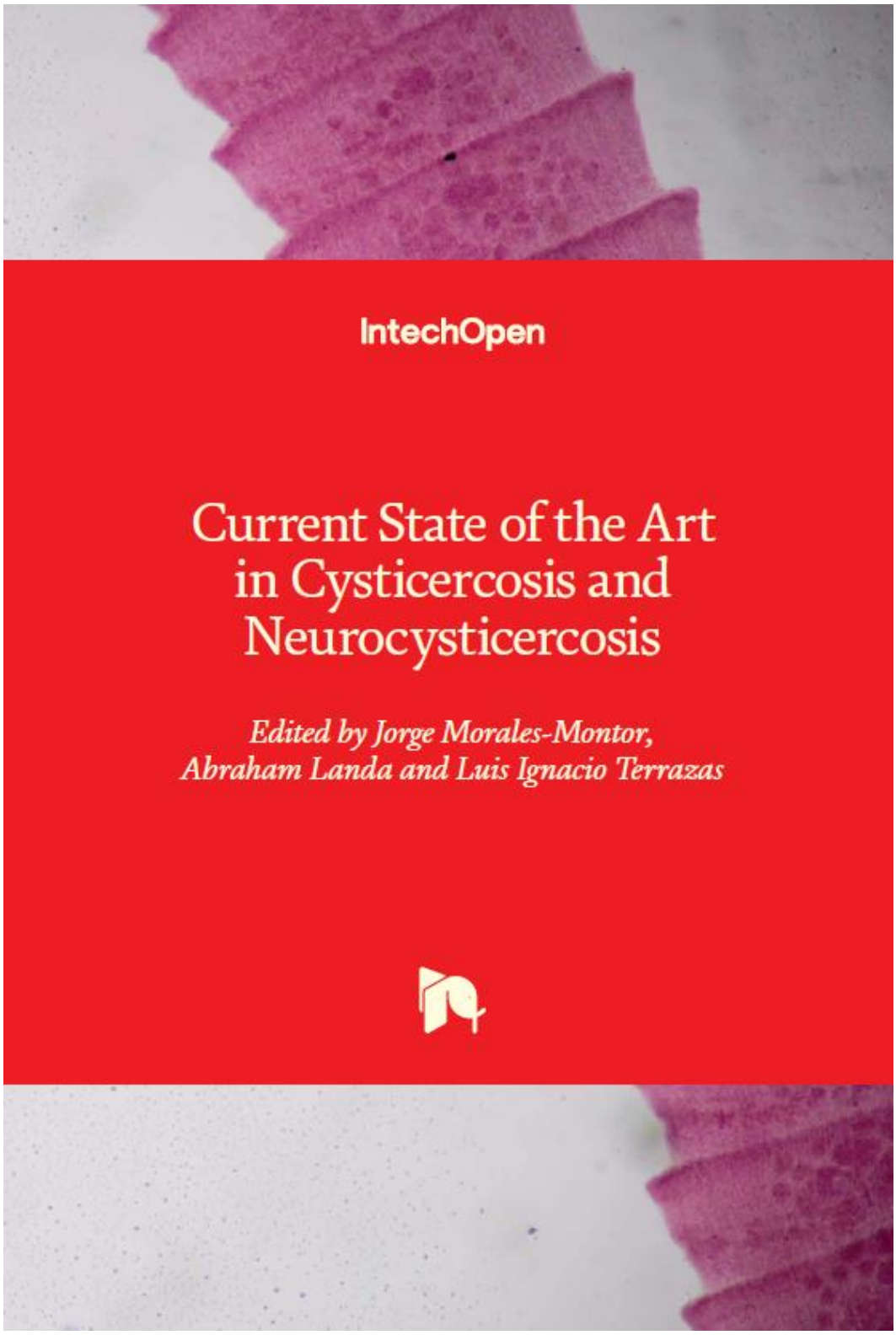
IntechOpen
Current State of the Art in Cysticercosis and Neurocysticercosis
Edited by Jorge Morales-Montor, Abraham Landa and Luis Ignacio Terrazas

Current State of the Art in Cysticercosis and Neurocysticercosis

Edited by Jorge Morales-Montor, Abraham Landa and Luis Ignacio Terrazas

Published in London, United Kingdom

Contents

Chapter 7

To Be or Not to Be a Tapeworm Parasite: That Is the Post-Genomic Question in *Taenia solium* Cysticercosis

Diana G. Ríos-Valencia, José Navarrete-Perea, Arturo Calderón-Gallegos, Jeannette Flores-Bautista and Juan Pedro Laclette

Abstract

Cestode parasites rely on their host to obtain their nutrients. Elucidation of tapeworm genomes has shown a remarkable reduction in the coding of multiple enzymes, particularly those of anabolic pathways. Previous findings showed that 10–13% of the proteins found in the vesicular fluid of *Taenia solium* cysticerci are of host origin. Further proteomic characterization allowed identification of 4,259 different proteins including 891 of host origin in the parasite's protein lysates. One explanation for this high abundance and diversity of host proteins in the parasite lysates is related to the functional exploitation of host proteins by cysticerci. Supporting this concept is the uptake of host haptoglobin and hemoglobin by the parasite, as a way to acquire iron. Surprisingly, internalized host proteins are minimally degraded by the parasite physiological machinery. Additional proteomic analysis demonstrated that these host proteins become part of the organic matrix of calcareous corpuscles; as 60–70% of the protein content are host proteins. In this review, a collection of available genomic and proteomic data for taeniid cestodes is assembled, the subject of the use and processing of host proteins is particularly addressed; a sketchy and unique cell physiological profile starts to emerge for these parasitic organisms.

Keywords: *Taenia solium*, Cestoda, Genome, Proteome, Host proteins, Calcareous Corpuscles

1. Introduction

Tapeworms are invertebrate metazoans producing zoonotic parasite diseases in animals and humans. These parasites have a worldwide distribution, but they especially affect human populations in developing countries and are considered neglected diseases [1]. Their larvae, known as metacestodes (including forms such as cysticercus in *Taenia solium* or hydatid or alveolar cysts in *Echinococcus* sp.) cause the highest morbidities due to tapeworms [2, 3], since they can produce generalized organ failure or seizures and can even result in patient's death [4–7].

Tapeworms produce long-term infections, being able to survive within its host for several years [8], maintaining a dynamic and complex host-parasite relationship [9]. Their lifecycles involve two host (intermediate and final) and include several developmental stages: embryo, larvae and adult stage [10] that can lodge in different tissues of their hosts producing diseases with a wide range of clinical presentations [11].

After description of the genomes of four tapeworms in 2013 [12], molecular studies of these organism have entered an integrative era; including approaches involving genomics, transcriptomics and proteomics [13]. These approaches are presented as promising avenues for the discovery of new pathways to improve our understanding of parasite diseases caused by cestodes, in the hope of developing better surveillance, treatment and control guidelines.

This chapter reviews current perspectives in the study of flatworms; special emphasis is placed on the genomics and proteomics of cestodes and taeniid parasites. The conspicuous and abundant presence of host proteins is particularly considered for taeniid larval forms.

2. The Platyhelminth genome

Access to massive sequencing technologies allowed characterization of entire genomes for some of the most relevant flatworms; being the free living *Schmidtea mediterranea* the first trematode to be reported in 2008 [14]. The timeline of all flatworms genome projects that have been published to date clearly shows the advent of the post-genomic era of flatworms (**Table 1**). A rapid characterization of the genomes of parasites with medical importance, such as *Schistosoma japonicum, S. mansoni, Clonorchis sinensis*, among others, followed by four cestodes: *Hymenolepis microstoma, Echinococcus granulosus, E. multilocularis and Taenia solium* [12]. Subsequently, the International Helminth Genomes Consortium carried out a project with a goal of 50 helminth genomes. These genomes are currently deposited in the WormBase Parasite database, where users can access 197 genomes [15], including 44 Platyhelminthes: 4 free-living flatworms, 20 trematodes, 19 cestodes and 2 monogeneans (**Figure 1**). This platform also allows searching protein domains and Gene Ontology terms,

	Genome size (Mb)	No. of Genes	Longest scaffold size (Mb)	N50 length (Mb)	N90 length (kb)	GC content (%)
T. solium	122.3	12490	0.7	0.07	5.3	43
T. multiceps	240	12890	10.5	44.8	8500	43.7
T. saginata	169	13,161	7.3	0.58	29.4	43.2
T. asiatica	168	13,323	4.2	0.34	14.3	43.1
E. multilocularis	115	10345	20.1	13.8	2900	42.2
E. granulosus	114.9	10231	16	5.2	200	42
E. canadensis	115	11449	0.574	0.075	3.8	42
E. oligarthrus	86	8756	16	10.2	11.6	41
H. microstoma	141.1	10241	2.4	0.5	82	35.9
H. diminuta	177	15169	6.9	2.3	412.2	35.3

Table 1.
Statistics of completed genome sequencing for several tapeworms.

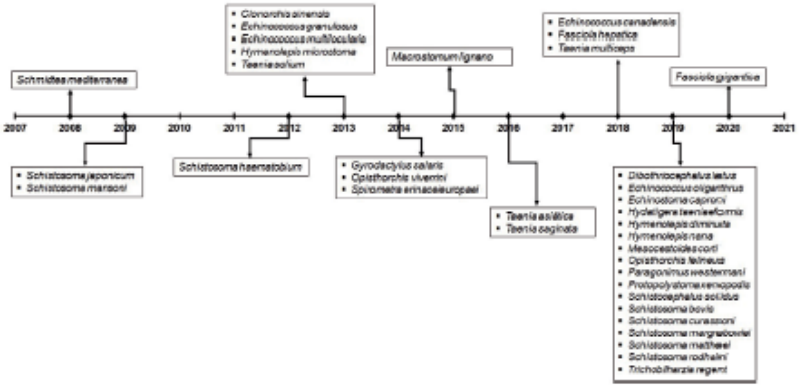

Figure 1.
Timeline of flatworms genome characterization [12, 14–39].

as well as performing comparative analysis of genes and alignments of RNA-Seq data sets, specific to the life stage genomes, among other useful functions [40, 41].

Other taeniid genomes have been reported outside the International Helminth Genomes Consortium during the past five years: *T. asiatica*, *T. saginata* [31] and *T. multiceps* [34], *E. canadensis* [32], *E. oligarthrus* [35], as well as *Hymenolepis diminuta* [36]; circumstances appear prone to greatly improve our understanding of the biology and evolution in those organisms, as well as to solve old unanswered questions on their host-parasite relationships. Availability of this genomic information allows integrative studies on this ancient lineage of organisms. **Table 1** includes the basic statistics of reported assemblies for several tapeworms of medical or veterinary importance, being *E. oligarthrus* the smallest assembly (86 Mb) and *T. multiceps* the largest one (240 Mb). The average GC content of these genomes is 35-43.7%, similar to trematode genomes [23] but different to bacterial genomes whose GC range content is 13.5%-74.9% [42]. As a reference, GC average content of vertebrates is 46% [43]; mice 41.7% [44] whereas human genome is 40.9% [45].

3. Gene gain/reduction along tapeworm evolution

The genomic data of the first four tapeworm genomes sequenced [12] permitted identification of reduction events for groups of genes such as Wnt, which corroborated some data that suggested the loss of these genes in trematodes [46]. Moreover, other genes as Nek kinases, peroxisomal genes and ParaHox members, as well as neuropeptides and G-protein coupled receptors (GPCRs) [15].

The loss of approximately 10 Hox gene families in tapeworms during their evolutionary pathway apparently affected the morphology of those organisms, i.e., the lack of eye-cups and gut [12]; Hox genes such as pax3/7, gbx, hbn and rax are mainly involved in neuronal development or eye development [47–50], as well as ParaHox genes in the formation of the digestive tract [51]. Another type of proteins absent in cestodes are those related to germ cells such as piwi, tudor and Vasa, although the latter have been found possible orthologues in the PL10 family [12].

Tapeworms have developed a specialized detoxification system that includes a single cytochrome p450 gene [12, 52], as well as a redox homeostatic system based on thioredoxin glutathione reductase and the expansion of glutathione

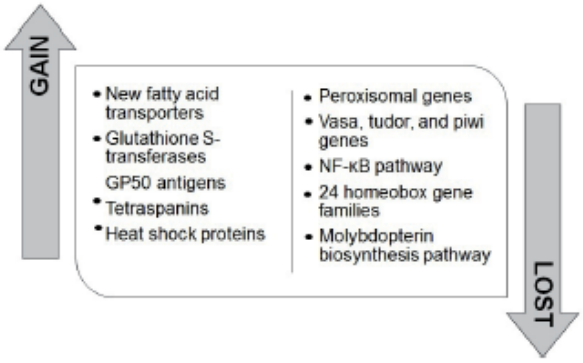

Figure 2.
Gains and losses of genes in taeniids. Phylogenetic study carried out with the genomes of the cestodes allowed finding important aspects about how these organisms acquired or lost some of their genomic traits to adapt to the conditions of their current environments.

S-transferases [53–55]. In addition, there was an expansion of some very specific protein families such as non-canonical heat shock proteins, with *Echinococcus* and *T. solium* having the highest number of genetic expansions in the cytosolic clade Hsp70 [12] suggesting that tapeworms have different mechanisms from nematodes to overcome stress [16]. In addition, taeniids have an expansion in some families of antigens such as GP50 [12, 15]. These antigens are useful for diagnostics; for example, coenurosis in goats [56] or cysticercosis in pigs [57]. For diagnosis of human cysticercosis, the use of GP50 as a diagnostic target allows a 100% specificity and 90% sensitivity using serum samples of patients [58, 59]. Some of the main gains and losses of genes in taeniids are summarized in **Figure 2**.

Our current knowledge on cestode's and taeniid's genomes is still limited but the speed of genomic data acquisition can advance significantly in this new era. We envisage a better understanding of these host–parasite interactions, at a molecular/evolutionary level that can help us unravel events that have permitted the adaptations of these platyhelminths to the host environment.

4. Metabolic adaptations of tapeworms

A great impact of having available complete tapeworm genomes is the characterization of the metabolic pathways in these organisms. Now we know that taeniid tapeworms cannot synthesize fatty acids and cholesterol de novo [25, 60]. For example, KEGG analysis for fatty acid biosynthesis in *T. solium* clearly shows that most of the components of the pathway are absent (**Figure 3**). Therefore, these parasites cannot carry out biosynthesis of fatty acids and are obligated to acquire host fatty acids through specific transporters [63]. Moreover, no genes related to the β-oxidation pathway were found in *Echinococcus* and *Hymenolepis,* although experimental data suggest that other flatworms do carry out this metabolic process [64] for utilization of lipids as a source of energy. It is clear that their major energy source are carbohydrates such as glucose and glycogen. This is supported by the fact that most enzymes participating in carbohydrate catabolism are expressed.

The synthesis of pyrimidines is also absent for taeniids [65], indicating that they acquire pyrimidines from their hosts. The biosynthesis of purines shows a similar landscape [15]. Parasitic flatworms are considered auxotrophic for eight

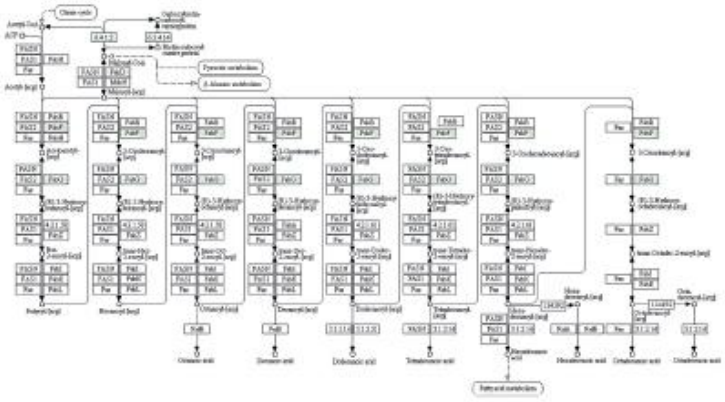

Figure 3.
KEGG analysis of the fatty acid biosynthesis in T. solium. *Enzymes available for this pathway are acetyl-CoA carboxylase (6.4.1.2), S-malonyltranferase (FabF), 3-Oxoacyl-[acyl-carrier-protein] synthetase II (FabF) and Ketoacyl-acyl carrier protein (FabG) [green squares] [61, 62].*

of the nine amino acids that are essential for humans (Phe, His, Lys, Leu, Met, Thr, Trp, and Val). Cestodes have a limited ability to synthesize amino acids, as an example, serine and proline are absent in *E. multilocularis* [16]; biosynthesis of lysine and the aromatic amino acids (Phe, Trp and Tyr) are also absent in most cestodes (**Figure 4**). Arginine is also an essential amino acid in helminths including flatworms, as they do not have all the necessary enzymes of the urea cycle to process

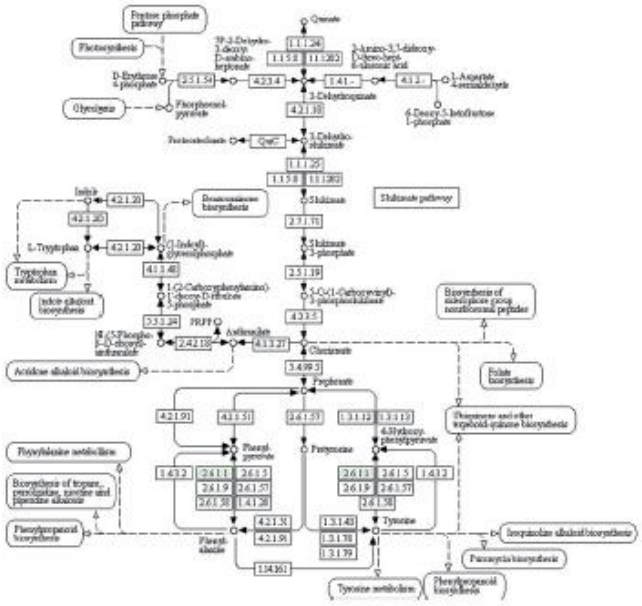

Figure 4.
KEGG analysis of phenylalanine, tyrosine and tryptophan biosynthesis in T. solium. *The only enzymes that are present in the* T. solium *genome are indicated in green within boxes [61, 62].*

ornithine, which is the precursor of arginine [15]. In summary, these parasitic organisms rely on their host for the acquisition of fatty acids, nucleosides and most amino acids. Metabolically speaking, they show highly simplified genomes.

5. Taeniid larval tissues contain large amounts of host proteins

The presence of host proteins in the tissues of the cystic larval forms of taeniids has been known for a long time [66–70]. It has been proposed that the mechanism for the uptake of these proteins is fluid pinocytosis in the cysticerci of *T. crassiceps* [69]. Moreover, in addition of entering the host proteins, these parasites can also secrete them [70, 71]. The biological role of those uptaken host proteins remains elusive, however, uptake of host albumin has been proposed to be involved in the maintenance of host-parasite osmotic pressure [68] and uptake of host immunoglobulins has been proposed as a mechanism of immune evasion and even as a source of amino acids [72].

Recent quantitative estimates indicated that host proteins might represent 11–13% of the protein content in the vesicular fluid of *T. solium* cysticerci, with albumin and immunoglobulins being the most abundant proteins. The use of high-throughput proteomics, allowed identifying 891 proteins of host origin from a total of 4,259 in a *T. solium* cysticerci whole protein extract [73]; thus, host proteins might represent up to 19% of the total protein species in the larval tissue lysates. Moreover, a fraction of these uptaken host proteins are intact and perhaps functionally active in the tissues of taeniid larvae [71].

6. Utilization of host proteins by cysticerci; iron chaperons and IgG

A known trait of parasitism is the use of the host as a provider of resources; sugars, amino acids, nucleosides, vitamins, coenzymes and/or microelements are good examples of resources that a parasite can acquire from its host. However, considering the abundance and diversity of host proteins present in the tissues of taeniid larvae, a pertinent question would be: are these parasites benefited by the accumulation of host proteins, beyond simply serving as a source of amino acids or as osmotic regulators? We have explored a couple of prospects: the use of host iron chaperones for the management of the parasite's iron necessities, as well as the use of host immunoglobulins as a source of amino acids [70, 71, 74].

Iron is an essential element for virtually all living organisms. Pathogens have evolved mechanisms to uptake iron from their hosts. Usually, iron is uptaken from plasma proteins: hemoglobin (heme prosthetic group) or haptoglobin-hemoglobin complexes, hemopexin (heme prosthetic group), transferrin or lactoferrin (iron), ferritin (iron), etc. In fact, the constant battle between host and pathogens for this element is well-studied [75, 76]. Hepcidin, the hormone that control iron levels in mammals, was first discovered as an antimicrobial peptide [76, 77]. In this light, it is expected that cestodes would acquire iron from their host, however, the mechanism remains elusive. Some evidence have suggested that hemoglobin or the haptoglobin-hemoglobin complexes could serve as an iron source for the cysts [78]. To support this notion, we have documented the immunolocalization of haptoglobin, hemoglobin, hepcidin and ferritin in the cyst; immunoblotting using crude larval extracts confirmed the finding [73]. We also showed that haptoglobin-hemoglobin complexes were detected in crude larval extracts in their expected molecular weight, indicating that those complexes are only marginally degraded. In fact, free haptoglobin purified from cysts protein lysates has been shown to retain

their hemoglobin binding activity, suggesting that the cyst are acquiring iron from those sources. However, future studies are needed to understand how the uptake is performed (is there a specific receptor?), how the heme prosthetic group or iron is removed from those complexes? and which parasite proteins are performing those roles.

Another aspect related to the host's protein uptake by tapeworm's larvae, is the utilization of these proteins as a source of amino acids. Internalization of IgG has been traced using a metabolically labeled (Leu-3H) IgG produced *in vitro* using a mice hybridoma [71]. Through *in vitro* culture of *T. crassiceps* (a closely related species of *T. solium*) cysts in the presence of (Leu-3H) mice IgG, uptake of the immunoglobulin can be monitored. Metabolic labelling also allowed tracking incorporation of Leu-3H into newly synthesized cyst proteins. The biochemical analyses revealed that within the tissue extracts, no other radiolabeled proteins were found. The two bands corresponding to the heavy (50 kDa) and light (25 kDa) chains remained intact after 3 days of culture. This would imply that these proteins are negligible used as a source of amino acids for the biosynthesis of the larvae's own proteins. Furthermore, the integrity and functionality of the Igs was conserved, as shown by SDS-PAGE and western blots marked with the Igs purified from tissue extracts. This finding led the research into a new direction: If immunoglobulins (and perhaps other uptaken host proteins) are only a minor source of amino acids [71], what is the fate of uptaken host proteins?

7. The calcareous corpuscles as a final deposit for host proteins

The tracking of metabolically radiolabeled IgG demonstrated that cysticerci do not significantly use these proteins as a major source of amino acids [71]. A possibility was that these proteins could end in the calcareous corpuscles (CC), that are known as a waste of toxic metabolites and other materials. These CC are microscopic calcifications occurring in the lumen of protonephridial canals, resulting after accretion of mineral salts (calcium carbonate and calcium phosphate) on an organic matrix composed by polysaccharides and other macromolecules [79, 80]. The CC

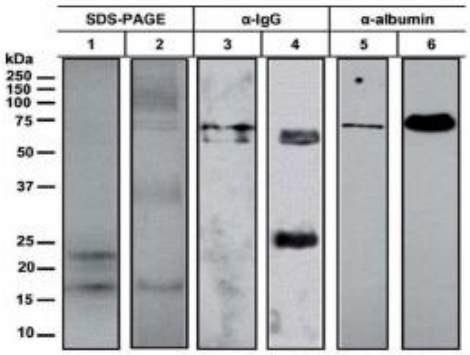

Figure 5.
Immunological identification of host IgG and albumin recovered from the protein matrix of calcareous corpuscles of T. solium *cysticerci. Lanes 1 and 2 correspond to Coomassie blue staining of protein extract from CC and silver staining of porcine serum respectively. Lanes 3 and 5 are western blots of protein extracts obtained from CC, lanes 4 and 6 are gels run with porcine serum, these blots were revealed with an α-IgG coupled to HRP (3 and 4) or sheep α-albumin and then with a rabbit α-sheep IgG coupled to HRP (5 and 6). This figure was originally published in [70].*

DOI: http://dx.doi.org/10.5772/intechopen.97306

Author details

Diana G. Ríos-Valencia[1], José Navarrete-Perea[2], Arturo Calderón-Gallegos[1], Jeannette Flores-Bautista[1] and Juan Pedro Laclette[1]*

1 Biomedical Research Institute, Universidad Nacional Autónoma de México, Mexico City, Mexico

2 Department of Cell Biology, Harvard Medical School, Boston Massachusetts, United States

*Address all correspondence to: laclette@iibiomedicas.unam.mx

References

[1] Webb C, Cabada MM. Intestinal cestodes. Current Opinion in Infectious Diseases 2017;30(5):504-510. DOI: 10.1097/QCO.0b013e3282ef579e

[2] Eckert J, Deplazes P. Biological, Epidemiological, and Clinical Aspects of Echinococcosis, a Zoonosis of Increasing Concern. Clinical Microbiology Reviews. 2004;17(1):107-135. DOI: 10.1128/cmr.17.1.107-135.2004

[3] Gripper LB, Welburn SC. Neurocysticercosis infection and disease–A review. Acta Tropica. 2016; 66:218-224. DOI: 10.1016/j.actatropica.2016.11.015Abba

[4] Abba K, Ramaratnam S, Ranganathan LN. Anthelmintics for people with neurocysticercosis. Cochrane Database of Systematic Reviews 2010;17;2010(3):CD000215. DOI: 10.1002/14651858.CD000215.pub3.

[5] O'Neal SE, Flecker RH. Hospitalization frequency and charges for neurocysticercosis, Emerging Infectious Diseases. 2015;21(6):969-976. DOI:10.3201/eid2106.141324

[6] Brunetti E, Kern P, Vuitton DA. Expert consensus for the diagnosis and treatment of cystic and alveolar echinococcosis in humans. Acta Tropica. 2010;114(1):1-16. DOI: 10.1016/j.actatropica.2009.11.001

[7] Garcia HH, Moro PL, Schantz PM. Zoonotic helminth infections of humans: echinococcosis, cysticercosis and fascioliasis. Current Opinion in Infectious Diseases. 2007;20(5): 489-494. DOI: 10.1097/QCO.0b013e3282a95e39

[8] Olson PD, Littlewood DTJ, Bray RA, Mariaux J. Interrelationships and evolution of the tapeworms (Platyhelminthes: Cestoda). Molecular Phylogenetics and Evolution. 2001;19(3):443-467. DOI: 10.1006/mpev.2001.0930

[9] Egger B. Making Heads or Tails of Tapeworms. Trends in Parasitology. 2016;32(7):511-512. DOI: 10.1016/j.pt.2016.04.003. DOI: 10.1016/j.pt.2016.04.003.

[10] Sulima A, Savijoki K, Bien J, Näreaho A, Salamatin R, Conn DB, et al. Comparative proteomic analysis of *Hymenolepis diminuta* cysticercoid and adult stages. Frontiers in Microbiology. 2018;15;8:2672. DOI:10.3389/fmicb.2017.02672.

[11] Craig P, Ito A. Intestinal cestodes. Current Opinion in Infectious Diseases. 2007;20(5):524-532. DOI: 10.1097/QCO.0b013e3282ef579e

[12] Tsai IJ, Zarowiecki M, Holroyd N, Garciarrubio A, Sanchez-Flores A, Brooks KL, et al. The genomes of four tapeworm species reveal adaptations to parasitism. Nature. 2013;496(7443):57-63. DOI: 10.1038/nature12031

[13] Marzano V, Mancinelli L, Bracaglia G, Del Chierico F, Vernocchi P, Di Girolamo F, et al. "Omic" investigations of protozoa and worms for a deeper understanding of the human gut "parasitome." PLoS Neglected Tropical Diseases. 2017;11(11):e0005916. DOI: 10.1371/journal.pntd.0005916.

[14] Robb SMC, Ross E, Alvarado AS. SmedGD: The *Schmidtea mediterranea* genome database. Nucleic Acids Researcher. 2008;36(SUPPL. 1):D599-D606. DOI:10.1093/nar/gkm684.

[15] Helminth I, Consortium G. Comparative genomics of the major parasitic worms. Nature Genetics. 2019;51(1):163-174. DOI: 10.1038/s41588-018-0262-1.

[16] Zheng H, Zhang W, Zhang L, Zhang Z, Li J, Lu G, et al. The genome of the hydatid tapeworm *Echinococcus granulosus*. Nature. 2013;45(10):1168-1175. DOI:10.1038/ng.2757

[17] Grohme MA, Schloissnig S, Rozanski A, Pippel M, Young GR, Winkler S, et al. The genome of *S. mediterranea* and the evolution of cellular core mechanisms. Nature Publishing Group. 2018;554(7690):56-61. DOI: 10.1038/nature25473.

[18] Rozanski A, Moon HK, Brandl H, Martín-Durán JM, Grohme MA, Hüttner K, et al. PlanMine 3.0 - improvements to a mineable resource of flatworm biology and biodiversity. Nucleic Acids Research. 2019;47(D1):D812–D820. DOI:10.1093/nar/gky1070

[19] Luo F, Yin M, Mo X, Sun C, Wu Q, Zhu B, et al. An improved genome assembly of the fluke *Schistosoma japonicum*. PLoS Neglected Tropical Diseases. 2019;13(8):e0007612. DOI: 10.1371/journal.pntd.0007612

[20] Zhou Y, Zheng H, Chen Y, Zhang L, Wang K, Guo J, et al. The *Schistosoma japonicum* genome reveals features of host-parasite interplay. Nature. 2009; 460(7253):345-351. DOI: 10.1038/nature08140

[21] Young ND, Jex AR, Li B, Liu S, Yang L, Xiong Z, et al. Whole-genome sequence of *Schistosoma haematobium*. Nature Genetics. 2012;44(2):221-225. DOI:10.1038/ng.1065

[22] Stroehlein AJ, Korhonen PK, Chong TM, Lim YL, Chan KG, Webster B, et al. High-quality *Schistosoma haematobium* genome achieved by single-molecule and long-range sequencing. Gigascience. 2019;8(9):1-12. DOI:10.1093/gigascience/giz108

[23] Berriman M, Haas BJ, Loverde PT, Wilson RA, Dillon GP, Cerqueira GC, et al. The genome of the blood fluke *Schistosoma mansoni*. Nature. 2009;460(7253):352-358. DOI: 10.1038/nature08160

[24] Protasio A V., Tsai IJ, Babbage A, Nichol S, Hunt M, Aslett MA, et al. A systematically improved high quality genome and transcriptome of the human blood fluke *Schistosoma mansoni*. PLoS Neglected Tropical Diseases. 2012;6(1):1455. DOI: 10.1371/journal.pntd.0001455

[25] Wang X, Chen W, Huang Y, Sun J, Men J, Liu H, et al. The draft genome of the carcinogenic human liver fluke *Clonorchis sinensis*. Genome Biology. 2011;12(10):R107. DOI: 10.1186/gb-2011-12-10-r107

[26] Huang Y, Chen W, Wang X, Liu H, Chen Y, Guo L, et al. The Carcinogenic Liver Fluke, *Clonorchis sinensis*: New Assembly, Reannotation and Analysis of the Genome and Characterization of Tissue Transcriptomes. PLoS One. 2013;8(1):e54732. DOI: 10.1371/journal.pone.0054732

[27] Wasik K, Gurtowski J, Zhou X, Ramos OM, Delás MJ, Battistoni G, et al. Genome and transcriptome of the regeneration-competent flatworm, *Macrostomum lignano*. PNAS. 2015;112(40):12462-12467. DOI:10.1073/pnas.1516718112

[28] Wudarski J, Simanov D, Ustyantsev K, De Mulder K, Grelling M, Grudniewska M, et al. Efficient transgenesis and annotated genome sequence of the regenerative flatworm model *Macrostomum lignano*. Nature Communications 2017;8(1):1-12. DOI: 10.1038/s41467-017-02214-8

[29] Hahn C, Fromm B, Bachmann L. Comparative Genomics of Flatworms (Platyhelminthes) Reveals Shared Genomic Features of Ecto- and Endoparastic Neodermata. Genome

Biology and Evolution. 2014;6(5):1105-1117. DOI:10.1093/gbe/evu078

[30] Young ND, Nagarajan N, Lin SJ, Korhonen PK, Jex AR, Hall RS, et al. The *Opisthorchis viverrini* genome provides insights into life in the bile duct. Nature Communications. 2014;5(13):1-11. DOI:10.1038/ncomms5378

[31] Wang S, Wang S, Luo Y, Xiao L, Luo X, Gao S, et al. Comparative genomics reveals adaptive evolution of Asian tapeworm in switching to a new intermediate host. Nature Communications. 2016;7(1):1-12. DOI:10.1038/ncomms12845

[32] Maldonado LL, Assis J, Araújo FMG, Salim ACM, Macchiaroli N, Cucher M, et al. The *Echinococcus canadensis* (G7) genome : a key knowledge of parasitic platyhelminth human diseases. BMC Genomics. 2017;1-23. DOI:10.1186/s12864-017-3574-0

[33] McNulty SN, Tort JF, Rinaldi G, Fischer K, Rosa BA, Smircich P, et al. Genomes of Fasciola hepatica from the Americas Reveal Colonization with Neorickettsia Endobacteria Related to the Agents of Potomac Horse and Human Sennetsu Fevers. PLOS Genetics. 2017;13(1):e1006537. DOI:10.1371/journal.pgen.1006537

[34] Li W, Liu B, Yang Y, Ren Y, Wang S, Liu C, et al. The genome of tapeworm *Taenia multiceps* sheds light on understanding parasitic mechanism and control of coenurosis disease. DNA Research. 2018;25(June):499-510. DOI:10.1093/dnares/dsy020

[35] Maldonado LL, Arrabal JP, Rosenzvit MC, Kamenetzky L. Revisiting the Phylogenetic History of Helminths Through Genomics , the Case of the New *Echinococcus oligarthrus* Genome. Frontiers in Genetics. 2019;10:708. DOI:10.3389/fgene.2019.00708

[36] Nowak RM, Jastr JP, Kuśmirek W, Sałamatin R, Rydzanicz M, Sobczyk-kopcioł A, et al. Assembly and annotation of the model tapeworm *Hymenolepis diminuta*. Scientific Data. 2019;3;6(1):302. DOI: 10.1038/s41597-019-0311-3

[37] Ershov NI, Mordvinov VA, Prokhortchouk EB, Pakharukova MY, Gunbin K V., Ustyantsev K, et al. New insights from *Opisthorchis felineus* genome: Update on genomics of the epidemiologically important liver flukes. BMC Genomics 2019;20(1):1-22. DOI: 10.1186/s12864-019-5752-8

[38] Oey H, Zakrzewski M, Narain K, Devi KR, Agatsuma T, Nawaratna S, et al. Whole-genome sequence of the oriental lung fluke *Paragonimus westermani*. Gigascience. 2018; 8(1):1-8. DOI: 10.1093/gigascience/giy146

[39] Oey H, Zakrzewski M, Gravermann K, Young ND, Korhonen PK, Gobert GN, et al. Whole-genome sequence of the bovine blood fluke Schistosoma bovis supports interspecific hybridization with *S. Haematobium*. PLoS Pathogens. 2019;15(1):e1007513–e1007513. DOI: 10.1371/journal.ppat.1007513

[40] Howe KL, Bolt BJ, Shafie M, Kersey P, Berriman M. WormBase ParaSite – a comprehensive resource for helminth genomics. Molecular and Biochemical Parasitology. 2017;215:2-10. DOI: 10.1016/j.molbiopara.2016.11.005

[41] Howe KL, Bolt BJ, Cain S, Chan J, Chen WJ, Davis P, et al. WormBase 2016: expanding to enable helminth genomic research. Nucleic Acids Reseacher. 2016;44(D1):D774–D780. DOI: 10.1093/nar/gkv1217

[42] Thomas SH, Wagner RD, Arakaki AK, Skolnick J, Kirby JR, Shimkets LJ, et al. The Mosaic Genome of *Anaeromyxobacter dehalogenans* Strain 2CP-C Suggests an Aerobic Common

Ancestor to the Delta-Proteobacteria. PLoS One 2008;3(5):e2103. DOI: 10.1371/journal.pone.0002103

[43] Vinogradov AE. Genome size and GC-percent in vertebrates as determined by flow cytometry: The triangular relationship. Cytometry. 1998;31(2):100-109. DOI:10.1002/(sici)1097-0320(19980201)31:2<100::aid-cyto5>3.0.co;2-q

[44] Zhao Z, Zhang F. Sequence context analysis in the mouse genome: Single nucleotide polymorphisms and CpG island sequences. Genomics.;87:68-74. DOI: 10.1016/j.ygeno.2005.09.012

[45] Piovesan A, Pelleri MC, Antonaros F, Strippoli P, Caracausi M, Vitale L. On the length, weight and GC content of the human genome. BMC Research Notes. 2019;12(1):106. DOI:10.1186/s13104-019-4137-z

[46] Riddiford N, Olson PD. Wnt gene loss in flatworms. Development Genes and Evolution. 2011;221(4):187-197. DOI: 10.1007/s00427-011-0370-8

[47] Philippidou P, Dasen JS. Hox Genes: Choreographers in Neural Development, Architects of Circuit Organization. Neuron. 2013;2;80(1):12-34. DOI:10.1016/j.neuron.2013.09.020

[48] Mathers PH, Grinberg A, Mahon KA, Jamrich M. The Rx homeobox gene is essential for vertebrate eye development. Nature. 1997;387(6633):603-607. DOI:10.1038/42475

[49] Castro LFC, Rasmussen SLK, Holland PWH, Holland ND, Holland LZ. A Gbx homeobox gene in amphioxus: Insights into ancestry of the ANTP class and evolution of the midbrain/hindbrain boundary. Developmental Biology. 2006;1;295(1):40-51. DOI: 10.1016/j.ydbio.2006.03.003

[50] Walldorf U, Kiewe A, Wickert M, Ronshaugen M, McGinnis W. Homeobrain, a novel paired-like homeobox gene is expressed in the Drosophila brain. Mechanisms of Development. 2000;96(1):141-144. DOI: 10.1016/s0925-4773(00)00380-4.

[51] Brooke NM, Garcia-Fernàndez J, Holland PWH. The ParaHox gene cluster is an evolutionary sister of the Hox gene cluster. Nature. 1998;15];392(6679):920-2. DOI: 10.1038/31933

[52] Pakharukova MY, Vavilin VA, Sripa B, Laha T, Brindley PJ, Mordvinov VA. Functional Analysis of the Unique Cytochrome P450 of the Liver Fluke Opisthorchis felineus. PLoS Neglected Tropical Diseases. 2015;9(12):e0004258. DOI: doi: 10.1371/journal.pntd.0004258

[53] Salinas G, Selkirk ME, Chalar C, Maizels RM, Fernández C. Linked thioredoxin-glutathione systems in platyhelminths. Trends in Parasitology. 2004, 20(7):340-346. DOI: 10.1016/j.pt.2004.05.002.

[54] Cvilink V, Lamka J, Skálová L. Xenobiotic metabolizing enzymes and metabolism of anthelminthics in helminthes. Drug Metabolism Reviews. 2009; 41(1):8-26. DOI: 10.1080/03602530802602880

[55] Harispe L, García G, Arbildi P, Pascovich L, Chalar C, Zaha A, et al. Biochemical analysis of a recombinant glutathione transferase from the cestode *Echinococcus granulosus*. Acta Tropica. 2010;114(1):31-36. DOI:10.1016/j.actatropica.2009.12.003

[56] Huang X, Xu J, Wang Y, Guo C, Chen L, Gu X, et al. GP50 as a promising early diagnostic antigen for *Taenia multiceps* infection in goats by indirect ELISA. Parasites and Vectors. 2016;9(1):618. DOI: 10.1186/s13071-016-1915-5

[57] Muro C, Gomez-Puerta LA, Flecker RH, Gamboa R, Barreto PV, Dorny P, et al. Porcine cysticercosis: Possible cross-reactivity of *Taenia hydatigena* to GP50 antigen in the enzyme-linked immunoelectrotransfer blot assay. The American Journal of Tropical Medicine and Hygiene. 2017;97(6):1830-1832. DOI: 10.4269/ajtmh.17-0378

[58] Hancock K, Pattabh S, Greene RM, Yushak ML, Williams F,et al. Characterization and cloning of GP50, a *Taenia solium* antigen diagnostic for cysticercosis. Molecular and Biochemical Parasitology. 2004;133(1):115-124. DOI:10.1016/j.molbiopara.2003.10.001

[59] Garcia HH, O'Neal SE, Noh J, Handali S, Gilman RH, Gonzalez AE, et al. Laboratory diagnosis of neurocysticercosis (*Taenia solium*). Journal of Clinical Microbiology. 2018;56(9). DOI: 10.1128/JCM.00424-18

[60] Frayha GJ. Comparative metabolism of acetate in the taeniid tapeworms *Echinococcus granulosus*, *E. multilocularis* and *Taenia hydatigena*. Comparative Biochemistry and Physiology Part B: Comparative Biochemistry Comp Biochem Physiol - Part B Biochem. Elsevier. 1971;39(1):167-170. DOI: 10.1016/0305-0491(71)90264-1

[61] Kanehisa M, Goto S. KEGG: Kyoto Encyclopedia of Genes and Genomes. Nucleic Acids Research, 2000; 1;28(1):27-30. DOI: 10.1093/nar/28.1.27.

[62] Kanehisa M. Toward understanding the origin and evolution of cellular organisms. Protein Science. 2019;28(11):1947-1951. DOI: 10.1002/pro.3715.

[63] Illescas O, Carrero JC, Bobes RJ, Flisser A, Rosas G, Laclette JP. Molecular characterization, functional expression, tissue localization and protective potential of a *Taenia solium* fatty acid-binding protein. Molecular and Biochemical Parasitology. 2012 Dec 1;186(2):117-125. DOI:10.1016/j.molbiopara.2012.10.002

[64] Pearce EJ, Huang SCC. The metabolic control of schistosome egg production. Cell Microbiology. 2015;17(6):796-801. DOI: 10.1111/cmi.12444

[65] Heath RL. Biosynthesis de novo of purines and pyrimidines in *Mesocestoides* (Cestoda) I. International Journal of Parasitology. 1970;56(1):98-102

[66] Hustead ST, Williams JF. Permeability studies on taeniid metacestodes. II. Antibody mediated effects on membrane permeability in larvae of *Taenia taeniaeformis* and *Taenia crassiceps*. Journal of Parasitology. 1977;63(2):322-326

[67] Machnicka B, Grzybowski J. Host serum proteins in *Taenia saginata* metacestode fluid. Veterinary Parasitology. 1986;19(1-2):47-54. DOI:10.1016/0304-4017(86)90031-2

[68] Hayunga EG, Sumner MP, Letonja T. Evidence for selective incorporation of host immunoglobulin by strobilocerci of *Taenia taeniaeformis*. Journal of Parasitology. 1989;75(4):638-642

[69] Ambrosio J, Landa A, Merchant MT, Laclette JP. Protein uptake by cysticerci of *Taenia crassiceps*. Archives of medical research. 1994; 25(3):325-330

[70] Aldridge JR, Jennette MA, Kuhn RE. Uptake and Secretion of Host Proteins by *Taenia crassiceps* Metacestodes. Journal of Parasitology. 2006;1;92(5):1101-2. DOI: 10.1645/GE-835R.1.

[71] Flores-Bautista J, Navarrete-Perea J, Fragoso G, Flisser A, Soberón X,

Laclette JP. Fate of uptaken host proteins in *Taenia solium* and *Taenia crassiceps* cysticerci. Biosciences Report. 2018;6;38(4). DOI: 10.1042/BSR20180636

[72] Damian RT. Presidential Address: The Exploitation of Host Immune Responses by Parasites. Journal of Parasitology. 1987;73(1):1. DOI:10.1017/s0031182097002357

[73] Navarreta-Pera J, Isasa M, Paulo JA, Corral-corral R, Flores-bautista J, Herna B, Gygi SP, et al. Quantitative multiplexed proteomics of *Taenia solium* cysts obtained from the skeletal muscle and central nervous system of pigs. 2017; 25;11(9):e0005962. DOI: 10.1371/journal.pntd.0005962

[74] Navarrete-Perea J, Moguel B, Mendoza-Hernández G, Fragoso G, Sciutto E, Bobes RJ, et al. Identification and quantification of host proteins in the vesicular fluid of porcine *Taenia solium* cysticerci. Experimental Parasitology. 2014 Aug;143(1):11-17. DOI: 10.1016/j.exppara.2014.04.011

[75] Kronstad JW, Caza M. Shared and distinct mechanisms of iron acquisition by bacterial and fungal pathogens of humans. Frontiers in Cellular and Infection Microbiology. 2013; 19;3:80. DOI: 10.3389/fcimb.2013.00080

[76] Barton JC, Acton RT. Hepcidin, iron, and bacterial infection. In: Vitamins and Hormones. Academic Press Inc. 2019;110:223-242. DOI:10.1016/bs.vh.2019.01.011

[77] Yiannikourides A, Latunde-Dada G. A Short Review of Iron Metabolism and Pathophysiology of Iron Disorders. Medicines. 2019;6(3):85. DOI:10.3390/medicines6030085

[78] Navarrete-Perea J, Toledano-Magaña Y, De La Torre P, Sciutto E, Bobes RJ, Soberón X, et al. Role of porcine serum haptoglobin in the host-parasite relationship of *Taenia solium* cysticercosis. Molecular and Biochemical Parasitology. 2016;1;207(2):61-7. DOI: 10.1016/j.molbiopara.2016.05.010

[79] Vargas-Parada L, Merchant MT, Willms K, Laclette JP. Formation of calcareous corpuscles in the lumen of excretory canals of *Taenia solium* cysticerci. Parasitology Research. 1999;85(2):88-92. DOI: 10.1007/s004360050514

[80] von Brand T, Nylen MU, Martin GN, Churchwell FK, Stites E. Cestode calcareous corpuscles: Phosphate relationships, crystallization patterns, and variations in size and shape. Experimental Parasitology. 1969;25(C):291-310. DOI: 10.1016/0014-4894(69)90075-7

[81] McCullough JS, Fairweather I. The structure, composition, formation and possible functions of calcareous corpuscles in *Trilocularia acanthiaevulgaris* Olsson 1867 (Cestoda, Tetraphyllidea). Parasitology Researcher. 1987;74(2):175-182. DOI: 10.1007/BF00536030

[82] Chung YB, Kong Y, Cho SY, Yang HJ. Purification and localization of a 10 kDa calcareous corpuscle binding protein of *Spirometra mansoni* plerocercoid. 2 Parasitology Research. 2003;235-237. DOI: 10.1007/s00436-002-0694-4

Anexo 2.

frontiers

The genomes of two strains of Taenia crassiceps the animal model for the study of human cysticercosis

Juan P. Laclette[1*], Raúl J. Bobes[1], Karel Estrada[2], Diana G. Rios-Valencia[1], Arturo Calderón-Gallegos[1], Patricia De La Torre[1], Julio C. Carrero[1], Alejandro Sanchez-Flores[2*]

[1]Universidad Nacional Autónoma de México, Biomedical Research Institute, Mexico, [2]Universidad Nacional Autónoma de México, Biotechnology Institute, Mexico

Submitted to Journal:
Frontiers in Cellular and Infection Microbiology

Specialty Section:
Parasite and Host

Article type:
Original Research Article

Manuscript ID:
876839

Received on:
15 Feb 2022

Journal website link:
www.frontiersin.org

frontiers

Conflict of interest statement

The authors declare that the research was conducted in the absence of any commercial or financial relationships that could be construed as a potential conflict of interest

Author contribution statement

KE performed the hybrid genome assembly, gene prediction, RNAseq differential expression and GO/KEGG enrichment analysis; PT performed initial sequencing, PT, DRV and RJB maintained and isolated the cysts in mice, RJB, KE, DRV, ACG and JCC carried out the gene annotation, differential protein expression analysis, ASF and KE did the comparative genomics (SNP and synteny analyses). JPL and ASF conceived the project. RJB, KE and DRV prepared the first draft and ASF and JPL developed the final version. JPL provided the budget from grants. All authors approved the submitted version.

Keywords

Taenia crassiceps, ORF, WFU, Comparative genomics, RNA-Seq, differential expression, Cysticercosis, animal model. 2

Abstract

Word count: 274

Human cysticercosis by Taenia solium is the major cause of neurological illness in countries of Africa, Southeast Asia, and the Americas. Publication of four cestode genomes (T. solium, Echinococcus multilocularis, E. granulosus and Hymenolepis microstoma) in the last decade, marked the advent of novel approaches on the study of the host-parasite molecular crosstalk for cestode parasites of importance for human and animal health. Taenia crassiceps is another cestode parasite, closely related to T. solium, which has been used in numerous studies as an animal model for human cysticercosis. Therefore, characterization of the T. crassiceps genome will also contribute to the understanding of the human infection. Here, we report the genome of T. crassiceps WFU strain, reconstructed to a noncontiguous finished resolution and performed a genomic and differential expression comparison analysis against ORF strain. Both strain genomes were sequenced using Oxford Nanopore (MinION) and Illumina technologies, achieving high quality assemblies of about 107 Mb for both strains. Dotplot comparison between WFU and ORF demonstrated that both genomes were extremely similar. Additionally, karyotyping results for both strains failed to demonstrate a difference in chromosome composition. Therefore, our results strongly support the concept that the absence of scolex in the ORF strain of T. crassiceps was not the result of a chromosomal loss as proposed elsewhere. Instead, it appears to be the result of subtle and extensive differences in the regulation of gene expression. Analysis of variants between the two strains identified 2,487 sites with changes distributed in 31 of 65 scaffolds. The differential expression analysis revealed that genes related to development and morphogenesis in the ORF strain might be involved in the lack of scolex formation.

Contribution to the field

The last decade has started the genomic era for Platyhelminthes; from only one genome available in 2008, we now have access to the genomes of 45 species, including 19 cestodes. Elucidation of the genomes of two strains of T. crassiceps (WFU and ORF) will improve the knowledge about the genomic similarities and differences that exist between taeniid species, allowing novel approaches to a number of unsolved questions on tapeworm infections, including human neurocysticercosis caused by T. solium. We identified several conserved proteins for all cestodes as well as some proteins that are unique to the Taenia genus and to the T. crassiceps species. These proteins are potential targets for novel drug design and vaccine or diagnostic tools development. Availability of high quality, chromosome level, assemblies of T. crassiceps strains, can also contribute to the definition of the usefulness and limits of this animal model, for improving the understanding of human cysticercosis. Our results also show that the absence of the scolex in the ORF strain, a structure that gives rise to the adult worm, was not due to a chromosomal loss as proposed earlier, but to more subtle changes in the expression of genes involved in embryonic development.

Funding statement

A1-S-11306 (CONACYT) and [IN 205820] PAPIIT-UNAM.

Ethics statements

Studies involving animal subjects

Generated Statement: The animal study was reviewed and approved by Institutional Committee for the Care and Use of Laboratory Animals (CICUAL), Biomedical Research Institute-UNAM with the register number 6329..

Studies involving human subjects

Generated Statement: No human studies are presented in this manuscript.

Inclusion of identifiable human data

Generated Statement: No potentially identifiable human images or data is presented in this study.

Data availability statement

Generated Statement: The datasets presented in this study can be found in online repositories. The names of the repository/repositories and accession number(s) can be found in the article/supplementary material.

The genomes of two strains of *Taenia crassiceps* the animal model for the study of human cysticercosis

Raúl J. Bobes[†1], Karel Estrada[†2], Diana G. Rios-Valencia[†1], Arturo Calderón-Gallegos[1], Patricia de la Torre[1], Julio C. Carrero[1], Alejandro Sanchez-Flores[2*] and Juan P. Laclette[1*]

[1]Biomedical Research Institute and [2]Biotechnology Institute, Universidad Nacional Autónoma de México.

† These authors contributed equally to this work and share first authorship

* These authors contributed equally to this work as corresponding authors

*Correspondence:

Juan P. Laclette, Biomedical Research Institute, Universidad Nacional Autónoma de México, Ciudad Universitaria, CP 04510, Coyoacán, Ciudad de México, México.

laclette@iibiomedicas.unam.mx

Alejandro Sanchez-Flores, Biotechnology Institute, Universidad Nacional Autónoma de México, Av. Universidad 201, Col. Chamilpa, CP 62210 Cuernavaca, Morelos, México.

alejandro.sanchez@ibt.unam.mx

Keywords: *Taenia crassiceps,* ORF, WFU, comparative genomics, RNA-seq, differential expression, cysticercosis, animal model.

Abstract

Human cysticercosis by *Taenia solium* is the major cause of neurological illness in countries of Africa, Southeast Asia, and the Americas. Publication of four cestode genomes (*T. solium*, *Echinococcus multilocularis*, *E. granulosus* and *Hymenolepis microstoma*) in the last decade, marked the advent of novel approaches on the study of the host-parasite molecular crosstalk for cestode parasites of importance for human and animal health. *Taenia crassiceps* is another cestode parasite, closely related to *T. solium*, which has been used in numerous studies as an animal model for human cysticercosis. Therefore, characterization of the *T. crassiceps* genome will also contribute to the understanding of the human infection. Here, we report the genome of *T. crassiceps* WFU strain, reconstructed to a noncontiguous finished resolution and performed a genomic and differential expression comparison analysis against ORF strain. Both strain genomes were sequenced using Oxford Nanopore (MinION) and Illumina technologies, achieving high quality assemblies of about 107 Mb for both strains. Dotplot comparison between WFU and ORF demonstrated that both genomes were extremely similar. Additionally, karyotyping results for both strains failed to demonstrate a difference in chromosome composition. Therefore, our results strongly support the concept that the absence of scolex in the ORF strain of *T. crassiceps* was not the result of a chromosomal loss as proposed elsewhere. Instead, it appears to be the result of subtle and extensive differences in the regulation of gene expression. Analysis of variants between the two strains identified 2,487 sites with changes distributed in 31 of 65 scaffolds. The differential expression analysis revealed that genes related to development and morphogenesis in the ORF strain might be involved in the lack of scolex formation.

Introduction

The tapeworm family Taeniidae has been extensively studied, particularly because of the importance of *Taenia solium*, *Taenia asiatica* (Wang et al. 2016, Gripper & Welburn 2017), *Echinococcus granulosus* and *Echinococcus multilocularis* (Battelli 2009, Deplazes et al. 2017) as public health threats. Other species also have veterinary importance such as *Taenia saginata* and *Taenia pisiformis* (Yang et al. 2012, Silva & Costa-Cruz 2012).

T. solium is the cestode parasite that generates a more significant economic and health burden on humans and pigs, this parasite, is responsible of porcine cysticercosis, human teniasis and neurocysticercosis, considered the most frequent parasite disease of the central nervous system (Garcia & Modi, 2008; Fleury et al.,2010; Carpio et al., 2018), and a neglected tropical disease by the World Health Organization in 2010 (WHO, 2010). Humans acquire cysticercosis through fecal-oral contamination with *T. solium* eggs from human tapeworm carriers. The most common places for the establishment of the larval form in the intermediate host are the skeletal muscles, the ocular system and the central nervous system. Cysticercosis is of great economic and public health importance, causing morbidity and mortality in countries and regions with deficient sanitary conditions. Many of these developing countries are located in Southeast Asia, Africa and the Americas (Ito et al. 2003, Flisser et al. 2006, Lustigman et al. 2012, Zammarchi et al. 2013, Ito 2015). In the last decades, cysticercosis has spread to Europe, the United States and Australia, mainly due to the increase in human migration from endemic regions (O'Neal & Flecker 2015, Gabriël et al. 2015). *T. solium* has been globally classified as the main foodborne parasite by the United Nations Food and Agriculture Organization (FAO) in 2014 and the World Health Organization (Torgerson et al. 2015).

Taenia crassiceps, a close relative of *T. solium*, can be easily maintained in most animal facilities and the cysticerci can be manipulated *in vivo* and *in vitro*, providing a suitable model for the study of several aspects of human cysticercosis (Willms & Zurabian 2010). Thus, the intraperitoneal murine infection by *T. crassiceps* has been widely used as a model of cysticercosis in studies of the host immune response, diagnosis, evaluation of anthelmintic drugs, vaccine development (Larralde et al. 1990; Toledo et al., 2001; Vargas-Villavicencio et al. 2005; Sciutto et al. 2011; Mahanty et al. 2013); sex and genetic influence on the susceptibility to infection (Sciutto et al., 1991), influence of the parasite on the hormonal status of the infected host (Morales-Montor et al., 2008), development of practical methods for transfection of exogenous genes (Moguel et al., 2015), among other aspects. Besides, *T. crassiceps* infections in humans are very rare, isolated cases have

been reported in immunosuppressed individuals (Heldwein et al. 2006, Willms & Zurabian 2010; Lescano and Zunt, 2013; Desplazes et al., 2019). Human infections by *T. crassiceps* include subcutaneous and intramuscular (Francois, 1998; Maillard, 1998; Heldwein, 2006; Goesseringer, 2011), intraocular (Shea, 1973; Arocker-Metinger, 1992; Mougeot, 1996; Chuck, 1997) and cerebellum locations (Ntoukas et al. 2011).

As an animal model, the metacestode stage of *T. crassiceps* is usually maintained through serial intraperitoneal passages of cysts from the peritoneal cavity of infected to recipient naïve mice, where they reproduce asexually by budding (Freeman, 1962; Esch and Smyth, 1976; Good & Miller 1976, Willms & Zurabian 2010). Definitive hosts for *T. crassiceps* are foxes, groundhogs, wolves, and dogs, intermediate hosts include field rats, mice and other small rodents, (Loos-Frank 2000).

Several strains of *T. crassiceps* have been reported, such as WFU (Everhart et al. 2004), HYG (Sally et al. 1976) or KBS (Dorais & Esch 1969), isolated from natural infections. The cysticercus possesses an invaginated scolex, which evaginates when ingested by the definitive host and develops into the adult worm. In contrast, the ORF strain of *T. crassiceps*, isolated in 1962 (Freeman et al., 1962), lacks an invaginated scolex and has been considered a mutant strain. It has been proposed that ORF suffered a chromosomal loss that impairs scolex formation (Smith et al., 1972), thus producing sterile larvae that cannot develop into adult worms in the wild (Mount, 1968; Dorais and Esch, 1969); can only be propagated in the laboratory and are considered safe for human manipulation (Freeman 1962).

In terms of genomic resources, the first genome reported for a flatworm was the free living *Schmidtea mediterranea* in 2008 (Robb et al. 2008). Since then, several genomes have been published including trematodes of medical importance such as *Schistosoma japonicum* (Zhou et al. 2009), *S. mansoni* (Berriman et al. 2009) and *Clonorchis sinensis* (Wang et al. 2011; Huang et al. 2013). In 2013, the genomes of four cestodes: *Hymenolepis microstoma*, *Echinococcus granulosus*, *E. multilocularis* and *Taenia solium* were reported (Tsai et al. 2013). Afterwards, the International Helminth Genomes Consortium started a project for genome characterization whose database (WormbaseParasite) already provides 45 Platyhelminthes and 19 cestodes (Helminth & Consortium, 2019).

In the last five years the genomes of other taeniidae have been reported: *T. asiatica*, *T. saginata* (Wang et al. 2016), *T. multiceps* (Li et al. 2018), *E. canadensis* (Maldonado et al. 2017), *E. oligarthrus* (Maldonado et al. 2019), *H. diminuta* (Nowak et al. 2019), *H. microstoma* (Olson et al, 2020). Availability of these genomes has increased the knowledge about gene numbers and

135 composition of these organisms, improving our understanding of their biology and
136 pathogenic mechanisms.

137 Here we report the high resolution characterization for the genome of *T. crassiceps*
138 WFU strain and a comparison analysis against ORF strain. Both genomes were
139 compared in order to find differences that could be related to the lack of scolex
140 development. Our results provide evidence that the absence of scolex in the ORF
141 strain was not the result of a catastrophic event such a chromosomal loss
142 proposed elsewhere. Instead, it appears to be the result of subtle differences in the
143 regulation of gene expression or unidentified mutations in specific genes.

144 **Materials and Methods**

145 **Parasite culture**

146 Cysticerci from *T. crassiceps* strains WFU and ORF were propagated in the
147 peritoneum of 4-week-old female BALB/c mice, which were inoculated
148 intraperitoneally with 10 cysticerci and after 90 days were sacrificed for the
149 recovery of the larvae. The cysticerci were thoroughly washed with sterile
150 Phosphate Buffer Saline (PBS), pH 7.4, and then frozen at -70°C until use. The
151 use and humanitarian handling of animals in this project was authorized by the
152 Institutional Committee for the Care and Use of Laboratory Animals (CICUAL),
153 UNAM with the register number 6329.

154 **Chromosome spreading for *Taenia crassiceps* karyotyping**

155 The protocol for spreading chromosomes was adapted from (Guo et al; 2018 and
156 Špakulová et al; 2018). Cysticerci recovered from the peritoneum of BALB/C mice
157 with three months of infection were selected and placed in 16-well culture plates
158 with RPMI-1640 media supplemented with 10% FBS and colchicine (0.25% w/v)
159 during 5 h at 37 °C. After incubation, cysticerci were washed twice with PBS and
160 then placed in deionized water for 20 min and then fixed with a Methanol-Acetic
161 acid solution (3:1) for 30 minutes. The chromosomes were spread by crushing the
162 cysts between two slides with strong physical pressure. The slides were then
163 frozen with liquid nitrogen and washed twice with PBS before being permeabilized
164 with PBS-Triton X-100 (1%) for 5 min. Finally, the spread was stained with DAPI
165 (1:500) for 20 minutes. Slides were mounted in Fluoroshield (Sigma) and observed
166 under an inverted fluorescence microscope (Olympus IX71). Image analysis was
167 made using FIJI software.

168 **DNA and RNA isolation and sequencing**

Fresh cysticerci (both WFU and ORF strains) obtained from the peritoneum of mice were used for DNA and RNA extraction after three times washing in PBS, pH 7.4. A 1 mL of supernatant from the PBS recovered cysticerci was centrifuged at 12,000 g. The pellet was resuspended in 200 µL of Biofluid & Solid Tissue Buffer, added with 20 µL of Proteinase K and 2 µL de RNAsa (10 mg/mL), and incubated at 55°C for one hour. The lysis reaction was transferred using a bore-tip to a tissue grinder for 10 minutes and 1 mL of phenol was added and after 2 minutes, the solution was centrifuged at 12,000 g for another 2 minutes. A 350 µL volume of the supernatant was transferred to a clean tube and 1mL of chloroform was added. Chloroform addition and centrifugation was repeated twice and 250 µL of the supernatant were recovered and placed in 150 µL of RNAse-free water. DNA was extracted using the Zymo Quick-DNA™ HMW MagBead Kit (Catalog No. D6060) according to the vendor's protocol. The same protocol was adapted for RNA extraction, skipping the 55 ºC incubation and harsher disruption using high-speed vortexing.

Different Illumina sequencing libraries were prepared using the extracted DNA from both WFU and ORF strains. Two Nextera XT DNA libraries, one with ~150 bp insert size and another with a ~500 bp insert size. Also, two Illumina Mate Paired libraries with 3-4 kb and 4-6 kb insert sizes, respectively. All libraries were prepared following the vendor's protocols. For Oxford Nanopore sequencing, the DNA libraries for WFU and ORF DNA samples were prepared using the SQK-LSK109 using 1µg of DNA for each sample and following the vendor's protocol. Sequencing was performed using a whole minION flow cell (v9.4) for each sample. Basecalling was done by the program Guppy v4.0.14 with default parameters.

RNA sequencing libraries were prepared using the Illumina TruSeq RNA Sample Prep Kit v2 (Illumina) following the manufacturer's protocol. High quality RNA samples from WFU and ORF strains, three biological replicates for each one with RIN numbers ranging from 8 to 10 were used for NGS library construction. The libraries were sequenced using the Illumina NextSeq 500 platform with a paired-end configuration using 150 cycles (2x75 reads).

Genome assembly, post-assembly improvement, gene prediction and annotation

A *de novo* genome assembly for WFU strain was performed using a hybrid approach with two different sequencing technologies. The first assembly was obtained using the AllPaths-LG v.52448 (Butler et al., 2008) assembler using default parameters, with Illumina paired-end and mate pair libraries. Then, a second *de novo* assembly was obtained using Oxford Nanopore long reads and Canu v.1.9 (Koren et al., 2017) assembler. This assembly was corrected using two

error correction tools, first Racon v1.3.1 (Vaser et al. 2002) with 3 iterations and later 3 iterations of Pilon v.1.23 (Walker et al. 2014), both used the illumina libraries employed in the first assembly. Finally, both assemblies were merged using the Ntjoin software v.1.0.8 (Coombe et al. 2020). The latest version of the genome can be found with the accession number JAKROA000000000, associated with the BioProject PRJNA807072.

For gene prediction, we first used RepeatModeler v1.0.11 and RepeatMasker v4.08 (Smit and Green. 2013) to softmasking the genome. We used Braker2 v2.1.6 (Brůna et al. 2021) and AUGUSTUS v3.3.2 (Stanke et al. 2006) using a set of 30,000 proteins that were obtained from the most similar orthologs with *T. solium*, *E. multilocularis and E. granulosus* and with the support of 10 Gb of RNAseq data. The protein annotation was achieved using an in-house pipeline with the following steps: first we used Blastp v2.11.0 (Camacho et al. 2009) to align these against the curated protein database Swiss-Prot and assign the function of the protein with the greatest similarity. We used HmmScan v3.3.2 (Eddy, 2009) to search protein domains using the Pfam-A database, additionally we used SignalP v4.1 (Petersen et al., 2011) to identify annotated signal peptides. Finally, we enriched the annotation with the GO and KEGG database, assigning the GO terms associated with each protein and their relationship with metabolic pathways, respectively.

SNPs Analysis

For variant calling and annotation, we used BWA v0.7.17 (Li and Richard2009) to map the Illumina DNA sequencing of the ORF strain vs the WFU genome. Then we used Freebayes v1.2.0 (Garrison and Gabor, 2012) to analyze the BAM resulting from the previous alignment and generate the VCF variants file.

Annotation of the variants was performed using SnpEff v4.3t (Cingolani et al., 2012); the program takes the WFU annotation file in GFF format and its genome as a database and the resulting VCF from the variant call.

Comparative genomics

For the comparative genomic analysis, the genomes available at Genbank for *E. multilocularis* (GCA_000469725.3) and *H. microstoma* (GCA_000469805.3) were used. The Proteinortho v6.02 (Lechner et al., 2011) was used to obtain protein clusters of WFU genomes analyzed here with the following parameters: E-value for blast: 1e-05, minimum percent identity of best blast alignments: 25, minimum coverage of best blast alignments in percent: 50, minimum similarity for additional hits: 0.95. The results from the protein orthologous was also used to verify the

annotation. Additionally, we used the Circos v0.69-8 (Krzywinski et al., 2009) package for circular data visualization.

Differential expression analysis

We used Bowtie2 v2.3.4.3 (Langmead and. Salzberg, 2012) to map the sequences from WFU and ORF RNAseq libraries to the coding sequences (CDS) of WFU strain. Subsequently, the counting matrices were obtained with Express v1.5.1 (Roberts et al., 2011) and finally the EdgeR v3.24.3 (Robinson et al., 2010) package was used to obtain the results of the differential expression analysis.

Gene Ontology Analysis

We used the R package TopGO v2.46.0 (Alexa and Rahnenfuhrer, 2010) to perform enrichment analysis of the differentially expressed gene set.

Results

Genome assembly and curation

The complete genome for the *T. crassiceps* WFU strain was sequenced using genomic DNA obtained from cysts and reconstructed through a hybrid approach using Illumina and Nanopore technologies. The initial assembly produced 179 scaffolds for a total of 118.7 Mb. However, several of the shorter scaffolds presented repetitive patterns or high similarity to regions in larger scaffolds. After performing the comparison analysis at sequence level, we confirmed that 114 scaffolds belonged to telomeric or collapsed regions. Therefore, the curated final assembly we obtained included only 65 scaffolds for a total of 107.05 Mb. The statistics of the two genomic assemblies are shown in Table 1.

Noncontiguous finished resolution for *T. crassiceps* genome and comparative genomics

We compared the ten largest scaffolds in the curated assembly of *T. crassiceps* with data from genomes of two closely related species with chromosome resolution assemblies. A CIRCOS plot comparison between *H. microstoma*, *E. multilocularis* and *T. crassiceps* is shown in Figure 1A. Three *T. crassiceps* scaffolds presented a similar degree of completeness and synteny to *E. multilocularis* chromosomes: scaffolds 1-3 of *T. crassiceps* vs. scaffolds 2, 4 and 3 from *E. multilocularis*, respectively. This suggested that these scaffolds might correspond to whole chromosomes. However, none of the compared *T. crassiceps* scaffolds showed a clear correspondence to *H. microstoma* scaffolds demonstrating a larger phylogenetic distance.

An extensive comparison of the identified proteins was carried out with five other species of cestodes to analyze their orthology with *T. crassiceps*. The proteomes of four taeniid species (*T. solium, E. multilocularis*, *E. granulosus* and *E. canadiensis*), as well as *H. microstoma* were compared against *T. crassiceps* proteins (Supplementary File 1). A total of 4,665 ortholog groups were found in all species (cestode pan-genome); 5,221 were found in the five species of the family *Taeniidae*; 6,842 ortholog groups were shared with *T. solium* which is the closest species with *T. crassiceps*. Finally, 2,822 proteins were unique to *T. crassiceps* and did not cluster with other proteins in any other genome. Among these, 2,173 didn't have a functional annotation.

Genomic variation between *T. crassiceps* WFU and ORF strains

Using the curated assembly of *T. crassiceps* WFU genome as a template, we evaluated the differences of the ORF strain. A dotplot analysis indicated that both assemblies were extremely close (Figure. 1B); no differences among them were found that might suggest that a catastrophic genomic event happened in the ORF strain, such as the loss of a complete chromosome. As for the differences in both strains, using short read mapping with the Illumina sequencing, we found 2,487 site variants in ORF, distributed in 31 of the 65 scaffolds in the WFU curated assembly. Of these, 155 variants affected 147 protein coding genes resulting in missense or frameshift mutations. Variants were mainly single-base substitutions, insertions or deletions. Since long read sequencing was also done for the ORF strain, we searched for larger structural changes but none was found. All the information regarding the variants between the two strains can be found in the Supplementary File 1.

WFU and ORF karyotype determination

It has been proposed that the lack of scolex in the ORF strain was due to an aneuploidy: a loss of a pair of chromosomes. Therefore, we also carried out a chromosome spreading to karyotype the metaphase nuclei of both strains. Interestingly the number 2n = 16 or 18 appeared with similar frequencies. This observation has been reported elsewhere (Špakulová et al., 2011). Whatever the number of chromosome pairs might be, we were unable to observe differences in both strains (not shown). It is worth mentioning that the morphologic resolution we achieved did not allow us to observe if differences in the chromosome structure existed.

Differential expression analysis between ORF and WFU strains of *T. crassiceps*

To elucidate the molecular basis of the phenotypic differences between WFU and ORF in relation with the lack of scolex development, we performed a differential expression analysis. A total of 231 genes were found differentially expressed in the ORF strain. Among them, 123 and 109 genes were up and down-regulated,

316 respectively (Supplementary File 1). Using a GO term enrichment analysis of the
317 59 down-regulated genes that had functional annotation in ORF, different protein
318 families were identified. Interestingly, some of them were related to embryonic
319 digestive tract morphogenesis, mesenchymal cell differentiation, maintenance of
320 animal organ identity, establishment of protein localization, among others
321 (Supplementary File 1). Differentially expressed genes were also characterized by
322 GO revealing a particular enrichment for both up and down-regulated genes
323 related to integral membrane proteins in the cellular component category (Figure
324 2). In the same category, a considerable number of genes related to cytoskeleton
325 were down-regulated. For up-regulated genes (Figure 3), in the biological
326 processes category, most of the differentially expressed genes were grouped
327 within response to stimulus. In total, 45 UF genes were also down regulated in
328 ORF (Supplementary File 1).

329 **Differentially expressed genes and genomic variation**

330 Analysis of genes with different expression levels whose coding sequence
331 contained SNPs allowed the identification of 17 genes, including 5 of unknown
332 function. Among the annotated genes, 3 were up-expressed and 7 were down-
333 expressed in ORF, including some related with development, such as homeobox
334 IRX-5 (TcrWFU_07074), rolling stone [rost] (TcrWFU_02139), as well as genes
335 participating in the cell cycle: ubiquitin carboxyl terminal hydrolase 16
336 (TcrWFU_00103) and others involved in signal transduction pathways: Axin-1
337 (TcrWFU_07383) that participates in the Wnt/ß catenin pathway (Supplementary
338 File 1).

339

340 **Discussion**

341 The present work describes the characterized genomes and RNAseq results of two
342 *T. crassiceps* strains (WFU and ORF), that are widely used as animal models for
343 the study of human cysticercosis. The use of *T. crassiceps* as an adequate animal
344 model seems justified in the light of our results of ortholog proteins in both species
345 shown here; 6,842 ortholog groups were shared with *T. solium* demonstrating a
346 high evolutionary closeness with *T. crassiceps*.

347 As mentioned above, the ORF strain lost the capacity to develop a scolex,
348 structure that gives rise to the adult worm. It has been proposed that the absence
349 of the scolex in the ORF strain was due to the loss of a pair of chromosomes
350 (Smith et al.,1972). We undertook a genomic and transcriptomic characterization of
351 these two strains as a way to approach this proposal. Initially, a dotplot analysis
352 using the two assemblies showed minimal differences between both strains.

Moreover, our karyotyping results did not reveal differences between the chromosome number in both strains, such as the absence of a whole chromosome pair (aneuploidy) reported previously (Smith et al., 1972). Even without a full chromosome resolution, the genomic information from both strains revealed no differences or massive structural changes that might support this catastrophic chromosomal event. Only minor differences were found in the genome drafts of both strains, including gene number, GC content and SNPs number. Instead, we hypothesize that the loss of scolex is the result of changes in the expression of genes involved in the development of this crucial structure in the ORF strain. In order to identify the network of genes resulting in the lack of scolex, we decided to analyze differences in gene expression (up or down-regulated) in the ORF strain. Considering that the scolex is the structure that gives rise to the adult stage of the parasite, we explored a diversity of genes related to embryonic development, formation of the anteroposterior axis, cell division, establishment of mitotic spindle orientation, among others.

The genome of *T. crassiceps* WFU strain was reconstructed using long and short read sequencing technologies. This allowed us to generate a noncontiguous high resolution genome, which was compared to the ORF strain and other cestode genomes with similar or higher resolution. According to the BUSCO completeness analysis, the reconstructed genome had a 78.5% completeness which is similar to the *E. multilocularis* genome (GCA_000469725.3). It is expected that genomes from parasitic species have a lower completeness due to a lack of proteins that are present in other free living eukaryotes. Interestingly, the ten largest fragments have a size similar to chromosomes in other species and five of them had a similar arrangement to chromosomes in *E. multilocularis*, which is a manually curated genome and a closely related species to *T. crassiceps*; both are included within the same family (Taenidae). Three *T. crassiceps* chromosomes (scaffolds 1-3) presented a very similar synteny to *E. multilocularis* but some of the comparisons suggested that other large fragments of *T. crassiceps* can also be arranged on the structure of other chromosomes in *E. multilocularis* (Figure 1A), although rearrangements cannot be ruled out. Therefore, other approaches like optical mapping can be used to resolve the assembly contiguity in the near future. Unfortunately, the current fragmentation of the *T. solium* genome, didn't allow us to include it in the comparison. We also evaluated the orthology between other cestodes and reported a pangenome of 5,221 ortholog groups found among five species of the Taeniidae family. Despite that more than half of the proteins (6,842 ortholog groups) were shared between *T. solium* and *T. crassiceps*, there were 2,822 unique proteins for the latter, where 2,173 remained without functional annotation and deserve further exploration to elucidate their role in this parasite.

A total of 232 genes were found with a change in their expression level, 140 of them had annotated function. Our RNA-seq results indicated that 123 were upregulated and 109 genes were downregulated in ORF, in comparison to the WFU strain, considered as the wild-type strain in this work. Those changes in expression included zinc finger proteins, transcription factors, oncosphere antigens, homeoboxes, etc., that had been identified in previous studies on other cestode species. For example, genes that encode for homeobox B7 (HoxB7) and the zinc finger protein are mainly correlated with processes of cell differentiation and segmentation in the adult stage, since they are presented distinctively in adult worms of cestode species. Some of these genes with a differential expression in *T. crassiceps* have also been found up or downregulated in other cestodes (Olson et al., 2018).

In the ORF strain, down-regulated genes included one homeobox that has been related to the strobilation process in cestodes. Strobilation is a process that occurs in adult worms in which new proglottids are produced from the neck region. Around 34 genes are related with this process, including 12 with known function (Wnt, TGFbeta/BMP or G-protein signaling pathways) and 22 missing functional annotation (Prado-Paludo et al., 2020). This suggested that some of the unidentified proteins in the *T. crassiceps* genome that are up or down-regulated could also participate in the strobilation. In the WFU strain of *T. crassiceps*, the higher expression of some of these genes could be related to the development of the adult phase.

A study of the expression of specific genes of each stage in *H. microstoma* shows the differential presence of proteins in several body regions of this cestode (Olson et al., 2018). In this case, one of the proteins that are up-regulated in the larva in comparison with the adult worm was frizzled (fzd), which plays an important role in the Wnt signaling pathway. Our data showed that frizzled (TcrWFU_07188) was down-regulated in the ORF strain. Proteins up-regulated in ORF such as Dystrobrevin-1 (TcrWFU_10303) and aquaporin-4 (TcrWFU_02255) have been found in the *Echinococcus* encystment process playing a role of vasopressor and water reabsorption (Fan et al., 2020). These mechanisms have been related to the transport of proteins, carbohydrates, and other substances (Park et al., 2015). Down-regulated in the ORF strain (in comparison to WFU) whose function could be related to its inability to form a scolex, were seven genes involved in embryonic development and morphogenesis (Supplementary File 1). Among them, transcription factor 21 (TcrWFU_01181), a member of a subfamily of basic-helix-loop-helix proteins (bHLH) showed a high differential expression (LogFC = -2.02). This factor has been reported to play an important role in embryonic development of mesodermal tissues (Quaggin et al, 1998). Since the mesoderm gives rise to the

notochord and the neural tube, it is also involved in the definition of the anteroposterior axis (Corallo et al., 2015). Another down-regulated protein (LogFC = - 2.23) in ORF is the Tyrosine protein-kinase src-1 (TcrWFU_10053), which together with Wnt, plays an essential role in embryonic development contributing to spindle orientation and endoderm specification in early development (Bei et al., 2002). Noteworthy, this gene is exclusively expressed in some head neurons of the nematode *Caenoharbditis elegans*, but not in its tail (Takashi, et al, 2003). Activated CDC42 kinase 1 (TcrWFU_02666), which is also down-regulated in the ORF strain (LogFC = -2.56), is a non-receptor tyrosine-protein and serine/threonine-protein kinase, implicated in reorganization of actin cytoskeleton for the regulation of the cellular protruding activity during cell spreading, mainly in neuronal development. Two other proteins also related to embryonic development, that were found down-regulated in ORF were the FMRF amide-activated amiloride-sensitive sodium channels (TcrWFU_03780 and TcrWFU_07460), whose LogFC were = -2.12 and -2.02, respectively. These proteins, which are voltage and cyclic nucleotide-gated ion channels, have been shown to be expressed prominently in the neuronal tissue of *D. melanogaster* (Marx et al., 1999). Since, the attachment of the worm to the surface of the intestinal epithelium would require some kind of anterior sensorial organ in the scolex of *T. crassiceps*, the deficiency of this channel in ORF could also be involved in scolex development. Finally, the other down-regulated genes in ORF also included the potassium/sodium hyperpolarization-activated cyclic nucleotide gated channel [(LogFC = -2.6) (TcrWFU_06892)], mediating responses to stimuli; and the fibroblast growth factor receptor-like 1 [(LogFC = -2.08) (TcrWFU_04317)], involved in the development of organisms and expressed in the anterior region (Lamb et al., 1995, Teven et al., 2014).

Regarding proteins that are up-regulated in the ORF strain, one was the G protein-signaling modulator 2 [(LogFC = 2.43) (TcrWFU_07618)] belonging to a group of proteins that have the ability to activate G proteins. They are proteins involved in different biological processes, for example, cell division, establishment and organization of mitotic spindle also playing an important role in asymmetric cell divisions via NuMA (Du et al., 2001; Zhu et al, 2011; Kiyomitsu and Cheeseman, 2012). Some reports focus on G protein regulators (GPRs) in asymmetric positioning of the mitotic spindle in the early *C. elegans* embryo (Manning, 2003).

Proteins related to maintenance of animal organ identity were also upregulated in ORF (Supplementary Table 2); among them, Fibronectins type III domain [(TcrWFU_10230, TcrWFU_10661, TcrWFU_10672 and TcrWFU_08319) (LogFC = 7.03, 8.13, 4.09 and 7.31)] are conserved proteins widely distributed in different species, three of them are reported as oncospheral proteins. In *Trichinella spiralis*,

these proteins may be involved in the mechanism allowing invasion of epithelial cells in the intestine (Ren et al., 2013). Also, an oncospheral fibronectin type III domain has been used to develop a successful vaccine against porcine cysticercosis (Flisser et al. 2004; González et al., 2005; Gauci et al., 2012). Finally, ORF cysticerci have a quicker reproductive rate in the peritoneal cavity of mice (Everhart et al., 2004; Fragoso et al., 2008; Willms and Zurabian 2010), suggesting that upregulation of proteins related to cell proliferation and differentiation are involved. These findings allow focusing future studies to determine the causative agent of the lack of scolex in ORF.

Genomic variation analysis of differentially expressed genes

In addition to the genes that were found differentially expressed between the two strains (Supplementary Table 1), we identified another group of 17 genes that were slightly down-regulated in ORF, containing moderate and high impact SNPs and other variations (Supplementary File 1). For example, the gene that codes for Iroquois-class homeodomain protein IRX-5 (TcrWFU_07074), which is a transcription factor that has been associated with craniofacial development through modulating the migration of progenitor cells in the branchial arches of *Xenopus laevis* embryos; mutation of this gene prevents the correct craniofacial development causing dysmorphism (Bonnard et al., 2012). In ORF, we found that the SNP on IRX-5 contains a missense change (c.290T>C) with respect to WFU, suggesting that this mutation could affect its function and contribute to the lack in the development of the scolex.

Other gene with a high impact change (frameshift c.260delG) was the ubiquitin carboxyl-terminal hydrolase 16 [(UBP16) (TcrWFU_00103)], resulting in an amino acid deletion which might affect its important role in the deubiquitination of histone H2A, necessary for the progress of M phase in the cell cycle (Cai et al., 1999, Joo et al., 2007). On the other hand, UBP16 has been observed in *X. laevis* embryos, playing a role in the regulation of HOX genes through deubiquitination of histone H2A, which leads to the correct development of the anterior-posterior embryonic pattern (Joo et al., 2007). Huntingtin (TcrWFU_07407), a large protein with a molecular mass of 348 kDa, included a SNP involving an amino acid deletion (c.1726delA). The normal function of this protein is not fully understood, however, it has been reported that targeted elimination of this protein in mice produces early embryonic lethality. All of its orthologs have a similar size and contain HEAT repeats: huntingtin, elongator factor 3, PR65/A (a regulatory subunit of PP2A) and Tor1 (Schulte et al., 2011). These are highly conserved proteins in vertebrates (Baxendale et al., 1995; Tartari et al., 2008). HEAT repeats are believed to mediate

508 protein-protein interactions (Takano et al., 2002); within huntingtin, its distribution
509 could confer a scaffolding role for the formation of protein complexes.

510 Another downregulated gene in the ORF strain was Axin-1/DIX (TcrWFU_07383);
511 which has been described as a protein with multiple functions, including the
512 regulation of Wnt/beta-catenin (cWnt) signaling pathway. Axin-1/DIX in ORF strain
513 presented a SNP (c.1131delC) producing a frameshift of high-impact effect. Being
514 a versatile scaffold protein involved in the separation of the centrosome and the
515 spindle assembly in mitosis, its malfunction in the Wnt/beta catenin (cWnt)
516 signaling pathway could impede important roles in different biological processes,
517 including cell growth, differentiation, polarity formation (Petersen and Reddien,
518 2009). Axins could interact with a beta-catenin paralog, limiting their accumulation;
519 having highly segregated expression patterns along the anteroposterior axis in *E.*
520 *multilocularis* and *H. microstoma*, this would indicate that beta-catenin destruction
521 complexes act during larval metamorphosis (Montagne et al., 2019).

522 Another down-regulated gene also containing a high impact SNP in the ORF strain
523 was the so-called rolling stone protein [rost] (TcrWFU_02139). The rost gene has
524 been identified in *Drosophila*, related to the regulation of a network of proteins
525 involved in the process of differentiation of the body wall musculature and in the
526 fusion of myoblasts to myotubes (Paululat et al., 1995, 1997). Rost in the ORF
527 strain showed a SNP producing a frameshift (c.213delA).

528 Taken together, the above data suggest that the lack of development of the scolex
529 of the ORF strain of *T. crassiceps* could result from the action of multiple genes
530 involved in the development of the anterior part of the parasite. Although a detailed
531 scheme cannot be advanced at this point, something that can be ruled out is the
532 proposal that the lack of scolex was due to a catastrophic genomic change, such
533 as the loss of complete chromosomes (Smith et al., 1972). Instead, our results
534 suggest that it was due to a series of smaller changes, including single point
535 mutations or differential expression of gene networks. Survival of this strain in
536 natural conditions appears to be impractical. The role of specific genes in the
537 formation of the scolex could be approached through gene silencing experiments
538 on WFU cysts (Guerrero-Hernández et al., 2021).

539 Elucidation of the genomes of two strains of *T. crassiceps* will improve our
540 knowledge about the genomic similarities and differences that exist between
541 taeniid species, allowing novel approaches to a number of unsolved questions on
542 tapeworm infections, including human neurocysticercosis caused by *T. solium*. We
543 identified several conserved proteins for all cestodes as well as some proteins that
544 are unique to the *Taenia* genus and the *T. crassiceps* species. In this respect,
545 improving the resolution of the *T. solium* genome is a must for future studies of

546 comparative genomics within Taeniidae. Comparison between genomes might
547 become a pipeline for the identification of potential targets and the design of new
548 drugs, diagnostic tools or vaccines. Finally, availability of these high quality
549 assemblies of *T. crassiceps* (WFU and ORF) can also contribute to defining the
550 usefulness and limits of this animal model for the improvement of our
551 understanding on human cysticercosis.

552 **Authors contributions**

553 KE performed the hybrid genome assembly, gene prediction, RNAseq differential
554 expression and GO/KEGG enrichment analysis; PT performed initial sequencing,
555 PT, DRV and RJB maintained and isolated the cysts in mice, RJB, KE, DRV, ACG
556 and JCC carried out the gene annotation, differential protein expression analysis,
557 ASF and KE did the comparative genomics (SNP and synteny analyses). JPL and
558 ASF conceived the project. RJB, KE and DRV prepared the first draft and ASF and
559 JPL developed the final version. JPL provided the budget from grants. All authors
560 approved the submitted version.

561 **Funding**

562 This report was supported in part by grants A1-5-11306 (CONACYT) and [IN
563 205820] PAPIIT-UNAM.

564 **Conflict of interest**

565 The authors declare that they have no known competing financial interests or
566 personal relationships that could have appeared to influence the work reported in
567 this paper.

568 **Acknowledgments**

569 We are grateful to R. Grande and J. Verleyen for sequencing and bioinformatic
570 support and to "Unidad de Secuenciación Masiva y Bioinformática" (UUSMB) of
571 the "Laboratorio Nacional de Apoyo Tecnológico a las Ciencias Genómicas,"
572 (CONACyT) in the Biotechnology Institute (UNAM). Infected mice were maintained
573 in the Unidad de Modelos Biológicos at the Biomedical Research Institute. We
574 thank G. Díaz and D. Garzón for the technical support.

575
576
577
578
579

References

Arocker-Mettinger E., Huber-Spitzy V., Auer H., Grabner G., Stur M. (1992). *Taenia crassiceps* in the anterior chamber of the human eye: A case report. *Klin Monbl Augenheilkd*. 201(1):34-7. doi: 10.1055/s-2008-1045865.

Alexa A., Rahnenführer J., and Thomas Lengauer. "Improved scoring of functional groups from gene expression data by decorrelating GO graph structure." *Bioinformatics* 22.13 (2006): 1600-1607.

Battelli., G. (2009). Echinococcosis: Costs, losses and social consequences of a neglected zoonosis. *Vet. Res. Commun.*, Suppl 1:47-52. doi: 10.1007/s11259-009-9247-y.

Baxendale S., Abdulla S., Elgar G., Buck D., Berks M., Micklem G., et al. (1995) Comparative sequence analysis of the human and pufferfish Huntington's disease genes *Nat. Genet.* 10:67. doi: 10.1038/ng0595-67.

Bei Y., Hogan J., Berkowitz, L. A., Soto, M., Rocheleau, C. E., Pang. (2002). SRC-1 and Wnt signaling act together to specify endoderm and to control cleavage orientation in early *C. elegans* embryos. *Developmental cell*, *3*(1), 113–125. doi: 10.1016/s1534-5807(02)00185-5.

Berriman M., Haas B.J., Loverde P.T., Wilson R.A., Dillon G.P., Cerqueira G.C., et al. (2009). The genome of the blood fluke *Schistosoma mansoni*. *Nature* 460: 352–358. doi: 10.1038/nature08160.

Bonnard C., Strobl A., Shboul., M. et al. (2012) Mutations in IRX5 impair craniofacial development and germ cell migration via SDF1. *Nat Genet* 44, 709–713. doi:10.1038/ng.2259.

Brůna T., Hoff K.J., Lomsadze A., Stanke M., Borodovsky M. (2021). BRAKER2: automatic eukaryotic genome annotation with GeneMark-EP+ and AUGUSTUS supported by a protein database. *NAR Genom Bioinform.* 3.1 : lqaa108. doi: 10.1093/nargab/lqaa108.

Butler J., MacCallum I., Kleber M., Shlyakhter I.A., Belmonte M.K., Lander E.S., et al. (2008). ALLPATHS: de novo assembly of whole-genome shotgun microreads. *Genome Research* **18:** 810–20. doi: 10.1101/gr.7337908.

Cai S.Y., Babbitt R.W., Marchesi V.T. A mutant deubiquitinating enzyme (Ubp-M) associates with mitotic chromosomes and blocks cell division (1999)." *Proc. Natl. Acad. Sci.* 96:2828-2833. doi: 10.1073/pnas.96.6.2828.

614 Camacho C., Coulouris G., Avagyan V., Ma N., Papadopoulos J., Bealer K., et al.
615 (2009). BLAST+: architecture and applications. *BMC bioinformatics* 10.1 : 1-9. oi:
616 10.1186/1471-2105-10-421.

617 Carpio A., Fleury A., Matthew L. Romo and Abraham R. (2018).
618 Neurocysticercosis: the good, the bad, and the missing, *Expert Rev Neurother.*
619 18:4, 289-301, doi:

620 Chuck R.S., Olk R.J., Weil G.J., Akduman L., Benenson I.L., Smith M.E., et al.
621 (1997) Surgical removal of a subretinal proliferating cysticercus of *Taeniaeformis*
622 *crassiceps*. *Arch Ophthalmol.* 115(4):562-3.
623 doi:10.1001/archopht.1997.01100150564028.

624 Coombe L., Nikolić V., Chu J., Birol I., Warren R.L. (2020). ntJoin: Fast and
625 lightweight assembly-guided scaffolding using minimizer graphs. *Bioinformatics.*
626 1;36(12):3885-3887. doi: 10.1093/bioinformatics/btaa253.

627 Cingolani P., Platts A., Wang le L., Coon M., Nguyen T., Wang L., et al. (2012). A
628 program for annotating and predicting the effects of single nucleotide
629 polymorphisms, SnpEff: SNPs in the genome of Drosophila melanogaster strain
630 w1118; iso-2; iso-3. *Fly* 6(2):80-92. doi: 10.4161/fly.19695.

631 Corallo D., Trapani V., and Bonaldo P. (2015). The notochord: structure and
632 functions. *Cellular and molecular life sciences: CMLS*, *72*(16), 2989–3008.
633 doi:10.1007/s00018-015-1897-z

634 Deplazes P., Rinaldi L., Alvarez-Rojas C.A., Torgerson P.R., Harandi M.F., Romig
635 T., et al. (2017). Global Distribution of Alveolar and Cystic Echinococcosis. *Adv.*
636 *Parasitol.* 95: 315–493. doi: 10.1016/bs.apar.2016.11.001.

637 Dorais FJ and Esch GW. (1969). Growth rate of two *Taenia crassiceps* strains.
638 *Exp. Parasitol.* 25: 395–398.doi: 10.1016/0014-4894(69)90086-1.

639 Du Q., Stukenberg P.T., Macara I.G. (2001). A mammalian Partner of inscuteable
640 binds NuMA and regulates mitotic spindle organization. *Nat Cell Biol.* 3(12):1069-
641 75. doi: 10.1038/ncb1201-1069.s

642 Eddy S.R. (2009). A new generation of homology search tools based on
643 probabilistic inference. *Genome Inform.* 23(1):205-11.

644 Esch G.W and Smyth J.D. (1976). Studies on the *in vitro* culture of *Taenia*
645 *crassiceps*. *Int. J. Parasitol.* 6, 143–149. doi:10.1016/0020-7519(76)90071-0

Everhart M.E., Kuhn R.E., Zelmer D.A. (2004). Infrapopulation dynamics of a wild strain of *Taenia crassiceps* (WFU) (Cestoda: Taeniidae) in BALB/cJ mice. *J Parasitol.* 90(1):79-84. doi: 10.1645/GE-3255.

Fan J., Wu H., Li K., Liu X., Tan Q., Cao W., et al. (2020). Transcriptomic Features of *Echinococcus granulosus* Protoscolex during the Encystation Process. *Korean J Parasitol.* 58: 287–299. doi: 10.3347/kjp.2020.58.3.287.

Fleury A., Moreno García J., Valdez Aguerrebere P., de Sayve Durán M., Becerril Rodríguez P., et al. (2010). Neurocysticercosis, a persisting health problem in Mexico. *PLoS Negl Trop Dis.* 24;4(8):e805. doi:10.1371/journal.pntd.0000805

Flisser A., Rodríguez-Canul R., Willingham AL. (2006). Control of the taeniosis/cysticercosis complex: Future developments. *Vet. Parasitol.* 139: 283–292. doi: 10.1016/j.vetpar.2006.04.019

Flisser A., Gauci C.G., Zoli A., Martinez-Ocana J.,Garza-Rodriguez A., Dominguez-Alpizar J.L., et al. (2004). Induction of protection against porcine cysticercosis by vaccination with recombinant oncosphere antigens. *Infect Immun.* 72(9):5292-7. doi: 10.1128/IAI.72.9.5292-5297.2004.

François A., Favennec L., Cambon-Michot C., Gueit I., Biga N., Tron F., Brasseur P., et al. (1998). *Taenia crassiceps* invasive cysticercosis: a new human pathogen in acquired immunodeficiency syndrome? *Am J Surg Pathol.* 22(4):488-92. doi: 10.1097/00000478-199804000-00015.

Fragoso G., Meneses G., Sciutto E., Fleury A., Larralde C. (2008). Preferential growth of *Taenia crassiceps* cysticerci in female mice holds across several laboratory mice strains and parasite lines. *J Parasitol.* 94(2):551-553. doi: 10.1645/GE-1287.1.

Freeman RS. (1962). Studies on the biology of *Taenia crassiceps* (ZEDER, 1800) RUDOLPHI, 1810 (CESTODA). *Can. J. Zool.* 40: 969–990.

Gabriël S., Johansen M.V., Pozio E., Smit G.S.A., Devleesschauwer B., Allepuz A., et al. (2015). Human migration and pig/pork import in the European Union: What are the implications for *Taenia solium* infections? *Vet. Parasitol.* 213: 38–45. doi: 10.1016/j.vetpar.2015.03.006.

Garcia H.H., Modi M. (2008). Helminthic parasites and seizures. *Epilepsia* 49: 25–32. doi: 10.1111/j.1528-1167.2008.01753.x.

678 Garrison E and Gabor M. (2012). Haplotype-based variant detection from short-
679 read sequencing. arXiv preprint arXiv:1207.3907

680 Gauci C.G., Jayashi C.M., Gonzalez A.E., Lackenby J., Lightowlers M.W. (2012).
681 Protection of pigs against *Taenia solium* cysticercosis by immunization with novel
682 recombinant antigens. *Vaccine*.6;30(26):3824-8.
683 doi:10.1016/j.vaccine.2012.04.019.

684 Goesseringer N., Lindenblatt N., Mihic-Probst D., Grimm F., Giovanoli P. (2011)
685 *Taenia crassiceps* upper limb fasciitis in a patient with untreated acquired
686 immunodeficiency syndrome and chronic hepatitis C infection--the role of surgical
687 debridement. *J Plast Reconstr Aesthet Surg*. 64(7):e174-6. doi:
688 10.1016/j.bjps.2011.02.011.

689 Good A.H., Miller K.L. (1976). Depression of the immune response to sheep
690 erythrocytes in mice infected with *Taenia crassiceps* larvae. *Infect. Immun.* 14:
691 449–456. doi: 10.1128/iai.14.2.449-456.1976.

692 Gonzalez A.E., Gauci C.G., Barber D., Gilman R.H., Tsang V.C., Garcia H.H., et al.
693 (2005). Vaccination of pigs to control human neurocysticercosis. *Am J Trop Med*
694 *Hyg*. 72(6):837-9.

695 Gripper L.B., Welburn S.C. (2017). Neurocysticercosis infection and disease-A
696 review. *Acta Trop*. 166:218-224. doi: 10.1016/j.actatropica.2016.11.015.

697 Guerrero-Hernández J., Bobes RJ., García-Varela M., Castellanos-Gonzalez A.,
698 Laclette JP. (2022). Identification and functional characterization of the siRNA
699 pathway in *Taenia crassiceps* by silencing Enolase A. *Acta Trop*. 225:106197. doi:
700 10.1016/j.actatropica.2021.106197.

701 Guo L., Accorsi A., He S., Guerrero-Hernández C., Sivagnanam S., McKinney S.,
702 et al., (2018). An adaptable chromosome preparation methodology for use in
703 invertebrate research organisms. *BMC Biol*. 26;16(1):25. doi: 10.1186/s12915-018-
704 0497-4.

705 Heldwein K., Biedermann H.G., Hamperl W.D., Bretzel G., Löscher T., Laregina D.,
706 et al. (2006). Subcutaneous *Taenia crassiceps* infection in a patient with non-
707 Hodgkin's lymphoma. *Am J Trop Med Hyg*. 75(1):108-11.

708 Helminth I Consortium G. (2019). Comparative genomics of the major parasitic
709 worms. *Nature Genetics*. 51(1):163-174. doi:10.1038/s41588-018-0262-1.

710 Huang Y., Chen W., Wang X., Liu H., Chen Y., Guo L., et al., (2013). The
711 Carcinogenic Liver Fluke, *Clonorchis sinensis*: New Assembly, Reannotation and
712 Analysis of the Genome and Characterization of Tissue Transcriptomes. *PLoS One*
713 8: e54732. 2013;8(1):e54732. doi: 10.1371/journal.pone.0054732.

714 Ito A. (2015). Recent advances and perspectives in molecular epidemiology of
715 *Taenia solium* cysticercosis. (2016). *Infect Genet Evol*. 40:357-367.
716 doi:10.1016/j.meegid.2015.06.022.

717 Ito A., Nakao M., Wandra T. (2003). Human taeniasis and cysticercosis in Asia.
718 *Lancet* 362: 1918–1920. doi:10.1016/S0140-6736(03)14965-3.

719 Joo H.Y., Zhai L., Yang C., Nie S., Erdjument-Bromage H., Tempst P., et al.
720 (2007). Regulation of cell cycle progression and gene expression by H2A
721 deubiquitination. *Nature*. 449, 1068-72. doi:10.1038/nature06256.

722 Kiyomitsu T and Cheeseman I.M. (2012). Chromosome- and spindle-pole-derived
723 signals generate an intrinsic code for spindle position and orientation. *Nat Cell Biol*.
724 12;14(3):311-7. doi:10.1038/ncb2440.

725 Koren S., Walenz B.P., Berlin K., Miller J.R., Bergman N.H., Phillippy A.M. (2017).
726 Canu: scalable and accurate long-read assembly via adaptive k-mer weighting and
727 repeat separation. *Genome research* 27(5) 722-736. doi: 10.1101/gr.215087.116.

728 Krzywinski M., Schein J., Birol I., Connors J., Gascoyne R., Horsman D., et al.
729 (2009). Circos: an information aesthetic for comparative genomics. *Genome*
730 *research 19(9):1639-45. doi: 10.1101/gr.092759.109.*

731 Lamb T.M., Harland R.M. (1995). Fibroblast growth factor is a direct neural
732 inducer, which combined with noggin generates anterior-posterior neural pattern.
733 *Development*. 121(11):3627-36.

734 Langmead B., Salzberg S.L. (2012). Fast gapped-read alignment with Bowtie 2.
735 *Nat Methods*. 4;9(4):357-9. doi: 10.1038/nmeth.1923.

736 Larralde C., Sotelo J., Montoya R.M., Palencia G., Padilla A., Govezensky T., et
737 al., (1990). Immunodiagnosis of human cysticercosis in cerebrospinal fluid.
738 Antigens from murine *Taenia crassiceps* cysticerci effectively substitute those from
739 porcine *Taenia solium*. *Arch. Pathol. Lab. Med*. 114: 926–928.

740 Lechner M., Findeiss S., Steiner L., Marz M., Stadler P.F., Prohaska S.J., et al.
741 (2011). Proteinortho: detection of (co-) orthologs in large-scale analysis. *BMC*
742 *bioinformatics* 28; 12:124. doi: 10.1186/1471-2105-12-124. 12.1: 1-9.

743 Lescano A.G., Zunt J. (2013). Other cestodes: sparganosis, coenurosis and
744 *Taenia crassiceps cysticercosis*. *Handb Clin Neurol*. 114:335-45.
745 doi:10.1016/B978-0-444-53490-3.00027-3.

746 Li W., Liu B., Yang Y., Ren Y., Wang S., Liu C., et al. (2018). The genome of
747 tapeworm *Taenia multiceps* sheds light on understanding parasitic mechanisms
748 and control of coenurosis disease. *DNA Res*. 25: 499–510.
749 doi:10.1093/dnares/dsy020.

750 Li Heng and Richard Durbin. (2009). Fast and accurate short read alignment with
751 Burrows–Wheeler transform. *Bioinformatics* 25(14):1754-60. doi:
752 10.1093/bioinformatics/btp324.

753 Loos-Frank B. (2000). An up-date of Verster's (1969) "Taxonomic revision of the
754 genus Taenia Linnaeus" (Cestoda) in table format. *Syst. Parasitol*. 45: 155–183.
755 doi:10.1023/a:1006219625792.

756 Lustigman S., Prichard R.K., Gazzinelli A., Grant W.N., Boatin B.A., McCarthy J.S.,
757 et al. (2012). A research agenda for helminth diseases of humans: The problem of
758 helminthiases. *PLoS Negl. Trop. Dis*. 6. doi:10.1371/journal.pntd.0001582.

759 Mahanty S., Madrid E.M., Nash T.E. (2013). Quantitative screening for anticestode
760 drugs based on changes in baseline enzyme secretion by *Taenia crassiceps*.
761 *Antimicrob. Agents Chemother*. 57(2):990-5. doi:10.1128/AAC.01022-12.

762 Maillard H., Marionneau J., Prophette B., Boyer E., Célerier P. (1998). *Taenia*
763 *crassiceps* cysticercosis and AIDS. *AIDS*. 20;12(12):1551-2.
764 doi:10.1097/00002030-199812000-00019.

765 Maldonado L.L., Arrabal J.P., Rosenzvit M.C., Kamenetzky L. (2019). Revisiting
766 the Phylogenetic History of Helminths Through Genomics, the Case of the New
767 *Echinococcus oligarthrus*. *Genome*. 7; 10:708. doi: 10.3389/fgene.2019.00708.
768 eCollection 2019.

769 Maldonado L.L., Assis J., Araújo F.M.G., Salim A.C.M., Macchiaroli N., Cucher M.,
770 et al. (2017). The *Echinococcus canadensis* (G7) genome: a key knowledge of
771 parasitic platyhelminth human diseases. *BMC Genomics*. 27;18(1):204.
772 doi:10.1186/s12864-017-3574-0.

773 Manning D.R. (2003). Evidence mounts for receptor-independent activation of
774 heterotrimeric G proteins normally in vivo: positioning of the mitotic spindle in *C.*
775 *elegans*. *Sci STKE*. 19;2003(196):pe35. doi:10.1126/stke.2003. 196.pe35.

776 Marx T., Gisselmann G., Störtkuhl, K. F., Hovemann B. T., and Hatt H. (1999).
777 Molecular cloning of a putative voltage- and cyclic nucleotide-gated ion channel
778 present in the antennae and eyes of Drosophila melanogaster. *Invertebrate*
779 *neuroscience : IN*, *4*(1), 55–63. doi:org/10.1007/pl00022368

780 Moguel B., Moreno-Mendoza N., Bobes R.J., Carrero J.C., Chimal-Monroy J.,
781 Díaz-Hernández M.E., et al. (2015). Transient transgenesis of the tapeworm
782 *Taenia crassiceps*. *Springerplus*. 15; 4:496. doi: 10.1186/s40064-015-1278-y.

783 Montagne J., Preza M., Castillo E., Brehm K., Koziol U. (2019). Divergent Axin and
784 GSK-3 paralogs in the beta-catenin destruction complexes of tapeworms. *Dev*
785 *Genes Evol*. 229(4):89-102. doi: 10.1007/s00427-019-00632-w.

786 Morales-Montor J., Escobedo G., Vargas-Villavicencio J.A., Larralde C. (2008).
787 The neuroimmunoendocrine network in the complex host-parasite relationship
788 during murine cysticercosis. *Curr Top Med Chem*. 8(5):400-7. doi:
789 10.2174/156802608783790866.

790 Mougeot G., Cambon M., Dimeglio V., Menerath J.M. (1996). Cestodose larvaire
791 intra-oculaire chez un jeune garçon de 14 ans en Auvergne [Intraocular Cestode
792 larva in a 14-year-old boy in Auvergne]. *Presse Med*. 7;25(25):1168.

793 Nowak R.M., Jastrzębski J.P., Kuśmirek W., Sałamatin R., Rydzanicz M., Sobczyk-
794 Kopcioł A., et al. (2019). Hybrid de novo whole-genome assembly and annotation
795 of the model tapeworm *Hymenolepis diminuta*. *Sci. Data*. 3;6(1):302.
796 doi:10.1038/s41597-019-0311-3.

797 Ntoukas V., Tappe D., Pfütze D., Simon M., Holzmann T. (2013). Cerebellar
798 cysticercosis caused by larval *Taenia crassiceps* tapeworm in immunocompetent
799 woman, Germany. *Emerg Infect Dis*. 19(12):2008-2011.
800 doi:10.3201/eid1912.130284

801 O'Neal S.E., Flecker RH. (2015). Hospitalization frequency and charges for
802 neurocysticercosis, United States. 2003–2012. *Emerg. Infect. Dis*. 21: 969–976.
803 doi: 10.3201/eid2106.141324.

804 Olson P.D., Tracey A., Baillie A., James K., Doyle S.R., Buddenborg S.K., et al.
805 (2020). Complete representation of a tapeworm genome reveals chromosomes
806 capped by centromeres, necessitating a dual role in segregation and protection.
807 *BMC Biol*. 9;18(1):165. doi: 10.1186/s12915-020-00899-w.

808 Olson P.D., Zarowiecki M., James K., Baillie A., Bartl G., Burchell P., et al. (2018).
809 Genome - wide transcriptome profiling and spatial expression analyses identify

signals and switches of development in tapeworms. *Evodevo*: 1–29. doi: 10.1186/s13227-018-0110-5.

Paululat A., Burchard S., Renkawitz-Pohl R. (1995). Fusion from myoblasts to myotubes is dependent on the rolling stone gene (rost) of *Drosophila*. *Development*. 121(8):2611-20.

Paululat A., Goubeaud A., Damm C., Knirr S., Burchard S., Renkawitz-Pohl R. (1997). The mesodermal expression of rolling stone (rost) is essential for myoblast fusion in Drosophila and encodes a potential transmembrane protein. *J Cell Biol*. 28;138(2):337-48. doi: 10.1083/jcb.138.2.337.

Prado-Paludo G., Thompson C.E., Miyamoto K.N., Lucas R., Guedes M., Zaha A., et al. (2020). Cestode strobilation: prediction of developmental genes and pathways. *BMC Genomics*. 16;21(1):487. doi: 10.1186/s12864-020-06878-3.

Park E.J., Kwon T.H. (2015). A Minireview on Vasopressin-regulated Aquaporin-2 in Kidney Collecting Duct Cells. *E & BP*. 13(1):1-6. doi: 10.5049/EBP.2015.13.1.1.

Petersen C.P., Reddien PW. (2009) A wound-induced Wnt expression program controls planarian regeneration polarity. *Proc Natl Acad Sci U S A* 106:17061–17066 1–6. doi: 10.1073/pnas.0906823106.

Petersen T., Brunak S., von Heijne, G. et al. (2011). SignalP 4.0: discriminating signal peptides from transmembrane regions. *Nat Methods* 8(10):785-6. doi: 10.1038/nmeth.1701. PMID: 21959131.

Quaggin S. E., Vanden H., and Igarashi P. (1998). Pod-1, a mesoderm-specific basic-helix-loop-helix protein expressed in mesenchymal and glomerular epithelial cells in the developing kidney. *Mech Dev*. 71(1-2), 37–48. doi:10.1016/s0925-4773(97)00201-3.

Ren H.J., Cui J., Yang W., Liu R.D., Wang Z.Q. (2013). Identification of differentially expressed genes of *Trichinella spiralis* larvae after exposure to host intestine milieu. *PLoS One*. 28;8(6):e67570. doi: 10.1371/journal.pone.0067570.

Robb S.M.C., Ross E., Alvarado A.S. (2008). SmedGD: The *Schmidtea mediterranea* genome database. *Nucleic Acids Res*. 36: D599-606. doi: 10.1093/nar/gkm684.

Roberts A., Trapnell C., Donaghey J., Rinn J.L., Pachter L. (2011). Improving RNA-Seq expression estimates by correcting for fragment bias. *Genome Biol* 12(3): R22. doi: 10.1186/gb-2011-12-3-r22.

843 Robinson M.D., McCarthy D.J., Smyth G.K. "(2010). edgeR: a Bioconductor
844 package for differential expression analysis of digital gene expression data.
845 *Bioinformatics* 26(1):139-40. doi: 10.1093/bioinformatics/btp616.

846 Sally C.Y., Chau J., Freeman R.S. (1976). Intraperitoneal passage of *Taenia*
847 *crassiceps* in rats. *J. Parasitol.* 62: 837–839.

848 Špakulová M., Orosová M., and Mackiewicz J. S. (2011). Cytogenetics and
849 chromosomes of tapeworms (Platyhelminthes, Cestoda). *Adv Parasitol.* 74:177-
850 230. doi: 10.1016/B978-0-12-385897-9.00003-3.

851 Sciutto E., Fragoso G., Larralde C. (2011). *Taenia crassiceps* as a model for
852 *Taenia solium* and the S3Pvac vaccine. *Parasite Immunol.* 2011 33(1):79-80. doi:
853 10.1111/j.1365-3024.2010.01257.x.

854 Sciutto E., Fragoso G., Diaz M.L., Valdez F., Montoya R.M., Govezensky T., et al.
855 (1991). Murine *Taenia crassiceps* cysticercosis: H-2 complex and sex influence on
856 susceptibility. *Parasitol Res.* 77(3):243-6. doi: 10.1007/BF00930866.

857 Schulte J., Littleton JT. (2011). The biological function of the Huntingtin protein and
858 its relevance to Huntington's Disease pathology. *Curr Trends Neurol.* 2011; 5:65-
859 78.

860 Shea M., Maberley A.L., Walters J., Freeman R.S., Fallis A.M. (1973). Intraocular
861 Taenia crassiceps (Cestoda). *Trans Am Acad Ophthalmol Otolaryngol.*
862 77(6):OP778-83.

863 Silva C. V., M. Costa-Cruz J. (2012). A Glance at *Taenia Saginata* Infection,
864 Diagnosis, Vaccine, Biological Control and Treatment. *Infect. Disord. - Drug*
865 *Targets* 10: 313–321. doi: 10.2174/187152610793180894.

866 Smith J.K., Esch G.W., Kuhn R.E. (1972). Growth and development of larval
867 *Taenia crassiceps* (cestoda). I. Aneuploidy in the anomalous ORF strain. *Int J*
868 *Parasitol.* 2(2):261-3. doi: 10.1016/0020-7519(72)90014-8.

869 Smit A. F. A., Hubley R., and Green P. (2015). RepeatMasker Open-4.0. 2013–
870 2015: 289-300.

871 Stanke M., Keller O., Gunduz I., Hayes A., Waack S., Morgenstern B. (2006).
872 AUGUSTUS: ab initio prediction of alternative transcripts. *Nucleic Acids Res.*
873 34.suppl_2 : W435-W439. doi: 10.1093/nar/gkl200.

874 Takano H., Gusella JF. (2002). The predominantly HEAT-like motif structure of
875 huntingtin and its association and coincident nuclear entry with dorsal, an NF-
876 kB/Rel/dorsal family transcription factor. *BMC Neurosci.* 3:15. doi: 10.1186/1471-
877 2202-3-15.

878 Tartari M., Gissi C., Lo Sardo V., Zuccato C., Picardi E., Pesole G., et al. (2008).
879 Phylogenetic comparison of huntingtin homologues reveals the appearance of a
880 primitive polyQ in sea urchin. *Mol. Biol. Evol.* 25:330. doi:
881 10.1093/molbev/msm258.

882 Toledo A., Fragoso G., Rosas G., Hernández M., Gevorkian G., López-Casillas F.,
883 et al., (2001). Two epitopes shared by *Taenia crassiceps* and *Taenia solium* confer
884 protection against murine *T. crassiceps* cysticercosis along with a prominent T1
885 response. *Infect Immun.* 69(3):1766-73. doi: 10.1128/IAI.69.3.1766-1773.2001.

886 Torgerson P.R., Devleesschauwer B., Praet N., Speybroeck N., Willingham A.L.,
887 Kasuga F., et al. (2015). World Health Organization Estimates of the Global and
888 Regional Disease Burden of 11 Foodborne Parasitic Diseases, 2010: A Data
889 Synthesis. *PLOS Med.* 3;12(12):e1001920. doi: 10.1371/journal.pmed.1001920.

890 Teven C.M., Farina E.M., Rivas J., Reid R.R. (2014). Fibroblast growth factor
891 (FGF) signaling in development and skeletal diseases. *Genes Dis.* 1;1(2):199-213.
892 doi: 10.1016/j.gendis.2014.09.005.

893 Tsai I.J., Zarowiecki M., Holroyd N., Garciarrubio A., Sanchez-Flores A., Brooks
894 KL., et al. (2013). The genomes of four tapeworm species reveal adaptations to
895 parasitism. *Nature.* 496: 57–63. doi: 10.1038/nature12031.

896 Vargas-Villavicencio J.A., Larralde C., León-Nava M.A De., Morales-Montor J.
897 (2005). Regulation of the immune response to cestode infection by progesterone is
898 due to its metabolism to estradiol. *Microbes Infect.* (3):485-93. doi:
899 10.1016/j.micinf.2004.12.015.

900 Vaser R., Sovic I., Nagarajan N., Sikic M. (2002). Racon-Rapid consensus module
901 for raw de novo genome assembly of long uncorrected reads. *Bioinformatics*
902 18.452-464: 6.

903 Walker B.J., Abeel T., Shea T., Priest M., Abouelliel A., Sakthikumar S., et al.
904 (2014). Pilon: an integrated tool for comprehensive microbial variant detection and
905 genome assembly improvement. *PloS one* 9.11: e112963. doi:
906 10.1371/journal.pone.0112963.

907 Wang X., Chen W., Huang Y., Sun J., Men J., Liu H., et al. (2011). The draft
908 genome of the carcinogenic human liver fluke *Clonorchis sinensis*. *Genome Biol.*
909 24;12(10): R107. doi: 10.1186/gb-2011-12-10-r107.

910 Wang S., Wang S., Luo Y., Xiao L., Luo X., Gao S., et al. (2016). Comparative
911 genomics reveals adaptive evolution of Asian tapeworm in switching to a new
912 intermediate host. *Nat Commun*. 22; 7:12845. doi: 10.1038/ncomms12845.

913 Willms K., Zurabian R. (2010). *Taenia crassiceps: in vivo* and *in vitro* models.
914 *Parasitology*. 137: 335–346. doi: 10.1017/S0031182009991442.

915 World Health Organization. (2011). Working to overcome the global impact of
916 neglected tropical diseases. First WHO report on neglected tropical diseases.
917 Summary. *Wkly Epidemiol Rec*.25;86(13):113-20.

918 Yang D., F.u Y., Wu X., Xie Y., Nie H., Chen L., et al., 2012. Annotation of the
919 transcriptome from taenia pisiformis and its comparative analysis with three
920 taeniidae species. *PLoS One* 7: e32283. doi: 10.1371/journal.pone.0032283.

921 Zammarchi L., Strohmeyer M., Bartalesi F., Bruno E., Muñoz J., Buonfrate D.
922 2013. Epidemiology and Management of Cysticercosis and *Taenia solium*
923 Taeniasis in Europe, Systematic Review 1990–2011. *PLoS One* 8: e69537. doi:
924 10.1371/journal.pone.0069537.

925 Zhou Y., Zheng H., Chen Y., Zhang L., Wang K., Guo J., et al. (2009). The
926 *Schistosoma japonicum* genome reveals features of host-parasite interplay. *Nature*
927 460: 345–351. doi: 10.1038/nature08140.

928 Zhu J., Wen W., Zheng Z., Shang Y., Wei Z., Xiao Z., et al. (2011). LGN/mInsc and
929 LGN/NuMA complex structures suggest distinct functions in asymmetric cell
930 division for the Par3/mInsc/LGN and Gαi/LGN/NuMA pathways. *Mol Cell*.
931 5;43(3):418-31. doi: 10.1016/j.molcel.2011.07.011.

932

933

934

935

936

937

Figure Legends

Figure 1. Comparative genomics between strains of *Taenia crassiceps* and with different cestode species. **(A)** Comparative genomics of three cestode genomes [*Hymenolepis microstoma* (HMN); *Echinococcus multilocularis* (EmW) and *Taenia crassiceps* WFU (TcrWFU)]. Scaffold sequences used for this comparison are available in the NCBI and WormBase databases. Genomic fragment names are those from the original source annotation **(B)** Dotplot comparison of WFU vs ORF strains at genomic level demonstrated a clear synteny discarding large structural variations.

Figure 2. Gene ontology enrichment analysis in the *T. crassiceps* ORF strain.

	Initial assembly	Curated assembly
Total bases	118.70 Mb	107.05 Mb
Total number of scaffolds	179	65
N50 / L50	6.70 Mb / 5	10.55 Mb / 4
N90 / L90	186.59 kb / 41	1.46 Mb / 18
Ave. scaffold size	663.16 kb	1.65 Mb
Largest scaffold	19.05 Mb	19.05 Mb
BUSCO (eukaryota dataset) completeness	78.5%	78.5%
Predicted coding genes	12,089	10,585
Annotated proteins	9,603	9,603
rRNA and tRNA	348 rRNA (18S(22), 5.8S(305) y 28S(21)) y 43 tRNA	76 rRNA (18S(4), 5.8S(67) y 28S(5)) y 43 tRNA
Gene average length	5,533.7 bases	5,568 bases
Protein average length	523.17 residues	503.52 residues
Average exon number per gene model	7.76	8.78
Exon mean size	201.4	201.6 bases
Intron mean size	626.7	626.8 bases

965

966 **Table 1.** *T. crassiceps* assemblies and genomic statistics

967

968

969

970

971

Figure 1.JPEG

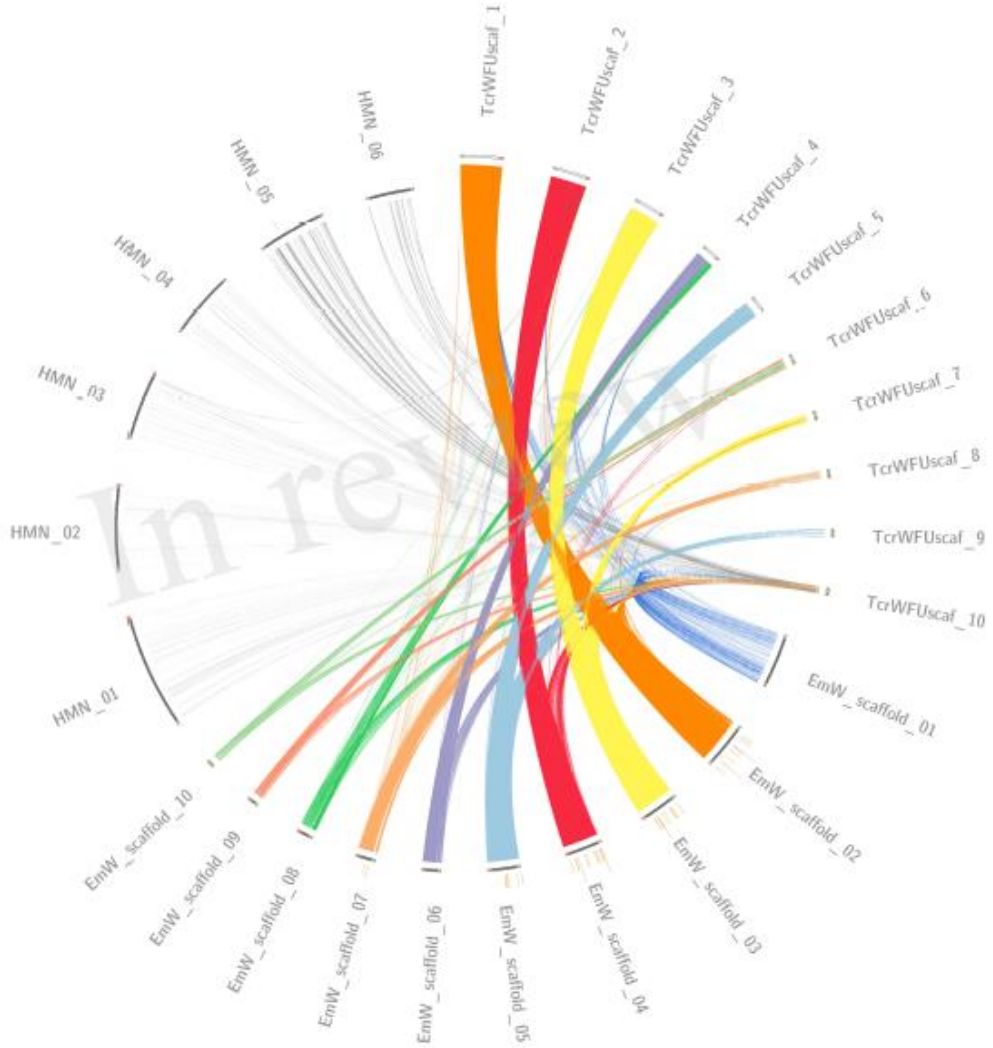

Figure 2.JPEG

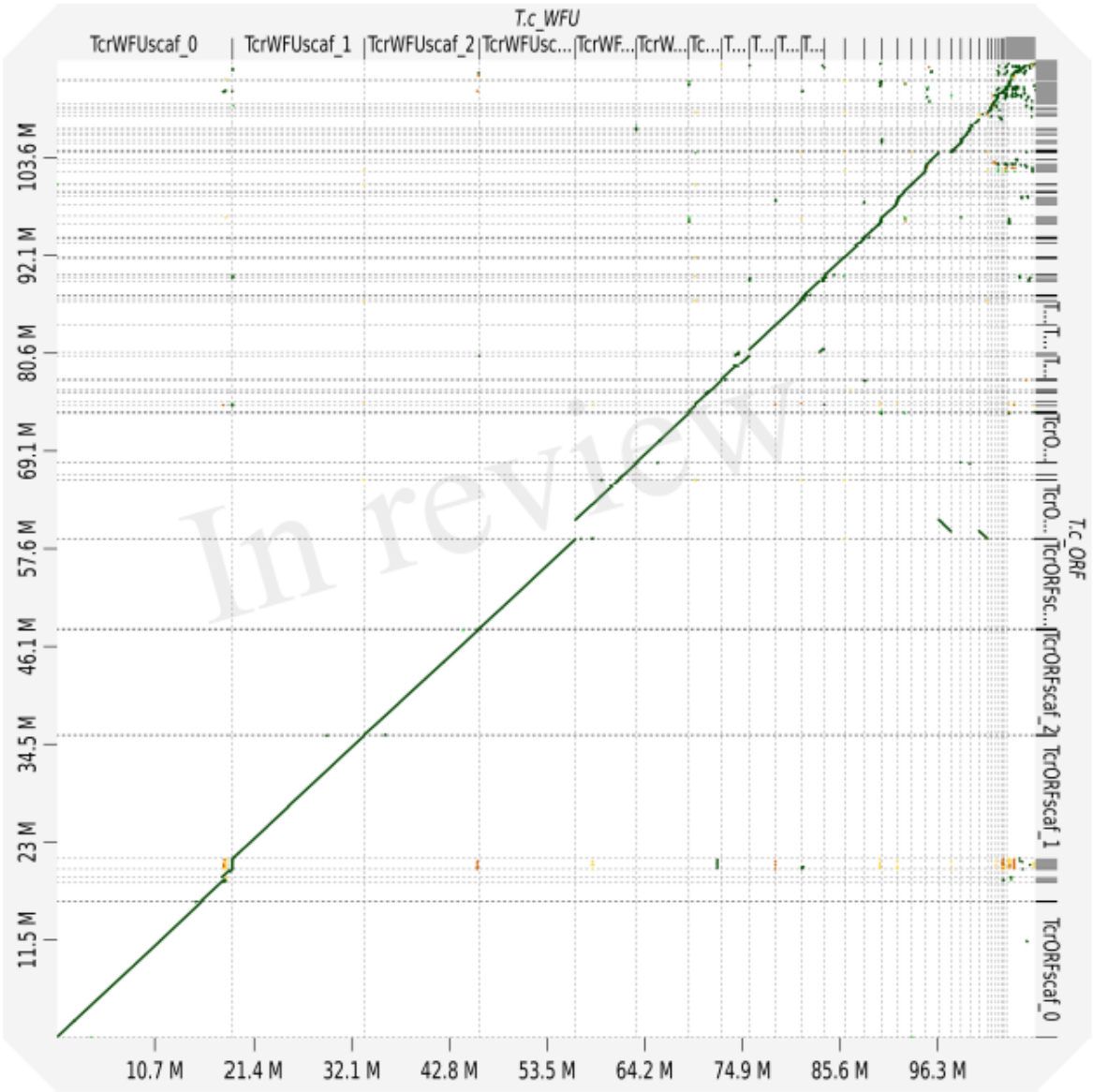

Figure 3.JPEG

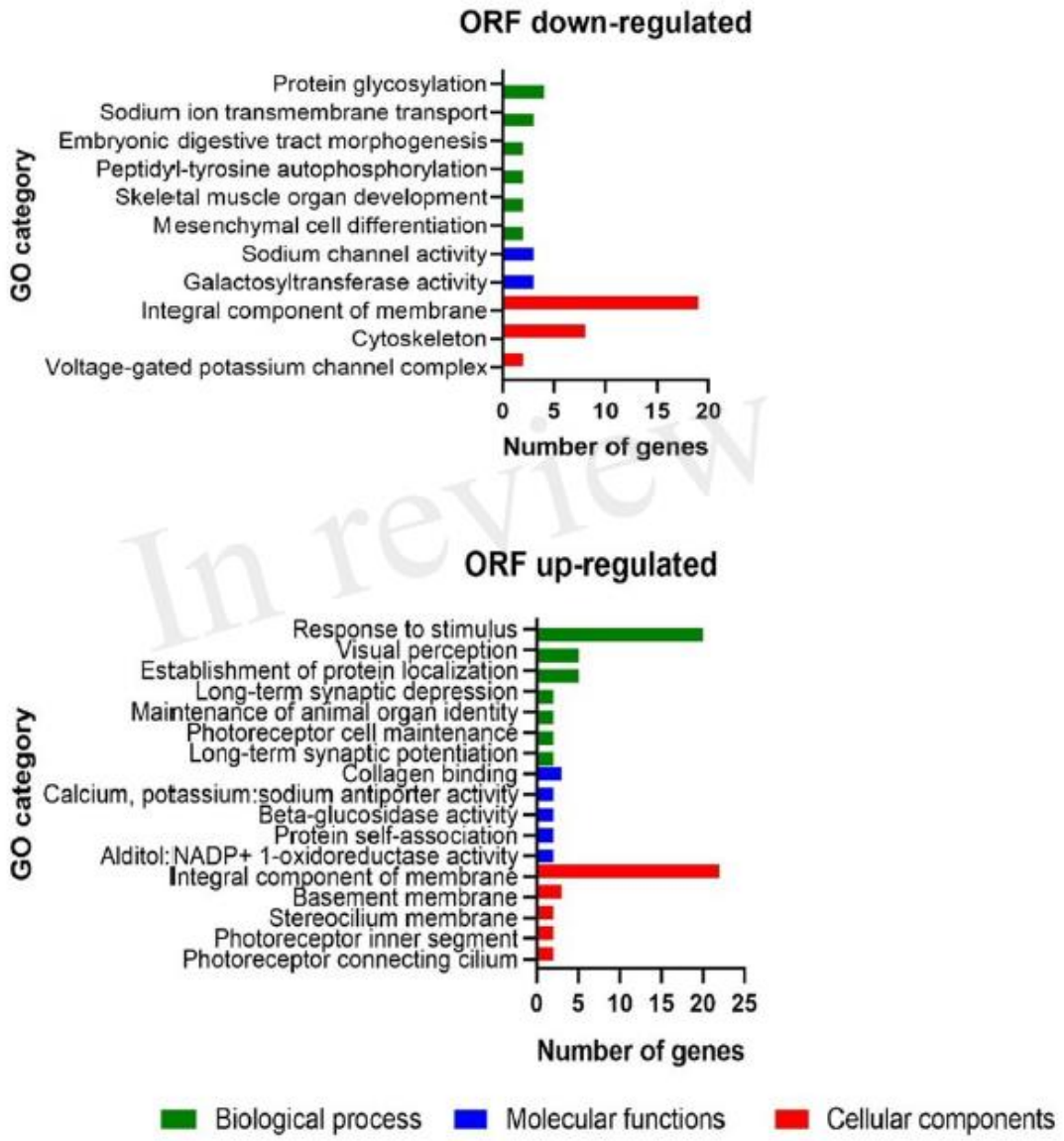

Anexo 3

pharmaceutics

MDPI

Article

Intranasal Methylprednisolone Ameliorates Neuroinflammation Induced by Chronic Toluene Exposure

Manuel F. Giraldo-Velásquez [1], Nicolas I. Pérez-Osorio[1], Alejandro Espinosa-Cerón[1], Brandon M. Bárcena[1], Arturo Calderón-Gallegos[1], Gladis Fragoso[1], Mónica Torres-Ramos[2], Nayeli Páez-Martínez[3,4]* and Edda Sciutto[1]*

[1] Departamento de Inmunología, Instituto de Investigaciones Biomédicas, Universidad Nacional Autónoma de México, Avenida Universidad 3000, Ciudad Universitaria, Coyoacán, C.P. 04510 Ciudad de México, México; manuel_f_er@hotmail.com (M.F.G.-V.); nicolas2309@outlook.es (N.I.P.-O.); alexec2803@gmail.com (A.E.-C.); bmbc1520@gmail.com (B.M.B.); arturo.calderon@comunidad.unam.mx (A.C.-G.); gladisfragoso@hotmail.com (G.F.).

[2] Unidad Periférica de Neurociencias, Facultad de Medicina UNAM-Instituto Nacional de Neurología y Neurocirugía, MVS-SSA, Insurgentes sur 3877, La Fama, Tlalpan, 14269 Ciudad de México, México; monica.torres@innn.edu.mx

[3] Laboratorio Integrativo Para el Estudio de Sustancias Inhalables Adictivas, Dirección de Investigaciones en Neurociencias, Instituto Nacional de Psiquiatría Ramón de la Fuente Muñiz, Calzada México-Xochimilco 101, Tlalpan, C.P. 14370 Ciudad de México, México; nayepam@yahoo.com.mx (N.P.-M.).

[4] Sección de Posgrado e Investigación, Escuela Superior de Medicina, Instituto Politécnico Nacional, Plan de San Luis y Díaz Mirón, Miguel Hidalgo, C.P. 11340 Ciudad de México, México

* Correspondence: nayepam@yahoo.com.mx (N.P.-M.); edda@unam.mx (E.S.); Tel.: +52-(55) 56223153 (E.S.), +52-(55)-4160-5116 (N.P.-M.).

Citation: M.F.G.-V.; N.I.P.-O.; A.E.-C.; B.M.B.; A.C.-G.; G.F.; M.T.-R.; N.P.-M.; E.S. Intranasal Methylprednisolone Ameliorates Neuroinflammation Induced by Chronic Toluene Exposure. *Pharmaceutics* 2022, *13*, x. https://doi.org/10.3390/xxxxx

Academic Editor: Piroska Szabó-Révész

Received: 10 November 2021
Accepted: 10 January 2022
Published: date

Publisher's Note: MDPI stays neutral with regard to jurisdictional claims in published maps and institutional affiliations.

Abstract: Inhalants are chemical substances that induce intoxication, and toluene is the main component of them. Increasing evidence indicates that a dependence on inhalants involves a state of chronic stress associated to the activation of immune cells in the central nervous system and release of proinflammatory mediators, especially in some brain areas such as the nucleus accumbens and frontal cortex, where the circuits of pleasure and reward are. In this study, anti-neuroinflammatory treatment based on a single dose of intranasal methylprednisolone was assessed in a murine model of chronic toluene exposure. The levels of proinflammatory mediators, expression levels of Iba-1 and GFAP, and histological changes in the frontal cortex and nucleus accumbens were evaluated after the treatment. The chronic exposure to toluene significantly increased the levels of TNF-α, IL-6, and NO, the expression of GFAP, and induced histological alterations in mouse brains. The treatment with intranasally administered MP significantly reduced the expression of TNF-α and NO and the expression of GFAP ($p < 0.05$); additionally, it reversed the central histological damage. These results indicate that intranasally administered methylprednisolone could be considered as a treatment to reverse neuroinflammation and histological damages associated with the use of inhalants.

Keywords: toluene; neuroinflammation; histological damage; intranasal administration; methylprednisolone

1. Introduction

Inhalant abuse is a worldwide problem especially common in youths from marginalized populations [1]. These substances are widely available and accessible to children and adolescents, in whom they have euphorigenic and highly toxic effects, which may be greater than in adults [2]. Toluene is the main substance contained in inhaled drugs [3,4], and its exposure is related to different neurological alterations [5,6]. The addiction within inhalant abuse underlies a neurochemical and neuroanatomical circuit of pleasure and reward. In this circuit, the nucleus accumbens, the hippocampus, the frontal cortex, and

the amygdala are the most important brain areas. Of them, the nucleus accumbens is critical for the beginning and the maintenance of the reinforcement of the drug abuse behavior [7]. Considering these reasons, in this study, histological analysis was performed in mouse frontal cortices (FCs) as well as nucleus accumbens (NA).

At cellular levels, chronic toluene administration impact cell viability by decreasing neurogenesis and promoting apoptosis [6]. Moreover, chronic toluene exposure produces several cognitive deficits, including learning and working memory impairment [8,9]. Among other effects, toluene inhalation induces changes in GABA and glutamate receptors, although the mechanisms that underlie these effects remain to be determined [10–13].

Neuroinflammation is the complex inflammatory response of neural tissue that initially participates in the brain fix and resolution process [14] but has also been attributed to the pathogenesis of a number of central nervous system diseases [15]. Neuroinflammation may be induced by toluene inhalant abuse due to the production of reactive oxygen species and glial cell activation [16]. In this way, different studies have demonstrated that drugs of abuse, such as toluene, interact with the neuroimmune system and alter immune gene expression and signaling, which in turn contribute to various aspects of addiction [17]. It has been reported that toluene exposure enhances IL-1β mRNA while decreasing TGF-β mRNA expression in the medial prefrontal cortex [16]. In addition, low toluene concentrations in mice may increase the expression of mRNA of TLR-4 and NF-KB mRNA in the hippocampus [18]. Furthermore, an increase in the expression of cell-specific markers ionized calcium binding adaptor molecule (Iba-1) and glial fibrillary acidic protein (GFAP) has been reported following exposure to toluene [16,19]. It has also been reported that repeated toluene administration (1500 ppm for 4 h/7 days) increased the expression of cytokine mRNA such as TNF-α, TGF-β, and glial markers such as GFAP in the rat hippocampus and cerebellum [20]. In mice chronically exposed to toluene, rapid absorption occurs. Once absorbed, toluene can readily cross the blood–brain barrier, resulting in brain damage by triggering neuroinflammation through the release of damage-associated molecular patterns.

Despite the worldwide use of toluene, the treatments for inhalant users are limited, and there is a clear need for more effective treatment options [21]. Some of these treatments include psychological and psychosocial interventions [22], and only a few studies have analyzed pharmacological approaches for the inhalant treatment [23]. In addition, in postmortem analysis of brains from patients undergoing inhalant addiction, it had been shown that gliosis, microglia migration and proliferation, cerebral atrophy, and myelin loss are the main effects of toluene exposure; it is important to say that for all the mentioned processes, neuroinflammation is critical for their establishment [24]. Altogether, these data suggest that neuroinflammation is a therapeutic target to reduce, at different levels, the harmful effects of toluene exposure.

Steroids are the drugs with the highest anti-inflammatory capacity and are commonly used in a wide range of pathologies such as allergies, asthma, neurodegenerative and autoimmune diseases, etc. [25,26]. Glucocorticoids are a class of steroids which regulate various cellular functions including, development, homeostasis, cognition, and the inflammatory response [27]. Despite the efficiency of glucocorticoids in controlling inflammation, high systemic doses are required to achieve central therapeutic doses required to control neuroinflammation, which may cause relevant adverse side effects [28]. Thus, its use is restricted to very particular neuroinflammatory conditions that endanger the patient's life.

In recent years, the intranasal (IN) route of administration has been recognized as a route to treat neurological disorders. The nasal pathway represents a non-invasive administration route of active pharmaceutical ingredients for local, systemic, and CNS action [29]. IN delivery not only avoids first-pass metabolism but also circumvents passage through the blood–brain barrier by allowing the transport of drugs from the nasal cavity to the brain through the nasal and trigeminal nerves [30]. On the other hand, the mucosa

and lamina propria are characterized by their extensive vascularization; likewise, the leaky epithelium provides an optimal absorption mechanism for the drug delivery [31]. To our knowledge, there are no reports on the use of the IN drug administration route to control toluene-associated neuroinflammation.

Considering that it has been reported that the repeated administration of different drugs of abuse in rodents causes a progressive increase in locomotor activity (Valjent et al., 2010) that is greater in magnitude compared to that induced by a single administration (a phenomenon known as locomotor sensitization), it is important to evaluate the impact of toluene inhalation and MP treatment on the addiction behavior. This activating effect of locomotion is easily perceptible and has a neurobiological substrate that is in part common with the one responsible for the reward effects. Thus, in this study, the impact of the anti-neuroinflammatory treatment in the addiction behavior was also evaluated.

The aim of this study was to evaluate the efficiency of the IN delivery of methylprednisolone (MP) to control the neuroinflammation induced by the chronic exposure of toluene in mice and its impact on the addiction behavior.

2. Materials and Methods

2.1. Mice

Male Swiss Webster mice of 30–35 days of age were employed in this study. Mice were obtained from Instituto Nacional de Psiquiatría Ramon de la Fuente Muñiz, México City, México, and housed at the same institution in an animal room maintained at 22 ± 3°C with a 12/12 h light–dark cycle. The age of mice approximately corresponds to human adolescence, which is the stage of life at which people generally start drug addictions. All mice were kept in plexiglass boxes with food (Teklad Sani-Chips® 7090, Envigo, Indianapolis, USA) and water (filtered, acidified, and sterilized) ad libitum.

Experimental procedures were conducted following the guidelines of the Institutional Committee of the Care and Use of Experimental Animals of the IIB at the Universidad Nacional Autónoma de México (UNAM) and of the U.S. National Institutes of Health. Experimentation protocol was approved by the animal safety and ethical committee of the IIB, UNAM (Protocol Number approval ID 140, approved in 4 April 2018).

2.2. Chronic Toluene Exposure

Mice were exposed to 4000 ppm toluene or air (control group) in an inhalation chamber, which consist in a 27 L glass cylinder with a polycarbonate lid. The lid contained an injection port in the outside part and a fan and a wire mesh in the inside part of the chamber. Animals are placed in the bottom of the chamber and an amount of toluene was dropped in the filter paper localized above of the wire mesh, then the fan was turned on. Exposure to toluene or air was conducted 30 min a day for 4 weeks, from Monday to Friday. A photoionization detector (2020 Combo Pro, Inficon, New York, NY, USA) were used to confirm the toluene concentration inside the inhalation chamber. The toluene exposure time and concentration were chosen according to previous studies from our lab, where behavioral and neurochemical alterations have been imitated by repeated toluene exposure [6,9,31,32,39].

2.3. Effect of Intranasal Methylprednisolone Administration

Two hours after the last toluene or air (0 ppm toluene) exposure, mice received a single dose of either intranasal isotonic saline solution (IN-SS) or intranasal methylprednisolone (IN-MP) (200 mg/kg). We employed a commercially available formulation of methylprednisolone for intravenous use (methylprednisolone sodium succinate (Pfizer, New York City, USA) and dissolved it with the ampule of injectable water and 2% benzyl alcohol that was provided. Mice received 10 µL in each nostril of the MP solution (200 mg/kg) adjusted to the weight of each mouse. Intranasal doses were applied with a micropipette, placing the tip and slowly releasing the solution into the nostril with the mouse

face up in the palm of the hand. Mice were lightly anesthetized with inhaled sevoflurane (10 s) before administration. The dose was ensured to be fully absorbed before the mouse was returned to the cage. Mice were randomly assigned in four experimental groups: toluene + saline solution (TSS), toluene + methylprednisolone (TMP), air + saline solution (ASS), and air + methylprednisolone (AMP). Mice of each group were anesthetized (90 mg of ketamine and 10 mg/kg of xylazine) and perfused with physiological saline followed by 4% paraformaldehyde solution previously cooled to 4 °C, and then euthanized (Figure 1). The expression of ionized calcium binding adaptor molecule (Iba-1) and glial fibrillary acid protein (GFAP) was performed by immunofluorescence analysis in the FC and NA. Hematoxylin and eosin staining were developed to assay histological changes as well as cellular infiltrates in FC and NA. The central level of cytokines (tumor necrosis factor TNF-α, interleukin IL-1β and IL-6) was measured in brain homogenates. Slices of the areas of interest—frontal cortex and nucleus accumbens—were selected according to a histological atlas [33]. Frontal cortex slices were made at 2.34 mm from Bregma, and for the nucleus accumbens, slices were made at 1.42 mm from Bregma.

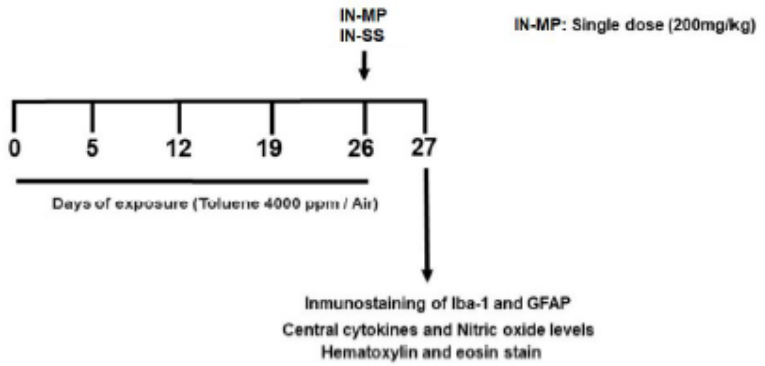

Figure 1. Experimental design. At the beginning animals were exposed to toluene 4000 ppm or air for four weeks. Two hours after the last exposure the animals received a single dose of intranasal MP (IN-MP) or intranasal SS (IN-SS). One day later, the expressions of Iba-1 and GFAP were assayed by immunofluorescence and central cytokines and nitric oxide levels were evaluated by enzyme-linked immunosorbent assay (ELISA) and Griess reaction, respectively. Histological analysis was performed with hematoxylin and eosin staining 24 h after the treatment.

2.4. Central Inflammatory Mediators

A mixture of ketamine (90 mg/kg) and xylazine (10 mg/kg) was used to anaesthetize all mice. Mice were submandibular bled before being euthanized. Mice were perfused by cardiac puncture with 250 mL of NaCl (0.15 M) to discard the presence of peripheral molecules in central tissues. Brains were removed and processed to determine the protein concentration and cytokine levels (TNF-α, IL-1β and IL-6) and nitric oxide (NO), following the procedure previously described [34].

Lysis buffer (50 mM HEPES, 150 mM NaCl, 1% Nonidet-p40, 0.5% sodium deoxycholate, 0.1% sodium dodecyl sulphate (SDS)) containing complete protease inhibitors (Roche, Basel, Switzerland) was employed to homogenate Snap-frozen full brains. Samples were then centrifuged at 16,000× *g* for 15 min at 4 °C and supernatants were collected and kept at −80 °C until analysis. The total amount of proteins in the soluble extract was measured using the Lowry method to normalize the central levels of cytokines [35].

2.5. Cytokine Enzyme-Linked Immunosorbent Assay (ELISA)

The concentrations of the proinflammatory cytokines IL-1β, IL-6, and TNF-α in brain extracts were measured using commercial kits (BioLegend, San Diego, CA, USA),

following the procedures previously reported [36]. ELISAs were performed in 96-well flat-bottomed MaxiSorp microtiter plates (Nunc, Roskilde, Demark). The capture antibody was placed in the microplates for 18 h at 48 °C and then washed with phosphate-buffered saline (PBS)—Tween 20 (0.05%) and blocking for 60 min at room temperature with 2% PBS bovine serum albumin (BSA). Plates were then incubated for 2 h at room temperature for 2 h with standard or samples, washed three times, and incubated at room temperature for 1 h with the detection antibodies at room temperature. Antibodies bounded were revealed using a d 1:1000 dilution of avidin-horseradish peroxidase (HRP) and 3,3′,5,5′-tetramethylbenzidine (TMB). The optical density was read before and after the reaction was stopped with H_2SO_4·2N at 450 and 630 nm, respectively, using an DR-200Bc microplate reader (Diatek Instruments, Wuxi, China). Results were expressed in pg/mL per mg of protein in the respective soluble extract. Groups of 4–5 mice for each experimental condition were employed.

2.6. Nitric Oxide Assay

Nitric oxide assay was carried out by indirect measurement of nitrite quantification (NO) using the Griess reaction [37]. The analysis was performed using 96-well MaxiSorp flat-bottom microtiter plates (Nunc, Roskilde, Denmark) where 25 µL of nitrite standards were initially added in duplicate at concentrations between 1.87 and 100 µM/mL followed by 25 µL of the samples in duplicate, then 25 µL of sulfanilamide was added to each well and incubated for 15 min at room temperature with constant shaking, and finally, 25 µL of the NED reagent was added to each well and the absorbance was measured at 10 min at 540 nm. The total amount of proteins in the soluble extract was measured using the Lowry method to normalize the central levels of NO [35]. The results were expressed in µM/mL per mg of protein in the respective soluble extract. Groups of 4–5 mice for each experimental condition were employed.

2.7. Immunofluorescence (IFC) Analysis

Immunohistological studies were performed using 30 µm-thick frozen brain coronal sections that were obtained through cryo-sectioning and preserved in phosphate-buffered saline (PBS) 1x until analysis. After the treatment with citrate buffer (0.01 M citric acid, 0.05% Tween 20, pH 6.0) at 70 °C for 50 min, samples were washed thoroughly with a solution of 2% immunoglobulin (Ig)G-free albumin (Sigma, St Louis, MO, USA) in TBS for 20 minutes at room temperature. Brain sections were then incubated overnight at 48 °C with either rabbit anti-GFAP (Invitrogen, Carlsbad, CA, USA) or anti-Iba-1 (Wako Chemicals Inc., Richmond, VA, USA) in TBS-2% BSA to detect astrocytes and microglia, respectively. After washing, sections were incubated for 1 h at room temperature with AlexaFluor 594 goat anti-rabbit IgG (Molecular Probes, Eugene, OR, USA) diluted in TBS-2% BSA. Sections were mounted onto glass slides in Vectashield medium (Vector Laboratories, Burlingame, CA, USA) containing 4′,6-diamidino-2-phenylindole (DAPI) to visualize nuclei The mean fluorescence intensity was quantified using Image J software (National Institute of health, Bethesda, MD, USA). Three mice for each experimental condition were analyzed.

2.8. Histological Analysis

Hematoxylin-eosin staining was carried out to assay histological changes and cell infiltrates. Briefly, brain sections were fixed with 4% paraformaldehyde for 24 h; subsequently, they were postfixed for 24 h more and embedded in paraffin. Using a microtome, sections with 10 µm thicknesses were obtained from both FC and NA and the slices were mounted onto glass slides. Once the brain sections were obtained, they were deparaffinized and rehydrated on an alcohol gradient, washed with distilled water, and stained with hematoxylin for 10 min. For the eosin staining, the glass slides, initially stained with hematoxylin, were washed in distilled water and treated with 1% acid alcohol and

saturated lithium carbonate solution; finally, the slides were placed in an eosin solution for 30 s. Photographs were obtained using a digital camera attached to a light microscope (Nikon DIGITAL SIGHT DS-Ri1, Nikon DIGITAL SIGHT DS-Ri1, Nikon, Tokyo, Japan).

2.9. Analysis of Addictive Behavior by Measuring the Locomotor Activity

To study the addictive behavior induced by chronic toluene inhalation, the locomotor activity of mice in the exposure chamber placed on a surface marked with 4 X 4 cm quadrants was recorded during the last 5 min of exposure, on day 1 and every 7 days during the following 28 days. The total number of quadrants that animals crossed during the test period was recorded.

Other group of mice that received the same schedule described above were treated on day 28 with saline or with methylprednisolone. The locomotor activity of all mice was measured 24 h after treatments.

2.10. Statistical Analysis

All data are expressed as the mean ± standard error. To evaluate the anti-neuroinflammatory effects of IN-MP administration, in animals previously exposed to toluene, ANOVA followed by Tukey test were performed. A difference was considered statistically significant at P-value less than 0.05. All analyses were carried out using the SigmaStat program (version 3.5, Jandel Scientific, California, USA).

3. Results

3.1. Effect of MP on the Central Levels of Cytokines

To evaluate the effect of IN delivery of MP on neuroinflammation induced by toluene exposure, central levels of proinflammatory cytokines were assayed (Figure 2). The exposure to toluene significantly increased the level of TNF-α and IL-6 in brain homogenates and did not affect the level of IL-1β. The administration of MP on the group previously exposed to toluene significantly reduced the levels of TNF-α but not IL-6 in brain homogenates 24 h after the treatment. No effect was observed in the levels of IL-1β. A slight but statistically significant increase in IL-6 levels was observed in the air MP-treated (AMP) group compared with air saline-treated (ASS) group.

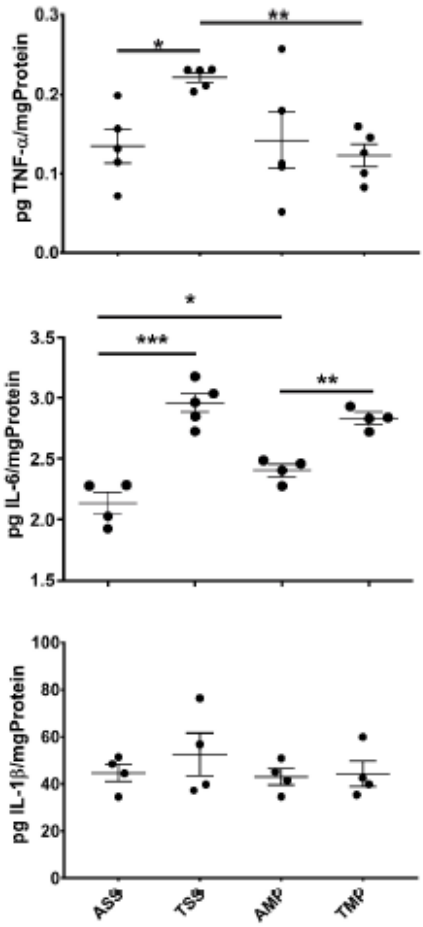

Figure 2. Central cytokine levels (pg/mg protein) in soluble extract from brain of mice chronically exposed to toluene and analyzed by ELISAs test. All results are showed as the mean ± standard error of groups values. * $p < 0.05$, ** $p < 0.01$, *** $p < 0.001$. ANOVA followed by Tukey's test was performed. Air + saline solution (ASS); toluene + saline solution (TSS); air + methylprednisolone (AMP); toluene + methylprednisolone (TMP).

3.2. *Intranasal Delivery of MP Effectively Reduced Central Levels of Nitric Oxide*

The effect of MP on the NO is shown in Figure 3. The results showed that chronic toluene exposure significantly enhanced the NO levels in brain homogenates that were significantly reduced after MP treatment.

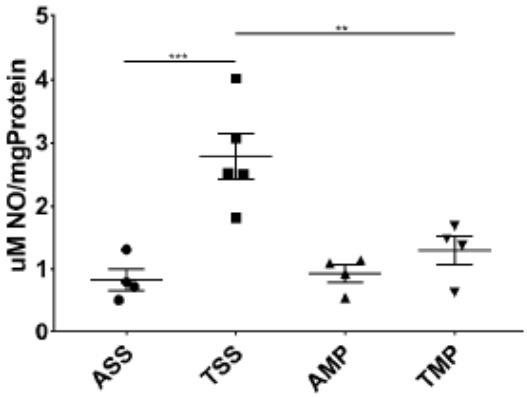

Figure 3. Central nitric oxide levels (μM/mg protein) in soluble extract from brain of mice repeatedly exposed to toluene and measured by Griess reaction. All results are shown as the mean ± standard error of groups values. * $p < 0.05$, ** $p < 0.01$. ANOVA followed by Tukey's test were performed. Air + saline solution (ASS); toluene + saline solution (TSS); air + methylprednisolone (AMP); toluene + methylprednisolone (TMP).

3.3. *Expression of Iba-1 and GFAP in FC and NA after 24 of Treatment*

Two hours after the chronic toluene exposure, mice received IN-SS or IN-MP. Twenty-four hours later, the effect of MP on the activation of microglia and astrocytes was evaluated in the NA and FC. Figure 4A shows an overview of the two regions (frontal cortex and nucleus accumbens) that were evaluated. Figure 4B shows a representative image of the expression of GFAP and Iba-1. As depicted, repeat toluene administration increased the immunoreactivity of GFAP ($p = 0.09$) in NA and FC. Meanwhile, MP treatment decreased the mean fluorescence intensity of GFAP expression, and no changes were observed in the AMP group (Figure 4C).

Toluene treatment does not significantly modify the expression of Iba-1 ($p > 0.05$) in both areas, in comparison to AMP or ASS groups. In contrast, in the TMP group, the expression of Iba1 was significantly increased compared to the TSS group ($p < 0.001$), probably due to the establishment of a M2 polarized microgliosis (Figure 4C).

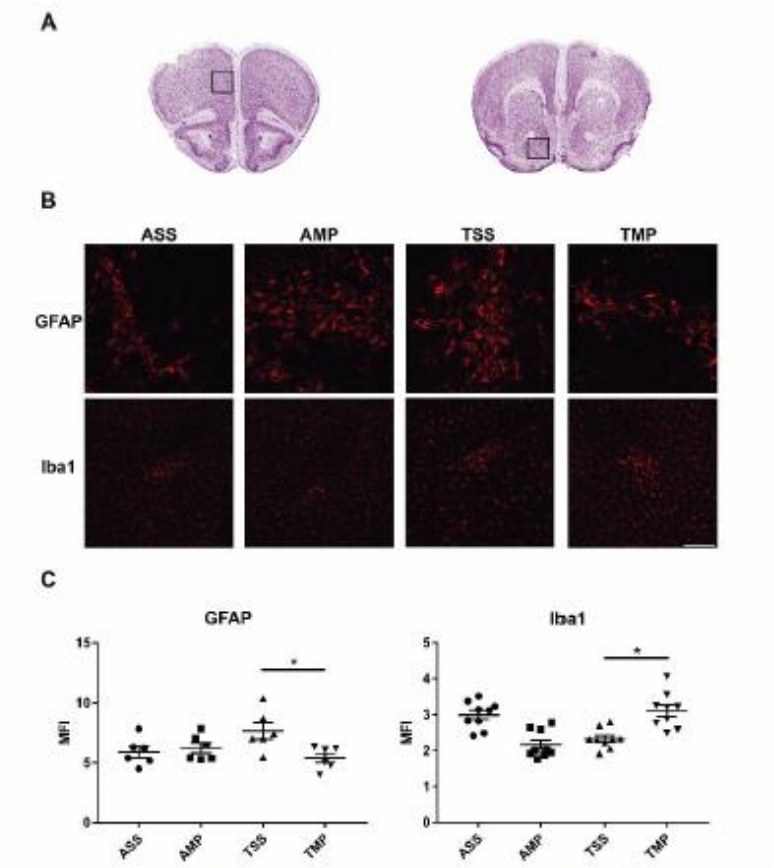

Figure 4. Analysis of brain GFAP and Iba-1 expression in exposed to toluene and non-exposed to toluene mice 24 h after the IN-MP administration. (**A**) Histological representation of analyzed areas. Squares points out areas in frontal cortex (**left**) and nucleus accumbens (**right**) which were analyzed. Images taken from "The mouse brain in stereotaxic coordinates" Reproduced from [30], OXFORD UNIV PRESS INC, 2020. (**B**) Representative images of GFAP and Iba-1 immunofluorescence stains. Scale bar represents 100 μm. (**C**) The mean fluorescence intensity (MFI) of GFAP and Iba-1 in frontal cortex and nucleus accumbens were quantified using the Image J software. All results are showed as the mean ± standard error of groups values. * $p < 0.05$. ANOVA followed by Tukey's test. Air + saline solution (ASS); air + methylprednisolone (AMP); toluene + saline solution (TSS); toluene + methylprednisolone (TMP).

3.4. Reduced Histological Alterations by Intranasal Methylprednisolone

Hematoxylin-eosin staining was performed to describe histological changes as well as cell infiltration induced by the toluene administration at the level of FC and NA (Figure 5). In the brains of mice that were only exposed to air, there were no abnormalities in the FC or in the NA. In the brain sections of the toluene-administered mice, nuclear pyknosis and cytoplasmic compaction, highly suggestive of apoptosis, were detected. In addition, hydrotropic degeneration, alteration in nuclear contours, and cell rupture—all characteristic cellular processes of necrosis—were found. Similar results were found in the NA (Figure 5). IN administration of MP results in a decrease in brain impairment in both areas.

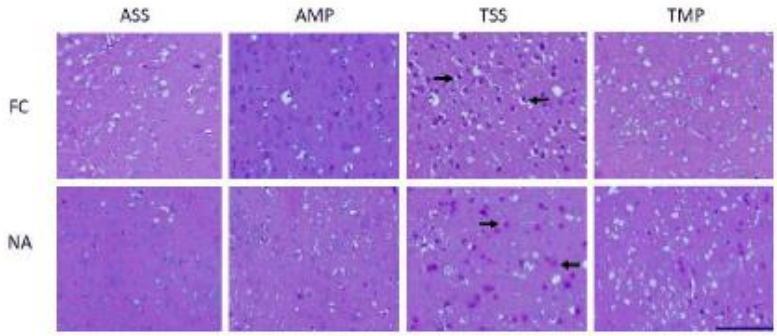

Figure 5. Histological examination of brains of mice repeatedly exposed to toluene and those with a previous exposure toluene and then treated with methylprednisolone. Hematoxylin-eosin stains of brain sections at frontal cortex (FC) and nucleus accumbens (NA). Scale bar represents 100 μm. Air + saline solution (ASS); air + methylprednisolone (AMP); toluene + saline solution (TSS); toluene + methylprednisolone (TMP). Arrows show nuclear damage in TSS group in both FC and NA regions. Treatment with IN-MP reduced nuclear damage (TMP).

3.5. Analysis of Addictive Behavior Measuring the Locomotor Activity

Figure 6 shows that exposure to 4000 ppm of toluene produced a significant increase in the locomotor activity from the first week of exposure that is maintained from day 14 to day 28. At day 28, one dose of MP was IN administered to all mice (air and toluene treated). One day later, the locomotor activity was recorded to measure the anti-neuroinflammatory effect on mice behavior. As shown in Figure 6, MP treatment did not modify the locomotor activity of toluene-treated mice. Moreover, MP significantly increased the locomotor of those mice only treated with saline isotonic solution.

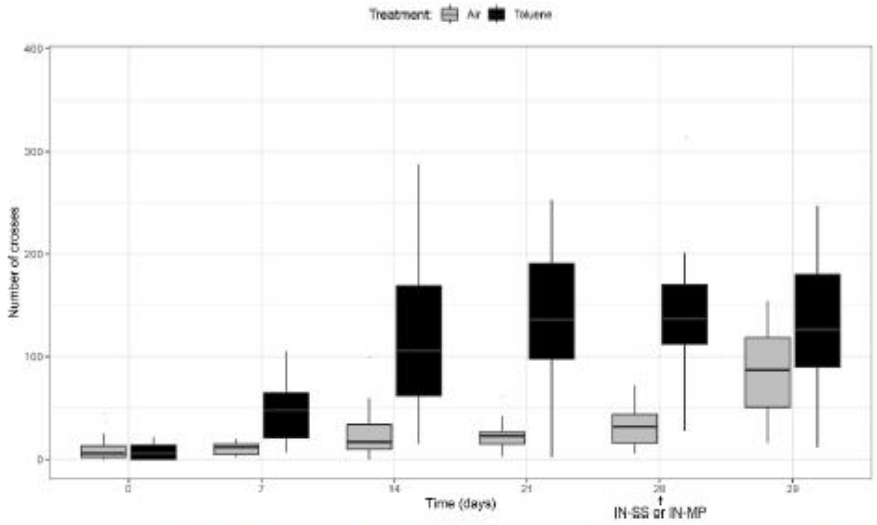

Figure 6. Mean ± SD of the number of crosses performed by 68 mice, half treated with air and the other half with toluene for 28 days. A group of 30 mice were then treated with one dose of IN-MP (200 mg/kg) and the locomotor activity was registered 24 h later. Values were compared by a T-student test.

4. Discussion

Based on the results obtained in the present study, chronic toluene exposure induced marked neuroinflammation characterized by increased levels of NO, TNF-α, and IL-6, as well as increased expression of GFAP. Moreover, histological alterations were observed by the toluene administration. Interestingly, IN-MP not only decreased the central levels of nitric oxide but also the levels of TNF-α. In addition, the expression of GFAP was significantly reduced after the IN-MP treatment. As a result, MP administration was able to reduce histological alterations produced by the chronic toluene treatment.

Clinical and neuroradiological findings sustain the central damage that is caused by repeated use of inhalants such as toluene [38]. The initial injury conceivably results in the expression of damage signals (DAMPS) and activation of the neuroinflammatory response. Once triggered, the sustained neuroinflammation induced by toluene may cause a succession of secondary brain-damage events leading to neuronal damage, such as the enhancement in apoptotic markers [6]. The present results are consistent with the literature on the neuroinflammatory effect of the toluene. Thus, repeated toluene exposure in rats enhances IL-1β in the FC [16]. Previous reports had shown how chronic exposure to toluene activated the NF-Kb signaling pathway through TLR-4 activation mediated by the expression of DAMPs [18]. Moreover, other works also demonstrated that toluene promoted the expression of TNF-α in different brain areas, such as the frontal cortex, hippocampus, and the substantia nigra [39]. Similarly, this study corroborates a previous work where repeated exposure to toluene induces oxidative stress, enhancing nitric oxide and reactive oxygen species production as well as reducing superoxide dismutase activity and glutathione levels in the FC and hippocampus [40]. Astrocytes and microglia are the main cells that respond to toxic damage in the central nervous system during toluene exposure. Experimental models have been used for the study of gliosis caused by toluene. From the present study, repeated doses of 4000 ppm of toluene administration enhance GFAP expression in mouse brains. In line with these results, in a rat study, toluene administration (1500 ppm for 4 h on 4–10 days) augmented GFAP immunoreactivity in the hippocampus and cerebellum [20]. Likewise, the mRNA of neuroimmune markers TNF-α, TLR-4, Iba-1, and GFAP have been found to be increased in the hippocampus of mice previously treated with a low level of toluene [19]. Likewise, toluene 8000 ppm, twice a day for five days increases the GFAP levels in the FC [16]. Altogether, these data corroborate that toluene can induce neuroinflammation. In our study, the chronic administration of toluene was able to increase several inflammatory conditions, such as NO, IL-6, TNF-α, and the expression of GFAP. No increase in IL-1β or Iba-1 could be attained. The production of IL-β requires two signals, one triggered by the recognition of DAMPs that induces the expression of the pro-IL-1β and the second coordinated by the activation of the inflammasome (which activates caspase 8 that cut the pro-IL-1, leading to the mature and active form of this inflammatory cytokine). It is possible that the inflammasome activation could not occur in our model induced by chronic inhalation of toluene. In contrast, in models of toluene with fewer administrations (10 exposures), the activation of NLRP3 inflammasome with the mRNA expression levels of IL-1β has been observed [16]. It is possible that the chronicity in the toluene administrations lead to different outcomes in the production of IL-β.

Herein, we explore the potential of anti-neuroinflammatory treatment using intranasal glucocorticoid administration. MP was selected considering that it is a synthetic glucocorticoid, extensively used orally or parenterally for its anti-inflammatory and immunosuppressive effects [26]. It has been widely administered to control the inflammatory process in several pathological diseases and it is the most common glucocorticoid employed for the treatment of relapses in multiple sclerosis [44–46]. However, high doses of MP have been used to reach the required concentration in the central nervous system to control neuroinflammation that may lead severe negative side effects that limit its use [47]. The intranasal (IN) route is a feasible alternative for drug delivery directly to the CNS [48–50] through the olfactory and trigeminal nerve structures avoiding the blood–brain

barrier. In our research group, we recently demonstrated that intranasally administered glucocorticoids are more effective to control the neuroinflammation that accompanied different diseases, in comparison to intravenously administered ones [36,51]. In the murine model of multiple sclerosis, we found that MP intranasally administered was able to reduce the inflammatory cytokines as well as the expression of activation markers of glia and astrocytes (Iba1 and GFAP, respectively) and improved the clinical score [27]. In this study, the treatment with only one dose of IN-MP significantly reduced some inflammatory features, such as TNF-α, ON, and astrocytes activation, results that are expected when potent anti-inflammatory drugs are employed [52]. Indeed, the damage induced by chronic exposure to toluene is partially reverted as soon as 24 h after IN-MP. This effect may be the result of the rapid reduction in neuroinflammation through the repression of inflammatory transcription factors together with the endothelial repair through the strengthen cell-to-cell contacts [53,54]. However, MP treatment could only partially reduce inflammation by lowering TNF-α and NO levels and maintaining slightly increased levels of the pleiotropic cytokine IL-6. IL-6 is a pro-inflammatory cytokine that is frequently accompanied by different neurological diseases and leads to astrogliosis [41]. However, when the inflammatory process begins to cease, IL-6 behaves as an anti-inflammatory cytokine inhibiting the expression of TNF-α- or IL-1β induced by ICAM-1 expressed in primary astrocytes. Additionally, it has been reported that IL-6 functions as an anti-inflammatory cytokine, helping to maintain the blood–brain barrier integrity in neuroinflammatory conditions. In line with these anti-inflammatory functions, IL-6 also induces the survival, proliferation, differentiation, and regeneration of neurons, influences the synaptic release of neurotransmitters, and promotes astrogliogenesis and oligodendrogenesis [42]. Thus, the high levels of this cytokine in MP-treated mice may reflect the restorative conditions of the inflamed brain. Although a single dose of MP showed benefits reducing some inflammatory markers, it is also likely that more time or additional doses of MP will be required to reverse the values of IL-6. A recent study evaluated minocycline, an anti-inflammatory agent, on the effects induced by toluene at the level of the FC. Similar to our results, minocycline also reduced neuroinflammatory marker IL-1β, while this drug was able to reduce the increased levels of GFAP induced by toluene [16]. A direct comparison is hard to conduct, on the aims of Cruz et al. study was to prevent the inflammatory response induced by toluene, the experiments were conducted in rats, the administration of minocycline was intraperitoneal and the neuroinflammation was evaluated in the FC. In the present study, the objective was to revert the brain damage already induced by toluene, mice were employed, the administration of the steroid was performed intranasally, and the whole brain was used to analyze the proinflammatory cytokines. Despite these differences, both studies show evidence that toluene can induce inflammation at the cerebral level and anti-inflammatory drugs are able to reduce some of those parameters of neuroinflammation. This study tries to conduct an approximation to evaluate the therapeutic potential of MP in the neuroinflammatory process induced by toluene; consequently, the whole brain was employed to analyze some neuroinflammation markers; however, a more specific analysis of the brain area is currently underway in our laboratory.

Exposure to toluene produces marked histological changes by altering the lipid structure of cells, as well as by interacting with different cellular proteins [39]. In patients who have been exposed for more than 10 years, chronic toluene usage leads to demyelination and axonal degeneration [43]. Moreover, there is evidence showing that toluene administration triggers tissue damage due to an increase in oxidative stress as well as the expression of proapoptotic proteins [6,40]. As we hypothesized, the reduction in neuroinflammation was reflected in greater integrity of the neuronal tissues, as observed in the histological profile, where less pyknotic and necrotic cells were observed in the group previously exposed to toluene as shown in Figure 5. The increased Iba-1 expression induced by MP could also contribute to this histological improvement. Indeed, it has been

extensively reported that steroids promote the activation of alternative activated microglia, M2 microglia [55].

In the present study, chronic exposure to toluene produced behavioral sensitization reflected in a progressive increase in locomotor activity (Figure 6). It is important to highlight that this increase was significant from the first week of exposure ($p < 0.001$), which allowed establishing the rapid effect of toluene to induce these changes. Our results coincide with those reported by other authors that found in a rat model that chronic exposure to toluene for 12 days for half an hour significantly increased locomotor activity. In our study, the administration of MP had no effect in reversing the behavioral sensitization induced by toluene. Moreover, MP administered to mice that only received air significantly increased their locomotion. These results are compatible with two aspects: on the one hand, the control of neuroinflammation does not reverse the addictive behavior at least in a short time. Additionally, the increased movements associated with the administration of the glucocorticoid MP may be due to changes in the mice metabolism resembling the result of the "corticoid-euphoria" reported in humans after glucocorticoids treatment [56]. Our results disagree with other reports that suggest that neuroinflammation caused by cell damage due to drug abuse could reinforce addictive behaviors [57,58]. Further research using different glucocorticoids schedules will be necessary to establish the relationship between neuroinflammation and addiction behavior.

Overall, the results obtained in this study showed that MP mitigated the proinflammatory markers and brain damage induced by the exposure to toluene, which allows us to propose the interest of evaluating other glucocorticoids and different administration regimens for the control of secondary damage induced by sustained neuroinflammation induced by chronic consumption of toluene, which could impact the quality of life of inhalant users.

Author Contributions: Conceptualization, M.F.G.-V., N.P.-M., and E.S.; methodology, N.I.P.-O., A.E.-C., and B.M.B.; validation, A.C.-G., G. F., and M.T.-R.; formal analysis, M.F.G.-V., N.P.-M., and E.S.; writing—original draft preparation, M.F.G.-V., G.F., and E.S.; writing—review and editing, N.I.P.-O., A.E.-C., G.F., and E.S.; funding acquisition, E.S. All authors have read and agreed to the published version of the manuscript.

Funding: This research was funded by Dirección General de Personal Académico, UNAM (DGAPA-UNAM, No. 207720), Mexico. This study was also supported by the Institutional program "Programa de Investigación para el Desarrollo y la Optimización de Vacunas, Inmunomoduladores y Métodos Diagnósticos del Instituto de Investigaciones Biomédicas" U.N.A.M, Consejo Nacional de Ciencia y Tecnología, México, grant number 300461 and Instituto Nacional de Psiquiatría Ramón de la Fuente Muñiz; Proyectos SIP-Instituto Politécnico Nacional.

Institutional Review Board Statement: The study was conducted according to the guidelines established by the Committee on the Care and Use of Experimental Animals of the IIB at the Universidad Nacional Autónoma de México (UNAM) and by the U.S. National Institutes of Health. Experimentation protocol was approved by the animal safety and ethical committee of the IIB, UNAM (Protocol Number approval ID 140).

Informed Consent Statement: Not applicable.

Data Availability Statement: Data available at 10.6084/m9.figshare.18343253.

Acknowledgments: We are grateful to Marisela Hernández for technical support and Daniel Garzón for the assistance with animal care. Manuel Giraldo Velázquez obtained his master's from Programa de Maestría en Ciencias Químicas, Universidad Nacional Autónoma de México, and received a fellowship from CONACYT. Also, we would like to thanks to Instituto Nacional de Psiquiatría Ramón de la Fuente Muñiz; Proyectos SIP-Instituto Politécnico Nacional.

Conflicts of Interest: The authors declare no conflicts of interest and the funders had no role in the design of the study; in the collection, analyses, or interpretation of data; in the writing of the manuscript, or in the decision to publish the results.

References

1. Dell, C.A.; Gust, S.W.; MacLean, S. Global Issues in Volatile Substance Misuse. *Subst. Use Misuse* **2011**, *46*, 1–7.
2. Anthony, J.C.; Warner, L.A.; Kessler, R.C. Comparative epidemiology of dependence on tobacco, alcohol, controlled substances, and inhalants: Basic findings from the National Comorbidity Survey. *Exp. Clin. Psychopharmacol.* **1994**, *2*, 244–268.
3. Cruz, S.L.; Rivera-García, M.T.; Woodward, J.J. Review of Toluene Actions: Clinical Evidence, Animal Studies, and Molecular Targets. *J. Drug Alcohol Res.* **2014**, *3*, 1–8.
4. Villatoro, J.A.; Cruz, S.L.; Ortiz, A.; Medina-Mora, M.E. Volatile Substance Misuse in Mexico: Correlates and Trends. *Subst. Use Misuse* **2011**, *46*, 40–45.
5. Cruz, S.L.; Torres-Flores, M.; Galván, E.J. Repeated toluene exposure alters the synaptic transmission of layer 5 medial prefrontal cortex. *Neurotoxicol. Teratol.* **2019**, *73*, 9–14.
6. Paez-Martinez, N.; Flores-Serrano, Z.; Ortiz-Lopez, L.; Ramirez-Rodriguez, G. Environmental enrichment increases doublecortin-associated new neurons and decreases neuronal death without modifying anxiety-like behavior in mice chronically exposed to toluene. *Behav. Brain Res.* **2013**, *256*, 432–440.
7. Ulloque, R.A. Sistema cerebral del placer y de la drogodependencia. *Biomédica* **1999**, *19*, 321.
8. Callan, S.P.; Hannigan, J.H.; Bowen, S.E. Prenatal toluene exposure impairs performance in the Morris Water Maze in adolescent rats. *Neuroscience* **2017**, *342*, 180–187.
9. Montes, S.; del Carmen Solís-Guillén, R.; García-Jácome, D.; Páez-Martínez, N. Environmental enrichment reverses memory impairment induced by toluene in mice. *Neurotoxicol. Teratol.* **2017**, *61*, 7–16.
10. Beckley, J.T.; Woodward, J.J. Volatile Solvents as Drugs of Abuse: Focus on the Cortico-Mesolimbic Circuitry. *Neuropsychopharmacology* **2013**, *38*, 2555–2567.
11. Beckstead, M.J.; Weiner, J.L.; Eger, E.I.; Gong, D.H.; Mihic, S.J. Glycine and gamma-aminobutyric acid(A) receptor function is enhanced by inhaled drugs of abuse. *Mol. Pharmacol.* **2000**, *57*, 1199–1205.
12. Cruz, S.L.; Balster, R.L.; Woodward, J.J. Effects of volatile solvents on recombinant N-methyl-D-aspartate receptors expressed in Xenopus oocytes. *Br. J. Pharmacol.* **2000**, *131*, 1303–1308.
13. Perrine, S.A.; O'Leary-Moore, S.K.; Galloway, M.P.; Hannigan, J.H.; Bowen, S.E. Binge toluene exposure alters glutamate, glutamine and GABA in the adolescent rat brain as measured by proton magnetic resonance spectroscopy. *Drug Alcohol Depend.* **2011**, *115*, 101–106.
14. Yang, Q.; Zhou, J. Neuroinflammation in the central nervous system: Symphony of glial cells. *Glia* **2019**, *67*, 1017–1035.
15. Chen, W.W.; Zhang, X.I.A.; Huang, W.J. Role of neuroinflammation in neurodegenerative diseases (Review). *Mol. Med. Rep.* **2016**, *13*, 3391–3396.
16. Cruz, S.L.; Armenta-Reséndiz, M.; Carranza-Aguilar, C.J.; Galván, E.J. Minocycline prevents neuronal hyperexcitability and neuroinflammation in medial prefrontal cortex, as well as memory impairment caused by repeated toluene inhalation in adolescent rats. *Toxicol. Appl. Pharmacol.* **2020**, *395*, 114980.
17. Cui, C.; Shurtleff, D.; Harris, R.A. Neuroimmune Mechanisms of Alcohol and Drug Addiction. *Int. Rev. Neurobiol.* **2014**, *118*, 1–12. https://doi.org/10.1016/B978-0-12-801284-0.00001-4.
18. Win-Shwe, T.-T.; Kunugita, N.; Yoshida, Y.; Fujimaki, H. Role of hippocampal TLR4 in neurotoxicity in mice following toluene exposure. *Neurotoxicol. Teratol.* **2011**, *33*, 598–602.
19. Win-Shwe, T.T.; Kunugita, N.; Yoshida, Y.; Nakajima, D.; Tsukahara, S.; Fujimaki, H. Differential mRNA expression of neuroimmune markers in the hippocampus of infant mice following toluene exposure during brain developmental period. *J. Appl. Toxicol.* **2012**, *32*, 126–134.
20. Gotohda, T.; Tokunaga, I.; Kubo, S.I.; Morita, K.; Kitamura, O.; Eguchi, A. Effect of toluene inhalation on astrocytes and neurotrophic factor in rat brain. *Forensic Sci. Int.* **2000**, *113*, 233–238.
21. Cruz, S.L.; Bowen, S.E. The last two decades on preclinical and clinical research on inhalant effects. *Neurotoxicol. Teratol.* **2021**, *87*, 106999. https://doi.org/10.1016/j.ntt.2021.106999.
22. Dell, D.; Hopkins, C. Residential Volatile Substance Misuse Treatment for Indigenous Youth in Canada. *Subst. Use Misuse* **2011**, *46*, 107–113. https://doi.org/10.3109/10826084.2011.580225.
23. Real, T.; Cruz, S.L.; Medina-Mora, M.E. Inhalant Addiction. In *Textbook of Addiction Treatment: International Perspectives*; Springer: Milan, Italy, 2015; pp. 597–619.
24. Filley, C.M.; Halliday, W.; Kleinschmidt-Demasters, B.K. The Effects of Toluene on the Central Nervous System. *J. Neuropathol. Exp. Neurol.* **2004**, *63*, 1–12.
25. Barnes, P.J. How corticosteroids control inflammation: Quintiles Prize Lecture 2005. *Br. J. Pharmacol.* **2006**, *148*, 245–254.
26. Whitehouse, M.W. Anti-inflammatory glucocorticoid drugs: Reflections after 60 years. *Inflammopharmacology* **2011**, *19*, 1–19.
27. Ramamoorthy, S.; Cidlowski, J.A. Corticosteroids. *Rheum. Dis. Clin. N. Am.* **2016**, *42*, 15–31.
28. Tuckermann, J.P.; Kleiman, A.; McPherson, K.G.; Reichardt, H.M. Molecular Mechanisms of Glucocorticoids in the Control of Inflammation and Lymphocyte Apoptosis. *Crit. Rev. Clin. Lab. Sci.* **2005**, *42*, 71–104.
29. Erdő, F; Bors, L.A.; Farkas, D.; Bajza, Á.; Gizurarson, S. Evaluation of intranasal delivery route of drug administration for brain targeting. *Brain Res. Bull.* **2018**, *143*, 155–170.

30. Rassy, D.; Bárcena, B.; Pérez-Osorio, I.N.; Espinosa, A.; Peón, A.N.; Terrazas, L.I.; Meneses, G.; Besedovsky, H.O.; Fragoso, G.; Sciutto, E. Intranasal Methylprednisolone Effectively Reduces Neuroinflammation in Mice with Experimental Autoimmune Encephalitis. *J. Neuropathol. Exp. Neurol.* **2020**, *79*, 226–237.
31. Lungare, S.; Bowen, J.; Badhan, R. Development and Evaluation of a Novel Intranasal Spray for the Delivery of Amantadine. *J. Pharm. Sci.* **2016**, *105*, 1209–1220.
32. Páez-Martínez, N.; Pellicer, F.; González-Trujano, M.E.; Cruz-López, B. Environmental enrichment reduces behavioural sensitization in mice previously exposed to toluene: The role of D1 receptors. *Behav. Brain Res.* **2020**, *390*, 112624.
33. Paxinos, G.; Franklin, K.B.J. *The Mouse Brain in Stereotaxic Coordinates*, 3rd ed.; Academic Press, New York, USA, 2007; ISBN 978-0-12-369460-7.
34. Meneses, G.; Gevorkian, G.; Florentino, A.; Bautista, M.A.; Espinosa, A.; Acero, G.; Díaz, G.; Fleury, A.; Osorio, I.N.P.; del Rey, A.; et al. Intranasal delivery of dexamethasone efficiently controls LPS-induced murine neuroinflammation. *Clin. Exp. Immunol.* 2017, *190*, 304–314.
35. Walker, J.M. *Protein Protocols Handbook*; Humana Press, New Jersey, USA, 2002; https://doi.org/10.1385/1592591698.
36. Meneses, G.; Cárdenas, G.; Espinosa, A.; Rassy, D.; Pérez-Osorio, I.N.; Bárcena, B.; Fleury, A.; Besedovsky, H.; Fragoso, G.; Sciutto, E. Sepsis: Developing new alternatives to reduce neuroinflammation and attenuate brain injury. Ann. N. Y. Acad. Sci. 2019, 1437, 43–56.
37. Bryan, N.S.; Grisham, M.B. Methods to detect nitric oxide and its metabolites in biological samples. *Free Radic. Biol. Med.* **2007**, *43*, 645–657.
38. Aydin, K.; Sencer, S.; Demir, T.; Ogel, K.; Tunaci, A.; Minareci, O. Cranial MR findings in chronic toluene abuse by inhalation. *AJNR. Am. J. Neuroradiol.* **2002**, *23*, 1173–1179.
39. Demir, M.; Cicek, M.; Eser, N.; Yoldaş; A; Sısman, T. Effects of Acute Toluene Toxicity on Different Regions of Rabbit Brain. *Anal. Cell. Pathol.* **2017**, *2017*, 1–6.
40. Montes, S.; Yee-Rios, Y.; Páez-Martínez, N. Environmental enrichment restores oxidative balance in animals chronically exposed to toluene: Comparison with melatonin. *Brain Res. Bull.* **2019**, *144*, 58–67.
41. Gao, Q.; Li, Y.; Shen, L.; Zhang, J.; Zheng, X.; Qu, R.; Liu, Z.; Chopp, M. Bone marrow stromal cells reduce ischemia-induced astrocytic activation in vitro. *Neuroscience* **2008**, *152*, 646–655.
42. Spooren, A.; Kolmus, K.; Laureys, G.; Clinckers, R.; De Keyser, J.; Haegeman, G.; Gerlo, S. Interleukin-6, a mental cytokine. *Brain Res. Rev.* **2011**, *67*, 157–183.
43. Sakai, T.; Honda, S.; Kuzuhara, S. Encephalomyelopathy demonstrated on MRI in a case of chronic toluene intoxication. *Rinsho Shinkeigaku* **2000**, *40*, 571–575.
44. Celik, F.; Göçmez, C.; Kamaşak, K.; Tufek, A.; Guzel, A.; Tokgoz, O.; Fırat, U.; Evliyaoğlu, O. The comparison of neuroprotective effects of intrathecal dexmedetomidine and metilprednisolone in spinal cord injury. *Int. J. Surg.* **2013**, *11*, 414–418. https://doi.org/10.1016/j.ijsu.2013.03.008.
45. Liu, S.; Liu, X.; Chen, S.; Xiao, Y.; Zhuang, W. Oral versus intravenous methylprednisolone for the treatment of multiple sclerosis relapses: A meta-analysis of randomized controlled trials. *PLoS ONE* **2017**, *12*, e0188644. https://doi.org/10.1371/journal.pone.0188644.
46. Hendler, J.V.; de Souza, L.; de Freitas Zernow, D.C.; Guimarães, J.; Bertotto, T.; Saldanha, C.F.; Brenol, J.C.T.; Monticielo, O.A. Survival analysis of patients with systemic lupus erythematosus in a tertiary hospital in southern Brazil. *Clin. Rheumatol.* **2017**, *36*, 2005–2010. https://doi.org/10.1007/s10067-017-3735-1.
47. Tischner, D.; Reichardt, H.M. Glucocorticoids in the control of neuroinflammation. *Mol. Cell. Endocrinol.* **2007**, *275*, 62–70. https://doi.org/10.1016/j.mce.2007.03.007.
48. Djupesland, P.G.; Messina, J.C.; Mahmoud, R.A. The nasal approach to delivering treatment for brain diseases: An anatomic, physiologic, and delivery technology overview. *Ther. Deliv.* **2014**, *5*, 709–733. https://doi.org/10.4155/tde.14.41.
49. Ducharme, N.; Banks, W.A.; Morley, J.E.; Robinson, S.M.; Nielhoff, M.L.; Mattern, C. Brain distribution and behavioral effects of progesterone and pregnenolone after intranasal or intravenous administration. *Eur. J. Pharmacol.* **2010**, *641*, 128–134. https://doi.org/10.1016/j.ejphar.2010.05.033.
50. Chapman, C.D.; Frey, W.H.; Craft, S.; Danielyan, L.; Hallschmid, M.; Schiöth, H.B.; Benedict, C. Intranasal Treatment of Central Nervous System Dysfunction in Humans. *Pharm. Res.* **2013**, *30*, 2475–2484. https://doi.org/10.1007/s11095-012-0915-1.
51. Espinosa, A.; Meneses, G.; Chavarría, A.; Mancilla, R.; Pedraza-Chaverri, J.; Fleury, A.; Bárcena, B.; Pérez-Osorio, I.N.; Besedovsky, H.; Arauz, A.; et al. Intranasal Dexamethasone Reduces Mortality and Brain Damage in a Mouse Experimental Ischemic Stroke Model. *Neurotherapeutics* **2020**, *17*, 1907–1918. https://doi.org/10.1007/s13311-020-00884-9.
52. Zou, H.; Guo, S.-W.; Zhu, L.; Xu, X.; Liu, J. Methylprednisolone Induces Neuro-Protective Effects via the Inhibition of A1 Astrocyte Activation in Traumatic Spinal Cord Injury Mouse Models. *Front. Neurosci.* **2021**, *15*, 628917. https://doi.org/10.3389/fnins.2021.628917.
53. Oberleithner, H.; Riethmüller, C.; Ludwig, T.; Shahin, V.; Stock, C.; Schwab, A.; Hausberg, M.; Kusche, K.; Schillers, H. Differential action of steroid hormones on human endothelium. *J. Cell Sci.* **2006**, *119*, 1926–1932. https://doi.org/10.1242/jcs.02886.
54. Gerber, A.N.; Newton, R.; Sasse, S.K. Repression of transcription by the glucocorticoid receptor: A parsimonious model for the genomics era. *J. Biol. Chem.* **2021**, *296*, 100687. https://doi.org/10.1016/j.jbc.2021.100687.
55. Tu, G.; Shi, Y.; Zheng, Y.; Ju, M.; He, H.; Ma, G.; Hao, G.; Luo, Z. Glucocorticoid attenuates acute lung injury through induction of type 2 macrophage. *J. Transl. Med.* **2017**, *15*, 181. https://doi.org/10.1186/s12967-017-1284-7.

56. Ciriaco, M.; Ventrice, P.; Russo, G.; Scicchitano, M.; Mazzitello, G.; Scicchitano, F.; Russo, E. Corticosteroid-related central nervous system side effects. *J. Pharmacol. Pharmacother.* **2013**, *4*, 94. https://doi.org/10.4103/0976-500X.120975.
57. Guerri, C.; Pascual, M. Impact of neuroimmune activation induced by alcohol or drug abuse on adolescent brain development. *Int. J. Dev. Neurosci.* **2019**, *77*, 89–98. https://doi.org/10.1016/j.ijdevneu.2018.11.006.
58. Harricharan, R.; Abboussi, O.; Daniels, W.M.U. Addiction: A dysregulation of satiety and inflammatory processes. *Prog. Brain Res.* **2017**, *235*, 65–91.

Anexo 4.

Vaccine

Towards the development of an epitope-focused peptide vaccine for SARS-CoV-2

--Manuscript Draft--

Manuscript Number:	JVAC-D-21-02872
Article Type:	Original article
Section/Category:	Human Viral Vaccines: Basic Research
Keywords:	vaccine; COVID-19; peptides; SARS-CoV-2; Mice; hamster
Corresponding Author:	Edda Sciutto-Conde, Ph.D. Universidad Nacional Autonóma de México Instituto de Investigaciones Biomédicas: Universidad Nacional Autonoma de Mexico Instituto de Investigaciones Biomedicas MEXICO
First Author:	Edda Sciutto-Conde, Ph.D.
Order of Authors:	Edda Sciutto-Conde, Ph.D.
	Jacquelynne Cervantes-Torres, Ph.D.
	Sergio Rosales, Ph.D.
	Carlos Cabello, Ph.D.
	Laura Montero, M.Sc.
	Juan Hernandez-Aceves, B.Sc.
	Guillermo Granados, B.Sc.
	Arturo Calderón-Gallegos, B.Sc.
	Francisco Zúñiga-Flores, B.Sc.
	Mima Ruiz-Rivera, B.Sc.
	Julio César Abarca-Magaña, B.Sc.
	Sandra Ortega-Francisco, B.Sc.
	Roxana Olguin-Alor, Ph.D.
	Georgina Díaz, B.Sc.
	Filipo Paczka-Garcia, B.Sc.
	Rubí Zavala-Gaytan, M.Sc.
	Ricardo Vázquez-Ramírez, B.Sc.
	Dolores Adriana Ayón-Nuñez, M.Sc.
	Julio César Carrero, Ph.D.
	Diana Rios, Ph.D.
	Mariana Jasso-Ramírez, B.Sc.
	Rebeca Vázquez-Hernández, B.Sc.
	David Venegas, B.Sc.
	Daniel Garzón, Ph.D.
	Laura Cobos, Ph.D.
	René Segura-Velázquez, Ph.D.
	Nelly Villalobos, Ph.D.
	Gabriela Meneses, Ph.D.

	Joaquín Zúñiga, Ph.D.
	Gerardo Gamba, Ph.D.
	Graciela Cárdenas, Ph.D.
	Marisela Hernández, Ph.D.
	Michael E Parkhouse, Ph.D.
	Marta C. Romano, Ph.D.
	Luis Alonso Herrera, Ph.D.
	Raúl J. Bobes, Ph.D.
	Mayra Pérez-Tapia, Ph.D.
	Leonor Huerta, Ph.D.
	Nora Fierro, Ph.D.
	Isabel Gracia, M.Sc.
	Gloria Soldevilla, Ph.D.
	Gladis Fragoso, Ph.D.
	Francisco Suárez-Güemes, Ph.D.
	Juan P. Laclette, Ph.D.
Abstract:	Highlights - A RBD-based synthetic peptide was shown safe when injected to mice and hamsters. - The vaccine candidate elicited antibodies that sustained for up to 2 months in mice. - Neutralizing antibodies and antigen-specific CD4+CD8+-IFNγ responses were detected.
Suggested Reviewers:	Luis Vaca Domínguez, Ph.D. Instituto de Fisiología Celular, UNAM lvaca@ifc.unam.mx
	Fernando Goldbaum, Ph.D. Instituto Leloir fagoldbaum@gmail.com
	Oscar Adelmo Bottasso, Ph.D. Instituto de Inmunología Clínica y Experimental de Rosario oscarbottasso@outlook.com
	Juliana Cassataro, Ph.D. Instituto de Investigaciones Biotecnológicas jucassat@ffyb.uba.ar
	Jesús Torres-Flores, Ph.D. Consejo Nacional de Ciencia y Tecnología: Consejo Nacional de Ciencia y Tecnologia chu_torrey@hotmail.com
	Carlos Federico Arias Ortiz, Ph.D. Instituto de Biotecnología UNAM arias@ibt.unam.mx
	Constantino López, Ph.D. Facultad de Química UNAM constantino.lopez@comunidad.unam.mx
Opposed Reviewers:	

Cover Letter

UNIVERSIDAD NACIONAL AUTÓNOMA DE MEXICO

INSTITUTO DE INVESTIGACIONES BIOMEDICAS
APARTADO POSTAL 70228
CIUDAD UNIVERSITARIA
04510 MÉXICO, D. F.

October 26, 2021

Dr. Gregory A. Poland
Editor-in-Chief
Vaccine

Dear Dr. Poland,

Enclosed please find the manuscript titled "Towards the development of an epitope-focused peptide vaccine for SARS-CoV-2," that we are submitting to be considered for publication as a full-length paper on *Vaccine*.

In our article, we report a platform for the development of a peptide-based vaccine against SARS-Cov-2 and an evaluation of its safety and immunogenicity. Our peptide-based vaccine targets one of the most immunogenic peptides in the RBD domain of the SARS-Cov2 virus. As you will notice, it proved to induce a robust immune response; furthermore, it was safe when parenterally administered to rodents. The results reported in this study support the feasibility of developing a peptide-based vaccine against SARS-Cov2. Given the low cost of our platform and its immunogenicity, it could provide a better alternative to control COVID-19 in medium- and low-income countries once it is optimized.

We hope you will find our manuscript of interest for the readers of your prestigious journal.

Best regards,

Dr. Edda Sciutto

Declaration of interests

☐The authors declare that they have no known competing financial interests or personal relationships that could have appeared to influence the work reported in this paper.

☒The authors declare the following financial interests/personal relationships which may be considered as potential competing interests:

Edda Sciutto reports financial support was provided by Dirección General de Personal Académico de la Universidad Nacional Autónoma de México. Edda Sciutto reports financial support was provided by Agencia Mexicana de Cooperación Internacional para el Desarrollo. Edda Sciutto reports financial support was provided by Programa Conjunto de Cooperación México-Chile, Secretaría de Relaciones Exteriores de México.

Towards the development of an epitope-focused peptide vaccine for SARS-CoV-2

Jacquelynne Cervantes-Torres[a], Sergio Rosales[b,c], Carlos Cabello[d], Laura Montero[a], Juan Hernandez-Aceves[a], Guillermo Granados[a], Arturo Calderón-Gallegos[a], Francisco Zúñiga-Flores[a], Mirna Ruiz-Rivera[a], Julio César Abarca-Magaña[a], Sandra Ortega-Francisco[a], Roxana Olguin-Alor[a], Georgina Díaz[a], Filipo Paczka-Garcia[a], Rubí Zavala-Gaytan[a], Ricardo Vázquez-Ramírez[a], Dolores Adriana Ayón-Nuñez[e], Julio César Carrero[a], Diana Rios[a], Mariana Jasso-Ramírez[a], Rebeca Vázquez-Hernández[a], David Venegas[a], Daniel Garzón[a], Laura Cobos[e], René Segura-Velázquez[e], Nelly Villalobos[e], Gabriela Meneses[f], Joaquín Zúñiga[d], Gerardo Gamba[a,g], Graciela Cárdenas[h], Marisela Hernández[a], Michael E Parkhouse[i], Marta C. Romano[j], Luis Alonso Herrera[k], Raúl J. Bobes[a], Mayra Pérez-Tapia[l], Leonor Huerta[a], Nora Fierro[a], Isabel Gracia[m], Gloria Soldevilla[a], Gladis Fragoso[a], Francisco Suárez-Güemes[e], Juan P. Laclette[a*], Edda Sciutto[a*]

[a]Instituto de Investigaciones Biomédicas, [e]Facultad de Medicina Veterinaria y Zootecnia, [m]Facultad de Química, Universidad Nacional Autónoma de México, Ciudad Universitaria s/n, Ciudad de México, 04510, Ciudad de México.

[b]Laboratorio de Biofarmacéuticos Recombinantes, Facultad de Ciencias Químicas, Universidad Autónoma de San Luis Potosí, Av. Dr. Manuel Nava 6, S.L.P, 78210, México.

[c]Sección de Biotecnología, Centro de Investigación en Ciencias de la Salud y Biomedicina, Universidad Autónoma de San Luis Potosí, Av. Sierra Leona 550, Lomas 2ª Sección, San Luis Potosí, 78210, México.

[d]Instituto Nacional de Enfermedades Respiratorias "Ismael Cosio Villegas". Calz. de Tlalpan 4502, Belisario Domínguez Secc. 16, Tlalpan, 14080 Ciudad de México, CDMX.

[f]Instituto de Diagnóstico y Referencia Epidemiológica "Dr. Manuel Martínez Báez". Francisco de P. Miranda 177, Lomas de Plateros, Álvaro Obregón, 01480 Ciudad de México, CDMX.

[g]Instituto Nacional de Ciencias Médicas y Nutrición "Salvador Zubirán". Vasco de Quiroga 15, Belisario Domínguez Secc. 16, Tlalpan, 14080 Ciudad de México, CDMX.

[h]Instituto Nacional de Neurología y Neurocirugía. Av. Insurgentes Sur 3877, La Fama, Tlalpan, 14269 Ciudad de México, CDMX.

[i]Instituto Gulbekian de Ciência, Portugal. R. Q.ta Grande 6, 2780-156 Oeiras, Portugal.

[j]Centro de Investigación y de Estudios Avanzados del Instituto Politécnico Nacional. Av. Instituto Politécnico Nacional 2508, San Pedro Zacatenco, Gustavo A. Madero, 07360 Ciudad de México, CDMX.

[k]Instituto Nacional de Medicina Genómica. Periférico Sur 4809, Arenal Tepepan, 4610 Ciudad de México.

[l]Unidad de Desarrollo e Investigación en Bioprocesos, Escuela Nacional de Ciencias Biológicas, Instituto Politécnico Nacional. Prolongación de Carpio y Plan de Ayala S/N, Col. Casco de Santo Tomas, Del. Miguel Hidalgo, C.P 11340. Ciudad de México, CDMX.

*Corresponding authors

Edda Sciutto and Juan P. Laclette, Department of Immunology, Biomedical Research Institute, Universidad Nacional Autónoma de México, Circuito escolar s/n, 04510 Coyoacán, Ciudad de México, México, 52(55) 5622-3153; E-mail: edda@unam.mx; laclette@iibiomedicas.unam.mx

Key words: vaccine, COVID-19, peptides, SARS-CoV-2, mice, hamster

Abstract

The rapid spread of COVID-19 on all continents and the mortality induced by SARS-CoV-2 virus, the cause of the pandemic coronavirus disease 2019 (COVID-19) has motivated an unprecedented effort for vaccine development. Inactivated viruses as well as vaccines focused on the partial or total sequence of the Spike protein using different novel platforms such us RNA, DNA, proteins, and non-replicating viral vectors have been developed. The high global need for vaccines, now and in the future, and the emergence of new variants of concern still requires development of accessible vaccines that can be adapted according to the most prevalent variants in the respective regions.

Here, we describe the immunogenic properties of a group of theoretically predicted RBD peptides to be used as the first step towards the development of an effective, safe and low-cost epitope-focused vaccine. One of the tested peptides named P5, proved to be safe and highly immunogenic. Subcutaneous administration of the peptide, formulated with alumina, induced high levels of specific IgG antibodies in mice and hamsters, as well as an increase of IFN-γ expression by CD8+ T cells in C57 and BALB/c mice upon *in vitro* stimulation with P5. Neutralizing titers of anti-P5 antibodies, however, were disappointingly low, a deficiency that we will attempt to resolve by the inclusion of additional immunogenic epitopes to P5. The safety and immunogenicity data reported in this study support the use of this peptide as a starting point for the design of an epitope restricted peptide vaccine.

Highlights

- A RBD-based synthetic peptide was shown safe when injected to mice and hamsters.
- The vaccine candidate elicited antibodies that sustained for up to 2 months in mice.
- Neutralizing antibodies and antigen-specific CD4+CD8+-IFNγ responses were detected.

1. Introduction

Vaccination has been demonstrated highly effective against SARS-CoV-2 coronavirus. However, despite all vaccines produced, there is still a need for more effective and safe vaccines against COVID-19, the cause of the worst pandemic public-health crisis in a century. Its rapid spread has promoted development of several vaccines in less than one year. Except for inactivated virus vaccines (Sinopharm and Sinovac), all have targeted the full length Spike (S) protein [1, 2]. mRNA-1273 (Moderna), 2BNT162b2 (Pfizer/BioNTech), ChAdOx1-S (University of Oxford/Astra Zeneca), Gam-COVID-Vac; Sputnik V (Gamaleya Institute), Ad5-nCoV (Cansino Biological Inc), Ad26.COV2.S (Janssen Pharmaceutical/Johnson & Johnson) and NVX-CoV2373 (Novavax). All have proven effective in preventing severe COVID-19 [1,3]. The RBD domain located at C-terminal domain in S the protein, has also been considered as an effective target-vaccine [1]. RBD comprises the domain responsible for the entrance of the virus through its association to the human receptor of angiotensin-converting enzyme 2 (hACE2) [4]. Indeed, antibodies against RBD are highly effective to block the receptor binding [5]. Thus, RDB has been expressed under different molecular platforms [6, 7, 8, 9, 10] and as a tandem-repeat dimeric RBD protein (ZF2001) formulated with alum-based adjuvant has been already accepted for human used [11].

Despite the biotechnological success of all vaccines developed in record time, many challenges remain to be solved to overcome the COVID-19 pandemic emergency. Population in many countries still remain without access to vaccine protection, including those sectors with high probability of morbidity and mortality.

The absence of immunity in a substantial portion of the world population offers the appropriate niche for the virus to evolve into new and eventually more pathogenic or more infectious variants, that can affect not only non-immune but also vaccinated individuals.

Therefore, the importance of achieving worldwide immunity as recommended by OMS against this new virus is clear, in order to interrupt transmission. Available vaccines continue to be effective against new variants of concern albeit the levels of protection have decreased. However, to compensate their decreasing efficiency, disregarding OMS recommendations, different developed countries have approved the use of a third dose of vaccine to reinforce the immunity of their populations. Favored by the lack of a global health coordination, the pandemic still poses a considerable threat. It is necessary a continued effort on vaccine development, to promote a global population immunity with an emphasis in supporting the poorest countries with more vaccines [12], as well as to become prepared against possible future changes in the virus.

Here, we propose the development of a reproducible and secure, epitope focused, synthetic peptide vaccine, containing crucial B-and T-cell epitopes of RBD, which may provide an affordable and scalable vaccine. Initial design relied on bioinformatic analysis of the spike protein, resulting in 6 short peptide sequences whose immunogenicity was assessed in mice. Of these, one (Peptide 5) was selected for a more extensive study on its humoral and cellular immunogenic properties. This work may be considered a simple and secure platform for the development of an effective anti-COVID-19 vaccine.

2. **Materials and Methods**

2.1. Mice

Mice from 9-16 weeks old used in this study were obtained from two different sources. Male and female BALB/c and female C57BL/6 were kindly provided by F. Rosetti from the Instituto Nacional de Ciencias Médicas y Nutrition Salvador Zubirán animal facilities. Other BALB/c mice were bred and obtained in the animal facilities of the Biomedical Research Institute. Eight to 10-week-old female and male golden Syrian hamsters were purchased from Facultad de Ciencias, UNAM animal facilities.

All procedures performed on animals in this study were conducted in accordance with national (Norma Oficial Mexicana, NOM-062-ZOO-1999) and institutional regulations for the use and care of laboratory animals, following two protocols approved by the Institutional Committee (approval numbers 6343 and 6345).

2.2. Bioinformatic analysis

Epitope prediction from the RBD of the SARS-CoV-2 spike protein

The sequence of the SARS-CoV-2 spike glycoprotein was obtained from the GenBank database (Gene ID: 43740568) (https://www.ncbi.nlm.nih.gov), and the RBD including residues 331 to 524 of the S protein [13] was analyzed for epitope prediction. We employed the Immune Epitope Database (IEDB) and IEDB-3D (http://www.iedb.org/) using the Bepipred Linear Epitope Prediction 2.0 with the scoring threshold set to 0.5 to Predict linear B cell epitopes and ElliPro: Antibody Epitope Prediction algorithms to predict discontinuous B cell epitopes using PDB ID: 7DF3 chain B, with a minimum score of 0.5 and maximum distance of 6 Å. To

determine if the predicted epitopes were exposed to the protein surface and the degree of contact to ACE2, tridimensional structures of the SARS-CoV-2 S protein (PDB ID: 7DF3, and the SARS-CoV-2 S RBD/ACE2 complex (PDB ID: 7DF4) were used. The homotrimeric complex (chains A-C) of protein S was visualized and the exposed residues of the predicted epitopes were identified by calculating the solvent accessible area with Swiss-PdbViewer software [13]. In addition, the residues of the predicted epitopes exposed to ACE2 were identified knowing the polar (hydrogen bonds) and hydrophobic (van der Waals) interactions established in the cocrystallizated complex RBD/ACE2 (PDB ID: 7DF4). The SARS-CoV-2 S RBD residues bound to ACE2 were identified using the Discovery Studio (https://www.3ds.com/products-services/biovia/products/molecular-modeling-simulation/biovia-discovery-studio/) software, establishing as geometric parameters of the interacting atoms, the following thresholds: 3.5 Å for hydrogen bond and 4.0 Å for hydrophobic interactions.

2.3. Peptides

Peptides were purchased from GenScript (NJ, USA) or from Synpeptide Co (Shangai, China); specifications from both manufacturers indicated >95% purity. Peptides were dissolved at 5 mg per mL according to their physicochemical properties: peptides 1 and 2 were dissolved in 0.9% saline solution (ISS), peptides 3 and 4 in sterile water, and peptides 5 and 6 in DMSO (1%) and sterile water. The helper peptide was prepared at 2 mg per mL in DMSO (1%) and sterile water.

2.4. Immunization

184 Groups of six to eight mice received three doses of each peptide diluted in saline
185 together with a single adjuvant by subcutaneous (sc) or intranasal (int) routes, every
186 7 days as described in figures legends and tables. For s.c. vaccination, mice were
187 immunized in the dorsal flank (27Gx13 mm needle) with a final volume of 100 µL,
188 and for int. vaccination mice received a maximum of 12.5 µL per nostril.

189 Adjuvants employed were AddaVax (MF59 analog, Invivogen) or aluminum
190 hydroxide [Al $(OH)_3$] (kindly donated by J. Garza-Ramos, PRONABIVE México).
191 AddaVax or Al $(OH)_3$ were mixed 1:1 with each peptide to a final volume of 100 µL.

192 Additionally, a group of nine mice were subcutaneously administered with
193 peptide 5 at 50 µg, plus influenza vaccine (Fluzone ®, SanofiPasteur) at 10 µg mixed
194 with aluminum hydroxide (1:1) to a final volume of 300 µL. Mice were kept with food
195 and water *ad libitum* and monitored daily and weighted before each immunization
196 and sacrificed. Blood samples were taken before immunization, and 7 days after the
197 last immunization to determine antibody levels of individual mice. The resulting sera
198 were frozen at -20°C until use. Broncho-alveolar fluids were also recovered 7 days
199 after the last immunization and kept at -70°C until use for antibody level
200 determination.

201 Groups of five to six hamsters including males and females were immunized s.c.
202 or int. with peptide 5 mixed with aluminum hydroxide or AddaVax (1:1) at a final
203 volume of 100 µL. The animals were immunized three times at an interval of seven
204 days, using doses of 50, 100 or 200 µg.

205 *2.5. Antibody detection by ELISA*

206 Serum antibody levels were determined by indirect ELISA, using the respective
207 peptide as antigen source, following a previously described procedure with minor
208 modifications [14]. Binding of the peptide or protein target to the wells was carried
209 out using 100 µL of each peptide (5 µg/mL) in carbonate buffer. The plates were
210 incubated overnight at 4°C, washed and then incubated with 100 µL of each serum
211 diluted 1:50 in PBS-BSA 1% for one h at 37°C. Antibodies were detected with 100
212 µL of goat anti-mouse IgG (H+L) alkaline-phosphatase conjugate (Sigma), diluted to
213 the optimum concentration (1:5000) and followed by substrate (p-nitrophenyl
214 phosphate, Sigma, 1 mg/mL). The reaction was stopped using 50 µL/well of NaOH
215 2N, and absorbance values were determined at 405 nm in a microplate
216 spectrophotometer reader (Epoch, Biotek, USA). Results were the average of
217 triplicate cultures.

218 2.6. *Cross-reactivity between anti-peptide 5 antibodies and the Spike protein*
219 *RBD domain*

220 For human sera, ELISA plates were coated with Peptide 5 at 5 µg per mL in
221 citrate buffer or with recombinant RBD expressed in eukaryotic cells (kindly provided
222 by UDIBI, at the National Polytechnic Institute) at 1 µg per mL in carbonate buffer.
223 Five sera from COVID-19 convalescent and 46 hospitalized patients were obtained
224 in the Instituto Nacional de la Nutrición, Instituto Nacional de Enfermedades
225 Respiratorias and Instituto Nacional de Neurología y Neurocirugía. Sera from
226 healthy donors obtained in 2014 were used as negative controls. Sera were diluted
227 in PBS containing 1% skimmed milk, incubated for 2 h at 25 °C and, after washing
228 5 times, the plates were developed with horseradish-peroxidase conjugated goat

anti-human IgG (1:10,000, 45 min.) and the absorbance at 450 nm was evaluated. Results were the average of triplicate determinations.

2.7. *Virus neutralization assay*

The assay was performed according to [15]. Fifty microliters of 2-fold serial diluted mouse sera were preincubated with an equal volume of SARS-CoV-2 (MOI=0.1) at 37 °C for 1 h. and the mixture was then added to VERO E6 cells seeded in 96-well plates for 3 days at 37 °C and 5% CO2. The resulting cytopathic effect (CPE) was visualized every day under the microscope. The cells were washed and fixed with ethanol:acetone (1:1) for 15 min. and finally stained with violet crystal for 20 min. Positive and negative controls were included in the assay. Results were the average of three sera per group.

2.8. *Cellular Immune Response*

Briefly, splenocytes were obtained from peptide P5 immunized or unimmunized control mice, and cultured in 24-well plates with 2 $x10^6$ cells per well. To evaluate the antigen-specific T cell response, cells were first incubated with Cell Trace Violet (CTV) (Invitrogen Inc, City State), for 15 min at 37 °C, washed and then stimulated with peptide 5 (10 µg/ml), anti-CD3+ anti-CD28 antibodies (1 µg/ml) as a positive activation control or as a negative control, with RPMI complete medium alone, for three days. Cells were harvested and stained for 20 minutes at room temperature with anti-CD4 APC, anti-CD8 PE and with Zombie NIR, as viability dye (all from Biolegend). Next, cells were permeabilized (Tonbo Permeabilization Kit) for 1 h at room temperature and Fc receptors were blocked with anti CD16/32 (Biolegend) for 20 minutes at 4°C followed by intracellular staining with anti-IFNγ BV510

252 (Biolegend), for 30 min 4°C. Samples were acquired in an Atunne NxT Acoustic
253 Focusing Flow Cytometer (Thermo Scientific) and analyzed with Flow Jo 10 software
254 (Tree Star Inc). Results were the average of triplicate cultures.

255 *2.9. Clinical and pathological evaluation in vaccinated and non-vaccinated*
256 *mice and hamsters*

257 To evaluate the safety of the vaccine candidate peptides, the number of deaths
258 or apparent undesirable clinical signs were registered. Body weights of male and
259 female immunized and non-immunized mice and hamsters of all treatment groups
260 were evaluated along the study period. Three mice or hamsters included in each of
261 the treatment groups were humanly sacrificed under anesthesia on day 7 after the
262 last immunization. The liver, heart, brain, lungs were fixed in 10% formaldehyde and
263 embedded in paraffin. Three µm thick serial-sections were prepared from non-
264 consecutive areas, stained with hematoxylin and eosin (H&E), and at least two
265 sections per tissue for each animal were examined for the presence of histological
266 abnormalities (magnification: 400× and 100×).

267

268 **3. Results**

269 *3.1. Bioinformatic identification of RBD vaccine epitopes*

270 Identification of highly immunogenic epitopes within RBD is essential for the
271 development of an effective peptide vaccine against COVID-19. Six different
272 epitopes (P1-P6) with high antigenic score were predicted between residues 407 to
273 506 of the RBD domain (Fig. 1). All of the epitopes were highly surface exposed, but
274 neither P2 nor P6 interact with ACE2, and P1 only had a polar interaction to ACE2

275 at Q42. The epitope P3 can potentially associated with ACE2 mainly with polar
276 interactions (F490, Q493, S494, G496, T500 and Y505) and some hydrophobic
277 interactions (Q493 and G502).

278 While P5, had the highest number of residues theoretically interacting with ACE2
279 (A475, G476, N487, F490 and Q493 via hydrogen bonds and Q474, G476, N487,
280 F490, and Q493 via hydrophobic interactions) (Supplementary Table 1).

281 *3.2. Antibody responses to the RBD synthetic peptides*

282 The predicted peptides were synthetized and tested for their ability to elicit
283 specific IgA and IgG antibodies in BALB/c and C57BL/6 mice. The mice were
284 immunized either subcutaneous (s.c.) or intranasal, three times every seven days
285 and bled before the first immunization as well as seven days after the last
286 immunization before being humanly sacrificed. Broncho-alveolar fluids were also
287 recovered. For the statistical analysis, mice were grouped by body weight.

288 Both P4 and P5 peptides elicited a significant IgG response in s.c. vaccinated
289 BALB/c and C57BL/6 mice. Only sera that were positive to peptide 5 recognized a
290 recombinant RBD produced in eukaryotic cells (Table 1). Intranasal administration
291 failed to elicit detectable levels of IgA antibodies in serum (Supplementary Table 2)
292 and bronchoalveolar fluid (data not shown). Thus, peptide P5 was selected for
293 subsequent analysis.

294 *3.3. Reported mutations within peptide 5 sequence*

295 The mutations reported worldwide in the Global Initiative on Sharing All Influenza
296 Data (GISAID; https://www.gisaid.org) [16] for P5 were identified (Supplementary

297 Table 3). The update shows that the entire P5 sequence has mutations; the reported
298 occurrence allows assessing the mutational influence for each P5 amino acid. The
299 relevant amino acids for being part of the worldwide circulation variants are: T478K
300 (Delta variant), E484K (Beta, Gamma and Iota variants), E484Q (Kappa variant).
301 Also, S477N and F490S should be considered for high incidence.

302 Mutations were ordered according to their reported occurrence. Considering the
303 most abundant mutation (the first on the left in each mutation), most of the
304 substitutions were conservative mutations, corresponding to similar biochemical
305 properties (e.g., size, polar, hydrophobic, or aromatic amino acid) compared to P5.
306 However, when considering amino acid charges, three mutations in the polar amino
307 acids can significantly change the electronic structure of P5, because they change
308 from neutral to polar basic (T478K, N481K) and from acidic to basic (E484K)
309 (Supplementary Table 3).

310

311 *3.4. Differential antibody responses between mice strains immunized with*
312 *peptide P5*

313 To define the optimal P5 dose inducing the highest specific antibody response,
314 female C57BL/6 and BALB/c mice were immunized 3 times. Similarly, high levels of
315 IgG were observed in C57BL/6 after s.c. immunization with all doses of P5. In
316 contrast, there was a dose dependent antibody response to P5 in BALB/c mice
317 (Table 2). Thus, subcutaneous immunization induced high antibody responses in
318 both strains of mice, with a higher antibody response at the lower dose of P5 in
319 C57BL/6 mice, the most inflammatory strain. Furthermore, intranasally immunized

mice elicited low but significant IgG specific antibody levels in C57BL/6 mice for all doses used. Finally, insignificant levels of anti-P5 IgA antibodies were detected in sera from s.c. or intranasally immunized mice (Supplementary Table 4).

3.5. Sexual dimorphism in the antibody response induced in peptide P5 immunized mice

Initial experiments pointed to the existence of sexual dimorphisms in the antibody levels induced by peptide P5 in mice (data not shown). This was further explored by immunizing female and male BALB/c mice using the same protocol described above. As shown in Supplementary Table 5, significantly higher levels of specific IgG antibodies were induced in female than in male mice after s.c. immunization with 3 doses of peptide P5.

3.6. Aluminum hydroxide is more effective adjuvant than AddaVax for vaccination of mice

To evaluate the best formulation for the vaccine, we performed experiments employing an oil-based adjuvant (AddaVax) or aluminum hydroxide (Aluminatrihydrate). Both adjuvants are approved for use in humans. Production of specific IgG anti-P5 antibodies was similar when mice were immunized s.c. using either adjuvant. Higher levels of antibodies were found in C57BL/6 mice relative to BALB/c, independent of the adjuvant used (Table 3). Low levels of specific IgA antibodies were detected in broncho-alveolar fluids of mice after s.c. and intranasal administration (Supplementary Table 6), but neither adjuvant induced detectable levels of IgA antibodies in serum (data not-shown).

342 *3.7. Aluminum hydroxide was more effective than AddaVax for the induction of*
343 *anti-P5 IgG antibodies in hamsters*

344 Considering that hamsters are natural hosts for SARS-CoV-2, the
345 immunogenicity of P5 was also evaluated in hamsters. High levels of specific IgG
346 antibodies were induced by s.c. immunization of hamsters with 3 doses of P5 using
347 AddaVax as adjuvant and they were dose dependent for P5 (Table 4). However,
348 higher levels of specific IgG antibodies were induced in hamsters immunized with
349 the lower dose of P5 using aluminum hydroxide as adjuvant. No sexual dimorphism
350 in the antibody response was observed in hamsters under these immunization
351 protocols. Finally, no IgG levels were detected in the sera after intranasal
352 immunization of hamsters with P5 (Table 4).

353 *3.8. No clinical and pathological features were associated with peptide P5*
354 *immunization*

355 No deaths or apparent clinical signs were found in any group of mice or hamsters
356 treated with 3 doses of P5 in combination with either of the two adjuvants. The weight
357 of both species of animals remained statistically unchanged, before and after
358 immunization with P5 (Suppl. Fig. 1). Furthermore, after histological inspection of
359 control and immunized mice, no abnormalities were found in the brains, kidneys,
360 spleen, pancreas, heart, small and large intestines (data no shown). The most
361 important hepatic alteration was vacuolar degeneration that occurred in 100% of the
362 samples and in mild to moderate grades (Suppl. Fig. 2 A, C). Some hepatocytes
363 were found with prominent karyomegaly and nuclei, and pyknotic nuclei in two
364 individuals. These findings were also found in the control group, so they are not

365 associated with treatment. In the lung. The most important alteration was alveolar
366 macrophage hyperplasia, which occurred in 80% of individuals and was associated
367 with antigenic stimulation independent of treatment (Suppl. Fig.2 B, D). As observed
368 in mice no histological abnormalities were found in hamsters (data not shown).

369 *3.9. Immunogenicity of peptide P5 vs. RBD*

370 In order to compare the relative effects of s.c. immunization using peptide P5
371 and recombinant RBD, specific antibody levels were determined at different time
372 points after 3 immunizations with each antigen. As shown in Fig. 2A, similar levels
373 of IgG antibodies were induced by peptide P5 and RBD, and remained detectable
374 up to 60 days after the last immunization.

375 *3.10. Anti-peptide P5 antibody virus neutralization assay*

376 The capacity of antibodies elicited by P5 peptide immunization to interfere with
377 the entrance of SARS-CoV-2 virus to the cells was measured. BALB/c mice were
378 immunized three times on days 0, 7 and 14 with 50 µg of peptide P5 mixed with
379 $Al(OH)_3$. Sera from three mice per group was collected on day 14, 21 and 44 days
380 after the first immunization and serial dilutions were incubated with the SARS-CoV-
381 2 virus and VERO E6 cells. Immunization significantly increased neutralization
382 antibody titers (4±0 and 4.74±0.58 at 21 and 44 days, respectively), whilst only a
383 tendency was obtained after the second immunization, as shown in Fig. 2B.

384 *3.11. Antibodies in sera from COVID-19 patients and convalescent individuals*
385 *recognize peptide P5*

386 Recent studies have demonstrated that sera from infected patients can recognize
387 the RBD domain of SARS-CoV-2 [28]. To test if SARS-CoV-2 infection induces

antibodies that also recognize P5, 46 sera from infected individuals were obtained from hospitals treating COVID-19 patients. All sera from convalescent individuals and 89% of sera from COVID-19 patients recognized peptide P5 and RBD (Fig. 3). This is in agreement with our observation that about half of the sera from mice immunized with P5 induced antibodies that react with both, P5 and RBD. (Fig.3)

3.12. Immunization of mice with human influenza vaccine reduced the antibody response to peptide P5

As the influenza vaccine may be administered in combination with a COVID-19 vaccine, particularly during future cold seasons, the effect of co-immunization of mice with peptide P5 plus human influenza vaccine was explored. Co immunization with influenza vaccine and the peptide reduced the antibody response to peptide P5, but not to the influenza vaccine (Suppl. Fig. 3).

3.13. Cellular immune response to the RBD synthetic peptide P5

To evaluate antigen specific T cell responses, splenocytes from 3 times immunized and unimmunized mice were re-stimulated *in vitro* for 72 h with peptide P5 (10 µg/ml). Intracellular IFNγ production of CD4+ and CD8+ T cell subpopulations was analyzed by flow cytometry (Fig. 4). Our results showed that significant IFNγ production was observed only in CD8+ T cells from mice that were s.c. immunized using aluminum hydroxide as adjuvant (Table 5).

To evaluate the kinetic of the cellular response along the time, splenocytes from peptide P5 immunized mice were tested at different times after 3 immunizations schedule with P5-aluminum hydroxide. As shown in Fig. 2C, whilst the number of

410 CD4+ T cells secreting IFNγ was only slightly increased during the evaluation period,
411 the number of IFNγ secreting CD8+ T cells was robustly increased after a week,
412 and then gradually decreased to similar levels as the CD4+ T cells.

413 Taken together, these findings reinforce our decision to use aluminum hydroxide
414 as the optimal adjuvant to induce both, a specific humoral response, as well as an
415 IFNγ producing T cell response.

416

4. Discussion

At present, several vaccines have been authorized for emergency use and only two (Pfizer and Moderna) have been assigned for marketing authorization, as they finished comprehensive safety and efficacy studies for the regulatory authorities of each country. However, despite great international efforts, availability of vaccines in many countries continues to be a problem, mostly in developing countries.

The S protein of SARS-CoV-2 is the major target of most anti-COVID-19 vaccines currently available. However, previous studies have reported enhanced respiratory disease in other coronaviruses infections, such as SARS-CoV and MERS-CoV, due to phenomenon of antibody-dependent enhancement (ADE) induced by IgG specific antibodies to the spike protein [4, 17]. The use of the S1 subunit, RBD domain or certain epitopes within it, could induce an efficient immune response against the most critical regions interacting with ACE2 receptor, avoiding potential ADE effects.

I*n silico* predictions of immunogenicity can be used for a rational design of multi-epitope peptide-based vaccines but their effectiveness still needs evaluation. In this study, immunogenic properties of 6 peptides predicted by *in silico* analysis of the S protein were tested through immunization of mice. A peptide of 34 aa named P5, induced the highest levels of specific IgG antibodies in two strains of mice, as well as in hamsters. Differences in the magnitude of the responses were observed depending of the route of administration, dose, number of doses, adjuvants employed in vaccine formulation, animal species, as well as strain and gender in mice.

Peptide P5 induced strong humoral and cellular immune responses when subcutaneously administered to both C57BL/6 and BALB/c mice. Similar responses were produced in hamsters. The lower dose of peptide was the most effective for the stimulation of both humoral and cellular responses. Although most of the experiments reported here were performed using 3 immunizations, mice also elicited a significant antibody response after the second dose of antigen. Indeed, detectable antibodies induced by two subcutaneous immunizations of P5 using aluminum hydroxide as adjuvant elicited both ELISA positive and virus neutralizing antibodies, which were maintained for at least 80 days after the last immunization, suggesting that peptide P5 includes relevant B-cell epitope(s) for the induction of a sustained and effective humoral and cellular response.

As in many viral infections, cellular immunity plays an important role in resistance to SARS-CoV2 [18]. Indeed, an inverse association has been reported in COVID-19 between the severity of the disease and the percent of activated and proliferating virus-specific CD8+ T cells, such as spike-specific CD8 + T cells [19]. Thus, the observation that peptide P5 induced a proliferative response of CD8+/IFNγ mouse cells is particularly significant. The T cell response was evaluated when P5 was administered with aluminum hydroxide as adjuvant, but not with AddaVax (Table 5). This is of particular practical relevance as aluminum salts have been used for the formulation of vaccines for almost 100 years. In addition to its safety, the low cost and lack of intellectual property claims makes aluminum hydroxide an ideal adjuvant for development of vaccines, particularly in developing countries.

462 An interesting sexual dimorphism in the antibody response of mice was also
463 observed; being females more responsive than males. Gender differences in favor
464 of women in the risk of contracting and dying from COVID-19 have been documented
465 in different countries and similar data were observed in recent epidemics, including
466 severe acute respiratory syndrome (SARS) and in the Middle East respiratory
467 syndrome (MERS) [20, 21]. The mechanisms underlying sex differences in vaccine-
468 induced innate and adaptive immunity has implicated hormonal, genetic, and even
469 microbiota differences between males and females [22]. Generally, testosterone has
470 an immunosuppressive effect while estrogen has an immunoenhancing effect on the
471 immune system [23, 24]. The X chromosome may be also involved in the sex-related
472 immune function [25]. Thus, a dimorphic response to vaccine-induced humoral
473 immunity similar to that reported here for peptide P5 immunized mice seems to be
474 frequent, and has been described for other vaccines [22, 26, 27, 28].

475 An important consideration for COVID-19 vaccines is the occurrence of mutations
476 in the spike protein. So far, all reported variants were conservative mutations
477 compared to P5; however, three mutations involving polar amino acids must be
478 considered for further experiments when considering their charges and mutational
479 occurrence, because, they change from polar neutral to basic (T478K, N481K) and
480 from acidic to base (E484K), such mutations may require appropriate modifications
481 in P5 sequence in order to maintain its potential as a protective vaccine, as is the
482 case for all COVID-19 vaccines (Supplementary Table 3).

483 Finally, we have addressed the possibility of vaccine induced immunopathology,
484 due to acute pro-inflammatory components in the vaccine or in its adjuvants. In this

485 respect, peptide P5 did not induce any behavioral or macroscopic evidence of
486 discomfort in the animals. In addition, there were no significant histological
487 differences between the organs of vaccinated and control mice. Some microscopic
488 findings observed during necropsies, were not correlated with the treatment and are
489 probably due to the maintenance conditions in our animal facilities. The possibility of
490 pathology due to Anti-peptide P5 Dependent Enhancement remains to be evaluated.

491 In conclusion, this study suggested that a short peptide (34 amino acids) whose
492 sequence was taken of RBD, shows immunogenic properties demanded for the
493 development of a vaccine against SARS-CoV2. At present, 43 vaccine candidates
494 based on protein subunits are being tested in clinical assays, including 15 based on
495 RBD or peptide antigenic sequences identified after analyzing different proteins of
496 SARS-CoV 2 [https://www.who.int/publications/m/item/draft-landscape-of-covid-19-
497 candidate-vaccines]. Our goal was to increase its immunogenic capacity by including
498 recently reported adjacent epitopes.

499 **Declaration of Competing Interest**

500 The authors declare that they have no known competing financial interests or
501 personal relationships that could have appeared to influence the work reported in
502 this paper.

503 Funding: This study was supported by Dirección General de Personal Académico
504 de la Universidad Nacional Autónoma de México (PAPIIT IV201020) and the
505 Institutional Program "Programa de Investigación para el Desarrollo y la
506 Optimización de Vacunas, Inmunomoduladores y Métodos Diagnósticos del IIB"

(PROVACADI). Agencia Mexicana de Cooperación Internacional para el Desarrollo (AMEXCID) y al Programa Conjunto de Cooperación México-Chile, Secretaría de Relaciones Exteriores de México (CH03 Project).

Acknowledgments

We are indebted to P. de la Torre and O. Rangel-Rivera for technical support; to the Unidad de Modelos Biológicos of our institute, as well as to A. Carmona School of Sciences-UNAM for animal lodging and handling. To LabNalCit for their support using flow cytometry, and to M. E. Carrasco for her advice on inter-institutional agreements.

Author contributions

All authors should have made substantial contributions to all of the following: (1) the conception and design of the study ES, JPL, GF, JCT performed the experiments JCT, SR, CC, LM, JHA, GG, ACG, FZF, MRR, JCAM, SO, RO, GD, FPG, RZG, NV, RVR, DAAN, LC, JCC, MJR, RVH, DV, DG, RSV, GM, JZ, DR, analysis and interpretation of data ES, JPL, GF, JCT, SR, NF, GS, RMEP, GG, GC, MH, MR, LAH, RJB, MPT, FSG, LH, NF, IG, CS,(2) drafting the article or revising it critically for important intellectual content ES, JPL, GF, GS, JCT, MR, NF, RMEP, (3) final approval of the version to be submitted ES, JPL, GF, JCT, RMEP, RJB.

529 **References**

530 [1] Dai L, Gao GF. Viral targets for vaccines against COVID-19. Nat Rev Immunol.
531 2021; 21:73–82 (). doi.org/10.1038/s41577-020-00480-0.

532 [2] Duman N, ALzaidi Z, Aynekin B, Taskin D, Demirors B, Yildirim A, Sahin IO,
533 Bilgili F, Turanli ET, Beccari T, Bertelli M, Dundar M. COVID-19 vaccine
534 candidates and vaccine development platforms available worldwide. J Pharm
535 Anal. 2021 Sep 14. doi: 10.1016/j.jpha.2021.09.004.

536 [3] Muhammed Y, Yusuf Nadabo A, Pius M, Sani B, Usman J, Anka Garba N,
537 Mohammed Sani J, Opeyemi Olayanju B, Zeal Bala S, Garba Abdullahi M,
538 Sambo M. SARS-CoV-2 spike protein and RNA dependent RNA polymerase
539 as targets for drug and vaccine development: A review. Biosaf Health. 2021 Jul
540 21. doi: 10.1016/j.bsheal.2021.07.003.

541 [4] Wan, Y. et al. Molecular mechanism for antibody dependent enhancement of
542 coronavirus entry. J. Virol. 94, e02015–e02019 (2020).

543 [5] Min L, Sun Q. Antibodies and Vaccines Target RBD of SARS-CoV-2. Front Mol
544 Biosci. 2021 Apr 22;8:671633. doi: 10.3389/fmolb.2021.671633. PMID:
545 33968996; PMCID: PMC8100443.

546 [6] Calina D, Docea AO, Petrakis D, Egorov AM, Ishmukhametov AA, Gabibov AG,
547 Shtilman MI, Kostoff R, Carvalho F, Vinceti M, Spandidos DA, Tsatsakis A.
548 Towards effective COVID‐19 vaccines: Updates, perspectives and challenges
549 (Review). Int J Mol Med. 2020; 46(1):3-16. doi: 10.3892/ijmm.2020.4596.

[7] Hodgson SH, Mansatta K, Mallett G, Harris V, Emary KRW, Pollard AJ. What defines an efficacious COVID-19 vaccine? A review of the challenges assessing the clinical efficacy of vaccines against SARS-CoV-2. Lancet Infect Dis. 2020; S1473-3099(20)30773-8. doi: 10.1016/S1473-3099(20)30773-8.

[8] Khan K, Dimtri F, Vargas C, Surani S. COVID-19: A Review of Emerging Preventative Vaccines and Treatment Strategies. Cureus. 2020; 12(5):e8206. doi: 10.7759/cureus.8206.

[9] Omersel J, Karas Kuželički N. Vaccinomics and Adversomics in the Era of Precision Medicine: A Review Based on HBV, MMR, HPV, and COVID-19 Vaccines. J Clin Med. 2020; 9(11): E3561. doi: 10.3390/jcm9113561.

[10] Shih HI, Wu CJ, Tu YF, Chi CY. Fighting COVID-19: A quick review of diagnoses, therapies, and vaccines. Biomed J. 2020; 43(4):341-354. doi: 10.1016/j.bj.2020.05.021.

[11] Yaling An, Shihua Li, Xiyue Jin, Jian-bao Han, Kun Xu, Senyu Xu, Yuxuan Han, Chuanyu Liu, Tianyi Zheng, Mei Liu, Mi Yang, Tian-zhang Song, Baoying Huang, Li Zhao, Wen Wang, A Ruhan, Yingjie Cheng, Changwei Wu, Enqi Huang, Shilong Yang, Gary Wong, Yuhai Bi, Changwen Ke, Wenjie Tan, Jinghua Yan, Yong-tang Zheng, Lianpan Dai, George F. Gao. A tandem-repeat dimeric RBD protein-based COVID-19 vaccine ZF2001 protects mice and nonhuman primates. Cold Spring Harbor. Preprint. bioRxiv 2021.03.11.434928; doi: doi.org/10.1101/2021.03.11.434928.

571 [12] Tai W, He L, Zhang X, Pu J, Voronin D, Jiang S, Zhou Y, Du L. Characterization
572 of the receptor-binding domain (RBD) of 2019 novel coronavirus: implication
573 for development of RBD protein as a viral attachment inhibitor and vaccine.
574 Cell Mol Immunol. 2020; 6 :613-620. doi: 10.1038/s41423-020-0400-4.

575 [13] Guex N, Peitsch MC. SWISS-MODEL and the Swiss-PdbViewer: an
576 environment for comparative protein modeling. Electrophoresis. 1997;
577 15:2714-23. doi: 10.1002/elps.1150181505.

578 [14] Sciutto E, Hernández M, García G, de Aluja AS, Villalobos AN, Rodarte LF,
579 Parkhouse M, Harrison L. Diagnosis of porcine cysticercosis: a comparative
580 study of serological tests for detection of circulating antibody and viable
581 parasites. Vet Parasitol. 1998; 78(3):185-94. doi: 10.1016/s0304-
582 4017(98)00129-0.

583 [15] Beales LP, Wood DJ, Minor PD, Saldanha JA. A novel cytopathic microtitre
584 plate assay for hepatitis A virus and anti-hepatitis A neutralizing antibodies. J
585 Virol Methods. 1996; 59(1-2):147-54. doi: 10.1016/0166-0934(96)02035-6.

586 [16] Elbe S, Buckland-Merrett G. Data, disease and diplomacy: GISAID's innovative
587 contribution to global health. Glob Chall. 2017; 1(1):33-46. doi:
588 10.1002/gch2.1018.

589 [17] Tseng CT, Sbrana E, Iwata-Yoshikawa N, Newman PC, Garron T, Atmar RL,
590 et al. Immunization with SARS coronavirus vaccines leads to pulmonary
591 immunopathology on challenge with the SARS virus. PloS One 2012;7:e35421.

592 [18] Chandrashekar A, Liu J, Martinot AJ, McMahan K, Mercado NB, Peter L,
593 Tostanoski LH, Yu J, Maliga Z, Nekorchuk M, Busman-Sahay K, Terry M, Wrijil
594 LM, Ducat S, Martinez DR, Atyeo C, Fischinger S, Burke JS, Slein MD,
595 Pessaint L, Van Ry A, Greenhouse J, Taylor T, Blade K, Cook A, Finneyfrock
596 B, Brown R, Teow E, Velasco J, Zahn R, Wegmann F, Abbink P, Bondzie EA,
597 Dagotto G, Gebre MS, He X, Jacob-Dolan C, Kordana N, Li Z, Lifton MA,
598 Mahrokhian SH, Maxfield LF, Nityanandam R, Nkolola JP, Schmidt AG, Miller
599 AD, Baric RS, Alter G, Sorger PK, Estes JD, Andersen H, Lewis MG, Barouch
600 DH. SARS-CoV-2 infection protects against rechallenge in rhesus macaques.
601 Science. 2020; 369(6505):812-817. doi: 10.1126/science.abc4776.

602 [19] Muraoka D, Situo D, Sawada SI, Akiyoshi K, Harada N, Ikeda H. Identification
603 of a dominant CD8+ CTL epitope in the SARS-associated coronavirus 2 spike
604 protein. Vaccine. 2020; 38(49):7697-7701. doi: 10.1016/j.vaccine.2020.10.039.

605 [20] Pirhadi R, Sinai Talaulikar V, Onwude J, Manyonda I. Could estrogen protect
606 women from COVID-19? J Clin Med Res. 2020; 10:634-639. doi:
607 10.14740/jocmr4303.

608 [21] Pinna G. Sex and COVID-19: A protective role for reproductive steroids.
609 Trends Endocrinol Metab. 2021; 32(1):3-6. doi: 10.1016/j.tem.2020.11.004.

610 [22] Fischinger S, Boudreau CM, Butler AL, Streeck H, Alter G. Sex differences in
611 vaccine-induced humoral immunity. Semin Immunopathol. 2019; 41(2):239-
612 249. doi: 10.1007/s00281-018-0726-5.

[23] Taneja V. Sex Hormones Determine Immune Response. Front Immunol. 2018; 9: 1931.doi: 10.3389/fimmu.2018.01931.

[24] Mauvais-Jarvis F, Klein SL, Levin ER. Estradiol, progesterone, immunomodulation, and COVID-19 Outcomes. Endocrinology. 2020; 161:1-8 doi: 10.1210/endocr/bqaa127.PMID: 32730568.

[25] Libert C, Dejager L, Pinheiro I. The X chromosome in immune functions: when a chromosome makes the difference. Nat Rev Immunol. 2010; 10(8):594–604. doi: 10.1038/nri2815.

[26] Flanagan KL, Fink AL, Plebanski M, Klein SL. Sex and gender differences in the outcomes of vaccination over the life course. Annu Rev Cell Dev Biol. 2017; 33:577-599. doi: 10.1146/annurev-cellbio-100616-060718.

[27] Ruggieri A, Anticoli S, D'Ambrosio A, Giordani L, Viora M. The influence of sex and gender on immunity, infection and vaccination. Ann Ist Super Sanita. 2016; 52(2):198-204. doi: 10.4415/ANN_16_02_11.

[28] Gadi N, Wu SC, Spihlman AP, Moulton VR. What's sex got to do with COVID-19? gender-based differences in the host immune response to Coronaviruses. Front Immunol. 2020; 11:2147. doi: 10.3389/fimmu.2020.02147.

634 **Figure Legends**

635 Fig. 1. Prediction of immunogenic peptides within RBD. Upper panel shows the
636 amino acid sequences for peptides 1 to 6. Lower panel shows 3D homotrimeric
637 complex of the SARS-CoV-2 S protein (PDB ID: 7DF3), each polypeptide chain is
638 indicated in red, blue and gold. Peptides are located in the RBD and correspond to
639 the apical region of the virus and the position of the 6 peptides are indicated by blue
640 spheres.

641 Fig. 2. Humoral and cellular immune response sustained. Antibodies induced by s.c.
642 immunization with P5 or RBD. **A)** Subcutaneous immunization of mice was carried
643 out in groups of six to twelve BALB/c mice female mice, using 50 µg of peptide 5 or
644 12.5 µg of RBD, in the presence of alumina. Each mouse received three doses of
645 peptide 5 or RBD each 7 days. Anti-peptide 5 or anti-RBD IgG antibodies were
646 determined at the indicated time points by ELISA. Mean + SEM are shown and
647 statistical differences are depicted as *P < 0.05. **B)** Microneutralizing antibody (MN)
648 titers against SARS-CoV-2 virus. Mice were immunized s.c. three times at weekly
649 intervals with P5, and sera were obtained at different time points. Neutralization of
650 SARS-CoV-2 infection (MOI=0.1) by individual diluted sera (n=3) from mice was
651 determined. Sera from convalescent patient were used as controls. Solid bars
652 represent geometric mean log2 titer with SEM shown by error bars. Statistically
653 different between before and after immunization (*P<0.05). **C)** Splenocytes from
654 BALB/c mice s.c. immunized with P5 adjuvanted either with Aluminum hydroxide
655 were recovered at weeks 1, 5 or 14 after the last immunization. Cells were
656 restimulated *in vitro* with P5 (10 µg/ml), anti-CD3+ anti-CD28 antibodies (1 µg/ml)

as positive control or medium alone (W/S) for 72h. The mean and SD of the intracellular IFNγ production of CD4+ and CD8+ T cell subpopulations, were plotted. Relative index (RI) was calculated with respect to non-immunized mice.

Fig. 3. Cross-reactivity between peptide 5 and RBD. IgG antibodies against peptide 5 or RBD were determined in sera from six COVID-19 recovered-convalescents subjects, 20 other patients with active COVID-19, and from 6 mice immunized with Peptide 5 as described above. Data are expressed as the mean ± SD of the IgG levels that recognized peptide 5 or the recombinant RBD.

Fig. 4. Cellular immune response induced by P5. Splenocytes from BALB/c mice s.c. immunized with P5 adjuvanted either with Aluminum hydroxide or ADDAVAX were recovered 7 days after the last immunization. Cells were restimulated in vitro with P5 (10 µg/ml), anti-CD3+ anti-CD28 antibodies (1 µg/ml) as positive control or medium alone (W/S) for 72h. **A)** Graphs show the gating strategy used to analyze CD4+ and CD8+ T cells. **B)** Intracellular IFNγ production of CD4+ and CD8+ T cell subpopulations was analyzed by flow cytometry. *Statistically different between before and after immunization ($P<0.05$).

Suppl. Fig. Legends

Suppl. Fig. 1. Subcutaneous immunization with peptide 5 does not modify the weight of mice. Mice of each experimental group were weighed on their arrival to the animal facilities and before each immunization (shown by an arrow in the Fig.).

Suppl. Fig. 2. Similar histopathological alterations found in (A, C) liver or B, D) lung from control and peptide 5 immunized BALB/c mice. Abbreviations: VD, vacuolar

679 degeneration; FN, focal necrosis; AlvMH, alveolar macrophage hyperplasia; LnfLP
680 Lymphoplasmotic inflammation; P5, peptide 5; Sc: Subcutaneous immunization; IN:
681 Intranasal Immunization.

682 Suppl. Fig. 3. Levels of IgG obtained before and seven days after the last
683 immunization. Subcutaneous co-immunization of influenza vaccine (IV) and P5
684 depleted the levels of antibodies elicited by P5 alone but not against influenza
685 vaccine. Individual values and Mean (black solid line) of the serum IgG levels of
686 mice immunized SC with 50 µg of P5 with Aluminum hydroxide or with 50 µg of
687 P5- Aluminum hydroxide + 10 µg of Influenza Vaccine. *Statistically different
688 between before and after immunization ($P<0.05$).

689

690

691

692

693 Table 1. Levels of sera IgG and IgA in mice subcutaneously immunized with different peptides derived from the RBD domain of the
694 Spike protein of SARS-CoV-2 virus

	Sera levels of IgG				Sera levels of IgA	
	Recognizing the specific peptide		Recognizing the RBD domain		Recognizing the specific peptide	
	Before Immunization	After Immunization	Before Immunization	After Immunization	Before Immunization	After Immunization
Immunizing with:						
P1	0.20±0.02	0.19±0.04	0.26±0.09	0.240.02±	0.16±0.10	0.22±0.11
P2	0.25±0.06	0.17±0.01	0.19±0.03	0.23±0.01	0.09±0.02	0.17±0.05
P3	0.25±0.12	0.25±0.10	0.24±0.10	0.24±0.09	0.090.02±	0.18±0.09
P4	0.44±0.07	1.69±1.60*	0.16±0.08	0.28±0.04	0.08±0.03	0.20±0.08
P5	0.22±0.02	1.10±0.34*	0.23±0.06	2.21±1.38*	0.17±0.00	0.17±0.09
P6	0.14±0.02	0.14±0.05	ND	ND	0.29±0.09	0.45±0.31

695

696 Mean ± SD of the Optical Density read at 405 nm of the ELISA to detect IgG and IgA level of immunoglobulins of six female mice
697 subcutaneously immunized with 50 µg of the respective peptide with ADDAVAX. Each mouse received three doses of the vaccine
698 each 7 days. Mice were bled before and seven days after the last immunization. ND: not determined. *Statistically different between
699 before and after immunization ($P<0.05$).

700

701 Table 2. Effect of different doses of P5 on the level of specific antibodies in Intranasal
702 and Subcutaneously immunized mice

	Anti-P5 IgG antibodies					
	Subcutaneous			Intranasal		
	P5 (μg/mouse)	Before Immunization	After Immunization	P5 (μg/mouse)	Before Immunization	After Immunization
Mouse Strain:						
C57Bl/6J	50	0.25±0.04	2.72±0.01*	10	0.25±0.05	0.41± 0.10*
BALB/c	50	0.21±0.01	0.32±0.01*	10	0.27±0.08	0.29 ± 0.02
C57Bl/6J	100	0.16±0.01	2.90±0.03*	50	0.38±0.16	0.55 ± 0.02*
BALB/c	100	0.30±0.01	1.43±1.20*	50	0.21±0.01	0.29 ± 0.07
C57Bl/6J	200	0.31±0.01	2.09±0.80*	100	0.26±0.04	0.37 ± 0.10*
BALB/c	200	0.33±0.02	2.82±0.06*	100	0.21±0.08	0.19 ± 0.01

703 Mean ± SD of the Optical Density read at 405 nm of ELISA to detect levels of IgG anti-P5
704 antibodies in female mice immunized with different doses of P5 adjuvanted with Addavax.
705 Each mouse received three doses of the vaccine each 7 days. Mice were bled before and
706 seven days after the last immunization. *Statistically different between before and after
707 immunization ($P<0.05$).

708

709

Table 3. The optimal humoral immune response was induced by subcutaneous immunization with peptide 5 and aluminum hydroxide

			Anti-peptide 5 IgG	
			Before Immunization	After Immunization
	Mouse Strain:	Adjuvant		
Subcutaneous immunization	C57BL/6J	ADDAVAX	0.21±0.01	2.58±0.20*
	BALB/c	ADDAVAX	0.25±0.04	0.32±0.02
	C57BL/6J	AL(OH)3	0.26±0.06	2.68±0.28*
	BALB/c	AL(OH)3	0.16±0.03	0.81±0.54*
Intranasal Immunization	C57BL/6J	ADDAVAX	0.25±0.05	0.37±0.10
	BALB/c	ADDAVAX	0.27±0.07	0.19±0.01
	C57BL/6J	AL(OH)3	0.26±0.06	0.36±0.14
	BALB/c	AL(OH)3	0.16±0.06	0.17±0.02

Mean ± SD of the Optical Density read at 405 nm of ELISA to detect sera levels of IgG anti-P5 antibodies from female mice immunized with P5 adjuvanted either with Aluminum hydroxide or ADDAVAX. Each mouse received three doses of the vaccine each 7 days. Mice were bled and sacrificed seven days after the last immunization. The level of IgG antibodies in the group in separates groups of two BALB/C, C57BL/6J or non- immunized mice, were determined. *Statistically different between before and after immunization ($P<0.05$).

Table 4. Effect of adjuvant and dose of P5 on the levels of IgG antibodies in subcutaneous and intranasal immunized female and male hamsters

				Sera IgG levels				
				Before Immunization	After Immunization	Route	Before Immunization	After
Adjuvanted with: ADDAVAX	Sex	Dose (μg)	Route					
	M F	10	SC	ND	ND	IN	0.16±0.01	0.17±0.01 0.21±0.07
	M F	50	SC	0.19±0.02	1.45±0.09* 1.42±0.45*	IN	0.15±0.01	0.20±0.08 0.29±0.09
	M F	100	SC	0.13±0.03	3.45±0.35* 3.72±0.07*	IN	0.14±0.01	0.17±0.04 0.29±0.09
	M F	200	SC	0.13±0.01	3.36±0.34* 3.59±0.06*	IN	ND	ND
Aluminum hydroxide								
	M F	50	SC	0.19±0.03	3.76 3.06±0.49*	IN	ND	ND
	M F	100	SC	ND	ND	IN	0.15±0.01	0.20±0.03 0.26±0.01

Mean ± SD of the Optical Density read at 405 nm of ELISA to detect sera levels of IgG anti-P5 in male and female hamsters immunized with different doses of P5 with either ADDAVAX or $AL(OH)_3$. Each hamster received three doses of the vaccine each 7 days. A pooled

742 serum from a group of non-immunized hamsters was employed and samples from each immunized hamster was obtained seven days
743 after the last immunization in those immunized. *Statistically different between before and after immunization (P<0.05

744

745 Table 5. The optimal cellular immune response was induced by subcutaneous
746 immunization with peptide 5 and aluminum hydroxide

			Cellular immune response (CD8+IFNγ+ cells)	
			Before Immunization	After Immunization
	Mouse Strain:	Adjuvant		
Subcutaneous immunization	C57BL/6J	ADDAVAX	ND	0.46±0.47
	BALB/c	ADDAVAX	0.86±0.68	0.76±0.03
	C57BL/6J	$AL(OH)_3$	ND	4.4± 2.6*
	BALB/c	$AL(OH)_3$	0.86±0.68	20.83± 7.3*
Intranasal Immunization	C57BL/6J	ADDAVAX	ND	0.58±0.05
	BALB/c	ADDAVAX	0.86±0.68	1.34±0.6
	C57BL/6J	$AL(OH)_3$	ND	0.60±0.08
	BALB/c	$AL(OH)_3$	0.86±0.68	0.75±0.40

747 Mean ± SD of the number of spleen CD8+IFNγ+ cells from female mice immunized with P5
748 adjuvanted either with Aluminum hydroxide or ADDAVAX. Each mouse received three
749 doses of the vaccine each 7 days. Mice were bled and sacrificed seven days after the last
750 immunization. The numbers of CD8+IFNγ+ cells in separates groups of two BALB/C,
751 C57BL/6J or non- immunized mice, were determined. *Statistically different between before
752 and after immunization ($P<0.05$).

753

754

Figure 1.tif

Peptide	Sequence
1	N_{439}NLDSKVGG$_{447}$
2	V_{407}RQIAPGQTGKIAD$_{420}$
3	F_{490}PLQSYGFQPTNGVGYQ$_{506}$
4	Y_{472}QAGSTPCNGV$_{483}$
5	C_{460}LKPFERDISTEIY$_{472}$QAGSTPCNGV$_{483}$EGFNCYF$_{490}$PLQ$_{493}$
6	G_{431}CVIAWNS$_{438}$

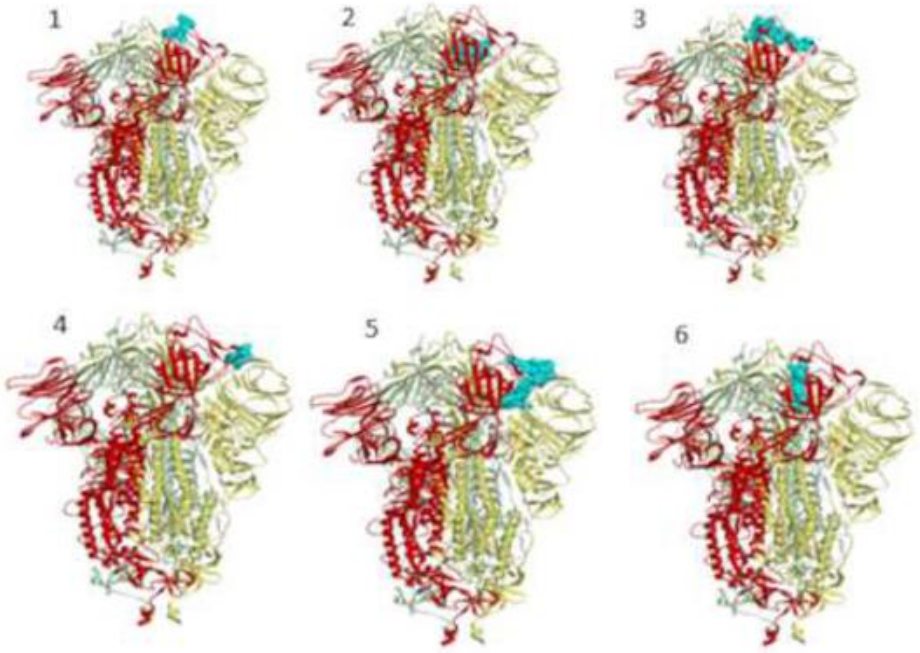

Figure 2

Click here to access/download;Figures;Figure 2.tif

Figure 4.tif

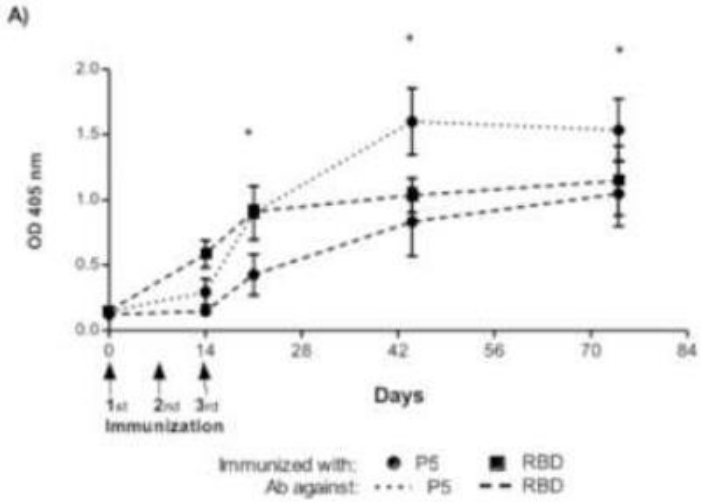

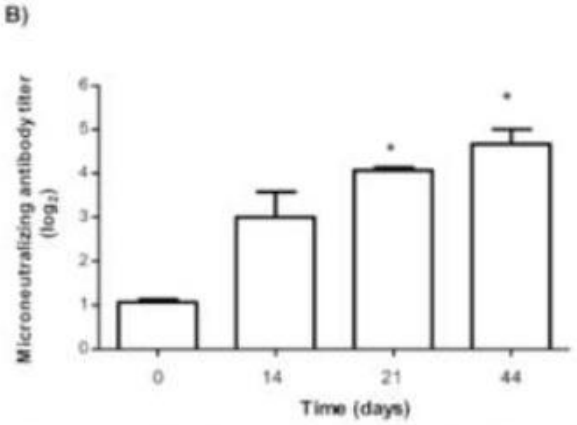

Positive control (Sera from convalescent patient): log_2 MN titer=9.58

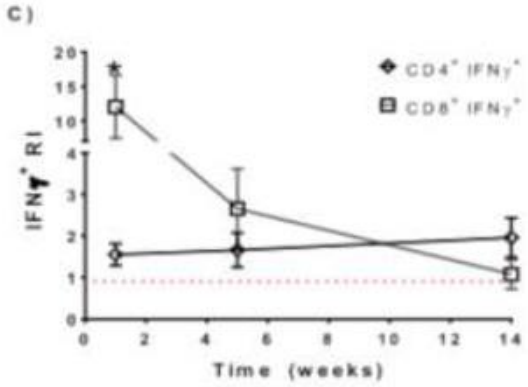

Figure 3

Click here to access/download;Figures;Figure 3.tif

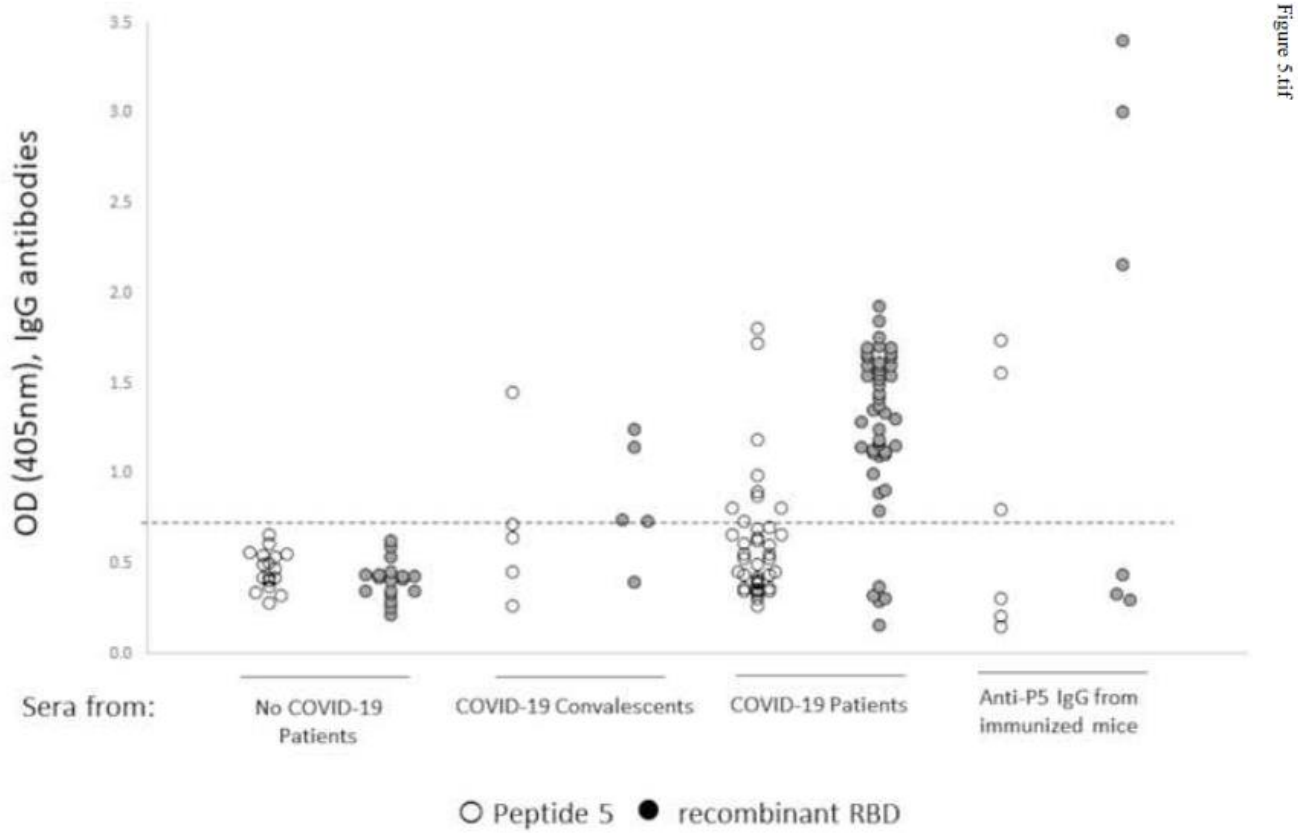

Figure 4

Click here to access/download;Figures;Figure 4.tif

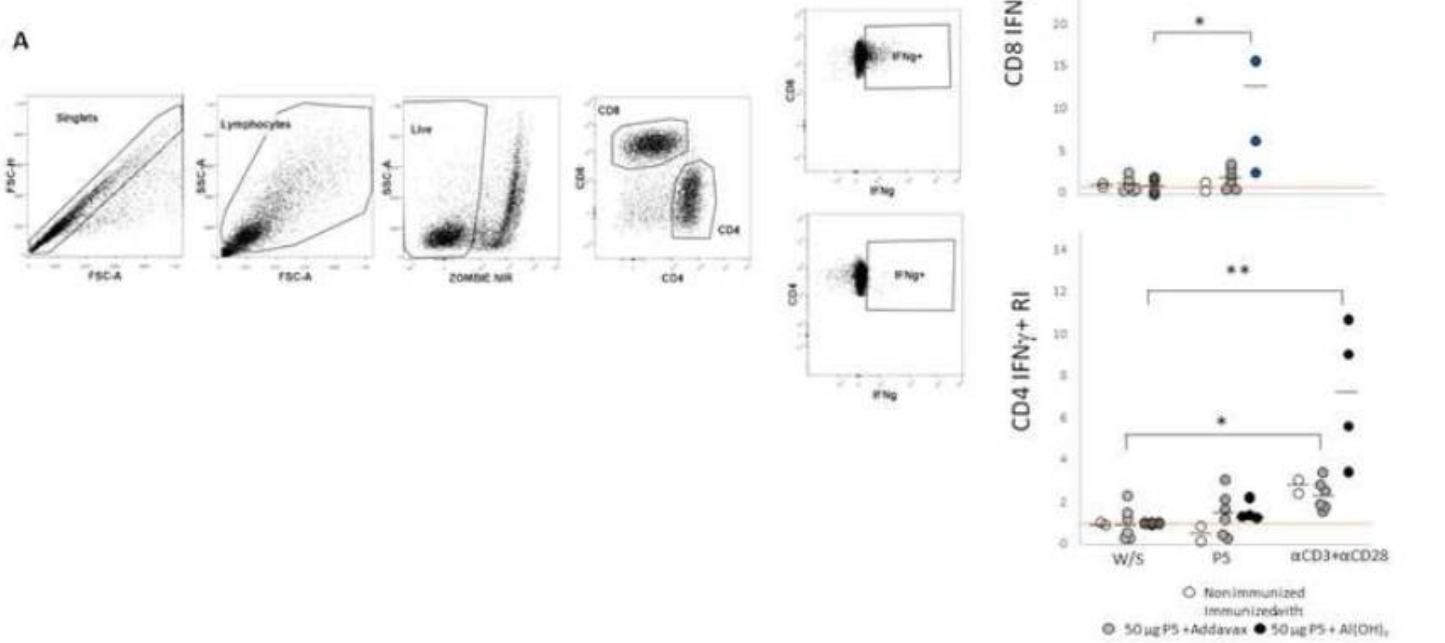

Figure 7.tif

Figure 2.tif

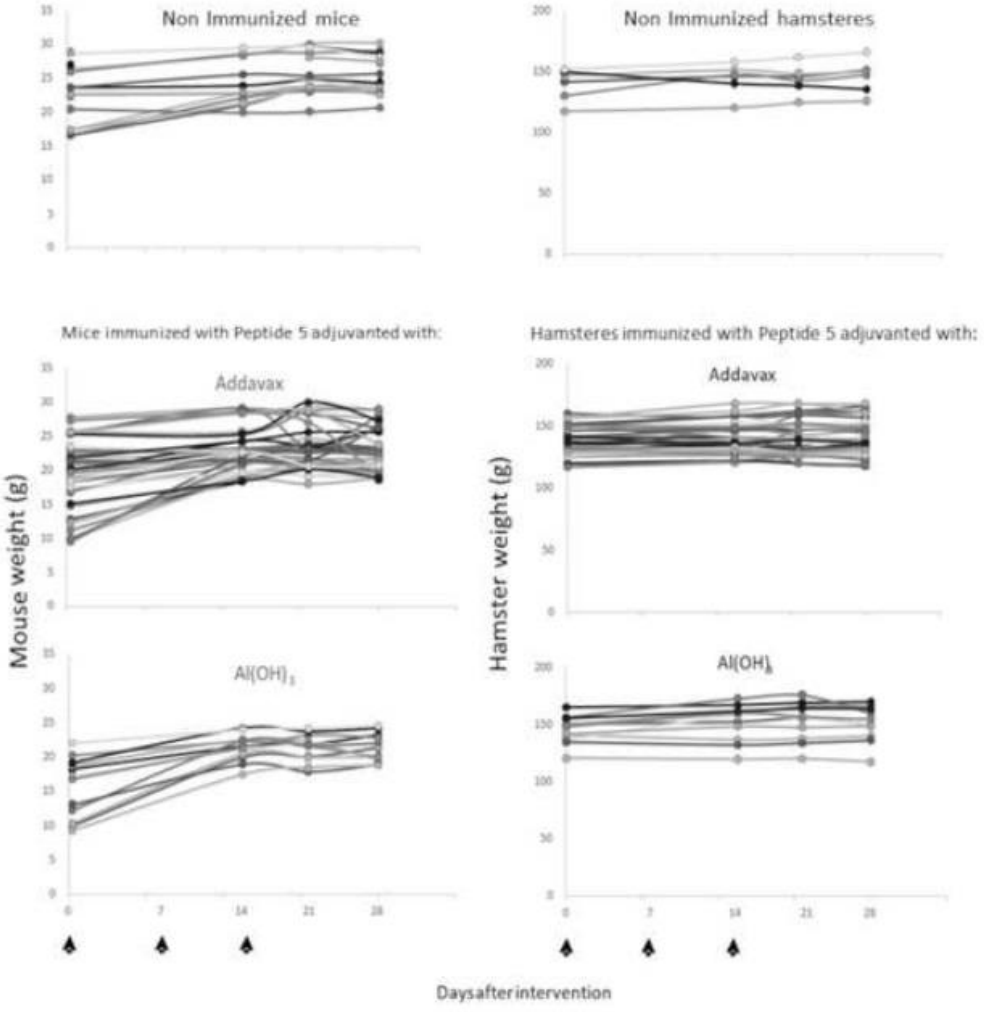
Non Immunized mice
Non Immunized hamsteres
Mice immunized with Peptide 5 adjuvanted with:
Hamsteres immunized with Peptide 5 adjuvanted with:
Addavax
Addavax
Al(OH)3
Al(OH)3
Mouse weight (g)
Hamster weight (g)
Days after intervention

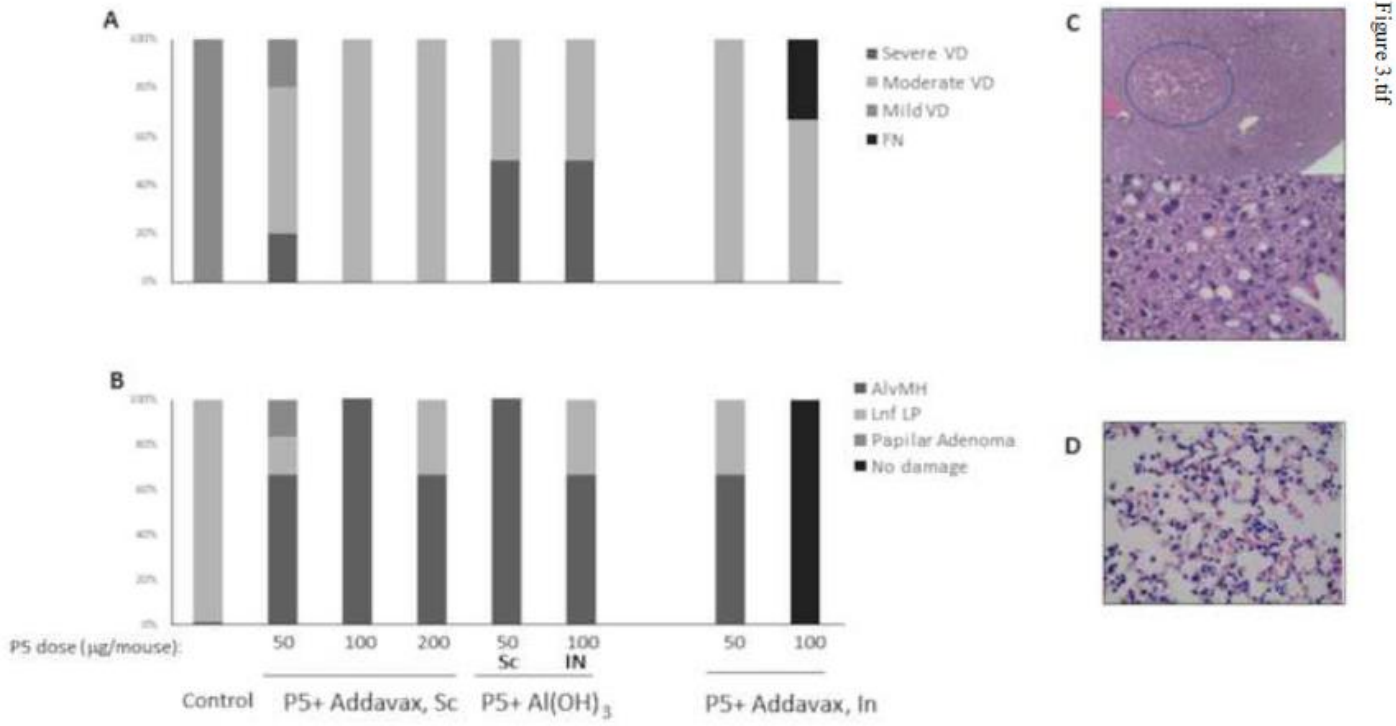

Figure 3.tif

Suppl. Fig, 3

Click here to access/download;Figures;Suppl. Fig, 3.tif

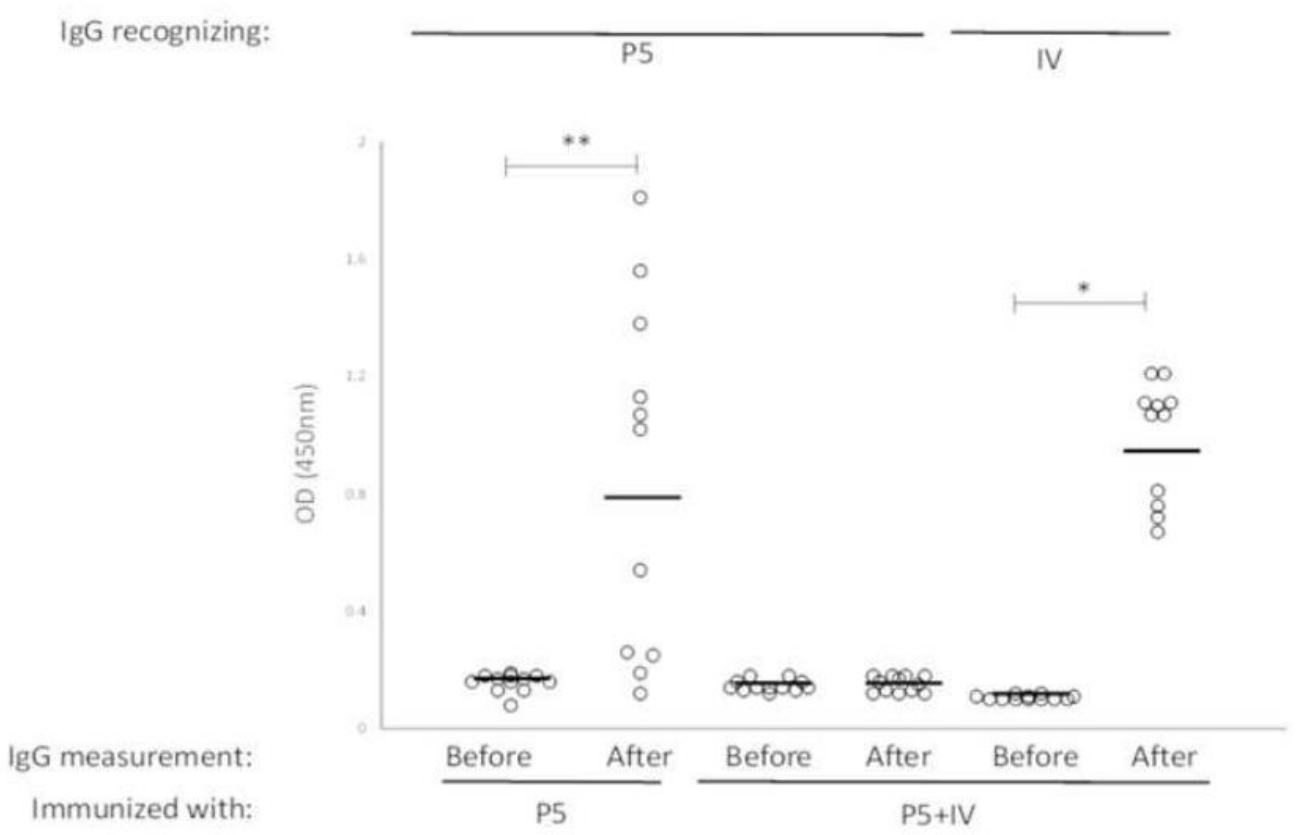

Figure 6.tif